

**A new inducible transgenic mouse model of  
endothelium-specific human endothelin-1  
overexpression.**

**Suellen Cristina Coelho**

Division of Experimental Medicine

McGill University, Montreal

Final thesis submission in October 2017

(A thesis submitted to McGill University in partial fulfillment of the requirements of the degree of PhD Experimental Medicine – Thesis)

## Abstract

The mechanisms of blood pressure (BP) regulation by endothelin (ET)-1 produced by endothelial cells (EC) are complex and remain unclear. Our laboratory has previously generated a constitutive EC-restricted specific human ET-1 (*EDN1*) mouse model. Constitutive EC-restricted *EDN1* overexpression induced endothelial dysfunction, vascular remodeling, oxidative stress, and inflammation in the absence of significant change in BP. It is worth noting that these aforementioned constitutive ET-1 overexpression-induced effects may be due, at least in part, to an ontogenic adaptation to life-long exposure to elevated ET-1 overexpression. To overcome these limitations, we developed a transgenic mouse with tamoxifen-inducible EC-restricted *EDN1* overexpression (ieET-1) using Cre/loxP technology. We hypothesized that induction of endothelium-restricted *EDN1* overexpression would allow the study of vascular and renal mechanisms involved in ET-1 regulation of BP in the absence of developmental effects.

The objectives of this thesis are: 1) to determine whether short term 3-week induction of EC-restricted *EDN1* overexpression in adult ieET-1 mice causes BP elevation and vascular and renal damage and 2) to determine whether longer term 3-month induction of EC-specific ET-1 overexpression in adult ieET-1 mice will maintain BP elevation and induce vascular and renal damage.

The first study shows that we successfully developed an ieET-1 mouse model using tamoxifen-inducible Cre/loxP technology. ieET-1 mice exhibited BP elevation after three weeks of induction in an ET type A (ET<sub>A</sub>) receptor-dependent manner, in absence of vascular and kidney injury.

The second study shows that a longer term 3-month exposure to EC-restricted *EDN1* ET-1 overexpression caused sustained BP elevation, small artery stiffening and endothelial dysfunction, which was associated to enhanced PVAT-derived oxidative stress and monocyte/macrophage infiltration. In addition, *EDN1* overexpression triggered an initial renal damage and immune cell infiltration.

To conclude, ET-1 plays an important role in the development and maintenance of HTN in an ET<sub>A</sub> receptor-dependent manner. ET-1-induced longstanding BP elevation

and vascular and renal inflammation might be important contributors to further induce vascular and renal injury.

## Résumé

Les mécanismes de la régulation de la pression artérielle (PA) par l'endothéline (ET)-1 produite par les cellules endothéliales (CE), sont fort complexes et demeurent incertains. Précédemment, notre laboratoire a généré un modèle de souris qui exprime l'endothéline humaine ET-1 (*EDN1*) spécifiquement et de manière constitutive restreinte aux CE. La surexpression constitutive de l'*EDN1* restreinte à ces cellules a induit une dysfonction endothéliale, un remodelage vasculaire, du stress oxydatif, de l'inflammation, en l'absence de changement significatif de la PA. Les effets induits par la surexpression de l'*EDN1* en absence d'élévation de la PA peuvent être dus en partie à une adaptation ontogénique causée par à une exposition élevée et à long terme à ET-1. Pour surmonter ces contraintes, nous avons développé des souris transgéniques ieET-1 présentant une surexpression de l'ET-1 inducible avec le tamoxifène (TAM) dans les CE à l'aide du système Cre/loxP. Ainsi, nous avons émis l'hypothèse que l'induction de la surexpression *EDN1* restreinte à l'endothélium permettra l'étude des mécanismes vasculaires et rénaux impliqués dans la régulation de la PA par l'ET-1 en l'absence d'effets induits par le développement.

Les objectifs de cette thèse sont : 1) Déterminer si une inhibition à court terme (3 semaines) de la surexpression *EDN1* restreinte aux CE chez les souris adultes ieET-1 provoquera une augmentation de la PA et des dommages vasculaires et rénaux. 2) Déterminer si à plus long terme (3 mois), l'induction de la surexpression de l'ET-1 spécifique aux CE chez les souris adultes ieET maintiendra la hausse de la PA et induira des dommages vasculaires et rénaux.

La première étude montre que nous avons réussi à développer des souris ieET-1 en utilisant la technologie Cre/loxP. Après trois semaines d'induction avec le TAM, les souris ieET-1 présentent une augmentation de la PA dépendante du récepteur ET de type A (ET<sub>A</sub>) avec absence de dommages vasculaires et rénaux.

La deuxième étude montre que l'exposition à long terme de l'ET-1 restreinte aux CE provoque une élévation soutenue de la PA, un durcissement des petites artères et un dysfonctionnement endothélial. Cette observation est associée à une augmentation

du stress oxydatif et à l'infiltration par des monocytes/macrophages dans le tissu adipeux périvasculaire (PVAT). De plus, la surexpression *EDN1* initie des dommages rénaux et une infiltration rénale de cellules immunitaires.

Pour conclure, l'ET-1 joue un rôle important dans le développement et le maintien de l'hypertension artérielle. Ces effets sont médiés par les récepteurs ET<sub>A</sub>. L'élévation soutenue de la PA ainsi que l'inflammation vasculaire et rénale induits par ET-1 pourraient provoquer davantage de dommages vasculaires et rénaux.

## Table of Contents

Abstract.....	ii
Résumé.....	iv
Abbreviations .....	ix
List of tables.....	xiv
List of figures.....	xv
Contribution of authors.....	xviii
Acknowledgements .....	iii
Statement of originality .....	v
CHAPTER I: Review of the Literature and Research Objectives.....	1
1. Introduction .....	2
2. Discovery of the endothelin family and sarafotoxin.....	4
3. General biology of endothelin-1 .....	6
3.1. Constitutive endothelin-1 regulation .....	6
3.2. Endothelin-1 synthesis .....	6
3.2.1. Endothelin-1 synthesis by non-ECE .....	8
3.3. Endothelin-1 storage and secretion .....	10
3.4. Endothelin receptors .....	11
3.4.1. ETR signaling and internalization .....	12
3.4.2. ET receptor antagonists .....	15
3.5. Endothelin-1 degradation .....	16
4. Physiological and pathophysiological effects of ET-1 .....	17
4.1 ET-1 actions within the vasculature .....	17
4.1.1 Anatomy and function of the vessels .....	17
4.1.2 Physiological effects of ET-1 on the vasculature .....	20
4.1.2.1 ET-1 effects on vascular tone .....	21

4.1.3 Pathophysiological effects of ET-1 in the vasculature .....	21
4.1.3.1 Endothelial dysfunction .....	22
4.1.3.2 Vascular remodeling and stiffening .....	25
4.1.3.2.1 Outward hypertrophic remodeling .....	28
4.1.3.2.2 Inward eutrophic and hypertrophic remodeling .....	28
4.1.3.3 Vascular immune response .....	30
4.2 ET-1 actions on the kidney .....	35
4.2.1 Anatomy and function of the kidney .....	35
4.2.2 Physiological effects of ET-1 on the kidney .....	38
4.2.2.1 ET-1 effects on renal hemodynamics .....	39
4.2.2.2 ET-1 effects on sodium and water excretion .....	40
4.2.3 Pathophysiological effects of ET-1 in the kidney .....	42
5. Experimental design .....	45
6. Hypothesis and objectives .....	45
CHAPTER II: Inducible Human Endothelin-1 Overexpression in Endothelium Raises Blood Pressure via Endothelin Type A Receptors .....	47
Abstract .....	49
Introduction .....	50
Methods .....	51
Results .....	53
Discussion .....	57
References .....	62
Figures and tables .....	67
Expanded materials and methods .....	75
Supplemental figures and tables .....	87
CHAPTER III: Three-month endothelial human endothelin-1 overexpression causes blood pressure elevation and vascular and kidney injury .....	93

Abstract.....	96
Introduction .....	97
Methods .....	98
Detailed Methods are available in the online-only Data Supplement.....	98
Data analysis .....	100
Results .....	100
Discussion.....	104
References.....	110
Figures .....	116
Expanded materials and methods .....	125
Supplemental figures and tables.....	139
CHAPTER IV: Discussion and conclusion .....	157
7. Discussion.....	158
7.1. Role of ET-1 in development and maintenance of hypertension .....	158
7.2. Role of ET-1 in the vascular function and mechanical properties .....	159
7.3. ET-1 and the immune system in HTN .....	163
7.4. ET-1 and renal damage during HTN .....	165
8. Conclusion .....	168
9. Limitations .....	168
10. Perspectives .....	169
References:.....	170

## Abbreviations

AA	Arachidonic acid
ACE	Angiotensin-converting enzyme
ADH	Anti-diuretic hormone
Akt	Protein kinase B
AMI	Acute myocardial infarction
Ang	Angiotensin
AP-1	Activator protein-1
APCs	Antigen presenting cells
ApoE	Apolipoprotein E
BP	Blood pressure
CAG	Chicken $\beta$ -actin promoter
<i>cat</i>	Chloramphenicol acetyltransferase
CBF	Cortical blood flow
CD ET-1 KO	Collecting-duct ET-1 knockout
CD ET <sub>A</sub> R KO	Collecting-duct ET <sub>A</sub> R knockout
CD ET <sub>B</sub> R KO	Collecting-duct ET <sub>B</sub> R knockout
CD ET <sub>A/B</sub> R KO	Collecting-duct ET <sub>A/B</sub> R knockout
cGMP	Cyclic guanosine monophosphate
CKD	Chronic kidney disease
CLCNKB	Chloride channel Kb
CNS	Central nervous system
COX	Cyclooxygenases
CreER <sup>T2</sup>	Cre recombinase protein fused to modified estrogen receptor ligand binding domain
CVD	Cardiovascular disease
DAG	Diacylglycerol
DAMPs	Damage-associated molecular patterns
DBP	Diastolic blood pressure
DCs	Dendritic cells

DOCA	Deoxycorticosterone acetate
EC	Endothelial cells
ECE	Endothelin converting enzyme
ECM	Extracellular matrix
EDHF	Endothelium-derived hyperpolarizing factor
EDRF	Endothelium-derived relaxing factor
eET-1	Endothelium-specific human ET-1 overexpression
EMA	European Medicines Authority
ENaC	Epithelial sodium channel
eNOS	endothelial nitric oxide synthase
ER	Endoplasmic reticulum
ERA	Endothelin receptor antagonists
ERK	Extracellular signal regulated kinase
ET	Endothelin
ET <sub>A</sub> R	Endothelin type A receptor
ET <sub>B</sub> R	Endothelin type B receptor
ETR	Endothelin receptor
FDA	Food and Drug Administration
FOXP3	Factor forkhead box P3
GC	Guanylate cyclase
GFR	Glomerular filtration rate
GPCR	G protein-coupled receptor
HIF	Hypoxia inducible factor
H <sub>2</sub> O <sub>2</sub>	Hydrogen peroxide
HTN	Hypertension
ICAM-1	Intracellular adhesion molecule-1
ieET-1	Inducible endothelium-specific human ET-1 overexpression
IFN- $\gamma$	Interferon- $\gamma$
IL	Interleukin
iNOS	Inducible nitric oxide synthase
IP	Prostacyclin receptor

IP <sub>3</sub>	Inositol triphosphate
JAK2/STAT	Janus kinase 2/signal transducer and activator of transcription
JNK	c-Jun N terminal kinase
L-NAME	N <sup>G</sup> -nitro-L-arginine methyl ester
LysM	Lysozyme M <sup>+</sup>
MAPK	Mitogen-activated protein kinase
MBF	Medullary blood flow
MCP-1	Monocyte chemoattractant protein-1
MCSA	Medial cross-sectional area
m-CSF	Macrophage colony-stimulating factor
MDSC	Myeloid-derived suppressor cell
MHC-I or II	Major histocompatibility complex
MLC	Myosin light chain
MMP	Matrix metalloproteinase
NAD(P)H	Nicotinamide adenine dinucleotide phosphate
NCC	Sodium chloride co-transporter
NEP	Neutral endopeptidase enzyme
NHE3	Sodium-hydrogen exchanger
NK	Natural killer
NKCC2	Sodium-potassium-chloride co-transport
NO	Nitric oxide
O <sub>2</sub> <sup>-</sup>	Superoxide
ONOO <sup>-</sup>	Peroxynitrate
op	Osteopetrotic
PAH	Pulmonary arterial hypertension
PAMPs	Pathogen-associated molecular patterns
PGH <sub>2</sub>	Prostaglandin H <sub>2</sub>
PGI <sub>2</sub>	Prostacyclin
PI3K	Phosphatidylinositol 3 kinase
PIP <sub>2</sub>	Phosphatidylinositol 4,3 biphosphate
PKA	Protein kinase A

PKB	Protein kinase B
PKC	Protein kinase C
PLA2	Phospholipase A2
PLC	Phospholipase C
PLD	Phospholipase D
PMCA	Plasmalemmal Ca <sup>2+</sup> -ATPase
PRRs	Pattern recognition receptors
PVAT	Perivascular adipose tissue
PWV	Pulse wave velocity
Rag1	Recombination activating gene-1
RAS	Renin angiotensin system
RBF	Renal blood flow
ROMK	Renal outer medullary potassium channel
ROS	Reactive oxygen species
SERCA	Sarcoplasmic reticulum Ca <sup>2+</sup> -ATPase
SBP	Systolic blood pressure
SHR	Spontaneously hypertensive rats
SIN	3-morpholino-sydnonimine chloride
SMC	Smooth muscle cells
SOD	Superoxide dismutase
SPC	Subtilisin-like pro-protein convertases
TAM	Tamoxifen
Tc	T cytotoxic
TCR	T cell receptor
Th	T helper
TGF-β1	Transforming growth factor-β1
Tie-2	Tie2/CD202b/TEK, tyrosine kinase receptor with immunoglobulin-like and epidermal growth factor-like domains 2, a receptor for angiopoietins
TIMPs	Tissue inhibitors of metalloproteinase
TLRs	Toll-like receptors
TNF-α	Tumor necrosis factor-α

Treg	T regulatory lymphocytes
VCAM-1	Vascular cell adhesion molecule
VEGF	Vascular endothelial growth factor
VSMC	Vascular smooth muscle cells
VIC	Vasoactive intestinal contractor
WBP	Weibel-Palade bodies

## List of tables

### CHAPTER II

Table II-1. Induction of ET-1 overexpression in the endothelium did not alter body or tissue weights .....	72
Table II-2. Induction of endothelin-1 overexpression in the endothelium did not cause vascular remodeling in resistance arteries .....	73
Table II-3. Induction of endothelin-1 overexpression in the endothelium did not affect renal perfusion and function or cause renal injury.....	74
Table II-S1. Oligonucleotides, product sizes and applications. ....	87

### CHAPTER III

Table III-S1. Body and tissue weight.....	139
Table III-S2. Long-term human ET-1 overexpression in endothelium decreased renal artery flow .....	139
Table III-S3. Masson's trichrome staining solutions .....	140
Table III-S4. Periodic Acid Schiff's staining solutions.....	141
Table III-S5. Antibodies for flow cytometry profiling of T cells.....	142
Table III-S6. Oligonucleotides used in quantitative PCR assays .....	142

## List of figures

### CHAPTER I

Figure I-1: The structure of ET-1, ET-2 and ET-3 peptides. ....	5
Figure I-2: Human ET-1 synthesis. ....	7
Figure I-3: Alternative human ET-1 synthesis. ....	9
Figure I-4: ET-1 secretion into the cell surface. Adapted from Servier Medical Art. ....	10
Figure I-5: ET-1 signaling pathway in the vasculature. Adapted from Mazzuca <i>et al.</i> <sup>59</sup> & Servier Medical Art. ....	13
Figure I-6: Structure of a normal artery. Adapted from Servier Medical Art. ....	18
Figure I-7: Large and small artery remodeling during HTN. Adapted from Integan <i>et al.</i> and Schiffrin <i>et al.</i> <sup>145, 162</sup> & Servier Medical Art. ....	28

### CHAPTER II

Figure II-1. Inducible endothelium-restricted human endothelin-1 overexpression mice. ....	67
Figure II-2. Induction of endothelin-1 overexpression in the endothelium increased systolic blood pressure in an endothelin type A receptor manner. ....	69
Figure II-3. Induction of endothelin-1 overexpression in the endothelium did not cause vascular dysfunction in resistance arteries. ....	70
Figure II-4. Induction of endothelin-1 overexpression in the endothelium was associated with an elevation in renal ET <sub>A</sub> and ET <sub>B</sub> receptors. ....	71
Figure II-S1. Genotyping of mice for CAG- <i>cat-EDN1</i> (A), <i>Tie2-CreER</i> <sup>T2</sup> (B) and <i>ROSA26</i> <sup>mT-mG/+</sup> (C). ....	89
Figure II-S2. Tissue specificity of Cre activation was determined using vehicle- and tamoxifen-treated ieCre/ <i>ROSA26</i> <sup>mT-mG/+</sup> reporter mice by determining the replacement of membrane-targeted tandem dimer tomato (mT) by membrane-targeted enhanced green fluorescent protein (mG) expression using confocal microscopy imaging. ....	90

Figure II-S3. Induction of endothelin-1 overexpression in the endothelium increased systolic blood pressure (SBP) in ieET-1-C170 mice. ....	91
Figure II-S4. Renal artery blood flow was determined by echography using two-dimensional short axis view and pulse wave (PW) Doppler as described in the Online Methods section. ....	92

### CHAPTER III

Figure III-1. Long-term endothelial human endothelin-1 overexpression increased blood pressure in an ET type A receptor-dependent manner. ....	116
Figure III-2. Long-term endothelial human endothelin-1 overexpression induced mesenteric artery endothelial dysfunction and vascular stiffening. ....	117
Figure III-3. Long-term human endothelin-1 overexpression increased monocyte/macrophage infiltration in the perivascular adipose tissue of mesenteric arteries. ....	119
Figure III-4. Long-term endothelial human ET-1 overexpression caused early renal damage. ....	120
Figure III-5. Long-term endothelial human endothelin-1 overexpression induced renal immune cell infiltration. ....	121
Figure III-6. After long-term endothelial human endothelin-1 overexpression, increased immune cell infiltration was associated with greater frequency of kidney and myeloid cells expressing the pattern-recognition receptor CD36. ....	123
Figure III-S1. Long-term endothelial human ET-1 overexpression enhanced plasma ET-1 levels. ....	143
Figure III-S2. Long-term endothelial human endothelin-1 overexpression increased blood pressure in an ET type A receptor-dependent manner. ....	144
Figure III-S3. Long-term endothelial human endothelin-1 overexpression did not affect mesenteric artery contractile responses to norepinephrine (NE), relaxation responses to acetylcholine (ACh) after inhibition of nitric oxide synthase (NOS) and to sodium nitroprusside (SNP), and caused vascular remodeling. ....	145

Figure III-S4. Long-term endothelial human endothelin-1 overexpression increased oxidative stress in mesenteric artery perivascular adipose tissue.....	146
Figure III-S5. Long-term endothelial human endothelin-1 overexpression did not modify mesenteric artery fibronectin expression.....	147
Figure III-S6. Long-term endothelial human endothelin-1 overexpression did not affect mesenteric artery collagen content. ....	148
Figure III-S7. Long-term endothelial human endothelin-1 overexpression did not alter the mRNA expression of ET <sub>A</sub> or ET <sub>B</sub> receptors in the mesenteric arteries. ....	149
Figure III-S8 Long-term endothelial human endothelin-1 overexpression did not alter the expression of monocyte chemoattractant protein (MCP)-1 in mesenteric arteries.....	150
Figure III-S9. Long-term endothelial human endothelin-1 overexpression increased monocyte/macrophage infiltration in the perivascular adipose tissue of mesenteric arteries. ....	151
Figure III-S10. Long-term endothelial human endothelin-1 overexpression did not alter the mRNA expression of renal ET <sub>A</sub> , ET <sub>B</sub> receptors or renal cortex renin. ....	152
Figure III-S11. Long-term endothelial human endothelin-1 overexpression did not alter plasma creatinine or urinary albumin excretion rate.....	153
Figure III-S12. Long-term endothelial human endothelin-1 overexpression did not cause evident kidney injury.....	154
Figure III-S13. Long-term endothelial human endothelin-1 overexpression increased immune cell infiltration in the kidney.....	155
Figure III-S14. Long-term endothelial human endothelin-1 overexpression increased the frequency of renal immune cell infiltration. ....	156

## Contribution of authors

First study - Inducible Human Endothelin-1 Overexpression in Endothelium Raises Blood Pressure via Endothelin Type A Receptors

Yohann Rautureau\*:

- Animal model generation
- Design of experiments
- Technical setup for most of the experiments
- Collection of samples
- ELISA
- Immunofluorescence
- Blood pressure analysis
- Myograph
- Ultrasound data analysis
- Statistical analysis

Suellen Cristina Coelho\*:

- Design of experiments
- Technical setup for most of the experiments
- Collection of samples
- Blood pressure analysis
- Myograph
- RT-qPCR
- Ultrasound data analysis
- Renal function and damage determination and analysis
- ELISA
- Statistical analysis
- Draft and revision of the manuscript

Julio César Fraulob Aquino:

- Collection of samples (Partial)

- Myograph (Partial)

Ku-Geng Huo

- Collection of samples (Partial)
- Myograph (Partial)

Asia Rehman:

- Myograph (Partial)

Stean Offermanns:

- Provided the Tie2-CreER<sup>T2</sup> mice

Pierre Paradis

- Design of experiments
- Supervision of work and evaluation of raw data
- Correction of manuscript

Ernesto L. Schiffrin:

- Originated the study as PI of a CIHR grant
- Design of experiments
- Supervision of work and evaluation of raw data
- Correction of manuscript
- Funding of studies

*\*These authors contributed equally*

Second study - Induction of Human Endothelin-1 Overexpression for 3 Months Causes Blood Pressure Rise and Small Artery Endothelial Dysfunction and Stiffening

Suellen Cristina Coelho:

- Design of experiments
- Technical setup for most of the experiments
- Collection of samples
- ELISA
- Blood pressure analysis
- Myograph
- Immunostaining
- Ultrasound data analysis
- Renal function and damage determination and analysis
- Metabolic cage
- RT-qPCR
- Statistical analysis
- Draft and revision of the manuscript

Julio César Fraulob Aquino:

- Collection of samples
- Immunohistochemistry (Partial)
- Histology
- Myograph (Partial)

Olga Berillo

- RT-qPCR
- Immunohistochemistry (Partial)
- ELISA
- Metabolic cage (Partial)

Antoine Caillon

- Flow cytometry

Sofiane Ouerd:

- Myograph (Partial)

- Immunohistochemistry (Partial)

Tlili Barhoumi

- Immunohistochemistry (Partial)

Stean Offermanns:

- Provided the Tie2-CreER<sup>T2</sup> mice

Pierre Paradis

- Design of experiments
- Supervision of work and evaluation of raw data
- Correction of manuscript

Ernesto L. Schiffrin:

- Originated the study as PI of a CIHR grant
- Design of experiments
- Supervision of work and evaluation of raw data
- Correction of manuscript
- Funding of studies

## Acknowledgements

I would like to express my sincerest thanks to several people, who were there at every step of the way to help and support me through my PhD.

To my family, specially my lovely husband and parents, who have always been very supportive and encouraged me to follow my dreams.

To Dr. Ernesto L. Schiffrin for his mentorship and supportive supervision throughout my graduate studies.

To Dr. Pierre Paradis for his important scientific expertise and academic advice.

To all my colleagues in Dr. Schiffrin's laboratory for their help, friendship, and support along the way.

To Adriana Cristina Ene, Veronique Michaud, Guillem Collodel and Isabelle Miguel for their excellent technical support.

To the members of my thesis committees Dr. Julie Lavoie, Dr. Eric Thorin, Dr. Lorraine Chalifour and Dr. Kostas Pantopoulos for their helpful comments.

To Canadian Institutes of Health Research (CIHR) grants 37917 and 102606, CIHR First Pilot Foundation Grant 143348, a Canada Research Chair (CRC) on Hypertension and Vascular Research by the CRC Government of Canada/CIHR Program and by the Canada Fund for Innovation for supporting the studies in this thesis. To Science without Borders offered by the National Council for Scientific and Technological Development of Brazil for their financial support.

To the Division of Experimental Medicine, including Ms. Dominique Besso and Ms. Marylin Linhares for their help.

To Les Laboratoires Servier Company/Servier Medical Art for providing medical vector images that were used to construct the figures in this thesis. These medical vector images are available under the Creative Common licenses: CC-BY.

### **Statement of originality**

The research presented in this thesis constitutes original work and collaboration from co-authors that is described in the section of contribution of authors. The studies distinctly contribute to the understanding of the pathophysiological role of endothelin-1 in blood pressure regulation and vascular damage. Moreover, the findings should stimulate the development of novel endothelin-1 antagonists with fewer side effects, ameliorating the success rate to treat hypertension, especially in resistant hypertension.

I declare that I wrote the content of this thesis, which was reviewed by my supervisor.

## **CHAPTER I: Review of the Literature and Research Objectives**

## 1. Introduction

The cardiovascular system, composed of the heart and blood vessels (arteries, veins and capillaries), is a dual circulatory system consisting of the pulmonary circulation and the systemic circulation. The pulmonary circulation connects the heart to the lungs, and allows deoxygenated blood to pass through the alveoli for re-oxygenation. The systemic circulation then delivers oxygenated blood, as well as transports nutrients, hormones and other bioactive peptides to peripheral tissues through blood vessels. The rate at which blood flow delivers these components into the peripheral tissues is influenced by the arterial blood pressure (BP), which, in turn, is regulated by the cardiac output and the total peripheral resistance. Under physiological conditions, the arterial BP generated during systole of the heart, termed systolic BP (SBP), rises to around 120mm Hg. The normal pressure during diastole of the heart, called diastolic BP (DBP), falls to around 80mm Hg. When BP is persistently at or above 140/90mm Hg the pathological condition is referred to as hypertension (HTN).

HTN is a multifactorial disorder that can arise as a consequence of pathophysiological changes in the heart, blood vessels, kidneys and adrenal glands. Obesity, insulin resistance, high alcohol and salt intake, sedentary lifestyle, stress, dyslipidemia and genetic components are all important factors that contribute directly or indirectly to the development and progression of HTN. Increase in BP is generally asymptomatic and, if left untreated, long standing BP elevation becomes a major risk factor for cardiovascular morbidity and mortality, such as heart failure, stroke, coronary artery disease and renal disease.<sup>1-3</sup>

The most common type of HTN, which accounts for 95% of all the cases, is essential, primary or idiopathic HTN. As the name suggests, the etiology for this pathology is unknown.<sup>4</sup> Conversely, secondary HTN is a result of a pre-existing disease, such as renal or renovascular disease, pheochromocytoma, mineralocorticoid-, drug- or pregnancy-induced HTN, or rarely renin-producing tumor. The secondary forms of HTN are a rare condition which affects no more than 1-5% of cases.<sup>5</sup> Finally, resistant HTN is a condition in which BP remains persistently elevated despite treatment with at least three antihypertensive agents, of which one is a diuretic, all at optimal

doses.<sup>6</sup> The prevalence of resistant HTN is estimated to be between 15-30% of treated hypertensive patients. It is difficult to estimate accurately the degree of true resistant HTN because not all studies monitor the medication adherence or provide medication at no charge.<sup>7</sup>

Worldwide, HTN is highly prevalent in both economically developing countries and in developed economies.<sup>8</sup> Despite the availability of various classes of anti-hypertensive drugs, the prevalence of uncontrolled HTN has increased worldwide due to population growth and aging,<sup>9</sup> independently of gender.<sup>10</sup>

The pathophysiology of HTN is complex and not completely understood. Given that HTN is a major risk factor for cardiovascular disease (CVD) and BP is still poorly controlled in about 50% of patients, HTN remains an important issue for further research. Endothelin (ET)-1, a powerful vasoconstrictor, is known to be involved in the pathophysiology of HTN. Under physiological conditions, ET-1 can modulate the function of different tissues. In relation, more specifically to the cardiovascular system and the kidney, ET-1 is responsible in maintaining the vascular tone, mediating the positive inotropic effects and contributing to renal hemodynamics and natriuresis and diuresis.

To study the potential role of ET-1 in the pathophysiology of HTN, many studies have relied on animal models with genetic gain-or-loss function, different diets, and pharmacological and surgical manipulations. Although these animal models have provided information about the potential role of ET-1 in HTN, those studies have limitations as it is difficult to clearly identify the role that ET-1 plays in HTN by itself. This thesis aims to demonstrate the role of endothelial ET-1 in BP regulation, vascular and renal function in the absence of confounding factors using a novel transgenic mouse with tamoxifen-inducible endothelium-restricted human ET-1 (ieET-1) overexpression using Cre/loxP technology.

In this chapter, a brief introduction will be given about different isoforms of ET, with particular focus on ET-1 and its synthesis, expression and degradation. Then, the subtypes of ET-1 receptors (ETRs) will be described. Next, the role of ET-1 in the physiology and pathophysiology of blood vessels and the kidney will be detailed. Our current understanding of the pathophysiological role of ET-1 in the context of HTN will

be presented. The literature review will be followed by two recent studies, respectively chapters II and III, that demonstrate that ET-1 can participate in the development and maintenance of HTN. Finally, a general discussion will be provided in chapter IV about the role of ET-1 in BP regulation, vascular and renal damage and inflammation. The differences and similarities of ET-1 effects will be compared between the animal models of HTN from the literature and our recently developed ieET-1 mouse model.

## 2. Discovery of the endothelin family and sarafotoxin

A potent vasoconstrictor substance, later defined as ET, was first isolated from the media of cultured bovine aortic endothelial cells (EC) in 1985 by Hickey *et al.*<sup>11</sup> Isolated pig coronary artery rings in EC-conditioned culture media contracted in a concentration-dependent manner which, was not reversed by  $\alpha$ -adrenergic, cholinergic, serotonergic and histaminergic blockade. This study suggested that EC effects were mediated by activation of a novel receptor. A year later, Yanagisawa *et al.* isolated a novel bioactive peptide and identified its 21-amino acid structure.<sup>12</sup> In this same year, it was shown that sarafotoxin S6, a peptide present in the venom of the snake *Atractaspis engaddensis*, induced a rapid and marked coronary vasoconstriction that could lead to cardiac arrest.<sup>13</sup> More importantly, its amino acid sequence presented a high degree of homology with the newly described ET.

In 1989, Inoue *et al.* found three putative endothelin precursors in human, rat and porcine genomic DNA samples.<sup>14</sup> These genes translated into peptides similar to the newly described ET. These peptides presented a 21-amino acid structure with a hydrophobic C-terminus and two intramolecular disulfide bonds between Cys residues at the N-terminus. The findings of this study revealed the existence of three isoforms of ET: ET-1, ET-2 and ET-3. The ET-2 and ET-3 peptides differ from ET-1 by two and six chemically similar amino acid residues, respectively. ET-2 contains Trp<sup>6</sup> and Leu<sup>7</sup> whereas ET-3 contains Thr<sup>2</sup>, Phe<sup>4</sup>, Thr<sup>5</sup>, Tyr<sup>6</sup>, Lys<sup>7</sup> and Tyr<sup>14</sup>. The conserved position of the four Cys residues among the members of the ET family is thought to determine the structure of the peptide (Figure I-1).

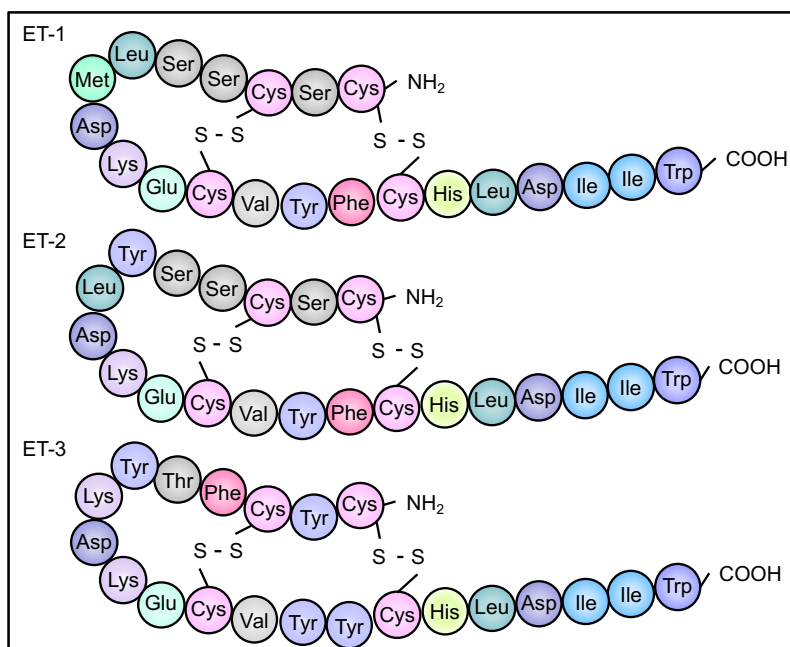


Figure I-1: The structure of ET-1, ET-2 and ET-3 peptides.

Despite the structural similarities, the contractile and pressor response of these peptides were shown to be different. In terms of molar potency, ET-1 was the most potent peptide, whereas the maximum contractile tensions were shown to be greatest for ET-2. ET-3 was the least potent, both with respect to sensitivity and maximal response. ET-1 and ET-2 produced a strong early pressor response, followed by a short duration depressor response, and a final long lasting pressor phase. These phases were not clear for ET-3, and the duration of the pressor response was shorter compared to ET-1 and ET-2.<sup>14</sup>

In 1989, Saida *et al.* described a new peptide of the ET family, ET-4, also known as vasoactive intestinal contractor (VIC).<sup>15</sup> This peptide was originally described to be expressed in the epidermal cells of the gut mucosa in rodents, and had a pressor activity similar to the ET family. The structure of VIC is analogous to human ET-2, however, differently from ET-2, VIC differs from ET-1 by the three amino acids Asn<sup>4</sup>, Trp<sup>6</sup> and Leu<sup>7</sup>.

All ET isoforms are detected in many tissues and organs, including the brain, the vasculature, lungs, kidneys and the heart.<sup>16, 17</sup> More specifically, ET-1 is produced mainly by EC, as well as by vascular smooth muscle cells (VSMCs), pulmonary and

renal epithelial cells, monocytes and macrophages, fibroblasts, cardiac myocytes, enteric glia cells, certain neurons and reactive glia cells in the central nervous system. ET-2 is expressed in the ovary and intestinal epithelial cells. ET-3 is found in endothelial cells, brain neurons, renal tubular and intestinal epithelial cells. Thus, the ET family plays complex roles in cardiovascular, neural, pulmonary, reproductive, and renal physiology. Among all the ET peptides, ET-1 is the most abundant isoform in the human cardiovascular system and has been shown to participate in CVD. This thesis will focus on the role of ET-1 in HTN and its effects on the vasculature and the kidney.

### **3. General biology of endothelin-1**

#### **3.1. Constitutive endothelin-1 regulation**

The ET-1 gene (*EDN1* in humans, *Edn1* in mice) is located on chromosome 6 and contains 9 exons in the human genome whereas it is situated on chromosome 13 and includes 5 exons in the mouse genome. Differential and tissue-specific production of ET-1 is tightly regulated transcriptionally by many binding sites and regulatory elements including activator protein (AP)-1,<sup>18</sup> GATA-2,<sup>19</sup> vascular endothelial growth factor (VEGF),<sup>20</sup> thrombin,<sup>21</sup> cytokines,<sup>22</sup> and other mediators.<sup>23</sup> Likewise, both physical and chemical stimuli contribute to changes in ET-1 gene expression levels in physiological and pathophysiological conditions. For example, under physiological conditions, shear stress, a force that acts on the surface of the endothelium due to blood flow velocity and plays an important role in vascular tone, changes EC shape and consequently down-regulates the transcription of ET-1 in bovine aortic EC.<sup>24</sup> Under pathological conditions, the transcriptional activation of hypoxia inducible factors (HIF) has been shown to enhance ET-1 expression in EC, which in turns leads to VEGF secretion that can promote tumor progression and metastasis.<sup>25</sup>

#### **3.2. Endothelin-1 synthesis**

Human ET-1 is generated from the 212-amino acid precursor peptide preproET-1.<sup>26</sup> This precursor contains an initial 17-amino acid sequence that functions as a signal peptide leading to its transport into the endoplasmic reticulum (ER). This short signal sequence is then removed to yield proET-1.<sup>27</sup> ProET-1 is cleaved at both C and N terminals by subtilisin-like pro-protein convertase (SPC) family enzymes. PC7 and furin belong to SPC family and are expressed in ECs. They act on proET-1 to produce a 38-amino acid intermediate peptide called big ET-1.<sup>28</sup> Similarly to ET-1, big ET-1 is able to increase BP and cause coronary constriction.<sup>29, 30</sup> It promotes as well diuresis and natriuresis in rats<sup>31</sup> and in humans.<sup>32</sup> Finally, big ET-1 is cleaved between positions Trp<sup>21</sup>-Val by a specific phosphoramidon-sensitive type II membrane-bound metalloprotease called ET-converting enzyme (ECE) to generate the bioactive form of ET-1 (Figure I-2).<sup>14</sup>

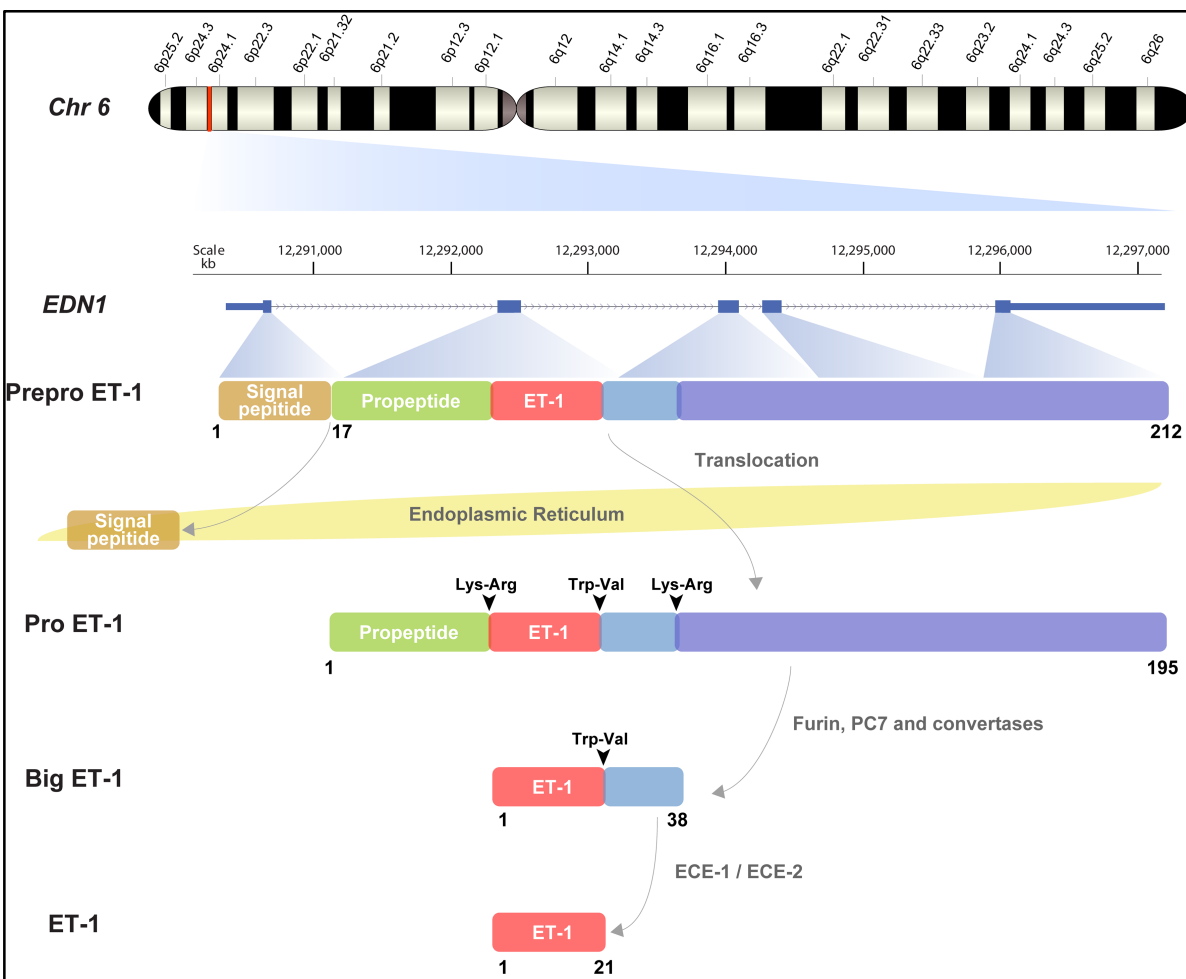


Figure I-2: Human ET-1 synthesis.

ECE is ubiquitously distributed within the cardiovascular system, adrenals, respiratory and central nervous systems.<sup>33</sup> In the vasculature, ECE is highly expressed in ECs but low or no expression has been observed in blood vessel VSMCs.<sup>34</sup> Two cDNA sequences for converting enzymes have been reported: ECE-1<sup>35</sup> and ECE-2.<sup>36</sup> These enzymes are structurally similar, and have a comparable selectivity to cleave big ET-1 into ET-1. Despite these similarities, ECE-1 seems to be the predominant enzyme.<sup>36</sup>

ECE-1 is localized in the Golgi membrane with its catalytic domain facing inside the Golgi and secretory vesicles. ECE-1 activity takes place in the cell probably during the transit of big ET-1 through the secretory pathway. Aside from ECE-1-mediated intracellular conversion of big-ET-1 to ET-1 in ET-producing cells, this enzyme can also convert exogenously provided big ET-1 into ET-1 on the cell surface of ET-1-target cells.<sup>35</sup> The ability of ECE-1 to convert intracellular and extracellular big ET-1 into ET-1 results from the existence of different isoforms (ECE-1a-d) and their localization.<sup>37, 38</sup> ECE-1a is found in intracellular vesicles and on the cell surface of ECs, ECE-1b is found in the trans-Golgi network, and ECE-1c and -1d are located on the extracellular side of the plasma membrane.

ECE-2 is a membrane protein and its C-terminal catalytic domain faces the lumen of the secretory vesicles where big ET-1 may be found. The differences between ECE enzymes are that ECE-2 is more sensitive to phosphoramidon than ECE-1 and its optimal pH for enzymatic activity is 5.5, whereas ECE-1 is enzymatically active at neutral pH.<sup>36</sup> Thus, while ECE-1 converts big ET-1 into ET-1 intracellularly in different parts of the cell, and extracellularly, ECE-2's activity takes place only intracellularly in the secretory vesicles where the optimal acidified pH range is available.

### **3.2.1. Endothelin-1 synthesis by non-ECE**

Big ET-1 can alternatively be cleaved between positions Tyr<sup>31</sup>-Gly<sup>32</sup> by the enzyme chymase to produce the 31-amino acid peptide ET-1 (1-31) (Figure I-3) in the lung,<sup>39</sup> heart<sup>40</sup> and vessels.<sup>30, 41</sup> Chymase is a chymotrypsin-like serine protease found mainly in degranulated mast cells under pathological conditions.<sup>39</sup> ET-1 (1-31) can either

promote its effects or be further converted into ET-1 by the enzyme neutral endopeptidase (NEP), and by ECE to a lesser extent.<sup>42</sup> It has been shown that contractile effects of ET-1 (1-31) are weaker compared to ET-1 in intact or endothelium-denuded porcine coronary arteries. However, its contractile activity was greater than that observed for big ET-1.<sup>30</sup> Although, ET-1 and ET-1 (1-31) present similar contractile effects on human coronary and mammary artery, it has been suggested that contraction in response to ET-1 (1-31) could possibly be due to its further cleavage to generate ET-1.<sup>40</sup> Besides ET-1 (1-31)-mediated contractility, this peptide is involved in VSMC proliferation<sup>43</sup> and inflammation.<sup>44</sup>

In addition to ECE, matrix metalloproteinase (MMP)-2, which is a serine protease that contributes to degrade the extracellular matrix (ECM) in the vasculature, can cleave big ET-1 at the Gly<sup>32</sup>-Leu<sup>33</sup> bond, generating a 32-amino acid peptide [ET-1 (1-32)]<sup>45</sup> (Figure I-3). Differently from ET-1 (1-31), ET-1 (1-32) is not likely to be cleaved into ET-1 due to the absence of the COOH-terminus structure necessary for recognition and cleavage by ECE-1. Nevertheless, ET-1 (1-32) induces a powerful contraction of rat mesenteric arteries<sup>45</sup> and rat thoracic aorta and vena cava.<sup>41</sup>

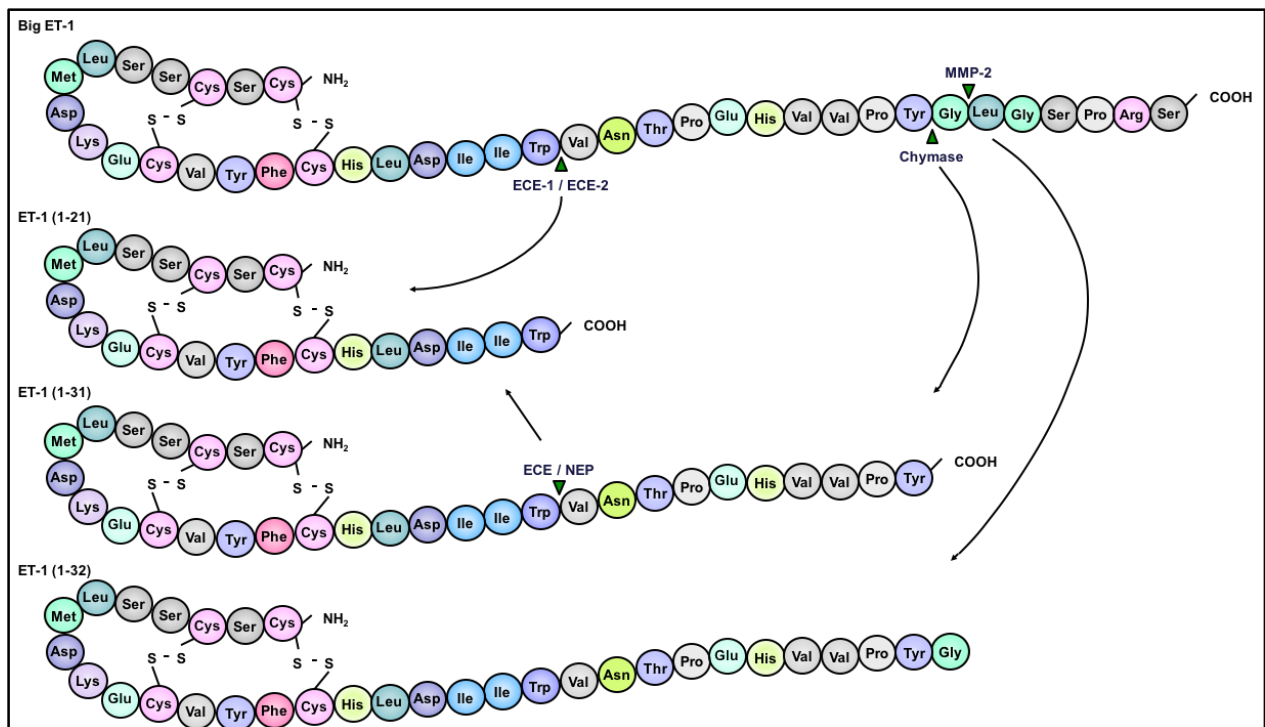
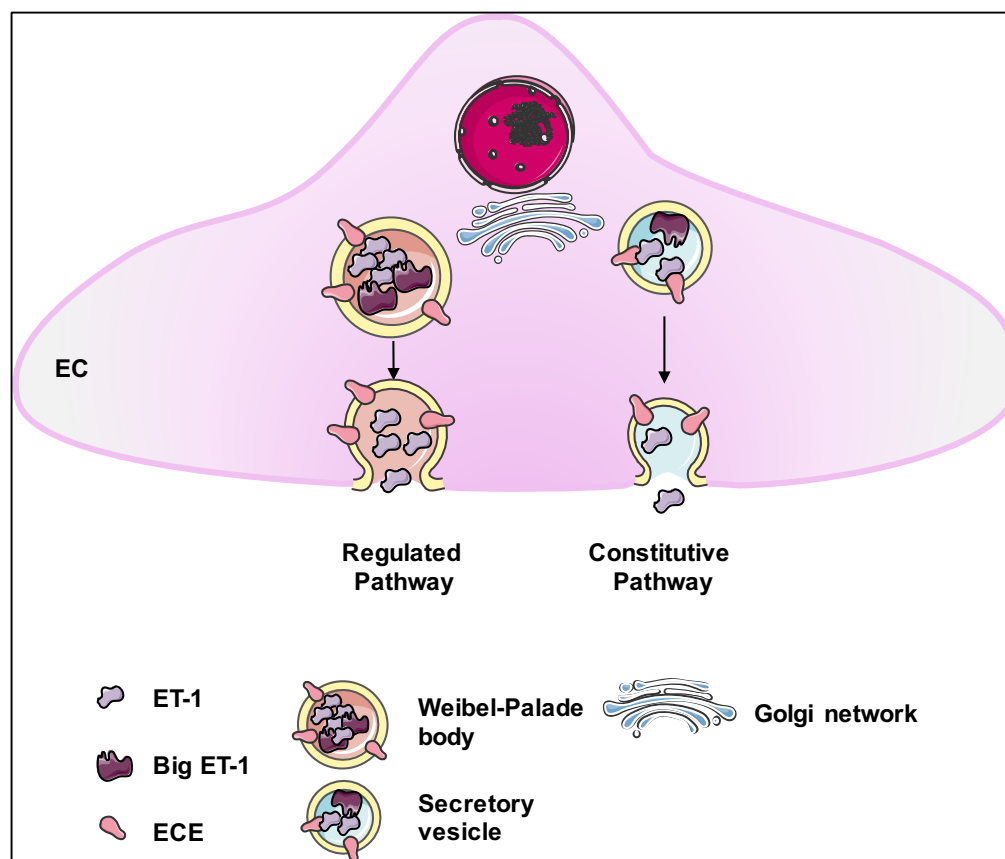


Figure I-3: Alternative human ET-1 synthesis.

### 3.3. Endothelin-1 storage and secretion

Beyond transcriptional regulation, ET-1 availability is also regulated through constitutive secretory and regulatory pathways. The constitutive secretory pathway employs secretory vesicles that continuously store and transport immature or mature proteins from the trans-Golgi network to the cell surface during physiological or pathophysiological conditions. Alternatively, proteins may also be secreted through a regulated pathway once they are sorted into endothelium-specific intracellular storage granules, also known as Weibel-Palade bodies (WPB). After stimuli, WPBs degranulate and mobilize to the cell surface (Figure I-4). These WPBs specifically store and release von Willebrand factor and P-selectin, among others vascular mediators.<sup>46</sup>

Figure I-4: ET-1 secretion into the cell surface. Adapted from Servier Medical Art.



Under normal conditions, ET-1 and its precursor have been detected in EC-derived secretory vesicles from bovine aortic cells.<sup>47</sup> ET-1 synthesis could take place in these vesicles since ECE is also present in these secretory vesicles from lung ECs.<sup>48</sup> In

chronic heart failure patients, high ET-like immunoreactivity has been observed in EC-specific coronary artery secretory vesicles as well as in WPB.<sup>49</sup> This strongly suggests that ET-1 transport and release can occur through both secretory and regulated pathways in the same cell type. In addition to ET-1, ECE-1 is present in high concentrations in EC abdominal aortic WPB from hypoxic rats. Increase in ET-1 and ECE-1 triggers degranulation and aggregation of WPBs on the EC plasma membrane.<sup>50</sup> Another study detected ECE-1a and b, and big ET-1, in WPB from EC-derived human umbilical vein. Cytosolic calcium influx stimulated the degranulation of these storage granules thereby releasing ET-1 into the media of the cultured cells. Hence, these findings indicate that the proteolytic conversion of big ET-1 to mature ET-1 by ECE-1a and b occurs in WPB.<sup>51</sup>

### 3.4. Endothelin receptors

In mammals, ET peptides mediate their actions only through activation of two subtypes of ETRs<sup>52</sup>, ET type A (ET<sub>A</sub>R)<sup>53</sup> and ET type B receptors (ET<sub>B</sub>R).<sup>54</sup> These receptors belong to the G protein-coupled seven transmembrane domain receptor (GPCR) family, and their sequence shares 59% similarity in humans.<sup>52</sup> The amino acid sequence of ET<sub>A</sub>R displays a high degree of conservation between species, e.g., human ET<sub>A</sub>R sequence has 93% and 92% homology with the rat and mouse sequence, respectively. ET<sub>B</sub>R presents a lesser degree of conservation between species, as human ET<sub>B</sub>R is 88% homologous to rat ET<sub>B</sub>R.<sup>16, 52</sup>

These receptors are widely distributed in tissues within the body.<sup>16</sup> ET<sub>A</sub>Rs are highly expressed in the heart and lung, whereas relatively low expression levels are found in the central nervous system (CNS). ET<sub>B</sub>Rs are predominantly expressed in CNS and lung. Among all tissues, the lungs have the highest density of ETRs. At the cellular level, vascular ET<sub>A</sub>Rs are highly expressed in VSMCs, whereas ET<sub>B</sub>Rs are expressed in the ECs and at lower levels in VSMCs. In the heart, ET<sub>A</sub>Rs are predominantly expressed in the cardiomyocytes, whereas both receptors are equally expressed on cardiac fibroblasts. In the lungs, ET<sub>B</sub>Rs are mainly present in the endothelium but also on airway SMCs. In the kidneys, both ETRs are expressed in glomeruli. ET<sub>B</sub>Rs are also

found in tubular epithelial cells. Consequently, the activation of ETRs promotes distinct cellular responses according to their tissue and cell location.

### 3.4.1. ETR signaling and internalization

The ET peptides bind to their receptors with different affinity. Ligand-displacement experiments have demonstrated that ET-1 and ET-2 peptides have similar affinity towards ET<sub>A</sub>R whereas ET-3 has less affinity to this receptor.<sup>53</sup> Conversely, all the three isotypes have equal affinity to ET<sub>B</sub>R.<sup>54</sup> ETR activation results in complex signaling cascades as these receptors are coupled with different members of G protein. Moreover, ETR responses vary according to the cell type and tissue location.<sup>55, 56</sup> The main focus of the following description of ETR signaling will be regarding the vasculature.

One of ET<sub>A</sub>R canonical signaling pathways is through activation of phospholipase C (PLC). PLC cleaves phosphatidylinositol 4,5 bisphosphate (PIP<sub>2</sub>) into inositol 1,4,5-triphosphate (IP<sub>3</sub>) and diacylglycerol (DAG) which, in turn, releases stored Ca<sup>2+</sup> from the ER into the cytosol<sup>54</sup> and activates protein kinase C (PKC).<sup>57</sup>

In the vasculature, intracellular SMC Ca<sup>2+</sup> binds to calmodulin to form a complex that will induce the activation of myosin light chain (MLC) kinase that phosphorylates MLC. Phosphorylated MLC enhances myosin-actin interactions resulting in VSMC contraction and consequent vasoconstriction. Activation of PKC stimulates the Ras/Raf/extracellular signal-regulated kinase (ERK) 1/2 cascade. PKC and the Ras/Raf/ERK 1/2 pathway phosphorylate diverse modulators of SMC contraction (Figure I-5).<sup>58</sup>

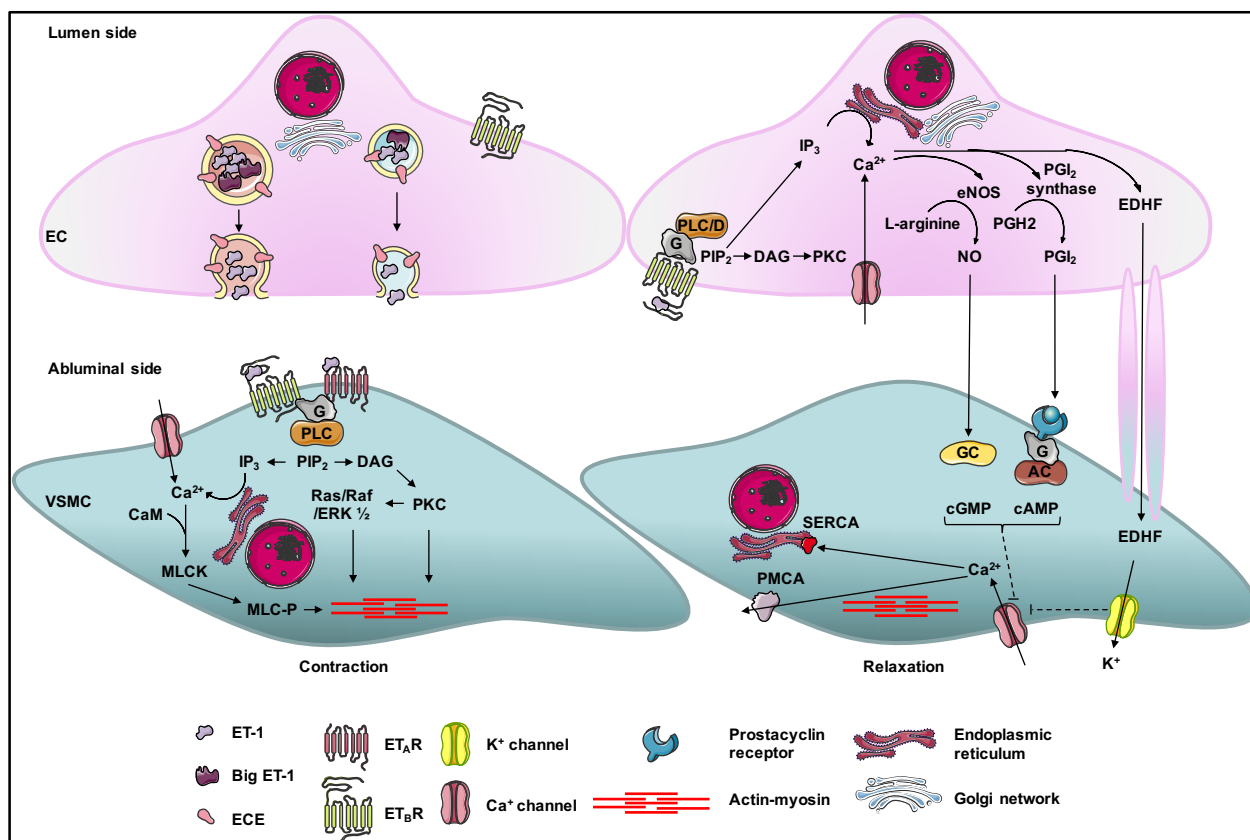


Figure I-5: ET-1 signaling pathway in the vasculature. Adapted from Mazzuca *et al.*<sup>59</sup> & Servier Medical Art.

ET<sub>A</sub>R can directly stimulate protein tyrosine kinases that activate protein kinase cascades involving mitogen-activated protein kinase (MAPK), ERK1/2, c-Jun N terminal kinase (JNK) and Janus kinase 2/signal transducer and activator of transcription (JAK2/STAT). Subsequently, this signaling pathway stimulates transcription factors that mediate cell growth, adhesion, and migration and intracellular matrix deposition in the vasculature and heart.<sup>60</sup>

Under normal conditions and depending on cell localization, ET<sub>B</sub>R activation may trigger opposite effects compared to ET<sub>A</sub>R activation. EC ET<sub>B</sub>Rs activate phosphatidylinositol 3 kinase (PI3K), which in turns recruits protein kinase B (PKB), also known as Akt. Protein Akt phosphorylates and activates endothelial nitric oxide synthase (eNOS) to enhance NO production.<sup>61</sup> Alternatively, EC ET<sub>B</sub>Rs induce NO production via PLC activation in a Ca<sup>2+</sup>-dependent manner<sup>59</sup> (Figure I-5). Briefly,

cytosolic  $\text{Ca}^{2+}$  binds to calmodulin. Subsequently, the  $\text{Ca}^{2+}$ -calmodulin complex binds to eNOS,<sup>62</sup> which then converts L-arginine into NO.<sup>63</sup> In the vasculature, NO diffuses from ECs into VSMCs to stimulate soluble guanylate cyclase (GC) to increase cyclic guanosine monophosphate (cGMP) formation. cGMP decreases VSMC intracellular  $\text{Ca}^{2+}$  by reducing  $\text{Ca}^{2+}$  entry through  $\text{Ca}^{2+}$  channels and by inducing  $\text{Ca}^{2+}$  removal via plasmalemmal (PMCA) and sarcoplasmic reticulum  $\text{Ca}^{2+}$ -ATPase (SERCA).<sup>59</sup> Ultimately, the decrease in cytoplasmic  $\text{Ca}^{2+}$  reduces the actin-myosin myofilament force sensitivity to  $\text{Ca}^{2+}$ , resulting in vascular relaxation. In addition to NO production,  $\text{ET}_B\text{R}$  activation leads the production of other endothelium-derived relaxing factors (EDRFs) such as prostacyclin ( $\text{PGI}_2$ )<sup>64</sup> and endothelium-derived hyperpolarizing factor (EDHF).<sup>65</sup>  $\text{ET}_B\text{Rs}$  mediate  $\text{PGI}_2$  synthesis through activation of the phospholipase D (PLD) pathway<sup>66</sup> and increases in intracellular  $\text{Ca}^{2+}$ . Intracellular  $\text{Ca}^{2+}$  binds to and activates phospholipase A2 (PLA2),<sup>67</sup> which in turn releases arachidonic acid (AA) from membrane-bound phospholipids. AA is converted to prostaglandin H2 (PGH2) by cyclooxygenase (COX)-2 and then it is further converted to  $\text{PGI}_2$  by prostacyclin synthase.  $\text{PGI}_2$  is a soluble lipid that diffuses from ECs to platelets or VSMCs to finally bind to its plasma membrane receptor. Activation of platelet prostacyclin receptor (IP) inhibits platelet aggregation, whereas activation of VSMC IP triggers the adenylate cyclase/cAMP/protein kinase A (PKA) signal transduction pathway, which induces vascular relaxation (Figure I-5).<sup>62, 68</sup>

The EDHF response is recognized as a transference of EC-originated hyperpolarization to VSMCs. The hyperpolarization on the SMC membrane leads to decrease in intracellular  $\text{Ca}^{2+}$  reducing vascular contraction.<sup>69</sup> ET-1-induced hyperpolarization effects have been observed in large arteries<sup>65</sup> and small mesenteric arteries.<sup>70</sup> The mechanism by which  $\text{ET}_B\text{Rs}$  activation induce endothelium-dependent hyperpolarization is unclear. Traditionally, ET-1-induced hyperpolarization effects have been attributed to a transient activation of  $\text{Ca}^{2+}$ -dependent  $\text{K}^+$  channels due to the increase in intracellular  $\text{Ca}^{2+}$  in the ECs. However, endothelial  $\text{Ca}^{2+}$ -dependent  $\text{K}^+$  channels do not participate on EDHF-mediated vascular relaxation responses upon activation of  $\text{ET}_B\text{Rs}$  in the rat carotid artery. Rather, voltage-dependent  $\text{K}^+$  channel

activation has been shown to cause the relaxation effects.<sup>65</sup> Furthermore, it has been shown that ET-1 does not promote direct hyperpolarization of VSMC.<sup>70</sup>

Following ETR stimulation, both receptors undergo internalization. Bremnes *et al.* have proposed an intracellular trafficking model for ETRs.<sup>71</sup> This process depends on the activation of GPCR kinases, arrestin, and dynamin/clathrin pathways. After internalization, ET<sub>A</sub>Rs and ET<sub>B</sub>Rs are directed to the sorting endosomes and then targeted to the recycling compartment to subsequently reappear on the plasma membrane or to go to lysosomes for degradation. Besides the varying ETR distribution within the organism, the different activated ETR signaling cascades and the distinct intracellular ETR trafficking may explain at least in part the different physiological responses mediated by these receptors.

### **3.4.2. ET receptor antagonists**

Current drugs that target ETRs are classified according to their receptor selectivity. ETR antagonists (ERA) can selectively block either ET<sub>A</sub>Rs and ET<sub>B</sub>Rs or both; sitazentan, ambrisentan, atrasentan, BQ-123, FR139317, zibotentan selectively block ET<sub>A</sub>Rs, BQ-788 and A192621 are selective ET<sub>B</sub>R antagonists and bosentan, macitentan, and tezosentan are dual antagonists.<sup>56, 72</sup>

ERAs have been extensively studied in clinical studies for treatment of several pathological conditions such as pulmonary arterial hypertension (PAH), essential HTN, heart failure, coronary artery disease, diabetic nephropathy and many others (ClinicalTrials.gov). Ambrisentan was approved by the Food and Drug Administration (FDA) in 2007 and by the European Medicines Authority (EMA) in 2008 for the treatment of PAH. Ambrisentan has good bioavailability, a long half-life and low hepatic toxicity. However, nasal congestion and peripheral edema are very common side effects of this drug.<sup>73</sup> Atrasentan is extensively used in preclinical studies. Although this drug is not yet approved by the FDA for clinical treatment, atrasentan has been shown to reduce albuminuria and improve BP and lipid profile in patients with type 2 diabetic nephropathy treated with renin-angiotensin system (RAS) inhibitors.<sup>74</sup> Zibotentan and sitaxentan are among the most ET<sub>A</sub>R selective peptides. These drugs are not approved

for clinical use as the former failed to improve survival of patients with prostate cancer in a Phase III trial<sup>75</sup> and the latter induced idiosyncratic hepatitis in patients with PAH.<sup>76</sup>

There are fewer ET<sub>B</sub>R antagonists due to the potential danger of blocking the beneficial actions mediated by this receptor such as vasodilation and ET internalization. The ET<sub>B</sub>R antagonists are mainly used in preclinical studies.

Bosentan was the first approved ERA for PAH treatment. Bosentan has good bioavailability and lower rate of fluid retention and edema compared to ET<sub>A</sub>R antagonists. However, this drug induces significant liver toxicity. Macitentan, also approved by the FDA for PAH treatment, was designed by changes in the molecular structure of bosentan to improve efficacy and tolerability. In comparison to bosentan, macitentan is more potent and has lower liver toxicity and induces less fluid retention. Moreover, macitentan enters the liver through passive diffusion. Therefore, there is no need to adjust the dose in patients with hepatic disease.<sup>16, 77</sup>

Apart from the ERA-related adverse side effects mentioned, ERAs also induce teratogenic effects during pregnancy, which lead to craniofacial and other organ malformations. Additionally, there are gastrointestinal side effects such as nausea, vomiting, and constipation. Combination of ERAs and angiotensin-converting enzyme (ACE) inhibitors may potentially induce hypotensive effects.<sup>56</sup>

### 3.5. Endothelin-1 degradation

ET-1 effects can be finely tuned at the degradation level. This process, which ultimately ends ET-1 effects, occurs at least in part by NEP enzymatic activity or ET<sub>B</sub>Rs-mediated clearance. NEP 24.11 hydrolysis activity occurs sequentially between the positions Ser<sup>5</sup>-Leu<sup>6</sup>, Asp<sup>18</sup>-Ile<sup>19</sup> and finally His<sup>16</sup>-Leu<sup>17</sup> of ET-1 molecule.<sup>78</sup> The role of NEP in ET-1 regulation was observed in several tissues and immune cells such as guinea pig trachea and human bronchi,<sup>79</sup> rat kidney<sup>80</sup> and in neutrophils from congestive heart failure patients.<sup>81</sup> Furthermore, ET-1 can also be metabolized by chymase and carboxypeptidase A, another type of NEP.<sup>82</sup> These proteases are secreted upon activation and degranulation of mast cells co-cultured with ECs. The authors have speculated that perhaps activated mast cells localized closely to ECs can regulate subendothelial ET-1 concentration in the vasculature.

Alternatively, ET-1 can be cleared from the body via ET<sub>B</sub>R. Following stimulation, the ET-1/ET<sub>B</sub>R complex is internalized and transported to the lysosome where the complex is degraded.<sup>71</sup> *In vivo* experiments indicate that circulating ET-1 clearance occurs in the lung, kidney and liver.<sup>83, 84</sup> In healthy subjects, exogenously infused ET-1 is also cleared from the circulation by lung, kidney and the splanchnic bed.<sup>85</sup> ET-1 clearance is impaired in EC-specific ET<sub>B</sub>R KO and ET<sub>B</sub> antagonist-treated mice,<sup>86</sup> further extending the evidence that ET<sub>B</sub>R mediate ET-1 clearance at the EC level.

#### **4. Physiological and pathophysiological effects of ET-1**

Under normal conditions, plasma ET-1 concentration is low and likely does not trigger a systemic effect. On the other hand, local tissue ET-1 concentrations are usually greater and hence are expected to have physiological significance. In CVD, such as chronic kidney disease (CKD), metabolic syndrome, heart failure and HTN, ET-1 expression and production is increased.<sup>87, 88</sup> In addition, plasma ET-1 concentrations are increased due to spillover of ET-1 into the circulation. Thus, systemic ET-1 effects may occur. In the next sections, the physiological and pathophysiological role of ET-1 in the vasculature and kidneys in the context of HTN will be described.

##### **4.1 ET-1 actions within the vasculature**

###### **4.1.1 Anatomy and function of the vessels**

The wall of blood vessels is composed of cells and matrix fibers organized in three layers: the intima (inner layer), the media and the adventitia (Figure I-6). The tunica intima consist of the endothelium, the basal lamina and internal elastic lamina.<sup>89</sup>

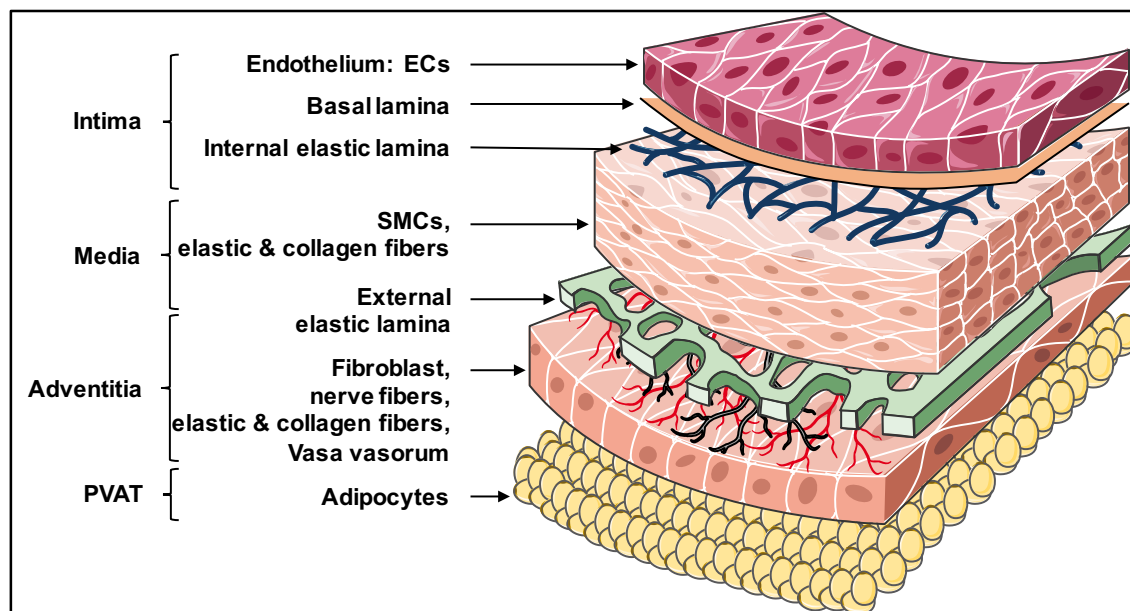


Figure I-6: Structure of a normal artery. Adapted from Servier Medical Art.

The endothelium has classically been described as a barrier between blood and the vessel wall. However, this monolayer is now known to be a dynamic organ that lies through the entire vascular system and could be considered the largest organ in the body. This layer composed of ECs controls vascular tone, platelet aggregation and thrombosis, inflammation in response to hormones, neurotransmitters and vasodilator agents.<sup>90, 91</sup> The shape of ECs is dictated by shear forces related to the blood flow. ECs are elongated polygonal cells and orientated in the direction of the blood flow when exposed to rapid, laminar and unidirectional shear stress. In contrast, ECs are less elongated and orientated when exposed to slow, complex and turbulent shear stress.<sup>91</sup> The following layer, the basal lamina, functions as a boundary between the endothelium and the underlying connective tissue. The outer layer of the tunica intima, the elastic lamina, contains a small amount of ECM, i.e. elastic and collagen fibers that provide, respectively, additional flexibility and strength to the vessel wall.<sup>89, 92</sup>

The media is the following tunica of the vessel wall. This layer is composed mainly of VSMCs, elastic and collagen fibers.<sup>89</sup> VSMCs control vascular diameter through vasoconstriction and vasodilation. Elastic and collagen fibers account for the passive mechanical properties of the vessels. Elastic fibers allow the vessels to expand and recoil in order to reduce the pulsatility of BP during ventricular contractions.<sup>92</sup> As the

pressure increases, collagen fibers are recruited and become circumferentially aligned to restrict distention and to provide support to the vascular wall.<sup>92, 93</sup> A large amount of collagen will prevent vascular rupture when vessels are exposed to high pressures. The largest arteries in the body, also known as elastic arteries or conduit arteries, have large amount of elastic and collagen fibers in the media. In contrast, the resistance arteries, which branch progressively starting from conduit arteries, contain the lowest amount of fibrous connective tissue in the media.<sup>89</sup> The media of resistance arteries consists mainly of SMCs that are highly innervated by sympathetic nerves, and elastic fibers. Thus, the resistance arteries regulate blood flow, through vascular constriction and dilation upon sympathetic activation,<sup>62</sup> and myogenic tone.

The outermost layer of the vessel wall that lies outside the external elastic lamina is the tunica adventitia that consists primarily of fibroblasts, which produce ECM such as collagen, elastin and fibronectin.<sup>89</sup> In the adventitia, collagen and elastin provide an additional structural support to the vessel wall. In addition to fibroblasts, the adventitia also contains terminal nerve fibers, resident macrophages, vascular progenitor cells and small blood vessels (also known as vasa vasorum).<sup>94</sup> The latter are small vessels that provide nourishment and oxygen to the adventitia and media. The adventitial layer was traditionally considered as a structural support for the vessels. However, recent studies have shown that adventitia is a source of reactive oxygen species (ROS), growth factors and vasoactive hormones. These components, under physiological conditions, maintain homeostatic balance in favor of normal wall thickness.<sup>94, 95</sup>

The distribution of collagen fibers within the three vascular wall layers depends on the region of the vascular tree. In a normal artery, collagen type I and III are the main elements of the intima, media and adventitia. Along with these collagens, collagen type IV and V are found in the ECs and SMCs basement membranes.<sup>96</sup>

Finally, beyond the outer limits of the adventitia we can find perivascular adipose tissue (PVAT). The amount and type (white, brown and beige) of PVAT varies according to vessel location and caliber. In rodents, the thoracic aorta is surrounded by brown PVAT whereas small arteries, such as mesenteric arteries, are surrounded by white PVAT.<sup>97</sup> PVAT has been traditionally considered a mechanical support for the vasculature and a site of lipid deposition for storage. However, the PVAT can also

modulate vascular function, thermoregulation, and VSMC proliferation and migration through secretion of pro-inflammatory and anti-inflammatory adipokines, chemokines, vasoactive substances, and gaseous molecules.<sup>98</sup> These mediators act in autocrine fashion on adipocytes, which are the main cell population in the PVAT, or paracrine fashion to stimulate or to inhibit the neighboring vascular cells such as fibroblasts, SMCs, ECs, as well as immune cells including T and B cells, macrophages and dendritic cells.<sup>97, 99</sup> The PVAT has important anticontractile effects that are mediated through endothelium-dependent and -independent mechanisms. The former mechanism is mediated by the PVAT-induced endothelial NO release and the latter mechanism involves the generation of hydrogen peroxide (H<sub>2</sub>O<sub>2</sub>).<sup>100</sup> An additional mechanism mediating the anticontractile actions of the PVAT is adiponectin. A decrease in PVAT-derived anticontractile effects has been associated with endothelial dysfunction in New Zealand obese mice, a model of human metabolic syndrome.<sup>101</sup> The possible mechanism for this observation is that reduction of adiponectin production by adipocytes contributes to an inflammatory milieu and ROS generation. Abnormalities in adiponectin-mediated anticontractile properties of PVAT have also been described in subcutaneous adipose tissue of obese subjects with metabolic syndrome.<sup>102</sup>

#### **4.1.2 Physiological effects of ET-1 on the vasculature**

Under basal conditions, EC-synthesized ET-1 is secreted in a polarized manner into the abluminal compartment of the vessel. Small amounts of ET-1 can spill over into the circulation, leading to ET concentration changes in blood.<sup>103</sup> In the vascular abluminal compartment, ET-1 functions as an autocrine and paracrine regulator by activating, respectively, the EC ET<sub>B</sub>Rs to stimulate the production of EDRFs to promote vasodilation and the underlying VSMC ET<sub>A</sub>Rs and ET<sub>B</sub>Rs to promote vasoconstriction.<sup>104, 105</sup> Infusion of ET-1 into the brachial artery of healthy subjects causes peripheral vasoconstriction whereas blockade of ET-1 effects by BQ-123 and inhibition of ET-1 synthesis by phosphoramidon induces forearm vasodilation.<sup>106</sup> Systemic administration of a non-selective ETR antagonist in healthy humans induced hypotensive effects and blocked forearm vasoconstriction effects after infusion of ET-1 in the brachial artery.<sup>107</sup> On the other hand, ET-1 gene KO mice present slightly

elevated BP.<sup>108</sup> Together, these studies indicate that the ET-1 system plays a role in the maintenance of vascular tone and BP.

#### **4.1.2.1 ET-1 effects on vascular tone**

ET-1 induces production of EDRFs, such as NO, PGI<sub>2</sub> and EDHF to modulate vascular tone. The mechanisms whereby ET-1 stimulates the secretion of these agents was described in the section 3.4.1. of this thesis. Among the EDRFs, NO is the major contributor to ET-1-induced vasodilation effects. ET<sub>A</sub>R blocker-induced vasodilation is reduced by 95% following inhibition of NO synthesis in healthy human resistance arteries.<sup>109</sup> Aside from its potent vasodilating effects that counteract ET-1-mediated vasoconstriction, NO reduces ET-1 effects through other mechanisms. NO interferes with ET-1-mediated vasoconstriction effects in VSMCs by accelerating the rate of intracellular Ca<sup>2+</sup> recovery, and by dissociating biotinylated ET-1 from ET<sub>A</sub>R in a cGMP-independent manner.<sup>110</sup> In addition, NO inhibits ET-1 formation via a cGMP-dependent pathway.<sup>111</sup> Thrombin-induced ET-1 secretion is potentiated when concomitantly secreted NO is inhibited by N<sup>G</sup>-nitro-L-arginine methyl ester (L-NAME), and when NO effects are prevented by an inhibitor of cGMP, methylene blue. These observations were further corroborated when ET-1 secretion was decreased by an NO donor, 3-morpholino-sydnnonimine HCl (SIN)-1, or by exposure to superoxide dismutase (SOD) in intact blood vessels. The modulation of ET-1 effects by NO seems to be more pronounced in arteries compared to veins.<sup>112</sup> The effects of NO in the vasculature are not limited to the maintenance of vascular tone; they can also inhibit platelet aggregation,<sup>113</sup> and smooth muscle proliferation.<sup>114</sup> Hence, NO and ET-1 have a complex intertwined relationship, as they counterbalance each other's vascular effects through different mechanisms.

#### **4.1.3 Pathophysiological effects of ET-1 in the vasculature**

Several studies have shown an increase in expression and circulating levels of ET-1 in humans with CVD. The expression levels of *EDN1* in small arteries from gluteal subcutaneous tissue were enhanced in patients with moderate-to-severe HTN.<sup>115</sup>

Plasma ET-1 levels were shown to be elevated in black and white hypertensive males and females compared to normotensive individuals. Plasma ET-1 levels were even higher in black than white hypertensive patients regardless of gender.<sup>116</sup> Additionally, circulating ET-1 levels were elevated in patients with essential HTN, which were even greater in patients with advanced more severe stages of HTN.<sup>117</sup> Similarly, circulating ET-1 levels were high in hypertensive patients with or without chronic renal failure undergoing or not dialysis.<sup>118</sup> Patients with acute myocardial infarction (AMI), with pulmonary edema, and with cardiogenic shock also presented increased levels of plasma ET-1.<sup>119, 120</sup>

These findings are not limited to humans, as plasma and expression levels of ET-1 are also increased in the blood vessels of different animal models of HTN such as deoxycorticosterone acetate (DOCA)-salt rat,<sup>121</sup> stroke-prone spontaneously hypertensive rats (SHR),<sup>122</sup> DOCA/salt-treated SHR,<sup>123</sup> Dahl salt-sensitive rats,<sup>124, 125</sup> one kidney, one clip Goldblatt rats,<sup>126</sup> and constitutive endothelium-restricted human ET-1 overexpressing (eET-1) mice.<sup>127, 128</sup> Although ET-1 plays an important role in the progression of HTN in these animal models, ET-1 seems to not be associated with HTN in SHR<sup>129</sup> and two-kidney, one clip hypertensive rats,<sup>126</sup> or to significantly raise BP in eET-1 mice.<sup>127</sup>

The increase in circulating ET-1 and its expression levels in the vasculature result in a number of cardiovascular consequences. In addition to BP elevation, the main consequence from ET-1 effects on vessels are endothelial dysfunction, vascular remodeling and stiffening, VSMC growth and proliferation and inflammation. These vascular changes will be addressed below.

#### **4.1.3.1 Endothelial dysfunction**

Endothelial dysfunction is a proinflammatory and prothrombotic state of the endothelium associated with impaired endothelium-dependent relaxation response to vasodilators.<sup>130</sup> Endothelial dysfunction is implicated with the progression of vascular diseases and is a common finding in HTN associated with enhanced expression and concentrations of ET-1. To investigate the effects of EC-derived ET-1 in the vasculature, two groups have generated distinct constitutive endothelium-specific ET-1 overexpressing transgenic

mouse models.<sup>127, 128</sup> In these studies, the authors have used tyrosine kinase (Tie)-1 and Tie-2 promoters to drive the expression of the respective mouse and human ET-1 genes specifically into ECs of these mice. The Tie-1 promoter drives the expression of ET-1 gene strictly to ECs from small vessels<sup>131</sup> whereas the Tie-2 promoter does it in ECs in the whole vasculature.<sup>132</sup> Under Tie-1 control, ET-1 overexpression induced MA and aortic endothelial dysfunction and increased BP in eET-1 mice.<sup>128</sup> Using the Tie-2 promoter, ET-1 overexpression induced endothelial dysfunction in resistance arteries with no significant change in BP in eET-1 mice, although systolic BP tracked 10 mm Hg above that of controls.<sup>127</sup> Under high-salt intake, eET-1 mice presented endothelial dysfunction in MA and increase in BP, which was prevented by ET<sub>A</sub>R and non-selective antagonists.<sup>133</sup>

The impaired relaxation response results from an imbalance of vasodilators and vasoconstrictors. The overproduction of ET-1 shifts the balance towards vasoconstriction. Moreover, the bioavailability of NO in the vasculature is reduced. One of the mechanisms whereby ET-1 reduces NO bioavailability is by decreasing the expression and activity of eNOS. Indeed, the expression level of eNOS has shown to be decreased in type-1 diabetic eET-1 mice with exacerbated endothelial dysfunction due to enhanced ROS formation.<sup>134</sup> In an animal model of rebound pulmonary HTN, reduction of NOS activity associated with inhaled NO therapy was prevented by ET<sub>A</sub>R antagonism.<sup>135</sup>

Alternatively, ET-1-induced ROS such as superoxide ( $O_2^-$ ) can reduce NO bioavailability by scavenging NO to form peroxynitrate ( $ONOO^-$ ). ROS are oxygen-derived by-products of activation of redox signaling pathways. NAD(P)H oxidase is the main source of ROS in the vasculature, and enzymatically transfers electrons from NAD(P)H to molecular oxygen to produce  $O_2^-$  anions.  $O_2^-$  can be further reduced to  $H_2O_2$  by superoxide dismutase (SOD).<sup>136</sup> Aside from decreasing NO bioavailability, excess ROS production may overwhelm the anti-oxidant defense mechanism resulting in oxidative stress. As a result, oxidative stress contributes to the development of HTN and end-organ damage by stimulating inflammation.

ET-1 increases vascular oxidative stress.<sup>134, 137-140</sup> In these studies, increased vascular ROS formation by ET-1 infusion was reduced by treatment with either a

superoxide scavenger (tempol, a superoxide dismutase mimetic) or a NAD(P)H oxidase inhibitor (apocynin, which may also function as an antioxidant).<sup>138, 139</sup> Likewise, enhanced arterial ROS production has been shown to be suppressed by ET<sub>A</sub>R blockade.<sup>140</sup>

The mechanisms whereby ET-1 activates ROS-generating systems are still debated. The enzymatic sources of ET-derived ROS include perhaps the mitochondrial respiratory chain enzymes.<sup>137</sup> Other studies have shown that ET-1 stimulates ROS formation through activation of NAD(P)H oxidase in human ECs,<sup>141</sup> and in carotid arteries of normotensive and DOCA-salt hypertensive rats.<sup>140</sup> The latter study showed that NAD(P)H oxidase activation was ET<sub>A</sub>R-dependent. Independently of the mechanism whereby ET-1 stimulates ROS production, it is clear that ET-1-induced ROS formation contributes to endothelial dysfunction in several experimental models of HTN. Indeed, ET-1 overexpression increased NAD(P)H oxidase activity in both mesenteric arteries and aortic vessels from eET-1 mice. This effect was associated with a decrease in endothelium-dependent relaxation response in mesenteric arteries, which was restored when vessels were pretreated with vitamin C, an antioxidant, or apocynin.<sup>127</sup> Additionally, NAD(P)H oxidase activity was enhanced when eET-1 mice were treated with a high-salt diet. This effect was accompanied by endothelial dysfunction and BP elevation. Increases in NAD(P)H oxidase activity, endothelial dysfunction and the BP elevation were normalized by ET<sub>A</sub>R and non-selective ETR antagonists.<sup>133</sup> The participation of ET-1-induced ROS in BP elevation remains unclear, as ET-1-induced BP elevation was abrogated when Sprague-Dawley rats were treated with tempol,<sup>138</sup> yet was unaffected when the rats were also fed with a high-salt diet.<sup>139</sup>

The process that induces endothelial dysfunction is not limited to ECs. The PVAT can also contribute to endothelial dysfunction by increasing PVAT-derived ROS formation and pro-inflammatory cytokines.<sup>142</sup> In addition, the imbalance between ET-1 and NO bioavailability might also occur at the PVAT level.<sup>143</sup> Removal of PVAT from small arteries attenuates NO release. Interestingly, treatment with an ET<sub>A</sub>R antagonist resulted in greater vasodilation and reduction of the inhibitory effect by L-NAME. During pathological states such as in obesity, the expression levels of vascular ET-1 and ET<sub>A</sub>R and the ET-1-mediated contractile effects are increased. Moreover, NAD(P)H oxidase-

derived ROS triggers eNOS uncoupling phenomenon that switches eNOS activity from an NO producing enzyme to a ROS-generating enzyme.<sup>143</sup> Similarly, endothelial ET-1 overexpression has been shown to exacerbate ROS formation in the periaortic fat in eET-1 mice crossed with atherosclerosis-prone mice and fed a high-fat diet.<sup>144</sup> Although, PVAT participates in the process of ROS generation and endothelial dysfunction, the significance of its participation in the progress of CVD is still unclear.

#### **4.1.3.2 Vascular remodeling and stiffening**

The increase in BP mediated by different vasoactive factors, such as ET-1, angiotensin (Ang) II and aldosterone, alters the function, the structure and the mechanical properties of the vasculature. These changes are elicited in part by vascular constriction and reduction in the lumen diameter, which according to Poiseuille's law, leads to an increase in vascular resistance to blood flow.<sup>145</sup> Resistance arteries and arterioles modulate about 70-90% of vascular resistance whereas, conduit arteries contribute only 10-30%.<sup>146</sup> The increase in peripheral vascular resistance is an important factor in the development of HTN, and contributes to the higher risk of cardiovascular events.<sup>147</sup> Changes in vascular function were addressed in the section above. Alterations in the structure of blood vessels and their properties such as vascular remodeling and stiffening are addressed below.

Vascular remodeling may be initially an adaptive response of the wall tension to BP elevation. However, it may become a maladaptive response over time. The vascular remodeling process entails several mechanisms, including cell growth and/or apoptosis, vascular fibrosis, low-grade inflammation, as well as changes in the interaction between anchoring proteins and ECM components. All these processes dynamically influence the degree and type of remodeling.

Vascular fibrosis is the deposition of structural proteins (e.g. collagen) and/or adhesive proteins (e.g. fibronectin) in the vascular wall. The deposition of these ECM components occurs through excessive biosynthesis of these proteins and/or as result of a decrease in their degradation by MMPs.<sup>148</sup> Collagen biosynthesis and deposition were increased in several vascular beds of DOCA-salt hypertensive rats and SHR,<sup>149</sup> effects that were reduced by antihypertensive treatment. In addition, mRNA expression levels

of fibronectin, collagen types I, III and IV, and laminin were increased in mesenteric arteries and in aorta of stroke-prone SHR.<sup>150</sup> Likewise, the collagen-elastin ratio was significantly greater in subcutaneous small arteries of hypertensive subjects.<sup>151</sup> MMP activity is regulated by tissue inhibitors of metalloproteinase (TIMP). A decrease in MMP activity contributes to enhanced ECM deposition that in turn participates in vascular remodeling in CVD.<sup>152</sup> Serum concentrations of MMP-1 were decreased whereas TIMP was increased in patients with essential HTN, contributing to a decrease in collagen type I degradation.<sup>153</sup> Another study using internal mammary artery has shown that MMP-1, MMP-2, MMP-9 and MMP inducer activity were downregulated in hypertensive subjects.<sup>154</sup> The decrease in MMPs and MMP inducer activity was associated with an increase in collagen deposition. Interestingly, TIMP levels were unaffected. In addition to MMP-induced vascular ECM accumulation, activated MMPs can create a proinflammatory environment by activating transforming growth factor (TGF)- $\beta$ 1, monocyte chemoattractant protein-1 (MCP-1), and pro ET-1.<sup>154-156</sup> Overall, imbalance between of MMPs and TIMPs, and activation of proinflammatory signaling and generation of proinflammatory factors leads to conditions prone to vascular remodeling and stiffening. ET-1 mediates early vascular changes by activating MMP-2 and MMP-9 expression and activity via ET<sub>A</sub>R activation independently of changes in BP.<sup>157</sup> Other studies have shown that blockade of the ET-1 system can exert beneficial effects on vascular remodeling, fibrosis and oxidative stress processes. ET<sub>A</sub>R blockade reduced collagen and fibronectin deposition, intracellular adhesion molecule (ICAM)-1 content, oxidative stress, and normalized vascular remodeling in blood vessels of Sprague-Dawley rats infused with aldosterone under a normal<sup>158</sup> or a salt-rich diet.<sup>159</sup> Non selective ETR antagonist prevented diabetes-associated vascular remodeling by decreasing MMP-2 activity, and reducing medial thickening in resistance vessels.<sup>160</sup> In another study, bosentan prevented intermittent hypoxia-induced vascular inflammatory remodeling. This effect seems to be mediated through HIF-1-dependent activation.<sup>161</sup>

During the vascular remodeling process, changes in vascular mechanical properties may also affect vascular stiffness due to changes in the collagen and elastin ratio. The stiffness of the wall is characterized by the distensibility and the compliance of the vessel to buffer changes in pressure.<sup>162</sup> During normal conditions, the contraction of

the heart generates a forward pressure wave that travels through the aorta to small vessels at relatively low pulse wave velocity (PWV). During distal propagation of the forward wave, it encounters regions of impedance mismatch that produces a wave reflection. The reflected waves from the arterial system form a backward-traveling reflected wave returning to the aorta in late systole and early diastole. The reflected wave raises diastolic BP and favours diastolic perfusion pressure of the coronary circulation, and as well dampens the pulsatile energy transmitted into the small vessels. When the aorta becomes stiffer, the PWV increases. Consequently, the reflected wave returns in early systole and increases the central pulse pressure. The former increases systolic pressure and afterload of the heart, while the diastolic pressure is reduced, which hinders coronary perfusion. At the same time, the impedance mismatch is reduced, which results in increased pulsatility being transmitted distally to a greater extent. Accordingly, pulsatile hemodynamic stress is enhanced in organs that are directly exposed to central pulse pressure, such as the heart, the brain and the kidney.<sup>163</sup> During stiffening of large- and medium-sized arteries, pulsatile energy is enhanced and transmitted deeper into the small vessels.<sup>162</sup> As a result, these effects promote changes in the function and structure of the microvasculature, contributing to end-organ damage.<sup>164</sup>

In HTN, both large vessels and resistance arteries exhibit vascular remodeling and stiffening. The type of remodeling and the time at which remodeling occurs are different between these arteries (Figure I-7)

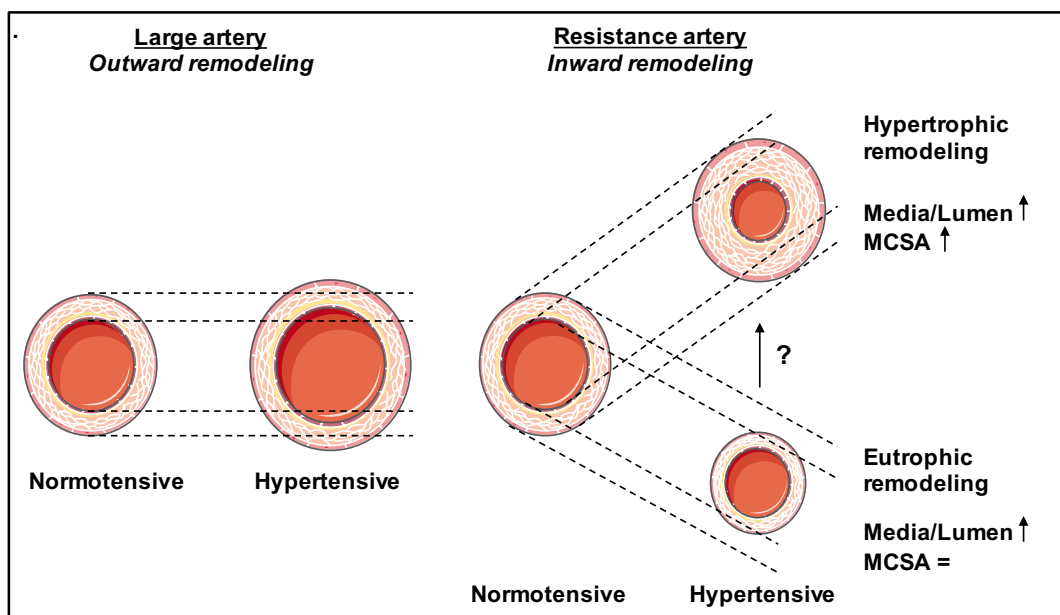


Figure I-7: Large and small artery remodeling during HTN. Adapted from Integan *et al.* and Schiffrin *et al.*<sup>145, 162</sup> & Servier Medical Art.

#### 4.1.3.2.1 Outward hypertrophic remodeling

Large arteries, such as aorta, undergo outward hypertrophic remodeling and stiffening with age. This process is accelerated in HTN.<sup>165</sup> Outward hypertrophic remodeling is characterized by an increase in lumen diameter and in media cross-sectional area (Figure I-7). VSMCs become hypertrophic (increase in size)<sup>166, 167</sup> and apoptosis of VSMC may occur to counterbalance or modify media growth.<sup>168, 169</sup> Additionally, alteration in the ECM, such as elastic fiber duplication and fragmentation,<sup>170</sup> and increase in collagen type I and III deposition and fibronectin,<sup>166, 171</sup> contribute to arterial stiffening. Along with changes in vascular components and geometry of the vessel, vascular distensibility and compliance are compromised.<sup>162</sup> As a result, stiffer vessels present less buffering ability to accommodate changes in BP.

#### 4.1.3.2.2 Inward eutrophic and hypertrophic remodeling

Remodeling of small arteries is one of the first manifestations of end-organ damage. Remodeling may precede endothelial dysfunction and left ventricular hypertrophy in mild hypertensive patients.<sup>172</sup> Resistance arteries present two types of vascular

remodeling: eutrophic and hypertrophic remodeling (Figure I-7). In eutrophic remodeling, the blood vessel diameter and lumen are decreased and the cross-sectional area of the media is unaltered.<sup>170</sup> Because lumen is reduced, the ratio between media thickness and lumen diameter is increased. The mechanism leading to eutrophic remodeling is still unclear, however some hypotheses have been proposed to explain it. One of the hypothesis involves a combination of inward vascular cell growth, which decreases the lumen diameter, and activation of an apoptotic process in the outer periphery of the vessel that could result in a reduction of the external diameter of the blood vessel.<sup>162</sup> Another hypothesis suggests changes in the interaction between ECM components and integrins, which are cell-matrix attachment sites localized on SMCs.<sup>173</sup> ECM components activate integrins to regulate cytoskeletal organization and motility, as well as cell growth and VSMCs contraction. During remodeling, the integrin profile is abnormal and collagen expression is high in SHR mesenteric arteries.<sup>174</sup> Thus, the interaction between SMCs and matrix proteins can quantitatively and topographically be shifted resulting in a rearrangement of SMCs and restructuring of the vascular wall.<sup>162</sup>

Eutrophic remodeling has been often described in animal models with an activated renin-angiotensin system,<sup>170</sup> such as SHR<sup>175</sup> and Ang II-infused rats.<sup>176</sup> Likewise, eutrophic remodeling has been described in essential and mild hypertensive patients,<sup>177, 178</sup> and this was corrected by the Ang II antagonist, losartan.<sup>179</sup> Long-standing HTN may modify the remodeling process. As HTN progresses, young SHR vessels, which initially presented eutrophic remodeling, change to hypertrophic remodeling in adult age, due to increase in medial cross-sectional area (MCSA).<sup>175</sup> This change is perhaps a result of more SMC proliferation than apoptosis. In addition to SMC proliferation, media growth can be a consequence of SMC hypertrophy<sup>180, 181</sup> and/or hyperplasia<sup>182</sup> which thickens the vessel in inward fashion encroaching on the lumen (Figure I-7). Thus, inward hypertrophic remodeling is also associated with an increase in media-lumen ratio. Hypertrophic remodeling is highly associated with severe HTN in which the ET system is activated such as DOCA-salt hypertensive rats,<sup>183</sup> SHR,<sup>123</sup> one-kidney renovascular hypertensive rats,<sup>184</sup> and eET-1 mice.<sup>127</sup> Likewise, hypertrophic remodeling has been observed in secondary HTN in humans.<sup>185</sup> Blockade of ET system regresses hypertrophic remodeling to different levels in some animal models of HTN.

ET<sub>A</sub>R blocker normalized hypertrophic remodeling in the mesenteric arteries of Dahl rats under high-salt diet<sup>125</sup> and in aldosterone-induced HTN.<sup>158</sup> A nonselective ET antagonist attenuated vascular hypertrophy and remodeling in mesenteric resistance arteries of DOCA-salt hypertensive rats.<sup>129</sup> In contrast, nonselective ET antagonist did not regress hypertrophic remodeling in renovascular hypertensive rats despite elevation of ET-1 gene expression level in the vessels.<sup>186</sup>

It has been speculated that ET-1 participates in vascular hypertrophy due to its growth-promoting properties.<sup>187</sup> ET-1 induced cell proliferation<sup>188</sup> and mitogenic effects<sup>189</sup> on VSMC, and as well increased protein synthesis in aortic VSMCs.<sup>190</sup> ET-1 can also induce VSMC proliferation by stimulating the expression and secretion of VEGF.<sup>20</sup> This growth factor is involved in angiogenesis and proliferation, migration and permeability of vascular ECs and SMCs. VEGF is produced by several cell types such as SMCs and macrophages and its production is stimulated by other factors as well as by ET-1, including growth factors, cytokines and hypoxia.<sup>191</sup>

#### **4.1.3.3 Vascular immune response**

Traditionally, inflammation has been recognized as a biological response whereby the immune cells are activated by pathogens, damaged cells, or tumor antigens to eliminate these harmful stimuli, as well as to clear out the damaged tissues and necrotic cells and promote repair. It is increasingly becoming clear that hypertensive stimuli, such as ET-1, Ang II, aldosterone, salt and genetic mutations can also trigger immune cell activation and response. These hypertensive stimuli initiate a subtle BP elevation leading to vascular injury that in turn may increase and/or modify the chemical composition and structure of proteins. These altered proteins will be recognized as non “self” protein, also known as neo-antigens or damage-associated molecular patterns (DAMPs).<sup>192, 193</sup> These components can then activate the immune response. Both innate and subsequent adaptive immune system responses are important contributors to the development and progression of HTN and vascular damage. Indeed, intravenous injection of splenic cells from DOCA-salt and renal hypertensive rats induce HTN in normotensive rats.<sup>194</sup> These recipient rats also presented with remodeling of renal and coronary arteries and infiltration of mononuclear cells in the vascular wall. Chronic

partial renal infarction did not induce renal degeneration and cell infiltration in the intrarenal arteries of nude mice, which present a genetic aplasia of the thymus. Moreover, the course of BP elevation in nude mice was lower compared with wild type mice.<sup>195</sup> Aside from activation and infiltration by immune cells associated with vascular inflammation, the increase in expression levels of chemokines and adhesion molecules, and the release of cytokines appear to be enhanced in HTN.<sup>196</sup>

In the next sections a brief overview of innate and adaptive immune systems will be described and their participation in the context of HTN will be addressed.

#### **4.1.3.3.1 Immune response**

##### **4.1.3.3.1.1 Innate immune response**

The first line of defense against pathogens is the innate immune system, since it takes a few days to the initial adaptive immune response to take place. This system is also characterized as a rapid and non-specific response to a variety but limited type of pathogens. The important components of innate immunity are: epithelial cells, which prevent pathogen entry; antigen-presenting cells (APCs) such as dendritic cells (DCs) and macrophages, neutrophils, mast cells; eosinophils, basophils, natural killer (NK) cells; and the complement system. Depending on the molecular nature of the antigens, different pattern recognition receptors (PRRs) are activated. Toll-like receptors (TLRs) are a family type of cell-surface PRRs present in some immune cells that identify “danger signals”, i.e. pathogen-associated molecular patterns (PAMPs), from pathogens such as the bacterial coat and toxins, and DAMPs such as heat shock proteins and double-stranded DNA. The recognition of DAMPs and PAMPs leads to phagocytosis and initiation of the inflammatory response. This is predominantly mediated by monocyte/macrophages and DCs. TLR activation leads as well to production of prostaglandins and cytokines. Some of these cytokines have chemoattractant effects (i.e. chemokines). These chemokines first attract and recruit a large number of neutrophils followed by monocytes to the site of infection by a process called chemotaxis. Recruited monocytes are then differentiated into macrophages. DCs are also attracted to the site of inflammation. The complement system facilitates the migration of immune cells from the circulation to the site of injury by a process known as diapedesis. Molecules expressed

in the vasculature, such as NO,  $O_2^-$ , cytokines regulate the expression of vascular cell adhesion molecule (VCAM)-1 on the vascular wall to facilitate the diapedesis process. At the injury site, recruited- and resident-derived macrophages are activated and differentiated into inflammatory/M1 or pro-repair/M2 macrophages that increase their phagocytosis capacity and activate T lymphocytes. DCs process the pathogens in phagosomes, carry them to the lymph nodes and present them as antigenic peptides to naïve lymphocytes to activate the adaptive immune system.<sup>197, 198</sup>

One of the first studies demonstrating the participation of the innate immune response in HTN used mice deficient in macrophage colony-stimulating factor (m-CSF or *Csf1*). These mice develop a spontaneous osteopetrotic (op) mutation within the gene m-CSF<sup>199</sup> that results in macrophage deficiency, monocytopenia, and defective bone formation.<sup>200</sup> Op/Op (or *Csf1*<sup>-/-</sup>) mice infused with Ang II remained normotensive and presented a major reduction in inflammatory responses demonstrated by a decrease in monocyte/macrophage infiltration, proinflammatory transcription factor NF $\kappa$ B activation, and VCAM-1 expression. Moreover, the degree of NAD(P)H oxidase activation and  $O_2^-$  generation was attenuated. Finally, the lack of vascular inflammation led to a lesser degree of vascular dysfunction and remodeling.<sup>201</sup> Similar results were also observed in Op/Op mice treated with DOCA-salt, which is a model that has ET-1-dependent effects,<sup>202</sup> as well as when Op/Op (or *Csf1*<sup>-/-</sup>) mice were crossed with eET-1 mice.<sup>203</sup>

To further understand the participation of monocyte/macrophages and neutrophils in vascular inflammation and HTN, another study used a mouse model that expresses Cre-inducible diphtheria toxin receptor targeted to lysozyme M<sup>+</sup> (LysM) monocytes. Administration of a low dose of diphtheria toxin leads to depletion of circulating monocytes and infiltrating macrophages in the aorta as indicated by a decrease in CD11b<sup>+</sup>Gr<sup>-1</sup>low F4/80 population. LysM monocyte ablation attenuated Ang II-induced HTN and vascular oxidative stress and dysfunction. A decrease in the expression level of inflammatory markers, such as COX-2, VCAM-1, CD68, inducible NOS (iNOS), and LysM was also observed, despite increase in neutrophil infiltration in the aorta. Moreover, the reconstitution of monocyte/macrophage reestablished the Ang II-mediated pathophysiological conditions in ablated animals.<sup>204</sup>

Overall, these studies have shed light on the pivotal role of inflammation in the vasculature in the context of Ang II- and ET-1-induced HTN. However, studies have not yet distinguished the role of different subpopulations of monocytes and macrophages involved in HTN.

#### **4.1.3.3.1.2 Adaptive immune response**

As briefly mentioned above, activated innate immunity initiates the adaptive immune response through the presentation of antigens by APCs. Adaptive immunity possesses a wide range of antigen recognition ability. Thus, differently from innate immunity, adaptive immunity is highly specific. T lymphocytes and B cells are the major cell types that participate in the adaptive immune response. CD3<sup>+</sup> T lymphocytes mature into either CD8<sup>+</sup> or CD4<sup>+</sup> cells. During antigen presentation process, APCs present the antigenic peptide via major histocompatibility complex (MHC)-I or II molecules to the T cell receptor (TCR) and to CD8 and CD4 co-receptors, activating and stimulating proliferation of CD8<sup>+</sup> and CD4<sup>+</sup> naïve T cells. In addition, co-stimulatory molecules, such as CD80 and CD86, and cytokines, induce the differentiation of effector T cells.<sup>205</sup> Thus, naïve CD8<sup>+</sup> T cells are differentiated into cytotoxic T (Tc) cells that produce perforin and granzyme as well as interferon (IFN)- $\gamma$  and tumor necrosis factor (TNF)- $\alpha$ , and predominantly function by killing damaged/infected cells. Naïve CD4<sup>+</sup> T helper (Th) cells (Th0) are polarized into Th1, Th2, or Th17, and T regulatory (Treg) lymphocyte subsets.<sup>206</sup> Each subset of CD4<sup>+</sup> Th and Treg cells produce their own panel of cytokines and perform specific functions. Effector T cells egress from lymphoid organs to the sites of inflammation.<sup>193, 207</sup> Overall, Th1 and Th17 cells present a pro-inflammatory phenotype by activating other immune cells such as macrophages and by producing pro-inflammatory cytokines, such as IFN- $\gamma$ , TNF- $\alpha$ , interleukin (IL)-6 and IL-17. In contrast, Th2 and Treg have anti-inflammatory phenotype. The former produces IL-4, IL-5, and IL-13, which promote B cell activation and suppress cell-mediated immunity. The latter produces IL-10 and TGF- $\beta$  and suppresses both innate and adaptive immune responses.<sup>207</sup> Thus, Treg cells are considered important to fine tune the immune response. In addition to the particular phenotype and cytokine secretion that each of

these effector T cells may have, they also present a certain plasticity and accordingly, they can change their phenotype depending on the milieu that they are exposed to.

The role of B and T cells in the context of the HTN state was first demonstrated in mice lacking recombination activating gene-1 ( $Rag1^{-/-}$ ). The RAG-1 enzyme is essential for genetic rearrangement and recombination of antibodies and TCR during maturation of B and T cells. The lack of the Rag-1 gene results in deficiency in mature B and T cells. Knockout of the Rag-1 gene blunted BP elevation, vascular remodeling and vascular  $O_2^-$  production in Ang II-infused and DOCA-salt mice.<sup>208</sup> Adoptive transfer of T cells but not B cells restored the response to Ang II.  $CD4^+$  and, to a lesser extent,  $CD8^+$  T cells accumulated in the aortic adventitia, particularly in the PVAT area in the hypertensive mice. Another study showed that Ang II-induced aortic adventitial collagen deposition and stiffness were abolished in  $Rag1^{-/-}$  mice.<sup>209</sup> The vascular collagen deposition and stiffening were partially prevented in  $CD8^{-/-}$  and  $CD4^{-/-}$  mice. These results indicate a possible synergistic effect of both T cell subtypes in HTN-related aortic remodeling and stiffening. ET-1 overexpression in atherosclerosis-prone mice exacerbated  $CD4^+$  T cell and monocyte/macrophage infiltration in aortic PVAT.<sup>144</sup> On the other hand, adoptive transfer of placental ischemia-stimulated  $CD4^+$  T cells stimulated the expression of ET-1 in normal recipient pregnant rats. This effect was followed by an increase in BP that was reduced by an  $ET_A$ R antagonist.<sup>210</sup> Adoptive transfer of placental ischemia-stimulated  $CD4^+$  T cells has also been shown to increase circulating pro-inflammatory cytokines such as TNF- $\alpha$ , IL-1 and IL-17 in recipient pregnant rats.<sup>211</sup>

Th17 cells, one of the pro-inflammatory arms of the adaptive immune response, have been suggested to play an important role in vascular inflammation during HTN. Ang II infusion increased the number of Th17 cells, the production of circulating IL-17, and its protein levels in aorta. IL-17 knockout prevented BP elevation, vascular stiffening and remodeling, as well as the increase in  $O_2^-$  formation and T cell infiltration, and preserved vascular function in Ang II-infused mice.<sup>209, 212</sup> *In vitro* experiments have shown that the ET-1 system can also regulate Th17-derived IL-17 production via  $ET_A$ R and in a APC-free environment.<sup>213</sup> However, ET-1/ $ET_A$ R signaling is not involved in Th17 differentiation.

Tregs mature under the influence of the transcription factor forkhead box P3 (FOXP3) and have been shown to have antihypertensive properties.<sup>207</sup> Treg adoptive transfer in Ang-II infused mice suppressed macrophage and T cell infiltration in the aorta, mesenteric artery dysfunction, stiffening, and ROS formation, and BP elevation.<sup>214</sup> Similar findings were observed in aldosterone-induced HTN.<sup>215</sup> Furthermore, Ang II-induced vascular damage, oxidative stress and inflammation were enhanced in Rag-1<sup>-/-</sup> mice receiving adoptive transfer of Scurfy T cells. Scurfy mice have a mutation in the Foxp3 gene resulting in deficient Tregs.<sup>216</sup> The lack of Treg in Ang II-infused Rag-1<sup>-/-</sup> mice increased proinflammatory macrophages. Furthermore, the injection of wild-type Tregs, but not Scurfy Tregs, was able to reduce the Ang II-mediated effects. The protective effect of Treg on the vasculature appear to be mediated by IL-10 release.<sup>217</sup> These results indicate that Tregs play a critical role in the regulation of BP and vascular damage in Ang II-induced HTN. On the other hand, Tregs are not altered in erythropoietin-induced HTN, where BP elevation and vascular injury depend on the preexisting increased ET-1 expression.<sup>218</sup>

## **4.2 ET-1 actions on the kidney**

As previously mentioned, HTN is a multifactorial and a complex disease. This complex phenotype is a result of participation of different organs and systems. The next section will briefly describe the participation of the kidney in BP regulation and how ET-1 controls multiple aspects of kidney function under physiological and pathological conditions.

### **4.2.1 Anatomy and function of the kidney**

The kidney plays a pivotal role in the short- and long-term regulation of BP, body fluid volume and acid-base balance, in the removal of toxic waste products and metabolized drugs, and in the production of erythropoietin and, active vitamin D. Changes in BP and secretion of different hormones promote changes in renal hemodynamics, altering renal function. Before describing the participation of ET-1 in renal hemodynamics and

function, the anatomy and the basic physiological function of the kidney will be briefly summarized.

The kidney is anatomically divided into the cortex, the medulla and the pelvis. The renal cortex is the outer region of the kidney where blood vessels connect to the nephron. The nephron is the structural and functional unit of the kidney that filters about 180 liters of blood per day to remove metabolic waste products and produce urine. In the nephron, blood arriving via the afferent arteriole undergoes the process of glomerular filtration. The glomerular filtration rate (GFR) represents the volume of glomerular filtrate formed per minute by the kidney. Under normal conditions, water, small molecular weight molecules and ions diffuse across the glomerular basement membrane and glomerular epithelial cells called podocytes. The former is an extracellular matrix layer that provides a permeable glomerular filtration barrier between the vasculature and the urinary space.<sup>219</sup> The podocytes stabilize the glomerular basement membrane and project foot processes that form a slit diaphragm that limits the passage of large molecules and cells into the renal tubules.<sup>220</sup> Under pathological conditions, alteration in the glomerular basement membrane and dysfunction of the slit membrane allow bigger molecular size proteins, such as albumin, to pass through the filter and enter the tubules. Most filtered components are reabsorbed by tubular cells by active or passive transport either through specialized channels or by paracellular transport through tight junctions.<sup>221, 222</sup>

The structure of the filtration barrier is not the only factor that regulates GFR. BP, blood volume and electrolyte concentrations in the blood alter renal hemodynamics, which influence GFR. The combination of the driving force exerted by the hydrostatic pressure and the opposing force exerted by the oncotic pressure of the plasma and by the pressure in the Bowman capsule produce an effective renal perfusion pressure that determines GFR. A decrease in renal perfusion pressure or in filtered sodium chloride, due to a reduction in BP for example, will stimulate the secretion of renin.<sup>223</sup> Renin is produced and secreted by juxtaglomerular cells of the afferent arteriole of the glomerulus. Renin cleaves angiotensinogen to form Ang I. Angiotensin-converting enzyme (ACE) converts Ang I into Ang II. Although Ang II is the main active component of the RAS, other peptides from alternative pathways also have biological activity, which

has demonstrated that the RAS system is a more complex cascade than the simple one described here.<sup>224, 225</sup> In the kidney, Ang II modulates GFR by directly increasing efferent arteriolar resistance more than afferent arteriolar constriction, as well as, inducing mesangial cell contraction, which in turn contracts and changes the surface area of the capillaries of the glomerulus.<sup>226</sup> Ang II has multiple actions directly on the nephron but description of these complex actions is beyond the scope of this review.<sup>227,</sup><sup>228</sup> In addition, Ang II stimulates aldosterone secretion from the zona glomerulosa of the adrenal cortex and releases anti-diuretic hormone (ADH) from the posterior pituitary gland. Aldosterone increases reabsorption of sodium through activation of renal tubular ion channels. ADH increases reabsorption of water in the distal tubule through aquaporin channels.<sup>229</sup> Overall, the production of hormones activates sodium-based regulatory mechanisms, which in turn modulate renal perfusion pressure to maintain an appropriate renal filtration and BP.

Sodium-based regulatory mechanisms occur along the nephron. In the proximal convoluted tubule, approximately 70% of the filtered sodium and water are absorbed together with 90% of the filtered bicarbonate. The luminal membrane sodium-hydrogen exchanger (NHE3) mediates the majority of sodium reabsorption. In addition, the basolateral (Na<sup>+</sup> K<sup>+</sup>)-ATPase actively pumps sodium out of the cell into the interstitium from where it diffuses into the circulation. Sodium transport into the circulation generates a low intracellular sodium concentration that creates a gradient that allows more sodium and other molecules, such as glucose and amino acids, to be reabsorbed. The thick ascending limb of the loop of Henle reabsorbs 20 to 30% of the filtered sodium chloride via Na<sup>+</sup>K<sup>+</sup>2Cl<sup>-</sup> co-transport (NKCC2) driven by the activity of basolateral (Na<sup>+</sup> K<sup>+</sup>)-ATPase. A functional NKCC also requires potassium to be recycled across the apical membrane via the renal outer medullary potassium channel (ROMK), and chloride to exit through the basolateral membrane chloride channel Kb (CLCNKB). In the distal tubule, 5 to 10% of the filtered sodium is reabsorbed via the luminal thiazide-sensitive sodium chloride co-transporter (NCC) driven by the basolateral (Na<sup>+</sup> K<sup>+</sup>)-ATPase. In the collecting duct, approximately 10 to 15% of the filtered water is reabsorbed via the luminal aquaporin 2 and basolateral aquaporin 3 channels, and a small percent of the filtered sodium is reabsorbed via the epithelial sodium channel

(ENaC). Despite the low amount of reabsorbed sodium in the collecting duct, this is the segment in which the hormonal fine-tuning of sodium reabsorption occurs.

The renal medulla is the inner region of the kidney and consists of multiple pyramidal tissue structures, appropriately called renal pyramids. This region contains parts of the nephron network originated in the renal cortex (cortical nephron) and the juxtamedullary nephron complex. Capillaries and the vasa recta present in the renal medulla are intertwined with the cortical and juxtamedullary nephron segment of the loop of Henle to exchange water and ion molecules. Water and sodium chloride transport create an osmotic gradient in the medullary interstitial space contributing to the countercurrent multiplication system. Although both cortical and juxtamedullary nephrons generate an osmotic gradient, it is the loop of Henle of juxtamedullary nephrons that is largely responsible for developing an osmotic gradient that contributes to the countercurrent mechanism responsible for urinary concentration. The renal pelvis is the concave part of the bean shape of the kidney also known as the hilum of the kidney. The renal pelvis is where renal artery and nerves enter and the renal vein as well as the ureter exit the kidney.

#### **4.2.2 Physiological effects of ET-1 on the kidney**

As in the vasculature, ET produced by the kidney acts locally in both autocrine and paracrine fashion. In contrast to the vasculature, renal ET-1 is produced and secreted by different cell types beyond ECs, including epithelial and mesangial cells, and podocytes.<sup>230, 231</sup> The renal ET-1 system controls multiple aspects of kidney function by regulating GFR, renal blood flow (RBF), renin release, sodium and water excretion, as well as proliferation and mitogenesis of mesangial cells and VSMCs. The mechanisms whereby ET-1 regulates renal hemodynamics and function under physiological conditions are complex due to the variety of ET-1 actions on different renal cell types. The levels of ETR expression and the ratio between ET<sub>A</sub>R and ET<sub>B</sub>R in the kidney varies among species,<sup>232</sup> making it difficult to extrapolate findings from rodents to humans. Despite these challenges, there is clear evidence that both ETRs are expressed in the kidney.<sup>233</sup> Within the renal vasculature, ET<sub>A</sub>R and ET<sub>B</sub>R are expressed

in VSMCs and ECs.<sup>234</sup> Glomerular mesangial cells and podocytes express ET<sub>A</sub>Rs that induce cell contraction. The vasa recta bundle expresses ET<sub>A</sub>Rs that induce contraction of pericytes, and vasodilatory ET<sub>B</sub>Rs on EC.<sup>235</sup> Epithelial cells of the proximal and distal convoluted tubules express ET<sub>B</sub>Rs and ET<sub>A</sub>Rs, respectively, whereas both receptors are found in the collecting duct.<sup>55, 234</sup>

#### 4.2.2.1 ET-1 effects on renal hemodynamics

Normal renal hemodynamics ensure a physiological GFR, and a balanced natriuresis, diuresis and medullary hyperosmotic conditions. There is a large body of evidence demonstrating that renal ET-1 alters renal hemodynamics, although the resulting physiological effects are unclear. Blockade of endogenous ET-1 by bosentan has been shown to increase preglomerular arteriolar resistance and decrease GFR, suggesting that ET-1 predominantly promotes vasodilation of afferent arterioles under physiological conditions.<sup>236</sup> The preglomerular effect seems to be mediated by ET<sub>B</sub>Rs, as BQ-123 treatment does not affect glomerular hemodynamics. Other studies have used isolated renal arteries from hydronephrotic kidney and suggested that ET-1 mediates long-lasting preglomerular vasoconstriction<sup>237</sup> through activation of both ET<sub>A</sub>Rs and ET<sub>B</sub>Rs.<sup>238, 239</sup> Similarly to preglomerular hemodynamics, the role of ET-1 in the regulation of postglomerular hemodynamics is still unclear. Endlich *et al.* have shown that ET-1 mediates cortical and juxtamedullary postglomerular vasoconstriction mainly through activation of ET<sub>B</sub>Rs<sup>238</sup> whereas Inscho *et al.* have demonstrated that activation of ET<sub>B</sub>R by sarafotoxin elicited juxtamedullary postglomerular vasodilation.<sup>239</sup> In addition to the complex relationship of ET-1 to its receptors in the glomerular vasculature, these vessels have different sensitivity to ET-1. Using isolated renal microvessels from normal Sprague-Dawley rats, efferent arteries were more sensitive to ET-1 than afferent arteries.<sup>240</sup> This indicates another potential ability of ET-1 to regulate glomerular filtration rate and glomerular hemodynamics. Thus, although ET-1 alters renal hemodynamics that in turn modulate GFR and BP, the exact mechanism is complex and the resulting effects are unclear.

ET-1-mediated hemodynamic effects are not limited to the glomeruli affecting GFR and to regulation of cortical blood flow (CBF). ET-1 also acts on the vasa recta to

modulate medullary blood flow (MBF). ET-1 decreased CBF and increased MBF in normal Wistar rats through activation of ET<sub>A</sub>Rs and ET<sub>B</sub>Rs respectively. ET-1-induced medullary vasodilation was dependent on NO and to a lesser extent on prostaglandins.<sup>241, 242</sup> ET<sub>A</sub>R blockade increased total RBF, CBF and MBF, whereas an ET<sub>B</sub>R antagonist decreased total RBF and CBF with no changes in MBF.<sup>243</sup> Another study corroborates the observation that ET-1-mediated vasodilation occurs through activation of ET<sub>B</sub>Rs. The same study has shown, however, that ET-1-induced renal vasoconstriction is a result of activation of both ETRs.<sup>244</sup> These results show, once again, the complex nature of ET-1 effects regulating renal hemodynamics.

#### **4.2.2.2 ET-1 effects on sodium and water excretion**

Regulation of sodium excretion takes place in several regions of the nephron. This process is regulated by systemic BP, glomerular pressure and renal hemodynamics, as well as by bioactive factors such as Ang II, aldosterone, ADH, NO and ET-1. The contribution of the renal ET-1 system to sodium and water handling appears to take place in the collecting duct. This hypothesis is supported by studies demonstrating that ET-1 is predominantly produced by epithelial cells in the inner medullary collecting duct region,<sup>245, 246</sup> ET<sub>B</sub>R expression levels are elevated in epithelial cells of the inner and outer medullary collecting duct region and glomeruli<sup>233, 235</sup> whereas ET<sub>A</sub>R expression is detectable in the cortical collecting duct.

The mechanism by which ET-1 physiologically regulates sodium and water transport is still unclear. The difficulties to clarify this issue are due to the inability to distinguish ET-1 effects on the nephron and on the vasculature. In addition, activation or inhibition of the renal ET-1 system alters RBF and GFR, which in turns has an effect on urinary sodium and water excretion. Systemic administration of ET-1 in normal rats impairs renal hemodynamics with a decrease in GFR and subsequent sodium retention.<sup>247</sup> Other studies have used low doses of ET-1 that do not alter renal hemodynamics to investigate the participation of ET-1 in sodium and water handling. Harris *et al.* reported that low doses of ET-1 caused profound diuresis and natriuresis.<sup>248</sup> Schnermann *et al.* described that low doses of ET-1 elicited diuresis

whereas, higher doses caused a reduction of GFR and no changes in water excretion.<sup>249</sup> Likewise, Denton *et al.* described that low doses of ET-1 increase the sodium excretion rate, whereas a higher dose of ET-1 does not change natriuresis.<sup>250</sup> Despite these contradictory observations, these findings suggest that renal ET-1 could inhibit sodium and water reabsorption in the cortical and medullary collecting duct, which can ultimately regulate BP. Indeed, knockout of collecting duct-specific *Edn-1* (CD ET-1 KO) reduced natriuresis and induced BP elevation in mice under a high salt diet.<sup>251</sup> In addition, plasma vasopressin levels were reduced, which impaired water excretion in CD ET-1 KO mice.<sup>252</sup> To investigate which ETR was responsible in mediating impaired natriuresis and diuresis and increased BP, collecting duct-specific ET<sub>A</sub>R (CD ET<sub>A</sub>R KO) and ET<sub>B</sub>R (CD ET<sub>B</sub>R KO) deficient mice have been studied. Deficiency in collecting duct-specific ET<sub>A</sub>R did not alter ET-1 effects on BP and sodium handling but reduced the hydrosmotic effects of vasopressin.<sup>253</sup> In contrast, ET<sub>B</sub>R deficiency induced HTN under normal diet conditions and elicited salt-sensitive HTN associated with early sodium retention, even though aldosterone and plasma renin activity were decreased.<sup>254</sup> Regardless of the diet, the degree of sodium retention and BP elevation was greater in CD ET-1 KO mice compared with CD ET<sub>B</sub> KO mice.<sup>254</sup> Interestingly, mice with disruption of both ETRs in the collecting duct presented BP elevation similar to CD ET-1 KO mice. Unexpectedly, sodium retention was observed in CD ET<sub>A/B</sub>R KO mice after two days of sodium loading.<sup>255</sup> An *in vitro* study using isolated microperfused collecting ducts also suggests that ET-1 inhibits sodium reabsorption through both ETRs.<sup>256</sup> These results suggest that collecting duct-derived ET-1 conceivably interacts with both ETRs to regulate systemic BP; it might exert an early natriuretic effect through paracrine actions on neighboring cells. Perhaps ET-1-mediated autocrine effects come into play later on. Overall, these findings further support the complex effects of ET-1 in BP regulation and sodium and water excretion.

The mechanism whereby ET-1 regulates sodium excretion in the collecting duct is by negatively modulating the activity of the ENaC. Patch-clamp electrophysiology studies showed that exogenous ET-1 decreased ENaC activity via collecting duct basolateral membrane ET<sub>B</sub>R but not via ET<sub>A</sub>R in wild-type mice<sup>257</sup> and rats.<sup>258</sup> Src and MAPK kinase signaling was required for the ET-1-induced reduction in ENaC activity.

Another study further suggests that ET-1-induced natriuresis and diuresis is partially mediated by NO production,<sup>259</sup> since renal NO production is decreased in CD ET-1 KO under normal and high salt diet associated with a decrease in neuronal NOS and eNOS activities. Thus, these results indicate that renal ET<sub>B</sub>R impair sodium and water reabsorption through NO-dependent mechanisms. The role of ET<sub>A</sub>R in ET-1-mediated sodium excretion remains unclear.

ET-1-mediated natriuretic and diuretic effects are not limited to the collecting duct region. ET-1 can also modulate sodium reabsorption in the proximal tubule through stimulation of the apical Na<sup>+</sup>/H<sup>+</sup> exchanger and the basolateral Na<sup>+</sup>/HCO<sub>3</sub><sup>-</sup> cotransporter.<sup>260</sup> In addition, low doses of ET-1 inhibit ENaC activity via ET<sub>B</sub>R in distal nephron cells, whereas high doses of ET-1 increase the channel activity via ET<sub>A</sub>R.<sup>261</sup>

#### **4.2.3 Pathophysiological effects of ET-1 in the kidney**

In HTN, the ability of the kidney to regulate glomerular pressure by pressure natriuresis is impaired and renal hemodynamics are altered, which explains at least in part the persistent BP elevation. Among other vasoconstrictor peptides, systemic ET-1 could be implicated in the progression and worsening of HTN by pathologically modulating natriuresis and diuresis as well as renal hemodynamics.<sup>262</sup> Infusion of a high dose of ET-1 in healthy subjects induced renal vasoconstriction associated with a decrease in GFR, RBF and sodium excretion and an increase in renal vascular resistance. Co-infusion of an ET<sub>A</sub>R antagonist partially restored ET-1-induced renal changes with the exception to GFR.<sup>263</sup> In presence of chronic kidney disease, plasma ET-1 levels are further increased in hypertensive patients.<sup>118</sup> Selective ET<sub>A</sub>R blockers appear to produce more beneficial systemic and renal hemodynamics effects than non-selective ETR blockers in hypertensive patients with chronic renal failure.<sup>264</sup> In addition to ET-1-induced sodium and water retention and a pathological alteration of renal hemodynamics, another study showed that overexpression of constitutive *Edn-1* for a year increased renal protein ET-1 levels associated with BP elevation, profound interstitial fibrosis, glomerulosclerosis, renal damage and decrease in renal function as indicated by a decrease in GFR.<sup>265</sup> Blockade with an ET<sub>A</sub>R reduced the severity of HTN and the renal injury, and improved renal function and the pressure/natriuresis curve in

Dahl salt-sensitive rats<sup>266</sup> and stroke-prone SHR<sup>267</sup> under high salt diet. Although ETR antagonists do not attenuate HTN in SHR,<sup>268</sup> ET-1-specific antibody treatment in SHR reduced BP and renal vascular resistance, and increased GFR and RBF.<sup>269</sup> Overall, ET-1-induced vasoconstriction alters renal hemodynamics thereby hindering renal function and as well leads to constriction of peritubular capillaries and descending vasa recta, with subsequent hypoxic damage which further cause and/or aggravate glomerular and tubular structural injury.<sup>270</sup>

Despite the large body of evidence indicating that high levels of plasma ET-1 are associated with renal damage and dysfunction in HTN, local renal ET-1 levels in HTN have been shown to be either increased or decreased. Perhaps the discrepancy in the renal ET-1 levels depends on the region of the kidney where ET-1 is measured. Urinary excretion of ET-1, an index of intrarenal ET-1 production, is increased in Ang II-induced hypertensive Sprague-Dawley rats associated with an increase in immunoreactive ET-1 in the kidney cortex.<sup>271</sup> In contrast, immunoreactive ET-1 content in the renal medulla was reduced in this animal model. Similar findings have also been reported in other animal models of HTN.<sup>272, 273</sup> The decrease in medullary ET-1 content could be at least in part due to a reduction of medullary collecting duct-derived ET-1 production. As collecting duct-derived ET-1 mediates natriuresis and diuresis, the decrease in ET-1 production in the medullary collecting duct can perhaps explain sodium and water retention, which could contribute to BP elevation. Indeed, urinary ET-1 levels and GFR from patients with essential HTN are decreased although plasma ET-1 is unchanged.<sup>274, 275</sup> However, urinary ET-1 levels from hypertensive patients with renal parenchymal disease are increased compared to patients with essential HTN.<sup>275</sup> High levels of urinary ET-1 in hypertensive patients with renal parenchymal disease are perhaps associated with an increase in renal ET-1 production due to the renal damage.<sup>276-278</sup>

Changes in renal ETR expression levels, ratio and activity are another conceivable explanation for ET-1-induced renal dysfunction and injury. Receptor ligand binding studies for renal cortical and medullary ETRs have shown that ETRs are modulated differently in the cortex and medulla after acute renal ischemia.<sup>277</sup> Furthermore, the distribution of ETRs within the cortical renal region is altered in SHR

compared to normotensive Sprague-Dawley rats. The affinity of ETRs is also higher, thereby inducing a more sensitive renal vasoconstrictor effects.<sup>279</sup>

ET-1 plays an important role in triggering vascular inflammation. ET-1 may also contribute to inflammation in the kidney. Ang II modulates T cell infiltration and differentiation in a differential manner within the kidney, as well as increases in the number of monocyte/macrophages.<sup>280</sup> ET<sub>A</sub>R antagonist decreased BP and the number of CD3<sup>+</sup> T cells within the kidney. Although triple antihypertensive therapy reduced BP, it attenuated CD3<sup>+</sup> T cell infiltration only in the renal medulla. These findings suggest that ET<sub>A</sub>R activation in Ang II-induced HTN participates in the increase in the number and proliferation of CD3<sup>+</sup> T cells in the renal cortex in a BP-independent manner and in the renal medulla in a BP-dependent manner. Likewise, ET<sub>A</sub>R antagonist attenuated BP elevation, renal inflammatory effects and growth response in aldosterone-induced HTN.<sup>281</sup> Thus, renal damage in Ang II and aldosterone-dependent HTN models is associated with inflammatory processes that are partly mediated by ET-1. Chronic infusion of ET-1 enhanced glomerular intercellular adhesion molecule (ICAM)-1 and MCP-1 expression, as well as macrophage and T cell infiltration in the renal cortex without affecting BP.<sup>282</sup> These renal inflammatory effects were mediated via ET<sub>A</sub>R independently of BP.

In HTN renal ET-1 plays a pivotal role in the regulation of BP by controlling sodium balance via both renal hemodynamic and tubular mechanisms. In addition, ET-1 contributes to initiation and progression of inflammation that can induce further renal damage independently or not of BP elevation.

## 5. Experimental design

Many experimental animal models of HTN have been developed to mimic the human forms of HTN. These animal models are the result of pharmacological, genetic, dietary and surgical manipulations that help to investigate the underlying pathophysiological mechanisms, in this case of ET-1, contributing to the development and progression of HTN.<sup>104</sup> In this section, the animal model used for the research presented in this thesis will be briefly described.

We generated our ieET-1 mouse by crossing a transgenic mouse line that expresses i) a ubiquitous early enhancer/chicken  $\beta$ -actin promoter (CAG), ii) followed by a loxP flanked-chloramphenicol acetyltransferase (*cat*) cDNA and iii) *EDN1* (CAG-*cat-EDN1*) with a transgenic mouse that expresses Cre recombinase protein fused to a tamoxifen (TAM)-inducible modified estrogen receptor ligand binding domain (CreER<sup>T2</sup>). CreER<sup>T2</sup> expression is under receptor tyrosine kinase *Tie2* promoter control and is therefore constitutively expressed selectively in ECs, although it remains inactive in absence of TAM treatment. Upon TAM treatment, the EC-specific CreER<sup>T2</sup> complex is activated, migrates to the nucleus and excises the loxP-flanked *cat* sequence allowing *EDN-1* to be expressed. Mice expressing only *Tie2*CreER<sup>T2</sup> were used as control group.

## 6. Hypothesis and objectives

Various experimental HTN models such as DOCA-salt rats, DOCA-salt-treated SHR, stroke-prone SHR, Dahl salt-sensitive rats, Ang II-infused rats, and one-kidney, one-clip Goldblatt rats have been used to investigate the pathophysiological role of ET-1.<sup>104</sup> These animal models, however, assess only the indirect pathophysiological participation of ET-1 in the progression of HTN. To overcome this limitation, in 2004 Amiri *et al.* generated a constitutive eET-1 mouse model. Constitutive eET-1 overexpression induced endothelial dysfunction, vascular remodeling, oxidative stress, and inflammation in the absence of significant change in BP (although systolic BP tracked 10 mm Hg above that of controls).<sup>127, 203, 283</sup> Furthermore, ET-1 overexpression

exacerbated aortic atherosclerosis and triggered abdominal aortic aneurysm formation in *Apoe*<sup>-/-</sup> mice crossed with eET-1 mice under a high fat diet.<sup>144</sup> Some of the effects associated with constitutive ET-1 overexpression may be due, at least in part, to an ontogenic adaptation to life-long exposure to elevated ET-1 expression. Accordingly, ieET-1 mice were generated to study the role of ET-1 on BP regulation in the absence of potential developmental effects.

The main objectives of this thesis are:

- Chapter II: To determine whether short-term 3-weeks induction of EC-selective ET-1 overexpression in adult ieET-1 mice causes BP elevation and vascular and renal injury.
- Chapter III: To determine whether long term 3-month induction of EC-restricted ET-1 overexpression in adult ieET-1 mice is associated with sustained BP elevation and induces vascular and renal injury.

**CHAPTER II: Inducible Human Endothelin-1 Overexpression in Endothelium  
Raises Blood Pressure via Endothelin Type A Receptors**

**Inducible human endothelin-1 overexpression in endothelium raises blood pressure via endothelin type A receptors**

Yohann Rautureau<sup>1\*</sup>, Suellen C. Coelho<sup>1\*</sup>, Julio C. Fraulob-Aquino<sup>1</sup>, Ku-Geng Huo<sup>1</sup>, Asia Rehman<sup>1</sup>, Stefan Offermanns<sup>3</sup>, Pierre Paradis<sup>1</sup>, Ernesto L. Schiffrin<sup>1,2</sup>

<sup>1</sup>Hypertension and Vascular Research Unit, Lady Davis Institute for Medical Research and <sup>2</sup>Department of Medicine, Sir Mortimer B. Davis-Jewish General Hospital, McGill University, 3755 Côte-Ste-Catherine Rd., Montreal, Montréal, Quebec, Canada, H3T 1E2; <sup>3</sup>Department of Pharmacology, Max-Planck-Institute for Heart and Lung Research, Ludwigstraße 43, 61231 Bad Nauheim, Germany.

\*Both authors contributed equally to this work.

Published in: Hypertension. 2015; 66:347-355

The manuscript is presented here according to the instructions of the journal in which it was published. The main manuscript is followed by the Online Supplemental material (including the expanded materials and methods section).

## Abstract

The mechanisms of blood pressure regulation by endothelin-1 produced by endothelial cells are complex and still unclear. Transgenic mice with endothelium-restricted human endothelin-1 (*EDN1*) overexpression presented vascular damage but no significant change in blood pressure, which could be due to adaptation to life-long exposure to elevated endothelin-1 levels. We now generated a tamoxifen-inducible endothelium-restricted *EDN1* overexpressing transgenic mouse (ieET-1) using Cre/loxP technology. Sixteen days after tamoxifen treatment, ieET-1 mice presented  $\geq 10$ -fold increase in plasma endothelin-1 ( $P < 0.01$ ) and  $\geq 20$  mmHg elevation in systolic blood pressure ( $P < 0.01$ ), which could be reversed by atrasentan ( $P < 0.05$ ). Endothelin-1 overexpression did not cause vascular or kidney injury or changes in kidney perfusion or function. However, endothelin type A and B receptor expression was differentially regulated in the mesenteric arteries and the kidney. Our results demonstrate using this ieET-1 mouse model that 21 days of induction of endothelin-1 overexpression caused endothelin-1-dependent elevated blood pressure mediated by endothelin type A receptors.

**Keywords:** endothelin-1, endothelium, blood pressure, endothelin type A receptor, inducible tissue specific transgenic mouse.

## Introduction

Endothelin (ET)-1 is one of the most potent vasoconstrictor peptides.<sup>1</sup> ET is produced by endothelial cells (EC) as well as other cell types.<sup>1,2</sup> The effects of ET-1 are mediated by two G-coupled receptors, ET type A (ET<sub>A</sub>) and B (ET<sub>B</sub>) receptors. ET-1 secreted by EC acts in paracrine fashion on ET<sub>A</sub> and ET<sub>B</sub> receptors on underlying vascular smooth muscle cells to induce contraction and growth. It also acts in autocrine fashion on EC ET<sub>B</sub> receptors to release vasodilator nitric oxide (NO) and prostacyclin. ET<sub>B</sub> receptors also play a role in ET-1 clearance, and mediate natriuresis by acting on the kidney.

ET-1 has been implicated in the development of hypertension and vascular damage.<sup>3,4</sup> Plasma ET-1 is elevated in patients with essential hypertension,<sup>5</sup> particularly in moderate-to-severe hypertension<sup>6</sup> and in hypertension associated with other disorders such as chronic kidney disease (CKD), metabolic syndrome and diabetes mellitus.<sup>3</sup> ET-1 expression is also increased in salt-dependent models of experimental hypertension such as deoxycorticosterone acetate (DOCA)-salt hypertension,<sup>7</sup> spontaneous hypertensive rats (SHR) treated with DOCA and salt,<sup>8</sup> stroke-prone SHR,<sup>9</sup> and in Dahl salt-sensitive rats.<sup>10</sup> In these rodents, enhanced ET-1 expression is associated with increased vascular oxidative stress, endothelial dysfunction and hypertrophic vascular remodeling. However, direct evidence that ET-1 may directly raise blood pressure (BP) has been difficult to obtain. Genetic manipulation of ET-1 gene (*Edn1*) expression levels has yielded contradictory results regarding the role of ET-1 on BP regulation. Homozygous *Edn1* null mice were not viable and presented craniofacial malformation.<sup>11</sup> On the other hand, *Edn1* haploinsufficiency (*Edn1*<sup>+/-</sup>) paradoxically caused hypertension. Endothelial-restricted *Edn1* knockout generated by crossing mice with floxed *Edn1* exon 2 (*Edn1*<sup>Flox/Flox</sup>) with mice expressing Cre recombinase under the transcriptional control of the endothelium-specific angiotensin-1 receptor (*Tek* also known as *Tie2*) promoter, caused mild hypotension and decrease in both plasma and tissue ET-1 levels. These findings demonstrated that ET-1 participates in the regulation of BP, and that EC are the main source of ET-1 production.<sup>12</sup> Transgenic mice bearing the entire human ET-1 (*EDN1*) gene presented no change in plasma ET-1, slightly elevated tissue ET-1 concentrations, renal disease

with aging (14-month-old) and no change in BP.<sup>13</sup> A similar finding was made in mice overexpressing a mouse *Edn1* cDNA under the control of the mouse *Edn1* promoter.<sup>14</sup> In addition, feeding a high-salt diet (8% NaCl) caused a 20 mmHg BP elevation in these mice. We have previously generated mice that overexpressed human *EDN1* cDNA in EC under transcriptional control of *Tie2* promoter (eET-1).<sup>15</sup> Although eET-1 mice presented increased plasma ET-1, mesenteric artery (MA) endothelial dysfunction, vascular remodeling, oxidative stress, and inflammation, BP was not significantly elevated.<sup>15, 16</sup> All the aforementioned models relied on constitutive loss- or gain-of-function of *Edn1*, suggesting that there is the possibility that ontogenic adaptation modified the effects of ET-1. Since the *Tie2* promoter has been shown to drive gene expression in EC during embryonic development,<sup>17</sup> it is possible that effects of ET-1 overexpression on vascular remodeling and function and absence of BP elevation are due, at least in part, to developmental changes or adaptation to life-long exposure to high ET-1 circulating and tissue concentrations.

In humans, selective ET<sub>A</sub> receptor or nonselective ET receptor antagonists were effective in reducing BP in resistant hypertensive subjects receiving ≥3 antihypertensive drugs, including a diuretic, at optimized doses, and ameliorated or reversed renal injury in patients with CKD.<sup>18</sup> However, the use of ET blockers was limited by adverse side effects such as liver toxicity, headaches and fluid retention. Further studies are required to better understand the complexity of the pathophysiology of ET-1 in hypertension and vascular injury.

In order to study the role of ET-1 on BP in absence of developmental effects, we generated a mouse model of inducible endothelium-specific ET-1 overexpression (ieET-1) using a Cre/loxP tamoxifen-inducible system. With this new model, we determined that induction of human ET-1 overexpression in EC of adult ieET-1 mice causes BP elevation mediated via ET<sub>A</sub> receptors.

## Methods

The Materials and Methods are described in detail in the online Supplement.

## Experimental design

The study was approved by the Animal Care Committee of the Lady Davis Institute for Medical Research and McGill University, followed recommendations of the Canadian Council for Animal Care and was in agreement with the Guide for the Care and Use of Laboratory Animals published by the US National Institutes of Health. The bacterial artificial chromosome (BAC) *Tie2-CreER<sup>T2</sup>* transgenic mice (renamed here ieCre) were produced by crossing ieCre mice with wild-type C57BL/6 mice (Harlan Laboratories, Indianapolis, IN). ieCre/*ROSA26<sup>mT-mG/+</sup>* reporter mice were generated by crossing ieCre mice with C57BL/6 *ROSA26<sup>mT-mG/mT-mG</sup>* reporter mice (Jackson Laboratories, Bar Harbor, ME). The transgenic *CAG-cat-EDN1* and ieET-1 mice were generated in our laboratory as described below and in the online Supplement and F4 and F5 C57BL/6 backcrossed generation were used in this study. Mice were treated for 5 days with tamoxifen (1 mg/day, s.c.) or vehicle, as indicated in the text, and studied 16 days later. In a subgroup, BP was determined by telemetry. Mice were anesthetized with isoflurane and surgically instrumented with PA-C10 BP telemetry transmitters (Data Sciences International, St. Paul, MN) as previously done.<sup>19</sup> Mice were allowed to recover for 7 additional days and BP was determined two days before (baseline), during vehicle or tamoxifen treatments, and the 16 following days. One group of tamoxifen-treated ieET-1 mice was also treated with the ET type A receptor blocker atrasentan (10 mg/kg/day P.O.) from day 10 to the end of the study. In another subgroup of mice, during the two last days of the study, 24-hour urine was collected using metabolic cages to determine kidney function and damage by measuring urinary creatinine, sodium, potassium and protein by the Diagnostic Research Support Services at the Comparative Medicine and Animal Resource Centre of McGill University, and urinary nephrin (Exocell, Philadelphia, PA) and lipocalin-2 (R&D Systems, Minneapolis, MN) by ELISA. Renal artery flow and resistive index were also assessed by ultrasound. At the end of the protocol, mice were weighed and then anesthetized with isoflurane. Blood was collected by cardiac puncture on EDTA and plasma stored at -80°C until used for ET-1 determination by ELISA (R&D Systems). The MA vascular bed was dissected, and other tissues and tibia harvested in ice-cold phosphate buffered saline (PBS). Tissues were weighed and tibia length measured. Kidney sections were dissected under the

microscope in order to separate renal cortex and medulla. Kidney sections and remaining tissues were frozen in liquid nitrogen and stored at  $-80^{\circ}\text{C}$  until used. Second-order MA were used for assessment of endothelial function and vessel mechanics function by pressurized myography. For the study of mRNA expression, the MA arcade was dissected away from the attached intestine under RNase-free conditions and stored immediately in RNAlater (Life Technologies, Burlington, ON, Canada) until RNA extraction. The expression of ET type A and B receptor (*Ednra* and *Ednrb*), renin (*Ren1*) and ribosomal protein S16 (*Rps16*) mRNA was determined in MA or renal cortex and medulla by reverse transcription/quantitative PCR (RT-QPCR). For determination of tissue specificity of Cre activation, *ieCre/ROSA26<sup>mT-mG/+</sup>* were anesthetized with 300-375 mg/kg IP of Avertin.<sup>20</sup> Depth of anesthesia was confirmed by rear foot squeezing. The mice were injected IP with heparin (100 USP units), then perfused through the left ventricle at a constant pressure of 100 mmHg for 5 min with PBS to remove the blood, followed by 15 min perfusion with 4% paraformaldehyde (PFA). Tissues were collected in 4% PFA and incubated in 4% PFA for 24 h with gentle agitation at  $4^{\circ}\text{C}$ . All tissues with exception of MA were dehydrated by incubation in 30% sucrose in PBS for 24 h with gentle agitation at  $4^{\circ}\text{C}$ . Tissues were embedded in VWR Clear Frozen Section Compound (VWR international, Edmonton, AL, Canada) and stored at  $-80^{\circ}\text{C}$  until used. MA were stored in PBS at  $4^{\circ}\text{C}$  until imaged. The numbers of mice used are indicated in the figure and table legends.

## Results

### **Inducible endothelium-restricted human ET-1 overexpressing mice.**

ieET-1 mice were generated in two steps. First, transgenic mice containing a Cre-inducible *EDN1* expression were generated as follows (Fig. II-1A). In brief, a DNA fragment containing the *EDN1* cDNA followed by the rabbit  $\beta$ -globin intron and polyadenylation signal (pA) was amplified by PCR and subcloned into multiple cloning sites (MCS) of the pCAG-*cat*-MCS.21 expression vector (generous gift of Dr. Thomas N. Sato, Nara Institute of Science and Technology, Ikoma, Nara, Japan). The resulting pCAG-*cat*-*EDN1* expression vector contains a CMV enhancer/chicken  $\beta$ -actin promoter

(CAG) that drives the expression of a LoxP-flanked, chloramphenicol acetyltransferase (*cat*) cDNA followed by a pA, before Cre-mediated excision, and *EDN1* cDNA followed by the rabbit  $\beta$ -globin intron and pA, after excision. A *Sall/NotI* DNA fragment containing the CAG-*cat-EDN1* transgene was used to generate transgenic mice at the Microinjection and Transgenesis core facility of Institut de recherches cliniques de Montréal (Montreal, QC, Canada). In order to eliminate the possibility that the effects of the *EDN1* transgene expression are due to the integration site, two CAG-*cat-EDN1* transgenic founders (C134 and C170) that transmitted the transgene, contained one integration site and expressed *cat* were selected for the study. Transgenic mice were backcrossed with C57BL/6 mice (Harlan Laboratories, Indianapolis, IN). No difference in plasma ET-1 levels could be observed between CAG-*cat-EDN1* C134 and C170 and control wild-type mice (Fig. II-1B), confirming that the expression of *EDN1* was blocked by the expression of *cat*. In the second step, two transgenic ieET-1 mouse lines were obtained by crossing the CAG-*cat-EDN1*-C134 and C170 mice with a transgenic mouse having an inducible endothelium restricted Cre (ieCre), the BAC transgenic *Tie2*-CreER<sup>T2</sup> mouse.<sup>21</sup> The ieCre mouse expresses a fusion protein of the Cre recombinase with the modified estrogen receptor (ER) binding domain (CreER<sup>T2</sup>)<sup>22</sup> under the control of the endothelium-specific *Tie2* promoter. CreER<sup>T2</sup> is activated by tamoxifen but not by natural ER ligands.<sup>21</sup> In presence of tamoxifen, CreER<sup>T2</sup> translocates from the cytoplasm to the nucleus, where it recombines the LoxP sites to remove the *cat*-pA DNA fragment, and consequently, induces the expression of *EDN1* (Fig. II-1A).

### **Tamoxifen induced ET-1 overexpression in ieET-1 mice.**

In order to evaluate the efficiency of tamoxifen-induced *EDN1* expression, ieET-1-C134 and C170 mice were treated for 5 days with tamoxifen (1 mg/day, subcutaneously) or vehicle, and plasma ET-1 levels were determined 16 days later. Tamoxifen-treated ieCre mice were also studied to control for induction of Cre with wild-type mice used as reference. Plasma ET-1 levels in vehicle-treated ieET-1-C134 and ieET-1-C170 were similar to wild-type mice (Fig. II-1B), demonstrating no leaky Cre activation in the absence of tamoxifen treatment. Similar plasma ET-1 levels were found in tamoxifen-treated ieCre mice, indicating that activation of CreER<sup>T2</sup> by tamoxifen or tamoxifen

treatment itself did not modify ET-1 expression. However, tamoxifen induced  $\geq 9$ -fold increase in plasma ET-1 in ieET-1-C134 and  $\geq 15$ -fold in ieET-1-C170 compared to vehicle-treated ieET-1 and tamoxifen-treated ieCre mice.

### **Tamoxifen induced endothelium-restricted Cre activation in ieCre mice.**

Tissue specificity of Cre activation was determined using ieCre/*ROSA26*<sup>mT-mG/+</sup> reporter mice, which express a loxP-flanked, membrane-targeted tandem dimer tomato (mT), before Cre-mediated excision, and a membrane-targeted enhanced green fluorescent protein (mG) after excision, under the control of the CAG promoter driving the expression in all cell types.<sup>23</sup> The ieCre/*ROSA26*<sup>mT-mG/+</sup> mice were treated with tamoxifen or vehicle as above, and the Cre activation was revealed by the replacement of mT by mG expression. Confocal microscopy imaging demonstrated that tamoxifen caused EC-restricted activation of Cre in MA, aorta and kidneys (Fig. II-1C and D) and in the heart and liver (Fig. II-S2). The EC-restricted Cre activation in kidneys, heart and liver was confirmed by colocalization of mG fluorescence with an endothelium marker, CD31. Tamoxifen-induced Cre activation in EC was partial in MA and aorta. Cre activation was not observed in the vehicle-treated mice.

### **Induction of ET-1 overexpression in the endothelium resulted in ET type A receptor-mediated systolic blood pressure rise.**

Systolic BP (SBP) was determined by telemetry in ieCre and ieET-1 (C134 and C-170) mice two days before (baseline), during vehicle or tamoxifen treatments as above, and the 16 following days. Tamoxifen increased SBP in ieET-1-C134 and C170 mice but not ieCre mice (Fig. II-2 and S3). SBP rose progressively during the 5 days of tamoxifen treatment in ieET-1-C134 and C170 mice. By the end of the study, nighttime SBP was  $\sim 25$  and 20 mmHg higher in tamoxifen-treated ieET-1-C134 and C170 mice, respectively, compared to tamoxifen-treated ieCre mice (Fig. II-2A and S3A). During the day, when the mice are resting, SBP was  $\sim 20$  mmHg higher in ieET-1-C134 and C170 mice, compared to ieCre mice (Fig. II-2B and S3b). In order to confirm whether ET-1 mediated SBP elevation through ET<sub>A</sub>R in ieET-1 mice, another group of ieET-1-C134 mice was treated as above with tamoxifen and then with an ET type A receptor blocker,

atrasentan (10 mg/kg/day), from day 10 until the end of the study. Atrasentan treatment abrogated SBP elevation during the night and day (Fig. II-2).

### **Induction of ET-1 overexpression in the endothelium did not alter body or organ weights.**

Induction of endothelial ET-1 overexpression affected neither growth of mice (body weight and tibia length) nor induced changes in heart, kidney, lung, liver or spleen weight in tamoxifen-treated ieET-1-C134 and C170 mice compared to tamoxifen-treated ieCre mice (Table II-1).

### **Induction of ET-1 overexpression in the endothelium did not cause resistance artery dysfunction nor remodeling but was associated with decrease in ET receptor expression**

Vascular function and remodeling were assessed in MA of vehicle and tamoxifen-treated ieET-1-C134 mice using pressurized myography. Contractile responses to norepinephrine and endothelium-dependent dilatory response to acetylcholine were unaffected by tamoxifen-induced ET-1 overexpression in ieET-1-C134 mice (Fig. II-3A-B). Likewise, induction of ET-1 overexpression in EC did not cause vascular remodeling within the timeframe of this experimental paradigm (Table II-2).

To better understand how induction of endothelial ET-1 overexpression caused a rise in SBP, contractile responses to ET-1 and angiotensin II were examined. The contractile responses to these peptides were identical in tamoxifen and vehicle-treated ieET-1 mice (Fig. II-3C-D). However, mRNA expression of ET<sub>A</sub> (*Ednra*) and ET<sub>B</sub> (*Ednrb*) receptors determined by RT-QPCR was decreased by ~60% or tended to decrease, respectively, in MA of tamoxifen-treated ieET-1-C134 mice compared to vehicle-treated mice (Fig. II-3E and F).

### **Kidney perfusion, function and damage and renal ET<sub>A</sub> and ET<sub>B</sub> receptor mRNA expression.**

The right renal artery diameter and blood flow were studied by echography using two-dimensional short axis view and pulse wave Doppler in tamoxifen-treated ieCre and

vehicle- and tamoxifen-treated ieET-1-C134 mice (Fig. II-S4). The renal artery diameter and flow were unaffected by 21 days of endothelial ET-1 overexpression (Table II-3). The heart rate and resistive index were also unaltered. Analysis of the urine collected in metabolic cages revealed that kidney function assessed by determining sodium/creatinine, potassium/creatinine and urea/creatinine, and renal injury by protein/creatinine, nephrin/creatinine and lipocalin-2/creatinine were unaffected by endothelial ET-1 overexpression iET-1.

mRNA expression of *Ednra* and *Ednrb* and renin (*Ren1*) was determined by RT-QPCR in renal cortex and medulla in the same groups as above. Induction of endothelial ET-1 overexpression was associated with a ~3-fold increase in *Ednra* expression in renal cortex but no change in renal medulla (Fig. II-4A and B). There was a 2-3-fold greater *Ednrb* expression in renal cortex and medulla (Fig. II-4C and D). Renin gene (*Ren1*) expression was similar in the three groups (Fig. II-4E and F).

## Discussion

This study demonstrated that generation of a novel mouse model with inducible endothelial ET-1 overexpression, which is devoid of developmental effects, results in ET-1-dependent elevated BP mediated by ET type A receptors. No vascular injury was observed in ieET-1 mice at 21 days after induction of ET-1 overexpression. Furthermore, ET type A and B receptor expression was differentially regulated in MA and kidney.

The ieET-1 mouse was designed to overexpress ET-1 in EC only upon tamoxifen treatment. This was realized in part by using ieCre mice expressing the tamoxifen-inducible CreER<sup>T2</sup> under the control of the EC-specific *Tie2* promoter. As previously observed,<sup>21</sup> this study showed that ieCre/*ROSA26*<sup>mT-mG/+</sup> reporter mice presented Cre activation only in EC of tamoxifen-treated mice. Furthermore, plasma ET-1 levels were increased only in tamoxifen-treated ieET-1 mice, which was independent of the transgene integration site, as this was observed in two distinct lines of ieET-1 transgenic mice. Altogether, these results confirmed that the overexpression of ET-1 was inducible and restricted to EC.

Induction of endothelium-restricted ET-1 overexpression in ieET-1 mice with tamoxifen increased BP without affecting at 21 days endothelial or vascular function, or mechanical properties of MA. Moreover, ET-1 overexpression had no effect on body or organ weight. These observations contrast with our previous findings using a constitutive endothelium-specific ET-1 (eET-1) transgenic mouse model.<sup>15</sup> A possible explanation for a different phenotypes observed might be due to developmental changes or adaptation to life-long exposure to elevated ET-1 circulating or tissue levels. In eET-1 mice, ET-1 expression was constitutively driven in EC under the control of the *Tie2* promoter. This promoter is known to drive gene expression early in development in all blood vessels<sup>17</sup> and thus *in utero* overexpression of ET-1 could have contributed to the observed vascular damage in the previous constitutive model. ieET-1 mice are devoid of ET-1 overexpression in the absence of induction with tamoxifen. Accordingly, it is likely that the Cre-loxP system was not activated long enough to allow ET-1 to cause vascular injury, whereas vasoconstriction to human ET-1 overexpressed in the endothelium resulted in elevated BP. Longer term experiments will be necessary to test this hypothesis that chronically the inducible model (ieET-1) will exhibit vascular injury.

The contractile response of MA upon exogenous ET-1 was the same between tamoxifen and vehicle-treated ieET-1 mice, suggesting that receptor activity was unaltered by ET-1 overexpression. Interestingly, the MA contractile response to ET-1 was similar to that observed by Yanagisawa *et al.* in porcine coronary arteries.<sup>1</sup> Likewise, the contractile response of MA to Ang II was not modified. Although no vascular dysfunction or remodeling were observed, ET<sub>A</sub> and ET<sub>B</sub> receptor mRNA expression was downregulated in MA of tamoxifen-treated ieET-1 mice. This suggests that despite the fact that duration of exposure to ET-1 overexpression did not cause vascular damage, it was long enough to induce an adaptive response. Whether the changes in mRNA expression of ET receptors translated into changes in protein is unknown, but they did not result in a reduction of the contractile response to exogenous ET-1. Current ongoing experiments of much longer chronic duration to elevated ET-1 overexpression will elucidate whether indeed in this model adult induction of ET-1 overproduction in the endothelium without exposure *in utero* will indeed lead to vascular

remodeling and modulation of vascular function not found in the present experimental paradigm.

The kidneys play a major role in long-term control of BP and in the development and maintenance of hypertension<sup>24</sup> Endothelial ET-1 overexpression-induced BP elevation could be modulated by the renal ET system that controls multiple aspects of kidney function through regulation of renal blood flow (RBF) and glomerular filtration rate (GFR), control of renin expression, and sodium and water excretion through activation of ET<sub>A</sub> and ET<sub>B</sub> receptors.<sup>25-27</sup> This was not the case in tamoxifen-treated ieET-1 mice, as renal artery flow, resistive index, sodium excretion and renin mRNA level were unaltered. In addition, short-term exposure to endothelial ET-1 overexpression did not cause renal injury, assessed by measuring urinary protein, nephrin and lipocalin-2 excretion, which may differ in longer-term exposure to endothelial ET-1 overexpression. However, the important conclusion is that BP rose in this inducible model in the short term without renal injury.

The expression of ET<sub>A</sub> receptors in the renal cortex and ET<sub>B</sub> receptors in renal cortex and medulla was increased. The renal ET system is complex given the fact that both ET receptors present distinct signaling pathways, whose effects depend on which cell type and at what nephron and vascular levels these receptors are present.<sup>26</sup> Changes in ET-1 receptor expression suggests some renal functional adaptation to induction of endothelial ET-1 overexpression and/or BP elevation. A large amount of renal ET receptor mRNA quantified by RT-QPCR might be coming from the tubular system since the collecting duct (CD) is a major renal site of ET receptor expression.<sup>26</sup> Furthermore, CD is also a major site of production of ET-1, an increase in extracellular fluid volume increases the expression of ET-1 in CD, and CD ET-1 KO mice present a reduction in sodium excretion and are hypertensive. An increase in endothelial ET-1 expression, ET-1 plasma level or the increase in BP could have affected the CD ET system and caused the increase in ET receptor expression. Further experiments to examine the regulation of CD ET system in the context of EC ET-1 overexpression could give further insight on mechanisms involved. Longer exposure to endothelial ET-1 overexpression and BP elevation could be required to cause more evident changes in

renal function and development of renal injury. It would also be interesting to determine whether the tamoxifen-treated ieET-1 mice have increased salt-sensitivity.

In conclusion, we generated a novel inducible EC-restricted *EDN1* overexpressing mouse. Twenty-one days of EC-restricted ET-1 overexpression caused ET-1-dependent BP elevation mediated by ET type A receptors, unaccompanied by vascular injury or evident alteration of kidney function or kidney injury.

### **Limitations**

Sex differences have been reported for both endothelin and NO systems (reviewed in<sup>28</sup>). In this study, the effects of the induction of ET-1 were determined only in male mice. Different results might be observed in female mice, which need to be addressed in another study. However, the results obtained in male mice translate to hypertension observed in men and postmenopausal women.

### **Perspectives**

Hypertension is the leading cause for heart disease and stroke, and the first cause of death and disease burden worldwide.<sup>29</sup> This novel mouse model of inducible endothelial restricted human ET-1 overexpression will facilitate understanding the role of ET-1 in the pathophysiology of hypertension and should stimulate development of novel ET-1 antagonists with fewer side effects than those currently available, improving our ability to successfully treat hypertension, particularly difficult to control or resistant hypertension, in order to improve outcomes of hypertensive subjects.

### **Acknowledgments**

We are grateful to our laboratory technicians (Adriana Cristina Ene, Heather Mlynarski and Guillem Colell Dinarès) and to Véronique Michaud, manager of the Lady Davis Institute for medical research imaging and phenotyping core, for excellent technical assistance.

**Funding Sources**

This work was supported by Canadian Institutes of Health Research (CIHR) grants 37917 and 102606, a Canada Research Chair (CRC) on Hypertension and Vascular Research by the CRC Government of Canada/CIHR Program and by the Canada Fund for Innovation (CFI), all to ELS, and by a fellowship to SCC and to JCFA from the program of Science without Borders (CsF) offered by the National Council for Scientific and Technological Development (CNPq) of Brazil.

**Disclosures**

None

## References

1. Yanagisawa M, Kurihara H, Kimura S, Tomobe Y, Kobayashi M, Mitsui Y, Yazaki Y, Goto K, Masaki T. A novel potent vasoconstrictor peptide produced by vascular endothelial cells. *Nature*. 1988;332:411-415.
2. Miyauchi T, Masaki T. Pathophysiology of endothelin in the cardiovascular system. *Annual review of physiology*. 1999;61:391-415.
3. Dhaun N, Goddard J, Kohan DE, Pollock DM, Schiffrin EL, Webb DJ. Role of endothelin-1 in clinical hypertension: 20 years on. *Hypertension*. 2008;52:452-459.
4. Rautureau Y, Schiffrin EL. Endothelin in hypertension: An update. *Current opinion in nephrology and hypertension*. 2012;21:128-136.
5. Saito Y, Nakao K, Mukoyama M, Imura H. Increased plasma endothelin level in patients with essential hypertension. *The New England journal of medicine*. 1990;322:205.
6. Schiffrin EL, Deng LY, Sventek P, Day R. Enhanced expression of endothelin-1 gene in resistance arteries in severe human essential hypertension. *Journal of hypertension*. 1997;15:57-63.
7. Lariviere R, Thibault G, Schiffrin EL. Increased endothelin-1 content in blood vessels of deoxycorticosterone acetate-salt hypertensive but not in spontaneously hypertensive rats. *Hypertension*. 1993;21:294-300.
8. Schiffrin EL, Lariviere R, Li JS, Sventek P, Touyz RM. Deoxycorticosterone acetate plus salt induces overexpression of vascular endothelin-1 and severe vascular hypertrophy in spontaneously hypertensive rats. *Hypertension*. 1995;25:769-773.
9. Blezer EL, Nicolay K, Goldschmeding R, Jansen GH, Koomans HA, Rabelink TJ, Joles JA. Early-onset but not late-onset endothelin-a-receptor blockade can modulate hypertension, cerebral edema, and proteinuria in stroke-prone hypertensive rats. *Hypertension*. 1999;33:137-144.

10. Ikeda T, Ohta H, Okada M, Kawai N, Nakao R, Siegl PK, Kobayashi T, Maeda S, Miyauchi T, Nishikibe M. Pathophysiological roles of endothelin-1 in Dahl salt-sensitive hypertension. *Hypertension*. 1999;34:514-519.
11. Kurihara Y, Kurihara H, Suzuki H, et al. Elevated blood pressure and craniofacial abnormalities in mice deficient in endothelin-1. *Nature*. 1994;368:703-710.
12. Kisanuki YY, Emoto N, Ohuchi T, Widyantoro B, Yagi K, Nakayama K, Kedzierski RM, Hammer RE, Yanagisawa H, Williams SC, Richardson JA, Suzuki T, Yanagisawa M. Low blood pressure in endothelial cell-specific endothelin 1 knockout mice. *Hypertension*. 2010;56:121-128.
13. Hofer B, Thone-Reineke C, Rohmeiss P, Schmager F, Slowinski T, Burst V, Siegmund F, Quertermous T, Bauer C, Neumayer HH, Schleuning WD, Theuring F. Endothelin-1 transgenic mice develop glomerulosclerosis, interstitial fibrosis, and renal cysts but not hypertension. *The Journal of clinical investigation*. 1997;99:1380-1389.
14. Shindo T, Kurihara H, Maemura K, et al. Renal damage and salt-dependent hypertension in aged transgenic mice overexpressing endothelin-1. *Journal of molecular medicine*. 2002;80:105-116.
15. Amiri F, Virdis A, Neves MF, Iglarz M, Seidah NG, Touyz RM, Reudelhuber TL, Schiffrin EL. Endothelium-restricted overexpression of human endothelin-1 causes vascular remodeling and endothelial dysfunction. *Circulation*. 2004;110:2233-2240.
16. Amiri F, Paradis P, Reudelhuber TL, Schiffrin EL. Vascular inflammation in absence of blood pressure elevation in transgenic murine model overexpressing endothelin-1 in endothelial cells. *Journal of hypertension*. 2008;26:1102-1109.
17. Schlaeger TM, Bartunkova S, Lawitts JA, Teichmann G, Risau W, Deutsch U, Sato TN. Uniform vascular-endothelial-cell-specific gene expression in both embryonic and adult transgenic mice. *Proceedings of the National Academy of Sciences of the United States of America*. 1997;94:3058-3063.
18. Bakris GL, Lindholm LH, Black HR, Krum H, Linas S, Linseman JV, Arterburn S, Sager P, Weber M. Divergent results using clinic and ambulatory blood

- pressures: Report of a darusentan-resistant hypertension trial. *Hypertension*. 2010;56:824-830.
19. Barhoumi T, Kasal DA, Li MW, Shbat L, Laurant P, Neves MF, Paradis P, Schiffrin EL. T regulatory lymphocytes prevent angiotensin ii-induced hypertension and vascular injury. *Hypertension*. 2011;57:469-476.
  20. Aries A, Paradis P, Lefebvre C, Schwartz RJ, Nemer M. Essential role of gata-4 in cell survival and drug-induced cardiotoxicity. *Proceedings of the National Academy of Sciences of the United States of America*. 2004;101:6975-6980.
  21. Korhonen H, Fisslthaler B, Moers A, Wirth A, Habermehl D, Wieland T, Schutz G, Wettschureck N, Fleming I, Offermanns S. Anaphylactic shock depends on endothelial gq/g11. *The Journal of experimental medicine*. 2009;206:411-420.
  22. Indra AK, Warot X, Brocard J, Bornert JM, Xiao JH, Chambon P, Metzger D. Temporally-controlled site-specific mutagenesis in the basal layer of the epidermis: Comparison of the recombinase activity of the tamoxifen-inducible cre-er(t) and cre-er(t2) recombinases. *Nucleic acids research*. 1999;27:4324-4327.
  23. Muzumdar MD, Tasic B, Miyamichi K, Li L, Luo L. A global double-fluorescent cre reporter mouse. *Genesis*. 2007;45:593-605.
  24. Guyton AC. Renal function curve--a key to understanding the pathogenesis of hypertension. *Hypertension*. 1987;10:1-6.
  25. Kohan DE, Barton M. Endothelin and endothelin antagonists in chronic kidney disease. *Kidney international*. 2014;86:896-904.
  26. Kohan DE, Rossi NF, Inscho EW, Pollock DM. Regulation of blood pressure and salt homeostasis by endothelin. *Physiological reviews*. 2011;91:1-77.
  27. Glenn ST, Jones CA, Gross KW, Pan L. Control of renin [corrected] gene expression. *Pflugers Archiv : European journal of physiology*. 2013;465:13-21.
  28. Vignon-Zellweger N, Relle K, Rahnenfuhrer J, Schwab K, Hoher B, Theuring F. Endothelin-1 overexpression and endothelial nitric oxide synthase knock-out induce different pathological responses in the heart of male and female mice. *Life sciences*. 2013

29. Lozano R, Naghavi M, Foreman K, et al. Global and regional mortality from 235 causes of death for 20 age groups in 1990 and 2010: A systematic analysis for the global burden of disease study 2010. *Lancet*. 2012;380:2095-2128.

## **Novelty and Significance**

### **1. What Is New?**

This is the first study that shows unambiguously that inducible human endothelin-1 overexpression will result in BP elevation in mice, and clearly demonstrates in this genetically engineered mouse the hypertensive effects of endothelin-1 mediated by ET<sub>A</sub> receptors.

### **2. What Is Relevant?**

Demonstration of the ET<sub>A</sub>-mediated hypertensive effect of human ET-1 should encourage the development of endothelin blockers for treatment of difficult to control or resistant hypertension in which the endothelin system is activated.

### **3. Summary**

Hypertension is the number one cause of morbidity and mortality worldwide, and is often uncontrolled or resistant to treatment. The endothelin (ET) system is activated particularly in difficult to control or resistant hypertension, or hypertension associated with chronic kidney disease or diabetes mellitus. However, the pressor significance in hypertension of endothelin-1, a potent vasoconstrictor, has been difficult to demonstrate. Here we show unambiguously that when transgenic human endothelin-1 overexpression is induced in endothelium of mice with a Cre/loxP tamoxifen system, it raises blood pressure via ET<sub>A</sub> receptors. These results should encourage the development of ET<sub>A</sub> receptor blockers for treatment of difficult to control or resistant hypertension, which has been slowed down by adverse effects of the antagonists developed in the past.

## Figures and tables

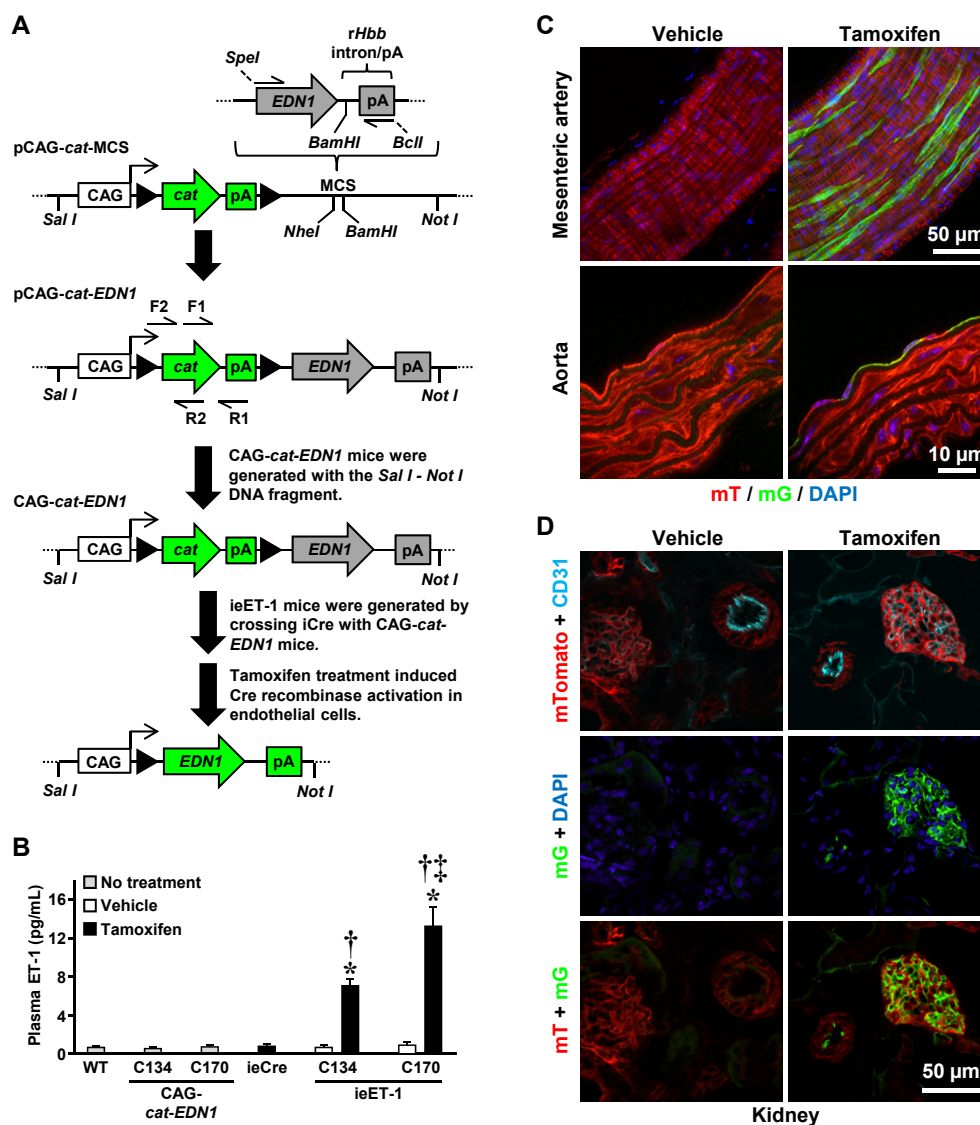


**Figure II-1. Inducible endothelium-restricted human endothelin-1 overexpression mice.**

**A.** The steps to generate the inducible endothelium-restricted human endothelin (ET)-1 (*EDN1*) overexpressing (ieET-1) mice are depicted. *rHbb*, rabbit  $\beta$ -globin; pA, polyadenylation signal; MCS, multiple cloning sites;  $\blacktriangleright$ , *loxP* site; CAG, ubiquitous human cytomegalovirus immediate early enhancer and chicken  $\beta$ -actin promoter; *cat*, chloramphenicol acetyltransferase; ieCre, mice expressing the tamoxifen-

inducible Cre recombinase CreER<sup>T2</sup> under the control of the angiopoietin-1 receptor *Tek* (also known as *Tie2*) promoter; right arrow linked to CAG box, initiation of the transcription site; half-arrows pointing to the right and left, primers used for genotyping and relative gene copy number determination (F1 and R1) and quantification of *cat* expression by reverse transcription/quantitative PCR (F2 and R2). **B.** Plasma ET-1 was determined in wild-type (WT), CAG-*cat*-EDN1-C134 and -C170, tamoxifen-treated ieCre, and vehicle- and tamoxifen-treated ieET-1-C134 and C170 mice. Data are presented as means  $\pm$  SEM, n = 13 for WT and 3-5 for the other groups. \* $P < 0.001$  vs. respective vehicle-treated ieET-1 group, † $P < 0.001$  vs. tamoxifen-treated ieCre and ‡ $P < 0.01$  vs. tamoxifen-treated ieET-1-C134. **C and D.** Tissue specificity of Cre activation was determined using vehicle- and tamoxifen-treated ieCre/*ROSA26*<sup>mT-mG/+</sup> reporter mice by determining the replacement of membrane-targeted tandem dimer tomato (mT) by membrane-targeted enhanced green fluorescent protein (mG) expression using confocal microscopy imaging. Representative mT (red) and mG (green) fluorescence images of mesenteric artery segments and aortic sections (**C**) and d mG, mT and the CD31 endothelium marker (cyan) fluorescence images of renal sections (**D**) are presented. Blue represents nuclear stain 4',6-diamidino-2-phenylindole (DAPI) fluorescence. n = 5 per group.

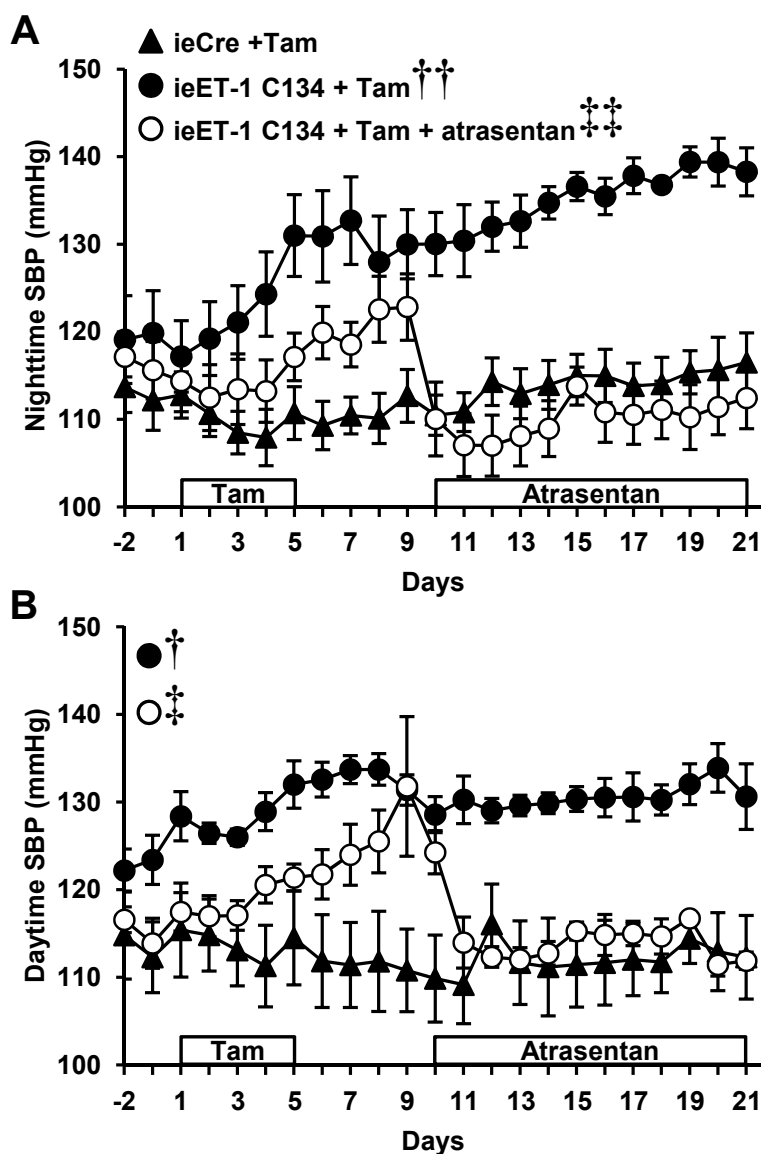


**Figure II-2. Induction of endothelin-1 overexpression in the endothelium increased systolic blood pressure in an endothelin type A receptor manner.**

Nighttime (A) and daytime (B) systolic blood pressure (SBP) were assessed by telemetry in ieCre treated with tamoxifen (Tam) and in ieET-1-C134 mice treated with Tam plus or minus the ET type A receptor blocker atrasentan from day 10 to the end of the study. The days of treatment with Tam and atrasentan are indicated by boxes. Data are presented as means  $\pm$  SEM,  $n = 4-5$ . † $P < 0.01$  and †† $P < 0.001$  vs. ieCre + Tam, and ‡ $P < 0.05$  and ‡‡ $P < 0.001$  vs. ieET-1-C134 + Tam.

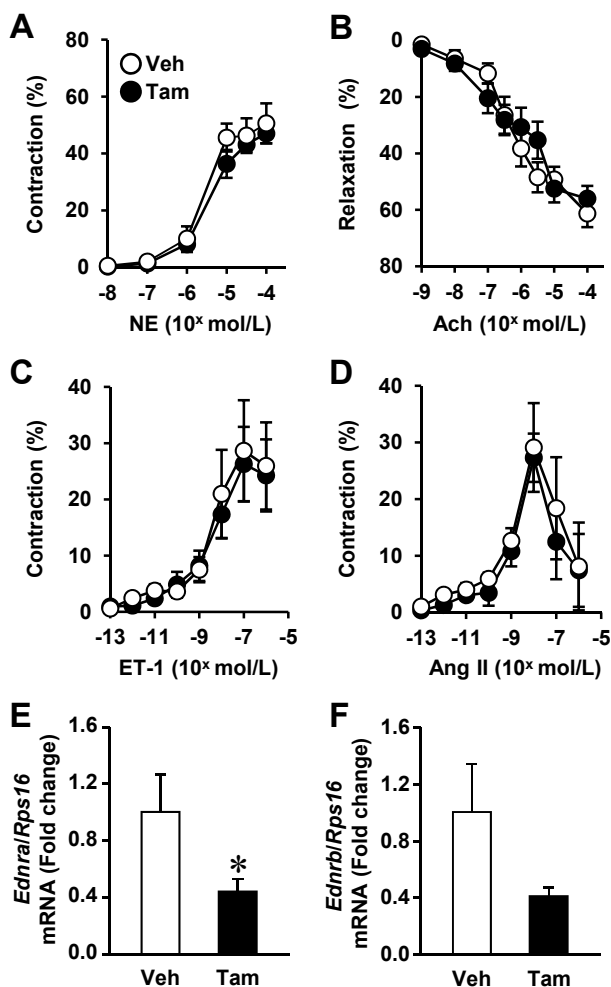


**Figure II-3. Induction of endothelin-1 overexpression in the endothelium did not cause vascular dysfunction in resistance arteries.**

Contractile responses to norepinephrine (NE, **A**), relaxation responses to acetylcholine (Ach, **B**), contractile responses to endothelin (ET)-1 (**C**) and angiotensin (Ang) II (**D**) and expression of the endothelin type A (*Ednra*, **E**) and B (*Ednrb*, **F**) receptors and ribosomal protein S16 (*Rps16*) mRNA were determined in mesenteric arteries of ieET-1-C134 mice treated with vehicle (Veh) or tamoxifen (Tam). The decrease in Ang II-induced contraction at concentration  $\geq 10^{-8}$  mol/L could be due to receptor desensitization. Data are presented as means  $\pm$  SEM, n = 5-8 for **A**, 4-5 for **B**, 5-7 for **C**, 5 for **D** and 5-7 for **E** and **F**. \**P* < 0.05 vs. Veh.

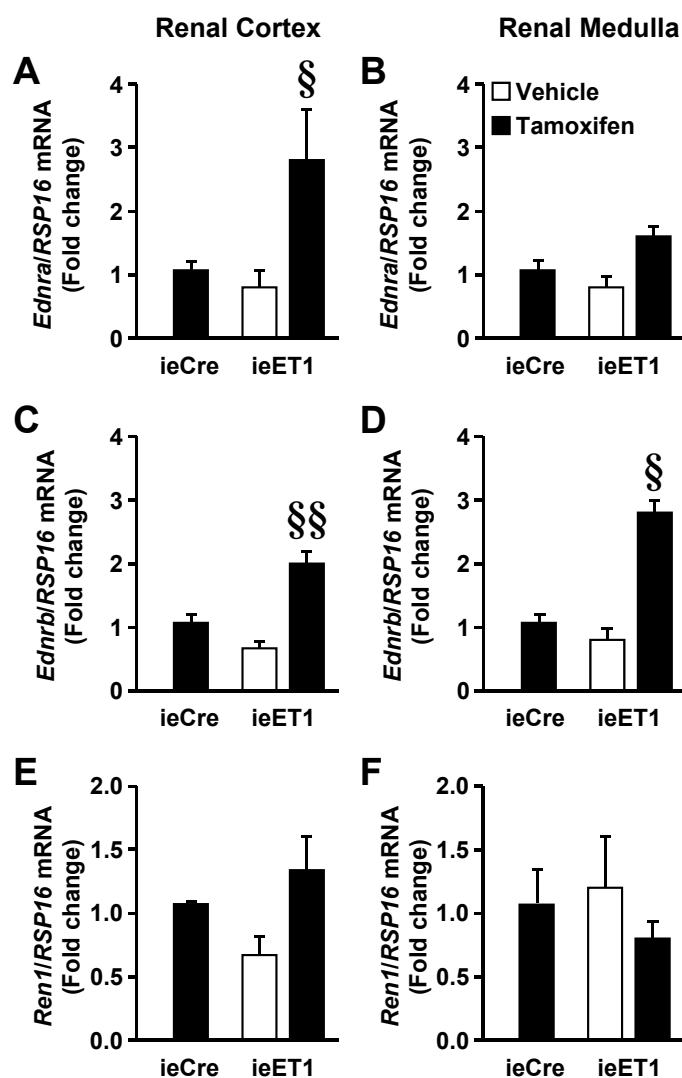


**Figure II-4. Induction of endothelin-1 overexpression in the endothelium was associated with an elevation in renal ET<sub>A</sub> and ET<sub>B</sub> receptors.**

The expression of the endothelin (ET) type A (*Ednra*, **A** and **B**) and B (*Ednrb*, **C** and **D**) receptors, renin (*Ren1*, **E** and **F**) and ribosomal protein S16 (*Rps16*) mRNAs was determined by reverse transcription/quantitative PCR in the renal cortex (**A**, **C** and **E**) and medulla (**B**, **D** and **F**) in tamoxifen-treated ieCre and ieET-1-C134 mice treated with vehicle or tamoxifen. Data are presented as means  $\pm$  SEM, n = 4-7. §*P*<0.05 and §§*P*<0.001 vs. combined other groups.

**Table II-1. Induction of ET-1 overexpression in the endothelium did not alter body or tissue weights**

Parameters	ieCre + tamoxifen	ieET-1- C134 tamoxifen	ieET-1- + C170 tamoxifen
n	11	9	7
BW (g)	27.7 ± 0.7	27.7 ± 1.0	26.6 ± 0.5
TL (mm)	18.50 ± 0.14	18.36 ± 0.20	18.37 ± 0.17
HW/TL (mg/mm)	7.44 ± 0.30	7.01 ± 0.21	6.62 ± 0.11
KW/TL (mg/mm)	18.7 ± 0.9	19.2 ± 0.5	19.2 ± 0.6
LuW/TL (mg/mm)	10.2 ± 0.7	10.9 ± 0.6	9.2 ± 0.6
LiW/TL (mg/mm)	77.0 ± 3.9	77.6 ± 2.8	72.7 ± 1.4
SW/TL (mg/mm)	4.80 ± 0.60	4.33 ± 0.12	4.43 ± 0.26

Body weight, tibia length (TL) and heart (HW), kidney (KW), lung (LuW), liver (LiW) and spleen (SW) weights were determined in tamoxifen-treated ieCre, ieET-1-C134 and ieET-1-C170 mice. n, number. Data are means ± SEM.

**Table II-2. Induction of endothelin-1 overexpression in the endothelium did not cause vascular remodeling in resistance arteries**

Parameters	Vehicle	Tamoxifen
n	5	9
Media/lumen (%)	4.30 ± 0.51	4.51 ± 0.27
Media cross-sectional area (μm <sup>2</sup> )	5956 ± 609	6160 ± 408

Media/lumen and media cross-sectional area (CSA) were determined in mesenteric arteries of ieET-1-C134 mice treated with vehicle or tamoxifen pressurized at 45 mmHg. n, number. Data are means ± SEM.

**Table II-3. Induction of endothelin-1 overexpression in the endothelium did not affect renal perfusion and function or cause renal injury**

Parameters	ieCre Tamoxifen	+ ieET-1- C134 + Veh	ieET-1- C134+ Tamoxifen
Renal artery diameter (mm)	0.40 ± 0.00	0.42 ± 0.03	0.40 ± 0.02
Renal artery flow (mL/min)	1.71 ± 0.16	1.96 ± 0.32	1.58 ± 0.19
Heart rate (bpm)	536 ± 8	536 ± 8	533 ± 5
Resistive index (arbitrary units)	0.77 ± 0.05	0.79 ± 0.05	0.69 ± 0.04
Sodium/Creatinine (mmol/mg)	0.45 ± 0.05	0.44 ± 0.04	0.47 ± 0.04
Potassium/Creatinine (mmol/mg)	1.31 ± 0.08	1.25 ± 0.06	1.24 ± 0.08
Urea/Creatinine (mmol/mg)	6.39 ± 0.30	6.26 ± 0.30	6.07 ± 0.30
Protein/Creatinine	1.17 ± 0.23	0.68 ± 0.07	0.86 ± 0.22
Nephrin/Creatinine (µg/mg)	1.71 ± 0.54	2.12 ± 0.33	2.07 ± 0.33
Lipocalin-2/Creatinine (ng/mg)	115 ± 7	123 ± 9	126 ± 7

Renal perfusion, function and damage were determined in tamoxifen-treated ieCre and vehicle- and tamoxifen-treated ieET-1-C134 mice. Renal perfusion was evaluated by measuring renal artery diameter, renal artery flow, heart rate and resistive index by echography using two-dimensional short axis view and pulse wave Doppler of the right renal artery. Renal function was assessed with the sodium/creatinine, potassium/creatinine and urea/creatinine, and renal injury with the protein/creatinine, nephrin/creatinine and Lipocalin-2/creatinine, all measured in the 24-h urine collected in metabolic cages. Data are presented as means ± SEM, n = 5-6 for renal perfusion and 5-7 for renal function, protein excretion and 5–6 for nephrin and lipocalin-2.

## Expanded materials and methods

### Engineering of the Cre-inducible endothelin-1 expression vector.

The Cre-inducible endothelin (ET)-1 expression vector was constructed using the pCAG-*cat*-MCS.21 expression vector (generous gift of Dr. Thomas N. Sato, Nara Institute of Science and Technology, Ikoma, Nara, Japan). This vector contains a ubiquitous cytomegalovirus immediate early enhancer/chicken  $\beta$ -actin promoter (CAG) driving the expression in all cell types, followed by a chloramphenicol acetyltransferase (*cat*) cDNA and a polyadenylation signal, which are flanked by loxP sites, and multiple cloning sites (MCS.21) (Fig. II-S1A). A DNA fragment containing the human ET-1 (*EDN1*) cDNA, a rabbit  $\beta$ -globin (*rHbb*) intron and polyadenylation signal (pA) was amplified from the p*Tie2*-ppET-1 plasmid used to generate our previous transgenic eET-1 mouse,<sup>1</sup> by PCR with Platinum® Pfx DNA polymerase (Life Technologies, Burlington, ON, Canada) using forward and reverse oligonucleotides containing *SpeI* and *BclI* restriction sites, respectively, and a GATC cap (Table II-S1). The transgenic DNA fragment was subcloned into the multiple cloning sites of pCAG-*cat*-MCS expression vector using *NheI* and *BamHI* restriction sites that have compatible cohesive ends to *SpeI* and *BclI*, respectively, to generate the pCAG-*cat*-*EDN1* expression vector. The subcloned DNA fragment was sequenced completely to ensure that artifactual mutations were not introduced accidentally by the Platinum® Pfx DNA polymerase (see Table S1 for sequencing primers).

### Generation of transgenic CAG-*cat*-*EDN1* founder mouse lines.

The pCAG-*cat*-*EDN1* plasmid was digested with *NotI* and *Sall* to free the CAG-*cat*-*EDN1* transgene from the vector backbone. One hundred  $\mu$ g of plasmid was digested with 150 Units of *NotI* in a final volume of 200  $\mu$ L overnight at 37°C. After confirmation of complete plasmid digestion by agarose gel electrophoresis, the *NotI* digesta was heat-inactivated at 65°C for 20 min. The buffer of the digestion was adjusted to perform the *Sall* digestion with 150 Units in a final volume of 500  $\mu$ L for 7 h at 37°C. Complete digestion of the plasmid was confirmed by agarose gel electrophoresis. Digested DNA and the picture of the gel with the transgenic fragment circle were sent to the

Microinjection and Transgenesis core facility of IRCM (Montreal, QC, Canada) for generation of transgenic mice. In brief, DNA was microinjected into the pronuclei of E0.5 zygotes F1 obtained from C3H crossed with C57BL/6 mice. Injected zygotes were transferred back into the oviducts of CD-1 pseudo-pregnant mice. Pups were weaned, identified and a 3 mm piece of tail was cut and stored in a sterile 1.5 mL microtube at -20°C for genotyping. Mice were housed at the Microinjection and Transgenesis core facility until mice positive for the transgene have been identified. Genotyping was performed by PCR (see **Genotyping**).<sup>2-4</sup> Fourteen out of 132 pups were found positive for the transgene. Ten transgenic founder mice were transferred to our mouse facility. Founders were backcrossed with C57BL/6 mice.

### **Selection of two CAG-*cat*-EDN1 transgenic lines for experimentation.**

In order to exclude a phenotype dependent on the site of integration of the transgene, two mouse founder transgenic lines were selected for the study as follows.

Seven out of the ten mouse founders transmitted the transgene to the F1 generation and were further studied.

Transgenic mice containing one integration site were determined as follows. The relative copy number of *CAG-cat-EDN1* in pups of F1 and F2 generations was determined by quantitative PCR (QPCR) for each transgenic line. No difference in the number *CAG-cat-EDN1* copy was observed between F1 and F2 descendent for each of the mouse lines, which suggest a unique site of integration. No mice were eliminated at this point.

Finally, the expression of *cat* transgene was used as a predictor for the expression of the *EDN1* transgene after activation by Cre recombinase to complete the selection of the transgenic mouse lines. The relative mRNA expression level of the *cat* transgene for all transgenic lines was determined in cardiac ventricles by reverse transcription (RT) followed by QPCR. The ventricles were obtained by removing the base of the heart and the atria. The ventricles were snap frozen in liquid nitrogen and stored at -80°C until used. Six transgenic mouse lines were studied, and the expression levels of *cat* were in the same range  $\pm$  1-fold. The transgenic mouse lines C134 and C170 named after their founders, who presented 2-fold different expression levels were

selected. When studied at the F2 generation, the *cat* relative expression level was  $1.23 \pm 0.08$  for the C134 mouse line ( $n = 6$ ) and  $0.45 \pm 0.03$  for the C170 mouse line ( $n = 6$ ). Selected CAG-*cat-EDN1* C134 and C170 transgenic mice were backcrossed with C57BL/6 mice obtained from Harlan Laboratories (Indianapolis, IN). Transgenic mice at F4 and F5 generation were used in this study.

### **Generation of inducible endothelial-restricted human ET-1 overexpression (ieET-1) mice.**

The ieET-1 mice were generated by crossing the CAG-*cat-EDN1* C134 and C170 mice with an inducible endothelial Cre (ieCre) mouse, the bacterial artificial chromosome (BAC) transgenic *Tie2-CreER<sup>T2</sup>* mouse.<sup>5</sup> The ieCre mouse expresses a fusion protein of the Cre recombinase with the modified estrogen receptor (ER) binding domain (CreER<sup>T2</sup>)<sup>6</sup> under the control of the endothelium-restricted angiotensin-1 receptor (*Tek*, also known as *Tie2*) promoter. CreERT2 can be induced by tamoxifen but not by natural ER ligands.<sup>5</sup>

### **Generation of a Cre activation reporter mouse.**

The reporter mouse was generated by crossing the ieCre mice with *ROSA26<sup>mT-mG/mT-mG</sup>* mice (Jackson Laboratories, Bar Harbor, ME).<sup>7</sup> These mice express a loxP-flanked, membrane-targeted tandem dimer tomato (mT) followed by a pA, before Cre-mediated excision, and a membrane-targeted enhanced green fluorescent protein (mG) followed by a pA, after excision, under the control of the CAG promoter driving the expression in all cell types. *ROSA26<sup>mT-mG/mT-mG</sup>* mice were crossed with ieCre mice to generate the reporter ieCre/*ROSA26<sup>mT-mG/+</sup>* mouse.

### **Genotyping.**

DNA was extracted using a quick method<sup>2</sup> with a modification.<sup>3</sup> Ninety  $\mu\text{L}$  of basic digestion buffer (25 mM NaOH and 0.2 mM EDTA, pH 12) was added to the tubes containing the piece of tail, and the mixture was heated at 95°C for 45 min. Then, the tubes were vortexed to ensure tissue disruption and maximal DNA release. The remaining material and lysis solution was brought down the tube by a quick

centrifugation at 12,000 x g, and incubation at 95°C was continued for an additional 15 min. At the end of the digestion, the tubes were vortexed and quickly centrifuged. Samples were stored at -20°C until used. Genotyping was done by PCR using 2 µL of supernatant tail digestion mixture.

Genotyping for *CAG-cat-EDN1* transgenic mice was done using TopTaq DNA polymerase kit (Qiagen, Mississauga, ON, Canada) by amplifying a 311 base pairs (bp) *cat* fragment contained within *CAG-cat-EDN1* transgene and a 516 bp fragment of MYB proto-oncogene protein gene (*Myb*) (Fig. II-S1A). *Myb* was used as an internal control to avoid any false-negative result. The oligonucleotides were designed to have a melting temperature ( $T_m$ ) of 60°C and a 3' GC clamp using Primer3 (Supplemental Table S1).<sup>4</sup> The PCR conditions were 3 min at 94°C, followed by 36 cycles of 1 min at 94°C, 1 min at 66°C and 1 min at 72°C.

Genotyping for *Tie2-CreER<sup>T2</sup>* (ieCre) transgenic mice was done using PCR by amplifying a 350 bp fragment containing a portion of *Tie2* gene and *CreER<sup>T2</sup>* transgene, and a 207 bp fragment of *Tie2* gene used as an internal control (Fig. II-S1B). These oligonucleotides sequences have been designed previously (Table II-S1).<sup>5</sup> The PCR conditions were 3 min at 94°C, followed by 35 cycles of 30 sec at 94°C, 30 sec at 60°C and 1 min at 72°C.

Genotyping for *ROSA26<sup>mT-mG/mT-mG</sup>* mice transgenic mice was done using PCR by amplifying a 250 bp fragment containing a portion of *Rosa26* gene and CAG promoter contained within *mT-mG* transgene and a 322 bp fragment of the *Rosa26* gene used as an internal control (Fig. II-S1C). These oligonucleotides sequences were obtained from Jackson Laboratories (Table II-S1). The PCR conditions were 3 min at 94°C, followed by 35 cycles of 30 sec at 94°C, 1 min at 61°C and 1 min at 72°C.

PCR products were run on a 2% agarose gel in 1x TAE (40 mM tris-acetate, 1 mM EDTA) buffer and picture taken (Fig. II-S1).

### ***CAG-cat-EDN1* transgene relative copy number.**

The relative copy number of *CAG-cat-EDN1* transgene was estimated by determining the ratio of the transgene over the  $\beta$ -actin (*Actb*) gene by QPCR. DNA was extracted from a segment of tail for each transgenic line as described in **Genotyping** section.

QPCR was performed with 2  $\mu$ L of supernatant tail digestion mixture diluted 50-times with water using the SsoFast EvaGreen Supermix (Bio-Rad Laboratories, Mississauga, ON, Canada) with the Mx3005P real-time PCR cycler (Agilent Technologies, Mississauga, ON, Canada). The QPCR conditions used were 2 min at 98°C, followed by 40 cycles of 5 sec at 98°C and 30 sec at 58°C. Oligonucleotides were designed with Primer3<sup>4</sup> as above to amplify a 311 bp fragment of *cat* contained within CAG-*cat-EDN1* transgene and a 207 bp fragment of *Actb* gene (Table II-S1).

#### **Confirmation of absence of CAG-*cat-EDN1* transgene leakage.**

Ten to 11-week old male CAG-*cat-EDN1*-C134 and CAG-*cat-EDN1*-C170 mice were treated for 5 days with tamoxifen (1 mg/kg/day, s.c.) and used 16 days later for determination of plasma ET-1 levels. Thirteen to 14-week old male C57BL/6 mice were used as reference for endogenous plasma ET-1 levels.

#### **Determination the tissue specificity and extend of Cre activation.**

Ten to 11-week old male ieCre/*ROSA26*<sup>*mT-mG/+*</sup> mice were treated for 5 days with tamoxifen as above or the vehicle (100  $\mu$ L of Miglyol 812, S.C., a generous gift of Unipex, Boucherville, QC, Canada) and used 16 days later to determine the tissue specificity and extend of Cre activation by determining the switch in expression of *mT* to *mG*.

#### **Effect of induction of ET-1 in endothelial cells on blood pressure regulation.**

Nine to 10-week old male ieCre and ieET-1-C134 and ieET-1-C170 mice were anesthetized with 3% isoflurane mixed with O<sub>2</sub> at 1 L/min. The depth of anesthesia was confirmed by rear foot squeezing. The non-steroidal anti-inflammatory drug carprofen (20 mg/kg) was administered subcutaneously to minimize the post-operation pain. The mice were then surgically instrumented with PA-C10 telemetry transmitters as recommended by the manufacturer (Data Sciences International, St. Paul, MN). Carprofen was administered as above once a day for the first 3 recovery days. Mice were allowed to recover for 7 additional days. Baseline blood pressure was determined every 5 min for 10 sec 2 days before treatment (Day -2 and, -1), during 5 days of

treatment with tamoxifen or vehicle as above, and during the 16 following days. An additional group of ieET-1-C134 mice was treated with tamoxifen as above, followed by the ET type A receptor blocker atrasentan (10 mg/kg/day p.o.) from day 10 to the end of the study.

### **Kidney function.**

Ten to 11-week old male ieCre and ieET-1-C134 mice were treated with tamoxifen or vehicle as above, and 24-hour urine was collected using metabolic cages to determine renal function during the two last days of the study. In addition, the renal artery flow and resistive index were determined by ultrasound.

### **Metabolic cages.**

Twenty-four-hour urine was collected as follows. In order to reduce stress, mice were first housed in metabolic cages (Tecniplast S.p.A., Buguggiate, VA, Italy) for two consecutive days, one week before the actual experiment to have them acclimatize to the environment and experimental procedure. On the last 2 study days, mice were housed in the metabolic cages, and 24-hour urine collection was initiated early in the morning (between 8 and 9 o'clock). Urine was collected at the end of the first 24-hour period. Food powder and feces attached to the urine collector system were removed by rinsing it extensively with water. The urine collector system was dried with paper towel and fixed to the metabolic cage for the second 24-hour urine collection. At the end of the experiment, 24-hour urine was collected, cleared by centrifugation at 10,000 *g* for 10 min, and stored at -80°C until used. Mice were anesthetized with isoflurane, and blood and tissues collected as described below. Water and foods were supplied *at libitum* during the whole procedure.

### **Renal artery flow and resistive index.**

Right kidney renal artery flow and resistive index were determined by ultrasound as follows. Briefly, the mice were anesthetized with 3 % isoflurane and 2 L/min O<sub>2</sub>. Depth of anesthesia was confirmed by rear foot squeezing. The mice were secured lightly on their chest on a warming pad, and their posterior right back was shaved. Echography

was performed using a Visual Sonic VEVO 770 ultrasound machine and a RMV™ 704 high frame rate scanhead with a center frequency of 40 MHz (VisualSonics Inc., Toronto, ON, Canada) as follows. The percentage of isoflurane was adjusted to maintain the heart rate (HR) between 500 and 550 beats/min. A two-dimensional short axis view of the right kidney was obtained and a view of the renal artery emerging from the aorta was positioned at the focus level. The pulse wave (PW) Doppler sample volume was positioned into the renal artery in the focal zone, the scanhead was angled to achieve a beam/flow angle of less than 60 degrees, and the PW Doppler spectrum was recorded. The heart rate (HR), renal artery velocity time integral (VTI), peak systolic velocity (PSV) and end diastolic velocity (EDV) were determined from the PW Doppler waveform on five consecutive beats located between two respirations. The renal artery diameter measured from a two-dimensional guided M-mode image, and HR were used to calculate the renal artery flow. The resistive index (RI) was calculated as follows.  $RI = (PSV-EDV)/PSV$ . Representative images of two-dimensional short axis view of the right kidney and PW Doppler spectrum of ieCre treated with tamoxifen, and in ieET-1-134 mice treated with vehicle or tamoxifen, are presented in Fig. II-S4.

### **Collection of tissues.**

At the end of the protocol, mice were weighed and then anesthetized with isoflurane as above, and blood collected by cardiac puncture on EDTA for plasma ET-1 determination. Blood samples were centrifuged at 1,000 g for 15 min at 4°C to remove blood cells, followed by centrifugation at 10,000 g for 10 min at 4°C to remove platelets. Plasma samples were stored at -80°C until tested. The mesenteric artery vascular bed was dissected with the intestine, and aorta, heart, lung, liver, two kidneys, spleen and tibia were harvested in ice-cold phosphate-buffered saline (PBS). Tissues were weighed and tibia length determined. Kidney sections were meticulously dissected under the microscope in order to separate renal cortex and medulla. Kidney sections and remaining tissues were frozen in liquid nitrogen and stored at -80°C until used.

For the study of vascular ET receptor mRNA expression, the mesenteric arcade was dissected away from the attached intestine under RNase-free conditions and stored immediately in RNAlater (Life Technologies) until RNA extraction.

For the determination of the tissue specificity and extent of Cre activation, *ieCre/ROSA26<sup>mT-mG/+</sup>* were anesthetized with 300-375 mg/kg IP of Avertin (2.5% solution of 1 mg/mL of 2,2,2-tribromoethanol dissolved in tert-amyl alcohol).<sup>8</sup> Depth of anesthesia was confirmed by rear foot squeezing. The mice were injected intraperitoneally with 100 USP units of sodium heparin (1000 USP units/mL), then perfused through the left ventricle at a constant pressure of 100 mmHg for 5 min with PBS to remove the blood, followed by 15 min perfusion with 4% paraformaldehyde (PFA). The mesenteric vascular bed, aorta, heart, kidneys and liver were collected in 4% PFA. Fat surrounding the mesenteric arteries was removed, and the vessels and other tissues were incubated in 4% PFA for 24 h with gentle agitation at 4°C. All tissues with exception of the mesenteric arteries were dehydrated by incubation in 30% sucrose in PBS for 24 h with gentle agitation at 4°C. Tissues were embedded in VWR Clear Frozen Section Compound (VWR international, Edmonton, AL, Canada) and stored at -80°C until used. The mesenteric arteries were stored in PBS at 4°C until imaged.

#### **Assesement of *mT* and *mG* expression.**

The expression of *mT* and *mG* was assessed by fluorescence microscopy imaging on 4- $\mu$ m thick cryosections or intact mesenteric artery segments. Four- $\mu$ m thick cryosections were stained with 4',6-diamidino-2-phenylindole (DAPI, 6  $\mu$ M, Life Technologies) for 20 min to label the nuclei. Isolated mesenteric arteries were whole-mount stained in nucleus staining solution overnight. Sections of tissues and isolated mesenteric arteries were mounted in Fluoromount (Sigma-Aldrich, St. Louis, MO) and imaged using a Wave FX Spinning Disc Confocal microscope (Quorum Technologies, ON, Canada).

The localization of endothelial cells within the tissue was determined by immunofluorescence in 4- $\mu$ m cryostat sections using CD31 staining. Tissue cryosections were permeabilized and blocked for 1 hour with buffer solution containing 50 mM of Tris, 150 mM of NaCl, 1% BSA, 0.4% Triton X-100 and 20% fetal bovine serum. Thereafter, sections were washed once with PBS. Sections were incubated overnight at 4°C with rat anti-mouse CD31 antibody (1:100, BD Biosciences Pharmingen, Ontario, CA). The sections were then washed 3 times with PBS and

incubated for 1 hour at room temperature with Alexa 647-conjugated goat anti-rat IgG antibody (1/200, Life Technologies). Sections were then washed 3 times with PBS and counterstained with DAPI and mounted with Fluoromount. Images were captured using Wave FX Spinning Disc Confocal microscope.

### **Assessment of endothelial function and vessel mechanics and structure.**

Second-order mesenteric arteries, of average lumen size  $\sim 220 \mu\text{m}$ , were dissected and mounted on a pressurized myograph as previously described.<sup>9</sup> Vessels were equilibrated for 45 min at 45 mmHg intraluminal pressure in Krebs solution (pH 7.4) containing (in mmol/L): 120 NaCl, 25 NaHCO<sub>3</sub>, 4.7 KCl, 1.18 KH<sub>2</sub>PO<sub>4</sub>, 1.18 MgSO<sub>4</sub>, 2.5 CaCl<sub>2</sub>, 0.026 EDTA and 5.5 glucose, bubbled continuously with 95% air and 5% CO<sub>2</sub>. Media and lumen diameter were measured by a computer-based video imaging system (Living Systems Instrumentation, Burlington, Virginia, USA). Contractile responses to cumulative concentrations of norepinephrine ( $10^{-8}$  to  $10^{-5}$  mol/L) were determined. Endothelium-dependent responses to acetylcholine ( $10^{-9}$  to  $10^{-4}$  mol/L) were determined in vessels precontracted with norepinephrine ( $10^{-5}$  mol/L). Contractile response to cumulative doses of ET-1 ( $10^{-12}$  to  $10^{-6}$  mol/L, Bachem, Torrance, CA) and angiotensin II ( $10^{-12}$  to  $10^{-6}$  mol/L, EMD Chemicals, San Diego, CA) were determined. Thereafter, vessels were perfused with Ca<sup>2+</sup>-free Krebs solution containing 10 mmol/L EGTA for 30 min to eliminate the tone. Media and lumen diameter were measured at 45 mmHg intraluminal pressure. Media cross-sectional area and media/lumen were calculated as previously described.<sup>10</sup>

### **Plasma and urine determinations.**

Plasma ET-1 was determined using a human Endothelin-1 QuantiGlo ELISA Kit (R&D Systems, Minneapolis, MN). Urinary sodium, potassium, urea, creatinine and protein were measured using a J&J Vitros 250 chemistry analyzer by Diagnostic Research Support Services at the Comparative Medicine and Animal Resource Centre of McGill University. Urinary nephrin and lipocalin-2 (also known as NGAL) were quantified using the Nephrin ELISA (Exocell, Philadelphia, PA) and Quantikine ELISA Mouse Lipocalin-2/NGAL Immunoassay (R&D Systems, Minneapolis, MN), respectively.

**Quantification of *cat*, *Ednra*, *Ednrb* and *Ren1* mRNA expression.**

The expression of chloramphenicol acetyltransferase (*cat*), ET type A and B receptor (*Ednra* and *Ednrb*), renin (*Ren1*) and ribosomal protein S16 (*Rps16*) was determined in cardiac ventricles or renal cortex and medulla or mesenteric arteries by RT-QPCR. RNA was extracted from frozen tissues using Trizol Reagent (Life Technologies) with a Polytron PT 1600 E homogenizer (Brinkmann Instruments, Mississauga, ON, Canada) and then processed as previously described.<sup>11</sup> The mesenteric arteries were dissected from surrounding tissues, perivascular fat and veins in RNAlater, then homogenized for 1 min with a Polytron PT 1600 E homogenizer and processed for total RNA extraction using the mirVana miRNA isolation kit (Life Technologies). RNA concentration was measured using a Nanodrop spectrophotometer ND-100 V3.1.2 (Thermo Fisher Scientific, Wilmington, DE) and RNA quality was assessed by determining the rRNA and mRNA profile by electrophoresis with a RNase free 1% agarose gel with 1X TAE electrophoresis buffer (2 M Tris-acetate and 50 mM EDTA). One and 0.4 µg of total RNA isolated from the frozen tissue and mesenteric arteries, respectively, were reverse-transcribed with the Quantitect RT kit (Qiagen). QPCR was performed using the SsoFast EvaGreen Supermix with the Mx3005P real-time PCR cyclers. Oligonucleotides for *cat*, *Ednra*, *Ednrb* and *Ren1* and *Rps16* were designed with Primer3 as above (Table II-S1). The QPCR conditions were 2 min at 96 °C, followed by 40 cycles of 5 sec at 96°C and 30 sec at 58°C. Results were normalized with *Rps16* and expressed as fold change over control.

**Data Analysis.**

Results are presented as means ± SEM. Blood pressure and plasma ET-1 data were compared by two-way analysis of variance (ANOVA) for repeated measures and one-way ANOVA respectively, all followed by a Student-Newman-Keuls *post-hoc* test. All other results were compared using a Student *t*-test or one-way ANOVA followed by a contrast *post-hoc* test, as appropriate.  $P < 0.05$  was considered statistically significant.

## References

1. Amiri F, Viridis A, Neves MF, Iglarz M, Seidah NG, Touyz RM, Reudelhuber TL, Schiffrin EL. Endothelium-restricted overexpression of human endothelin-1 causes vascular remodeling and endothelial dysfunction. *Circulation*. 2004;110:2233-2240.
2. Wang Z, Storm DR. Extraction of DNA from mouse tails. *BioTechniques*. 2006;41:410, 412.
3. Javeshghani D, Barhoumi T, Idris-Khodja N, Paradis P, Schiffrin EL. Reduced macrophage-dependent inflammation improves endothelin-1-induced vascular injury. *Hypertension*. 2013;62:112-117.
4. Rozen S, Skaletsky H. Primer3 on the www for general users and for biologist programmers. *Methods in molecular biology*. 2000;132:365-386.
5. Korhonen H, Fisslthaler B, Moers A, Wirth A, Habermehl D, Wieland T, Schutz G, Wettschureck N, Fleming I, Offermanns S. Anaphylactic shock depends on endothelial *gq/g11*. *The Journal of experimental medicine*. 2009;206:411-420.
6. Indra AK, Warot X, Brocard J, Bornert JM, Xiao JH, Chambon P, Metzger D. Temporally-controlled site-specific mutagenesis in the basal layer of the epidermis: Comparison of the recombinase activity of the tamoxifen-inducible *cre-er(t)* and *cre-er(t2)* recombinases. *Nucleic acids research*. 1999;27:4324-4327.
7. Muzumdar MD, Tasic B, Miyamichi K, Li L, Luo L. A global double-fluorescent *cre* reporter mouse. *Genesis*. 2007;45:593-605.
8. Aries A, Paradis P, Lefebvre C, Schwartz RJ, Nemer M. Essential role of *gata-4* in cell survival and drug-induced cardiotoxicity. *Proceedings of the National Academy of Sciences of the United States of America*. 2004;101:6975-6980.
9. Leibovitz E, Ebrahimian T, Paradis P, Schiffrin EL. Aldosterone induces arterial stiffness in absence of oxidative stress and endothelial dysfunction. *Journal of hypertension*. 2009;27:2192-2200.

10. Neves MF, Endemann D, Amiri F, Virdis A, Pu Q, Rozen R, Schiffrin EL. Small artery mechanics in hyperhomocysteinemic mice: Effects of angiotensin ii. *Journal of hypertension*. 2004;22:959-966.
11. Simeone SM, Li MW, Paradis P, Schiffrin EL. Vascular gene expression in mice overexpressing human endothelin-1 targeted to the endothelium. *Physiological genomics*. 2011;43:148-160.

## Supplemental figures and tables

Table II-S1. Oligonucleotides, product sizes and applications.

Gene	Primers	Product size (bp)	Application
<i>EDN1-rHbb</i>	F: 5' -GATC <u>ACTAGT</u> ATGGATTATTTGCTCATGATTTT-3' R: 5' -GATC <u>TGATCA</u> TGTCCTTCCGAGTGA-3'	1525	PCR subcloning of the <i>EDN1-rHbb</i> fragment
<i>EDN1-rHbb</i>	Seq: 5' -GGGACCCTTGATTGTTCTTTC-3' Seq: 5' -AAAATTCGTTACAAATGCAAGC-3' Seq: 5' -CCCTGAGTTCTTTTCCTGC-3'	N/A	Sequencing of the subcloned <i>EDN1-rHbb</i>
<i>cat</i>	F: 5' -TTTCGTCTCAGCCAATCCC-3' R: 5' -TGCCATTCATCCGCTTATTATC-3'	311	PCR genotyping and
<i>Myb</i>	F: 5' -GCCTGCTGTCCCTTCAGCTC-3' R: 5' -CCAGTCACGTTCCCTATCCT-3'	516	Control for CAG- <i>cat</i> - <i>Edn1</i>
<i>Actb</i>	F: 5' -cggtgctaagaaggctgttc-3' R: 5' -acctgggtcatcttttcacg-3'	272	Reference gene for QPCR copy
<i>Tie2</i> - CreER <sup>T2</sup>	F: 5' -GAAGTCGCAAAGTTGTGAGTTG-3' ( <i>Tie2</i> ) R: 5' -TGGCTTGCAGGTACAGGA-3' (CreER <sup>T2</sup> )	350	PCR genotyping of Tie2-CreER <sup>T2</sup> .
<i>Tie2</i>	F: 5' -GAAGTCGCAAAGTTGTGAGTTG-3' R: 5' -GAGAATGGCGAGAAGTCACTG-3'	207	Control for Tie2-CreER <sup>T2</sup>
<i>cat</i>	F: 5' -ATCCCAATGGCATCGTAAAG-3' R: 5' -TGCCATTCATCCGCTTATTATC-3'	314	RT-QPCR mRNA
<i>Ednra</i>	F: 5' -TGGCCCTTGGAGACCTTATC-3' R: 5' -GCTCGCCCTTGTATTCTGAAG-3'	339	RT-QPCR mRNA
<i>Ednrb</i>	F: 5' -TGTTTCGTGCTAGGCATCATC-3' R: 5' -CTGCTGTCCATTTTGAACC-3'	327	RT-QPCR mRNA
<i>Ren1</i>	F: 5' -ATCTTTGACACGGGTTTCAGC-3' R: 5' -AGAACACCGTCAAACCTTGGC-3'	278	RT-QPCR mRNA
<i>Rps16</i>	F: 5' -ATCTCAAAGGCCCTGGTAGC-3' R: 5' -ACAAAGGTAAACCCCGATCC-3'	211	Housekeeping gene

Forward (F) and reverse (R) oligonucleotides used to subclone by PCR the human endothelin-1/rabbit beta-globin transgene (*EDN1-rHbb*) contain respectively *Spe I* and *Bcl I* restriction sites (bold italic) and both a cap GATC sequence (underline). *Actb*,  $\beta$ -actin; *cat*, chloramphenicol acetyltransferase; *Ednra* and *Ednrb*, endotheline type A and B receptor; *Myb*, mouse transcriptional activator myeloblastosis; *Ren1*, renin; *Rps16*, 40S ribosomal protein S16; *Tie2-CreER<sup>T2</sup>*, a fusion protein of Cre recombinase with the modified estrogen receptor binding domain (CreER<sup>T2</sup>) under the control of the endothelium-specific *angiopoietin-1 receptor* (*Tie2* and alias of *Tek*) promoter.

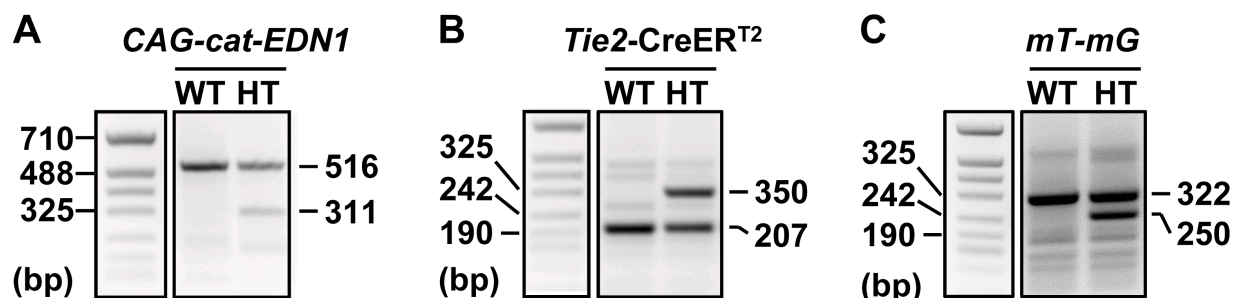


**Figure II-S1. Genotyping of mice for CAG-*cat-EDN1* (A), *Tie2-CreER<sup>T2</sup>* (B) and *ROSA26<sup>mT-mG/+</sup>* (c).**

Representative images of agarose gel for genotyping of wild-type (WT, **A-C**) and heterozygote (HT) *cat-EDN1* (**A**), *Tie2CreER<sup>T2</sup>* (**B**) and *ROSA26<sup>mT-mG/+</sup>* (**c**) mice are shown. **a.** CAG-*cat-EDN1* genotyping: PCR product of 516 base pairs (bp) is used for detection of *Myb* control gene (WT) and 311 bp for detection of CAG-*cat-EDN1* (*cat*) transgene. **B.** *Tie2-CreER<sup>T2</sup>* genotyping: PCR product of 207 bp is used for detection of *Tie2* gene (WT) and PCR product of 350 bp for detection of *Tie2-CreER<sup>T2</sup>* transgene (Cre). **C.** *ROSA26<sup>mT-mG/+</sup>*: PCR product of 322 bp is used for detection of *Rosa26* gene and 250 bp for detection of CAG promoter contained within *mT-mG* transgene. Sizes in bp on the left side of each panel are for the DNA ladder.

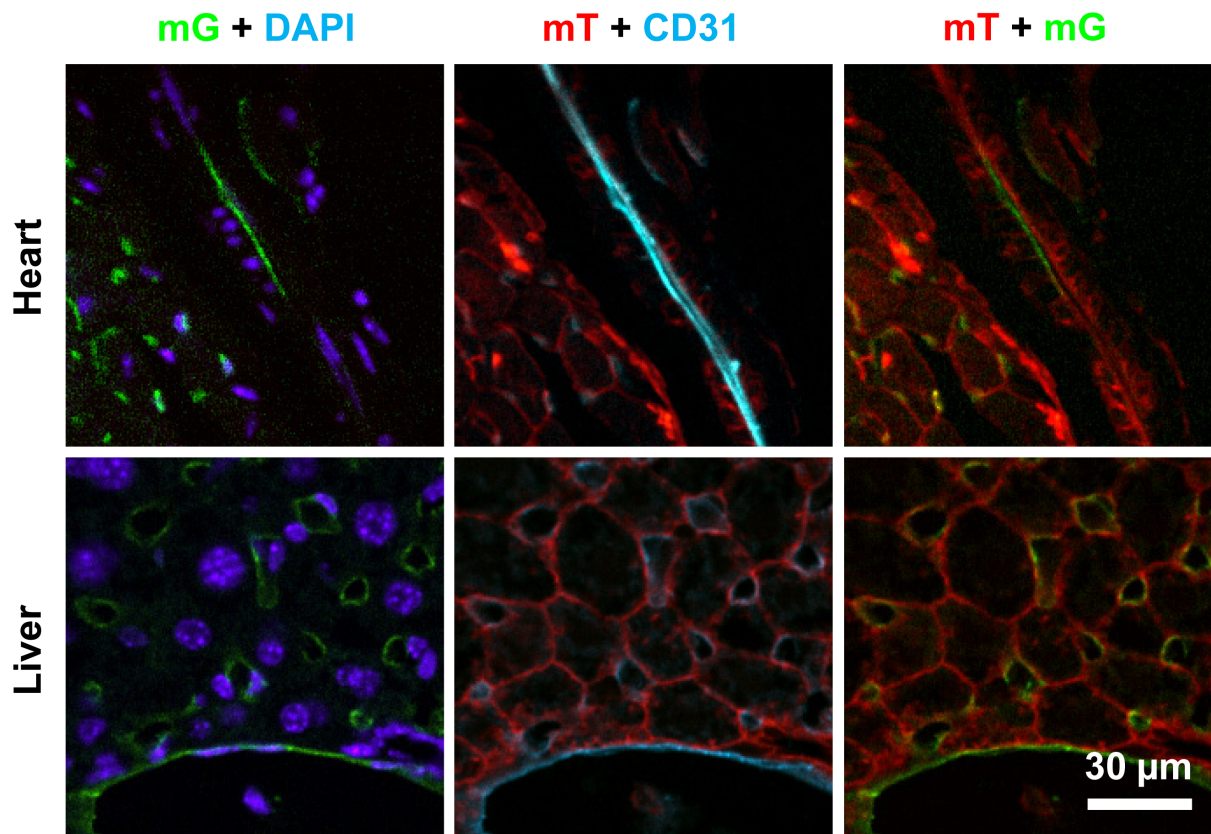


**Figure II-S2. Tissue specificity of Cre activation was determined using vehicle- and tamoxifen-treated  $ieCre/ROSA26^{mT-mG/+}$  reporter mice by determining the replacement of membrane-targeted tandem dimer tomato (mT) by membrane-targeted enhanced green fluorescent protein (mG) expression using confocal microscopy imaging.**

Representative mG, mT and the CD31 endothelium marker (cyan) fluorescence images of heart and liver sections are presented. Blue represents nuclear stain DAPI fluorescence.  $n = 5$  per group.

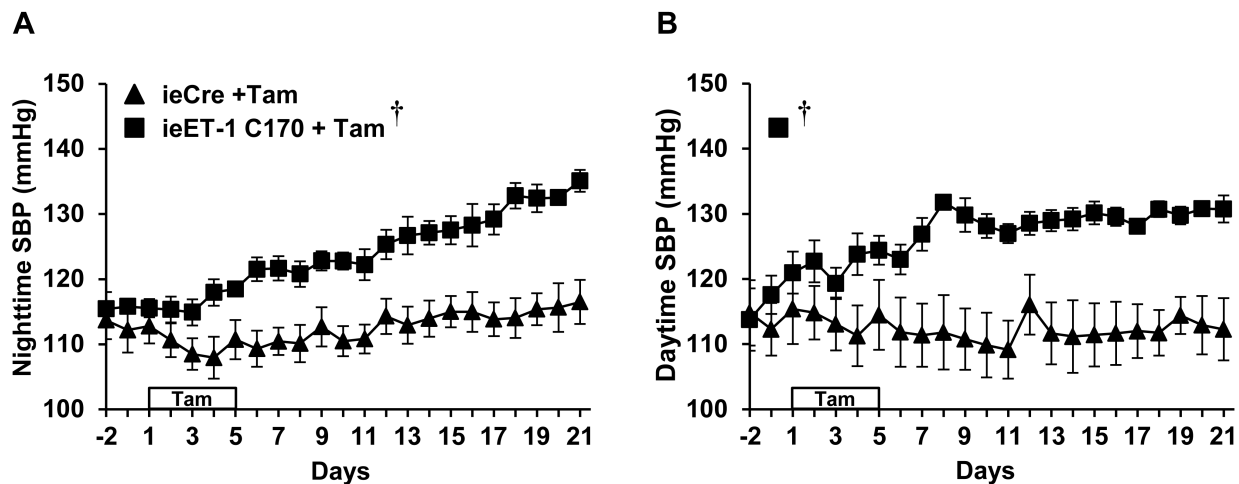


**Figure II-S3. Induction of endothelin-1 overexpression in the endothelium increased systolic blood pressure (SBP) in ieET-1-C170 mice.**

Nighttime (**A**) and daytime (**B**) SBP was assessed by telemetry in ieCre and in ieET-1-C170 mice treated with tamoxifen (Tam). Days of Tam treatment are indicated by a box. Data are presented as means  $\pm$  SEM,  $n = 5$ . † $P < 0.05$  vs. ieCre + TAM.

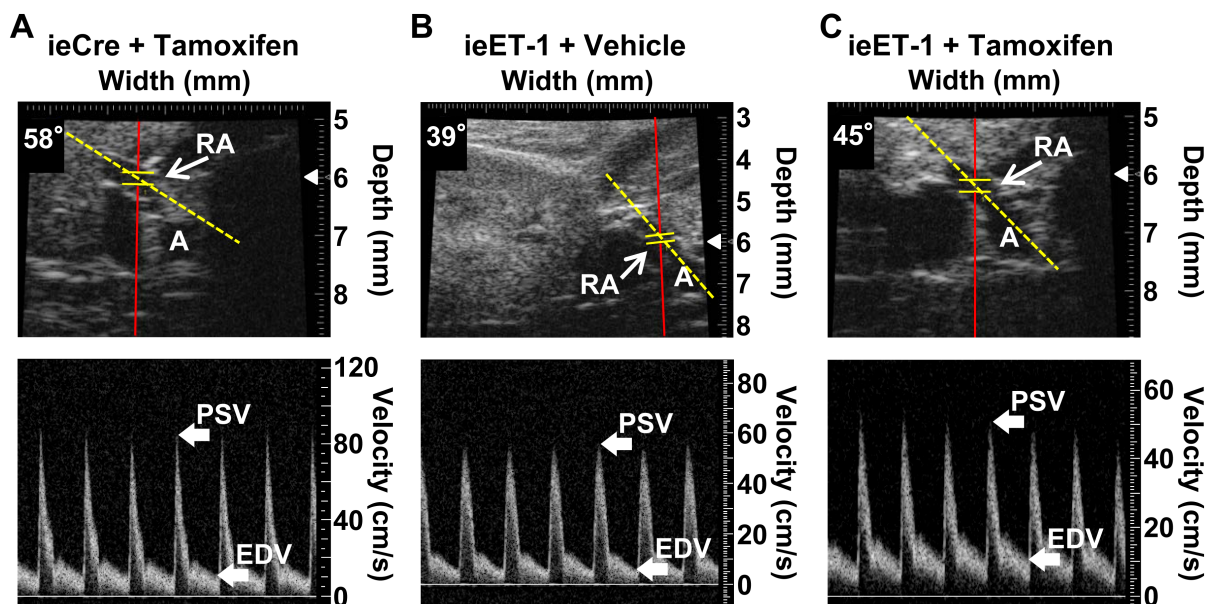


**Figure II-S4. Renal artery blood flow was determined by echography using two-dimensional short axis view and pulse wave (PW) Doppler as described in the Online Methods section.**

Representative images of two-dimensional short axis view of the right kidney (upper panels) and PW Doppler spectrum (lower panels) of ieCre treated with tamoxifen (A) and in ieET-1-134 mice treated with vehicle (B) or tamoxifen (C). The PW Doppler sample volume indicated by a pair of yellow lines was positioned into the renal artery (RA) at the focal zone indicated by an arrow head. The PW Doppler angle line (yellow dashed line) was positioned parallel to the blood flow. The PW angle was measured between the PW Doppler line of acquisition (red line) and PW Doppler angle line. Aorta, A, PSV, peak systolic velocity and EDV, end diastolic velocity.

**CHAPTER III: Three-month endothelial human endothelin-1 overexpression  
causes blood pressure elevation and vascular and kidney injury**

## Hypothesis and objectives

Plasma ET-1 is increased in patients with essential<sup>117</sup> and moderate-to-severe hypertension,<sup>115</sup> as well as in hypertension associated with other disorders such as chronic kidney disease and metabolic syndrome.<sup>284</sup> Several experimental hypertensive models such as DOCA-salt rats, DOCA-salt-treated SHR, stroke-prone SHR, Dahl salt-sensitive rats, Ang II-infused rats, and one-kidney, one-clip Goldblatt rats have shed light on the pathophysiological role of ET-1 in blood pressure elevation and vascular damage.<sup>104</sup> Generation of a constitutive eET-1 overexpressing transgenic mouse has further established the role of ET-1 in vascular inflammation,<sup>203, 283</sup> ROS-induced vascular damage<sup>127, 133</sup> in the absence of significant change in BP. Moreover, ET-1 overexpression exacerbated aortic atherosclerosis and triggered abdominal aortic aneurysm formation in Apoe<sup>-/-</sup> mice crossed with eET-1 mice under a high fat diet.<sup>144</sup> Some of the effects associated with the constitutive ET-1 overexpression might have been due, at least in part, to an ontogenic adaptation to life-long exposure to elevated ET-1 expression. Thus, ieET-1 mice were generated to study the pathophysiological role of ET-1 on BP regulation, and vascular and renal damage in the absence of potential developmental effects. In the first study, we demonstrated the successful generation of an inducible endothelium-restricted *EDN1* overexpressing transgenic mouse. In addition, we have shown that vasoconstriction induced by *EDN1* overexpression raised blood pressure via ET<sub>A</sub>R. Vascular and kidney injury were not observed at this time point of the study possibly due to the short time of ET-1 exposure. Thus, we sought to investigate whether longer exposure to endothelial ET-1 overexpression is associated with sustained BP elevation, and causes vascular and renal damage.

The specific objectives of this study include:

- To determine whether longer term (3 months) endothelial ET-1 overexpression causes BP elevation.
- To determine whether longer term (3 months) endothelial ET-1 overexpression induces damage and initiates inflammation in the vasculature and kidneys.

**Three-month endothelial human endothelin-1 overexpression causes blood pressure elevation and vascular and kidney injury**

Suellen C. Coelho<sup>1</sup>, Olga Berillo<sup>1</sup>, Antoine Caillon<sup>1</sup>, Sofiane Ouerd<sup>1</sup>, Júlio C. Fraulob-Aquino<sup>1</sup>, Tlili Barhoumi<sup>1</sup>, Stefan Offermanns<sup>3</sup>, Pierre Paradis<sup>1</sup>, Ernesto L. Schiffrin<sup>1,2</sup>

<sup>1</sup>Hypertension and Vascular Research Unit, Lady Davis Institute for Medical Research and <sup>2</sup>Department of Medicine, Sir Mortimer B. Davis-Jewish General Hospital, McGill University, 3755 Côte-Ste-Catherine Rd., Montreal, Montréal, Quebec, Canada, H3T 1E2; <sup>3</sup>Department of Pharmacology, Max-Planck-Institute for Heart and Lung Research, Ludwigstraße 43, 61231 Bad Nauheim, Germany.

Published in: Hypertension. 2017

The manuscript is presented here according to the instructions of the journal in which it was published. The main manuscript is followed by the Online Supplemental material (including the expanded materials and methods section).

## Abstract

Endothelium-derived endothelin (ET)-1 has been implicated in the development of hypertension and end-organ damage but its exact role remains unclear. We have shown that tamoxifen-inducible endothelium-restricted human ET-1 overexpressing (ieET-1) mice exhibited blood pressure (BP) rise after 3-week induction in an ET type A receptor (ET<sub>A</sub>R)-dependent manner, in absence of vascular and renal injury. It is unknown whether long-term ET-1 overexpression results in sustained BP elevation and vascular and renal injury. Adult male ieET-1 and control tamoxifen-inducible endothelium-restricted Cre recombinase (ieCre) mice were induced with tamoxifen and 2.5 months later were treated or not with the ET<sub>A</sub>R blocker atrasentan for 2 weeks. Three-month induction of endothelial human ET-1 overexpression increased BP ( $P<0.01$ ), reduced renal artery flow ( $P<0.001$ ), caused mesenteric small artery (MA) stiffening ( $P<0.05$ ) and endothelial dysfunction ( $P<0.01$ ). These changes were accompanied by enhanced MA *Col1A1* and *Col3A1* expression, and perivascular adipose tissue oxidative stress ( $P<0.05$ ) and monocyte/macrophage infiltration ( $P<0.05$ ). Early renal injury was demonstrated by increased kidney injury molecule-1 expression in renal cortex tubules ( $P<0.05$ ), with however undetectable lesions using histochemistry staining, and unchanged urinary albumin. There was associated increased myeloid (CD11b<sup>+</sup>) and myeloid-derived suppressive cell (CD11b<sup>+</sup>Gr-1<sup>+</sup>) renal infiltration ( $P<0.01$ ) and greater frequency of myeloid and renal cells expressing the pro-inflammatory marker CD36 ( $P<0.05$ ). Atrasentan reversed or reduced all of the above changes ( $P<0.05$ ) except the endothelial dysfunction and collagen expression and reduced renal artery flow. These results demonstrate that long-term exposure to endothelial human ET-1 overexpression causes sustained BP elevation and vascular and renal injury via ET<sub>A</sub>R.

**Keywords:** Endothelial human endothelin-1, hypertension, vascular injury, kidney injury, inflammation

## Introduction

Endothelin (ET)-1 was first described as a potent vasoconstrictor peptide.<sup>1</sup> The primary source of ET-1 is vascular endothelial cells (EC), but it is also produced by other cell types.<sup>2</sup> ET-1 mediates its actions through activation of G protein-coupled ET type A (ET<sub>A</sub>) and B (ET<sub>B</sub>) receptors. ET-1 secreted by EC acts in paracrine fashion to cause constriction of underlying vascular smooth muscle cell (VSMC) mostly through ET<sub>A</sub> receptors. ET-1 has also been reported to act in autocrine fashion on EC ET<sub>B</sub> receptors to induce relaxation mostly through release of nitric oxide (NO), but also prostacyclin or endothelium derive hyperpolarizing factor, depending on vascular bed. ET<sub>B</sub> receptors also play a role in the clearance of ET-1 in the lungs, liver and kidney, and on natriuresis and diuresis in the kidney.

Although ET-1 participates in physiological regulation of BP and vascular function, dysregulation of endothelial ET-1 (eET-1) expression could lead to hypertension and vascular and kidney injury.<sup>3</sup> ET-1 is elevated in plasma of patients with essential hypertension<sup>4</sup> and in small artery ECs of gluteal subcutaneous tissue of moderate-to-severe hypertensive subjects.<sup>5</sup> Moreover, ET-1 blockade decreased BP in patients with essential hypertension<sup>6,7</sup> and resistant hypertension.<sup>8</sup> Vascular ET-1 expression was increased in salt-dependent rat models of experimental hypertension, such as deoxycorticosterone acetate (DOCA)-salt treated uninephrectomized rats,<sup>9</sup> DOCA-salt treated rats,<sup>10</sup> DOCA-salt treated spontaneously hypertensive rats (SHR)<sup>11</sup> and stroke-prone SHR (SHR-SP).<sup>12</sup> ET receptor blockade reduced blood pressure (BP) and vascular remodeling in DOCA-salt uninephrectomized rats, DOCA-salt rats and SHR-SP.<sup>9,10,12</sup> Genetic loss- and gain-of-function approaches have as well demonstrated the importance of eET-1 in BP regulation. Indeed, plasma ET-1 was reduced by 80% and systolic BP (SBP) by ~10 mm Hg in mice with EC restricted ET-1 gene disruption.<sup>13</sup> Moreover, we have shown using tamoxifen-inducible EC-restricted human ET-1 overexpression (ieET-1) mice that after three week induction BP rises in an ET<sub>A</sub> receptor-dependent manner.<sup>14</sup> However, ieET-1 mice did not develop vascular or renal injury.

We hypothesized that a longer exposure to eET-1 overexpression and sustained BP rise may be necessary to cause vascular and kidney injury. In order to test this hypothesis, we determined whether 3 months (long-term) exposure to eET-1 overexpression will cause sustained BP rise and vascular and renal damage. In addition, oxidative stress and immune cell infiltration were examined since they have been implicated in the development of small artery dysfunction, remodeling and stiffening that result in elevated peripheral resistance and finally lead to target organ damage, such as renal injury.<sup>15-19</sup>

## Methods

Detailed Methods are available in the online-only Data Supplement.

## Experimental design

This study was approved by the Animal Care Committee of the Lady Davis Institute for Medical Research and McGill University, followed recommendations of the Canadian Council for Animal Care and was in agreement with the Guide for the Care and Use of Laboratory Animals published by the US National Institutes of Health. Control mice expressing a tamoxifen-inducible Cre recombinase (CreER<sup>T2</sup>)<sup>20</sup> under the control of endothelium-specific *Tie2* promoter (named hereafter ieCre) and ieET-1 mice have been previously described<sup>14,21</sup> and were generated in our animal facility. The endothelial specificity of tamoxifen-induced Cre recombination was demonstrated previously<sup>14</sup> in MAs, aorta, heart, liver and kidney using ieCre mice crossed with *ROSA26*<sup>mT-mG/+</sup> reporter mice, which expressed a loxP-flanked, membrane-targeted tandem dimer tomato (mT), before Cre mediated excision, and a membrane-targeted enhanced green fluorescent protein (mG) after excision, under the control of the CMV enhancer/chicken  $\beta$ -actin promoter (CAG) promoter driving the expression in all cell types. Nine-to-12 week-old male ieCre and ieET-1 mice were treated with tamoxifen (1 mg/day, S.C.) for 5 days and studied 3 months later. As previously described,<sup>14</sup> 24-hour urine was collected using metabolic cages to determine urinary albumin and creatinine in the week before or after the third month, and renal artery flow was determined using ultrasound

the following day. At the end of the protocol, mice were weighed, anesthetized with isoflurane and blood was collected by cardiac puncture on EDTA for plasma ET-1 determination. The mesenteric artery (MA) vascular bed was harvested with the intestine in ice-cold Krebs solution. The heart, lung, kidneys and right tibia were harvested in ice-cold phosphate buffered saline (PBS). Tissues were weighed and tibia length determined. The right kidney was used for immune cell profiling by flow cytometry. Second-order MA was used for determination of endothelial function and vascular mechanics by pressurized myography. Sections of MAs with perivascular adipose tissue (PVAT) and the left kidney were embedded in VWR Clear Frozen Section Compound (VWR International, Edmonton, AB, Canada) for determination of reactive oxygen species (ROS) production, fibronectin, monocyte chemoattractant protein (MCP)-1 or kidney injury molecule (KIM)-1 expression or monocyte/macrophage and T cell infiltration by immunofluorescence. Sections of MAs and left kidney were fixed in 4% paraformaldehyde in PBS for 48 h at 4°C and embedded in paraffin for investigation of collagen content with Sirius red staining, kidney injury using Masson's trichrome and Periodic Acid Schiff (PAS) staining or immune cell infiltration using CD45 immunohistochemistry.

In a subgroup of tamoxifen-treated ieCre and ieET-1 mice, blood pressure (BP) was determined by telemetry as described previously.<sup>22</sup> BP was assessed during the last 2 days of the third-month period and thereafter mice were studied as above.

Another subset of tamoxifen-treated ieET-1 mice were treated with the ET type A receptor blocker, atrasentan (10 mg/kg/day PO) mixed with the food, during the last two weeks of the third month. BP was determined by telemetry two days before and during atrasentan treatment, and thereafter mice were studied as above.

A separate group of ieCre and ieET-1 mice treated or not with atrasentan was used to examine the long-term effects of eET-1 overexpression on the expression of ET type A (*Ednra*) and B (*Ednrb*) receptors, collagen type I alpha 1 (*Col1A1*) and III alpha 1 (*Col3A1*) and renin (*Ren1*) in MAs or kidney by reverse transcription/quantitative PCR.

### **Data analysis**

Results are presented as means  $\pm$  SEM. Data were compared with two-way analysis of variance (ANOVA) for repeated measures or one-way ANOVA, with all ANOVA tests followed by a Student–Newman–Keuls *post-hoc* test, or with an unpaired *t*-test, as appropriate. Correlations were evaluated with a Pearson test.  $P < 0.05$  was considered statistically significant.

### **Results**

#### **Long-term induction of endothelial human ET-1 overexpression increased plasma ET-1 levels and blood pressure in ET<sub>A</sub> receptor-dependent manner**

Three months after tamoxifen injections, plasma ET-1 levels were 11-fold higher in ieET-1 mice compared to ieCre mice, and was unaffected by ET<sub>A</sub> receptor blockade with atrasentan (Figure III-S1 in online-only Data Supplement). Mean hour SBP and diastolic BP (DBP) were 22 and 16 mm Hg higher respectively, and heart rate (HR) unchanged in ieET-1 mice compared to ieCre mice (Figure III-1A and Figure III-S2A and B in online-only Data Supplement). The BP elevation was ET<sub>A</sub> receptor-dependent, since treatment with atrasentan reversed nighttime and daytime SBP rise in ieET-1 mice (Figure III-1B). DBP tended to be lower whereas HR was unchanged in atrasentan treated ieET-1 compared to control ieET-1 mice (Figure III-S2C and D in online-only Data Supplement). Body weight, heart, lung and kidney weight were unaffected by the long-term induction of eET-1 overexpression or atrasentan treatment (Table III-S1 in online-only Data Supplement).

#### **Long-term induction of endothelial human ET-1 overexpression induced mesenteric artery endothelium dysfunction**

Contractile responses to norepinephrine were similar between groups (Figure III-S3A in online-only Data Supplement). Maximal relaxation response to acetylcholine in vessels pre-contracted with norepinephrine was decreased by 48% in ieET-1 mice compared to ieCre mice, and was not corrected by atrasentan treatment (Figure III-2A). Vasodilatory responses to acetylcholine were completely abrogated by the NO synthase inhibitor N<sup>ω</sup>-

nitro-L-arginine methyl ester in all groups (Figure III-S3B in online-only Data Supplement), indicating that NO was the major mediator of the vasodilator response. Endothelium-independent relaxation responses to the NO donor, sodium nitroprusside, were similar in all groups (Figure III-S3C in online-only Data Supplement), suggesting that MA vasodilatory impairment was not due to a vascular smooth muscle defect.

### **Long-term induction of endothelial human ET-1 overexpression caused mesenteric artery stiffening**

eET-1 overexpression caused MA stiffening in ieET-1 mice, as indicated by a leftward displacement of the stress-strain curves compared to ieCre mice (Figure III-2B). Vascular stiffening was normalized by treatment with atrasentan. In contrast, long-term exposure to eET-1 overexpression did not cause vascular remodeling, as MA media/lumen and media cross-sectional area were similar in all groups (Figure III-S3D-E).

### **Long-term induction of endothelial human ET-1 overexpression increased oxidative stress in perivascular adipose tissue of mesenteric arteries**

To explain the endothelial dysfunction, ROS generation was studied in the media and perivascular adipose tissue (PVAT) of MA. ROS generation was unaltered in MA media but increased 1.4-fold in the MA PVAT (Figure III-2C-D and Figure III-S4 in online-only Data Supplement). Atrasentan treatment of ieET-1 decreased MA ROS generation by 47% compared to ieCre mice and reversed the eET-1-induced elevation in PVAT ROS generation.

### **Long-term induction of endothelial human ET-1 overexpression increased mesenteric artery collagen expression**

To investigate the mechanisms leading to vascular stiffening, fibronectin expression and collagen content were assessed in MAs. Fibronectin expression in MA wall was similar in ieCre and ieET-1 mice (Figure III-S5 in online-only Data Supplement). Quantification of the Sirius red-stained mesenteric artery polarized images did not reveal changes in collagen content in the adventitia and media (Figure III-S6 in online-only Data

Supplement) in ieET-1 compared to ieCre mice. However, since the collagen content in the media was at the limit of detection, collagen was also determined at mRNA level in MAs. *Col1a1* and *Col3a1* mRNA expression were increased 2.5- and 1.8-fold respectively in ieET-1 compared to ieCre mice (Figure III-2D-E). *Col1a1* mRNA expression was similar whereas *Col3a1* mRNA expression tended to be lower in atrasentan-treated ieET-1 compared to ieET-1 mice. MA mRNA expression of ET<sub>A</sub> and ET<sub>B</sub> receptors was unaffected at 3 months of induction of eET-1 overexpression or by atrasentan treatment (Figure III-S7 in online-only Data Supplement).

### **Long-term induction of endothelial human ET-1 overexpression increased monocyte/macrophage infiltration in the perivascular adipose tissue of mesenteric arteries.**

Vascular inflammation was investigated by determining the expression of MCP-1 in the vascular wall, and the infiltration of monocyte/macrophages and T cells in the MA PVAT. MA wall MCP-1 expression was similar in all the groups (Figure III-S8 in online-only Data Supplement). Monocyte/macrophage infiltration was 1.5-fold higher in ieET-1, which was reversed by atrasentan treatment (Figure III-3A and Figure III-S9A in online-only Data Supplement). On the other hand, CD3<sup>+</sup> T cell infiltration was similar in all groups (Figure III-3B and Figure III-S9B in online-only Data Supplement).

### **Long-term induction of endothelial human ET-1 overexpression decreased renal artery flow**

To determine the contribution of the kidney in eET-1-induced BP rise, RAF and renal mRNA expression of renin and ET<sub>A</sub> and ET<sub>B</sub> receptors were assessed. Long-term eET-1 overexpression decreased renal artery flow by 42%, which was not corrected by atrasentan treatment compared to ieCre mice (Table III-S2 in online-only Data Supplement). This change was not due to an alteration in renal artery diameter and heart rate. The mRNA expression levels of renal *Ednra* and *Ednrb* and renal cortex *Ren1* were similar in ieCre and ieET-1 mice (Figure III-S10 in online-only Data Supplement). Plasma creatinine was similar in all groups (Figure III-S11A in online-only

Data Supplement), which suggests that the decrease in RAF was not associated with a reduction in glomerular filtration rate.

### **Long-term induction of endothelial human ET-1 overexpression caused early renal damage and inflammation**

To evaluate renal injury, KIM-1 expression, which is upregulated in proximal tubular epithelium in kidney injury,<sup>23</sup> Masson's trichrome- and PAS-stained kidney sections and urine albumin were examined. KIM-1 expression was increased 4-fold in renal cortex tubules of ieET-1 compared to ieCre mice, and this increase was corrected by atrasentan treatment (Figure III-4A-B). However, no obvious renal lesions were detected on Masson's trichrome- or PAS-stained kidney sections (Figure III-S12 in online-only Data Supplement). Furthermore, urinary albumin/creatinine ratio and albumin excretion were similar in all groups (Figure III-4C and Figure III-S11B in online-only Data Supplement).

Early renal injury was accompanied by immune cell infiltration. Examination of the CD45 immunohistochemically-stained sections revealed increased CD45<sup>+</sup> cell infiltration in the interstitial space and in glomeruli in ieET-1 compared to ieCre mice, which was reversed by atrasentan treatment (Figure III-S13 in online-only Data Supplement). The infiltration of immune cells was further investigated by flow cytometry. The frequency and number of immune cell (CD45<sup>+</sup>) were increased 2.1-fold and 3.4-fold respectively in the kidney of ieET-1 compared to ieCre mice (Figure III- 5A-B and Figure III-S14A in online-only Data Supplement). The renal infiltrating CD45<sup>+</sup> cells in ieCre mice are made up of 52% myeloid cells (CD11b<sup>+</sup>), which contained 17% of myeloid derived suppressive cells (MDSCs, CD11b<sup>+</sup>Gr-1<sup>+</sup>) (Figure III-S14B-C in online-only Data Supplement). The frequency of these cells was similar in all groups. However, the number of infiltrating myeloid cells and MDSCs was increased >4-fold in the kidney of ieET-1 compared to ieCre (Figure III-5C-F). In addition, the frequency of myeloid and non-immune (CD45<sup>-</sup>) cells expressing the pro-inflammatory typical pattern recognition receptor CD36, which has been involved in chronic kidney disease,<sup>24-28</sup> was examined. CD36 was detected in 7.5% of myeloid cells and 3% of non-immune cells in ieCre mice (Figure III-6A-D). The frequencies of myeloid and non-immune (kidney) cells expressing

CD36 were increased 3- and 1.5-fold respectively in the kidney of ieET-1 animals compared to ieCre mice, and were reduced and reversed respectively by atrasentan. Furthermore, a high correlation between the frequency of CD36<sup>+</sup> non-immune cells and infiltrating immune cells was observed (Figure III-6E), which suggests a role for CD36 in the renal inflammatory process. Interestingly, atrasentan treatment of ieET-1 mice reduced or reversed the infiltration of all studied immune cells and reversed the increased frequency of CD36<sup>+</sup> kidney expressing cells (Figure III-5 and 6A-D).

## Discussion

In this study, we demonstrate that 3-month induction of human eET-1 overexpression in mice resulted in sustained BP elevation, resistance artery endothelial dysfunction and stiffening, associated with increased MA collagen mRNA expression, PVAT oxidative stress and monocyte/macrophage infiltration. Furthermore, long-term exposure to eET-1 overexpression resulted in early renal damage and immune cell infiltration in the kidney. Except for MA endothelial dysfunction and collagen mRNA expression, all the above were reversed or reduced by 2 weeks of treatment with the ET<sub>A</sub> antagonist atrasentan.

In our initial study of ieET-1 mice, we observed that BP progressively rose during the 3 weeks following induction of eET-1 overexpression, in the absence of development of vascular injury.<sup>14</sup> This was in contrast to our previous findings using a constitutive eET-1 transgenic mouse model, which presented endothelial dysfunction and vascular remodeling in absence of BP rise.<sup>29</sup> We have postulated that the different phenotypes observed might be due to developmental effects or adaptation to life-long exposure to elevated ET-1 circulating or tissue levels.<sup>14</sup> We have also hypothesized that longer exposure to eET-1 overexpression is required to induce vascular injury, which is demonstrated in the present study. However, ieET-1 mice presented a different phenotype from the constitutive eET-1 overexpressing mice,<sup>29</sup> as the BP remained elevated and there was no vascular remodeling after 3-month induction of eET-1 overexpression. This was not due to different eET-1 overexpression levels as similar plasma ET-1 levels were observed using both constitutive eET-1 overexpressing mice previously<sup>29</sup> and ieET-1 mice in this study. The difference between the two models may

be due to the fact that the ieET-1 mice are devoid of confounding developmental effects as eET-1 is not expressed *in utero* but induced in the adult mice. In addition, this study also showed that most of the long-term eET-1 overexpression effects, except for MA endothelial dysfunction, could be reversed or reduced by the ET<sub>A</sub> receptor blocker atrasentan during the last 2 weeks of the study. Three-month eET-1 overexpression might have caused irreversible damage to the endothelium that could not be corrected by atrasentan, at least not in the 2 weeks examined. Perhaps continuation of the atrasentan treatment for a longer time could prevent further vascular injury as it attenuated or eliminated other factors, i.e. elevated BP, oxidative stress and immune cell infiltration. It should be noted that MA expression of ET receptors was unaffected by long-term exposure to eET-1 overexpression, whereas ET receptors were downregulated after a 3-week exposure to eET-1 overexpression.<sup>14</sup> This might represent an adaptation to the 3-month exposure to eET-1 overexpression. Altogether, the results indicate that ieET-1 may be a better model to study the role of endothelial-derived ET-1 in hypertension and vascular remodeling. Furthermore, our results showed that eET-1 plays an important role in the development and maintenance of hypertension in an ET<sub>A</sub> receptor-dependent manner.

Long-term induction of eET-1 overexpression had vascular effects that were limited to MA stiffening, which was corrected by atrasentan treatment. The increase in stiffness was not explained by changes in media fibronectin expression or adventitia and media collagen content, but was associated with increased mRNA expression of *Col1a1* and *Col3a1*. Whether these changes explain the MA stiffening is unclear since *Col1a1* and *Col3a1* mRNA expression was not significantly reduced by atrasentan treatment. Alternatively, vascular stiffening could be explained by changes in vascular smooth muscle cells (VSMCs). Sehgel *et al.* showed that aortic stiffening could result in SHR from increases in VSMC stiffness and adhesion properties in absence of aortic collagen and elastin changes,<sup>30</sup> which could play a role here, but this requires further study.

The absence of vascular remodeling might be expected considering that the level of BP elevation achieved in tamoxifen-induced ieET-1 mice was moderate. In fact, a role of ET-1 in vascular remodeling was previously demonstrated in animal models of

hypertension presenting greater BP elevation, including DOCA-salt uninephrectomized rats,<sup>9</sup> DOCA-salt rats<sup>10</sup> and SHR-SP.<sup>12</sup> Furthermore, d'Uscio *et al.* demonstrated a correlation between vascular remodeling and SBP with pressure values between ~150 and ~200 mm Hg.

It is well recognized nowadays that innate and adaptive immune systems contribute to hypertension, endothelial dysfunction and vascular remodeling.<sup>19,31</sup> Both monocyte/macrophage and T lymphocyte perivascular infiltration has been observed in animal models of hypertension. Long-term induction of eET-1 overexpression may have resulted in the initiation of the inflammatory response as only monocyte/macrophage perivascular infiltration was observed. Furthermore, the extent of monocyte/macrophage infiltration was smaller in ieET-1 mice compared to angiotensin II or aldosterone infused mice.<sup>22,32</sup> This, and the lack of T cell infiltration could be explained at least in part by the absence of increase in MCP-1 expression, as this chemokine has been demonstrated to attract not only monocytes but also T cells.<sup>33,34</sup> Nevertheless, the perivascular infiltrating monocyte/macrophages could have contributed to the development of endothelial dysfunction and vascular stiffness in ieET-1 mice. ET-1 might represent one component of a multifactorial system involved in development of hypertension and vascular injury in animal models as well as in humans. This hypothesis might be confirmed by combining the induction of eET-1 overexpression with other hypertensive stimuli.

The kidneys play a key role in BP regulation and hypertension.<sup>35</sup> Long-term induction of eET-1 overexpression may raise BP through a direct action on renal microvascular resistance through activation of ET receptors.<sup>36</sup> Indeed, a decrease in RAF was observed in ieET-1 mice. However, this was not observed 3 weeks after induction of eET-1 overexpression.<sup>14</sup> Therefore, the kidneys could play a role in the maintenance but not in the initiation of ET-1-induced BP elevation. The reduction in renal artery flow was not corrected by atrasentan, which could be due to the tight attachment and remaining action of eET-1 on renal ET<sub>B</sub> receptors that could mediate efferent vasoconstriction when ET-1 levels reach 1-10 nM.<sup>36</sup> Similarly to the short-term ieET-1 overexpression study,<sup>14</sup> renin seems not to be implicated in eET-1-induced sustained BP elevation. In contrast to the short-term ieET-1 overexpression study, renal ET receptor expression were unaffected by long-term induction of eET-1

overexpression, which suggests renal adaptation of ET receptors to long-term exposure to eET-1 overexpression.

Long-term induction of eET-1 overexpression caused early renal injury and immune cell infiltration. The early renal injury was demonstrated by the increased expression of KIM-1 in renal cortex tubules, accompanied however by undetectable histologic lesions as shown by Masson's trichrome or PAS staining, and absence of increased urinary albumin excretion. KIM-1 is a phosphatidylserine and scavenger receptor that is expressed in injured tubular epithelial cells early in the development of renal proximal tubule injury.<sup>37</sup> Increased expression of KIM-1 transforms epithelial cells into semiprofessional phagocytes that eliminate apoptotic and necrotic cellular debris, thus limiting the inflammatory response.<sup>23,38</sup> Furthermore, it has been recently shown that recombinant KIM-1 may activate macrophages *in vitro*.<sup>39</sup> Renal infiltrating immune cells are made up in large part of myeloid cells and of a myeloid cell subpopulation, MDSCs. MDSCs are anti-inflammatory cells that have been shown to be increased in the blood and the spleen in murine models of hypertension and in the kidney in a model of acute kidney injury.<sup>40,41</sup> We observed an increase in the fraction of myeloid cells and kidney non-immune cells expressing the pro-inflammatory B scavenger/pattern recognition receptor CD36, which could contribute to the development of kidney injury.<sup>26,28,42</sup> *Cd36* knockout protects high-fat diet (HFD)-fed *ApoE*<sup>-/-</sup> mice<sup>25</sup> and mice with 5/6 nephrectomy infused with angiotensin II from development of renal injury and immune cell infiltration.<sup>25,27</sup> Furthermore, antagonism of CD36 by 5A peptide protects mice with 5/6 nephrectomy infused with angiotensin II and CD-1 mice with unilateral ureteral obstruction.<sup>27</sup> CD36 can bind a broad range of ligands including apolipoprotein (apo) A-I, apoL1, thrombospondin-1, serum amyloid A, lipopolysaccharides, oxidized low density lipoprotein (oxLDL), fatty acids, apoptotic cell surfaces, and microparticles (reviewed in <sup>27</sup>). CD36 has been shown to play a role in innate immune cell activation and renal cell injury.<sup>25,43</sup> Activation of CD36 by oxLDL, in cooperation with the Toll-like receptor 4 and TLR6 heterodimer, primes macrophages for Il-1 $\beta$  production.<sup>28</sup> Palmitic acid increased CD36 expression, lipid uptake, leading to podocyte apoptosis.<sup>42</sup> Plasminogen stimulation of podocytes increases ROS generation that promotes ET-1 synthesis and CD36 expression, and subsequent increased intracellular cholesterol

uptake followed by podocyte apoptosis.<sup>26,42</sup> As well, activation of CD36 expressed in macrophages and proximal tubular cells could potentiate an inflammatory signaling loop involving these cells and their associated macrophages.<sup>25</sup> Accordingly, we demonstrated that the fraction of non-immune renal cells expressing CD36 was highly correlated with the fraction of infiltrating immune cells.<sup>25</sup> This may also occur in humans since increased CD36 expression has been reported in renal tubules and glomeruli of patients with diabetic nephropathy and hyperlipidemia.<sup>42</sup> Interestingly, atrasentan treatment reversed the increase in KIM-1 expression and reduced immune cell infiltration and kidney non-immune CD36-expressing cells. Altogether, these results indicate that eET-1 plays an important role in the development of kidney injury.

In conclusion, we demonstrate that long-term induction of endothelium-restricted human ET-1 overexpression caused sustained BP rise, small artery stiffening and endothelial dysfunction, and early renal damage, which were reversed or reduced by 2-week treatment with the ET<sub>A</sub> receptor antagonist atrasentan.

### **Limitations**

The present study did not examine whether 3-month induction of human eET-1 overexpression in mice alters renal function. ET receptor expression was determined in the renal cortex and medulla. Changes in vascular ET receptor expression could be masked by ET receptors expressed in renal tubules. It would be interesting to determine whether 3-month induction of human eET-1 overexpression causes an elevation in CD36 expression in podocytes or tubular epithelial cells. This could play an important role in rendering the mice more susceptible to a second hit.

### **Perspectives**

Hypertension is the leading risk factor for global burden of disease.<sup>44</sup> This novel model of inducible endothelium-restricted human ET-1 overexpression devoid of developmental confounding effects will facilitate understanding the role of ET-1 in the pathophysiology of hypertension. This study adds to a substantial body of evidence showing that ET<sub>A</sub> receptor antagonists could be beneficial in hypertension and other diseases associated with renal inflammation, particularly in patients with difficult to control or resistant

hypertension.

### **Acknowledgments**

We are grateful to Adriana Cristina Ene, Guillem Colell Dinarès and Isabelle Miguel, and to Véronique Michaud, manager of the Lady Davis Institute for medical research imaging and phenotyping core, for excellent technical assistance.

### **Funding Sources**

This work was supported by Canadian Institutes of Health Research (CIHR) grants 37917 and 102606, CIHR First Pilot Foundation Grant 143348, a Canada Research Chair (CRC) on Hypertension and Vascular Research by the CRC Government of Canada/CIHR Program and by the Canada Fund for Innovation, all to ELS, and by a fellowship to SCC and to JCFA (Science without Borders (CsF) of the National Council for Scientific and Technological Development (CNPq) of Brazil), SO (CIHR Canada Graduate Scholarship-Master's scholarship), AC (Canadian Vascular Network), OB (Société québécoise d'hypertension artérielle [SQHA]) and TB (SQHA and Richard and Edith Strauss Postdoctoral Fellowship)

### **Disclosures**

None

## References

1. Yanagisawa M, Kurihara H, Kimura S, Tomobe Y, Kobayashi M, Mitsui Y, Yazaki Y, Goto K, Masaki T. A novel potent vasoconstrictor peptide produced by vascular endothelial cells. *Nature*. 1988;332:411-415.
2. Davenport AP, Hyndman KA, Dhaun N, Southan C, Kohan DE, Pollock JS, Pollock DM, Webb DJ, Maguire JJ. Endothelin. *Pharmacological reviews*. 2016;68:357-418.
3. Schiffrin EL. Vascular endothelin in hypertension. *Vascular pharmacology*. 2005;43:19-29.
4. Saito Y, Nakao K, Mukoyama M, Imura H. Increased plasma endothelin level in patients with essential hypertension. *The New England journal of medicine*. 1990;322:205.
5. Schiffrin EL, Deng LY, Sventek P, Day R. Enhanced expression of endothelin-1 gene in resistance arteries in severe human essential hypertension. *Journal of hypertension*. 1997;15:57-63.
6. Krum H, Viskoper RJ, Lacourciere Y, Budde M, Charlon V. The effect of an endothelin-receptor antagonist, bosentan, on blood pressure in patients with essential hypertension. Bosentan Hypertension Investigators. *The New England journal of medicine*. 1998;338:784-790.
7. Nakov R, Pfarr E, Eberle S, Investigators H. Darusentan: an effective endothelinA receptor antagonist for treatment of hypertension. *American journal of hypertension*. 2002;15:583-589.
8. Weber MA, Black H, Bakris G, Krum H, Linas S, Weiss R, Linseman JV, Wiens BL, Warren MS, Lindholm LH. A selective endothelin-receptor antagonist to reduce blood pressure in patients with treatment-resistant hypertension: a randomised, double-blind, placebo-controlled trial. *Lancet*. 2009;374:1423-1431.
9. Li JS, Lariviere R, Schiffrin EL. Effect of a nonselective endothelin antagonist on vascular remodeling in deoxycorticosterone acetate-salt hypertensive rats. Evidence for a role of endothelin in vascular hypertrophy. *Hypertension*. 1994;24:183-188.

10. d'Uscio LV, Barton M, Shaw S, Moreau P, Luscher TF. Structure and function of small arteries in salt-induced hypertension: effects of chronic endothelin-subtype-A-receptor blockade. *Hypertension*. 1997;30:905-911.
11. Schiffrin EL, Lariviere R, Li JS, Sventek P, Touyz RM. Deoxycorticosterone acetate plus salt induces overexpression of vascular endothelin-1 and severe vascular hypertrophy in spontaneously hypertensive rats. *Hypertension*. 1995;25:769-773.
12. Sharifi AM, He G, Touyz RM, Schiffrin EL. Vascular endothelin-1 expression and effect of an endothelin ETA antagonist on structure and function of small arteries from stroke-prone spontaneously hypertensive rats. *Journal of cardiovascular pharmacology*. 1998;31 Suppl 1:S309-312.
13. Kisanuki YY, Emoto N, Ohuchi T, Widyantoro B, Yagi K, Nakayama K, Kedzierski RM, Hammer RE, Yanagisawa H, Williams SC, Richardson JA, Suzuki T, Yanagisawa M. Low blood pressure in endothelial cell-specific endothelin 1 knockout mice. *Hypertension*. 2010;56:121-128.
14. Rautureau Y, Coelho SC, Fraulob-Aquino JC, Huo KG, Rehman A, Offermanns S, Paradis P, Schiffrin EL. Inducible Human Endothelin-1 Overexpression in Endothelium Raises Blood Pressure via Endothelin Type A Receptors. *Hypertension*. 2015;66:347-355.
15. Schiffrin EL. Vascular remodeling in hypertension: mechanisms and treatment. *Hypertension*. 2012;59:367-374.
16. Guzik TJ, Skiba DS, Touyz RM, Harrison DG. The role of infiltrating immune cells in dysfunctional adipose tissue. *Cardiovascular research*. 2017;113:1009-1023.
17. Guzik TJ, Touyz RM. Oxidative Stress, Inflammation, and Vascular Aging in Hypertension. *Hypertension*. Epub ahead of print on August 7, 2017;DOI: 10.1161/HYPERTENSIONAHA.117.07802
18. Idris-Khodja N, Ouerd S, Mian MO, Gornitsky J, Barhoumi T, Paradis P, Schiffrin EL. Endothelin-1 Overexpression Exaggerates Diabetes-Induced Endothelial Dysfunction by Altering Oxidative Stress. *Am J Hypertens*. 2016;29:1245-1251.
19. Mian MO, Paradis P, Schiffrin EL. Innate immunity in hypertension. *Current hypertension reports*. 2014;16:413.

20. Indra AK, Warot X, Brocard J, Bornert JM, Xiao JH, Chambon P, Metzger D. Temporally-controlled site-specific mutagenesis in the basal layer of the epidermis: comparison of the recombinase activity of the tamoxifen-inducible Cre-ER(T) and Cre-ER(T2) recombinases. *Nucleic acids research*. 1999;27:4324-4327.
21. Korhonen H, Fisslthaler B, Moers A, Wirth A, Habermehl D, Wieland T, Schutz G, Wettschureck N, Fleming I, Offermanns S. Anaphylactic shock depends on endothelial Gq/G11. *The Journal of experimental medicine*. 2009;206:411-420.
22. Barhoumi T, Kasal DA, Li MW, Shbat L, Laurant P, Neves MF, Paradis P, Schiffrin EL. T regulatory lymphocytes prevent angiotensin II-induced hypertension and vascular injury. *Hypertension*. 2011;57:469-476.
23. Ichimura T, Brooks CR, Bonventre JV. Kim-1/Tim-1 and immune cells: shifting sands. *Kidney international*. 2012;81:809-811.
24. Cho S. CD36 as a therapeutic target for endothelial dysfunction in stroke. *Curr Pharm Des*. 2012;18:3721-3730.
25. Kennedy DJ, Chen Y, Huang W, Viterna J, Liu J, Westfall K, Tian J, Bartlett DJ, Tang WH, Xie Z, Shapiro JI, Silverstein RL. CD36 and Na/K-ATPase-alpha1 form a proinflammatory signaling loop in kidney. *Hypertension*. 2013;61:216-224.
26. Raij L, Tian R, Wong JS, He JC, Campbell KN. Podocyte injury: the role of proteinuria, urinary plasminogen, and oxidative stress. *American journal of physiology Renal physiology*. 2016;311:F1308-F1317.
27. Souza AC, Bocharov AV, Baranova IN, et al. Antagonism of scavenger receptor CD36 by 5A peptide prevents chronic kidney disease progression in mice independent of blood pressure regulation. *Kidney international*. 2016;89:809-822.
28. Stewart CR, Stuart LM, Wilkinson K, van Gils JM, Deng J, Halle A, Rayner KJ, Boyer L, Zhong R, Frazier WA, Lacy-Hulbert A, El Khoury J, Golenbock DT, Moore KJ. CD36 ligands promote sterile inflammation through assembly of a Toll-like receptor 4 and 6 heterodimer. *Nat Immunol*. 2010;11:155-161.
29. Amiri F, Viridis A, Neves MF, Iglarz M, Seidah NG, Touyz RM, Reudelhuber TL, Schiffrin EL. Endothelium-restricted overexpression of human endothelin-1

- causes vascular remodeling and endothelial dysfunction. *Circulation*. 2004;110:2233-2240.
30. Sehgel NL, Sun Z, Hong Z, Hunter WC, Hill MA, Vatner DE, Vatner SF, Meininger GA. Augmented vascular smooth muscle cell stiffness and adhesion when hypertension is superimposed on aging. *Hypertension*. 2015;65:370-377.
  31. Idris-Khodja N, Mian MO, Paradis P, Schiffrin EL. Dual opposing roles of adaptive immunity in hypertension. *Eur Heart J*. 2014;35:1238-1244.
  32. Kasal DA, Barhoumi T, Li MW, Yamamoto N, Zdanovich E, Rehman A, Neves MF, Laurant P, Paradis P, Schiffrin EL. T regulatory lymphocytes prevent aldosterone-induced vascular injury. *Hypertension*. 2012;59:324-330.
  33. Carr MW, Roth SJ, Luther E, Rose SS, Springer TA. Monocyte chemoattractant protein 1 acts as a T-lymphocyte chemoattractant. *Proceedings of the National Academy of Sciences of the United States of America*. 1994;91:3652-3656.
  34. Rudemiller NP, Crowley SD. The role of chemokines in hypertension and consequent target organ damage. *Pharmacol Res*. 2017;119:404-411.
  35. Guyton AC. Renal function curve--a key to understanding the pathogenesis of hypertension. *Hypertension*. 1987;10:1-6.
  36. Kohan DE, Rossi NF, Inscho EW, Pollock DM. Regulation of blood pressure and salt homeostasis by endothelin. *Physiol Rev*. 2011;91:1-77.
  37. Prozialeck WC, Edwards JR, Lamar PC, Liu J, Vaidya VS, Bonventre JV. Expression of kidney injury molecule-1 (Kim-1) in relation to necrosis and apoptosis during the early stages of Cd-induced proximal tubule injury. *Toxicol Appl Pharmacol*. 2009;238:306-314.
  38. Ichimura T, Asseldonk EJ, Humphreys BD, Gunaratnam L, Duffield JS, Bonventre JV. Kidney injury molecule-1 is a phosphatidylserine receptor that confers a phagocytic phenotype on epithelial cells. *The Journal of clinical investigation*. 2008;118:1657-1668.
  39. Tian L, Shao X, Xie Y, Wang Q, Che X, Zhang M, Xu W, Xu Y, Mou S, Ni Z. Kidney Injury Molecule-1 is Elevated in Nephropathy and Mediates Macrophage Activation via the Mapk Signalling Pathway. *Cell Physiol Biochem*. 2017;41:769-783.

40. Shah KH, Shi P, Giani JF, Janjulia T, Bernstein EA, Li Y, Zhao T, Harrison DG, Bernstein KE, Shen XZ. Myeloid Suppressor Cells Accumulate and Regulate Blood Pressure in Hypertension. *Circulation research*. 2015;117:858-869.
41. Zhang C, Wang S, Li J, Zhang W, Zheng L, Yang C, Zhu T, Rong R. The mTOR signal regulates myeloid-derived suppressor cells differentiation and immunosuppressive function in acute kidney injury. *Cell Death Dis*. 2017;8:e2695.
42. Hua W, Huang HZ, Tan LT, Wan JM, Gui HB, Zhao L, Ruan XZ, Chen XM, Du XG. CD36 Mediated Fatty Acid-Induced Podocyte Apoptosis via Oxidative Stress. *PloS one*. 2015;10:e0127507.
43. Okamura DM, Pennathur S, Pasichnyk K, Lopez-Guisa JM, Collins S, Febbraio M, Heinecke J, Eddy AA. CD36 regulates oxidative stress and inflammation in hypercholesterolemic CKD. *Journal of the American Society of Nephrology : JASN*. 2009;20:495-505.
44. Lim SS, Vos T, Flaxman AD, *et al*. A comparative risk assessment of burden of disease and injury attributable to 67 risk factors and risk factor clusters in 21 regions, 1990-2010: a systematic analysis for the Global Burden of Disease Study 2010. *Lancet*. 2012;380:2224-2260.

**Novelty and Significance:****1. What Is New?**

- This study demonstrates that three-month induction of human endothelin (ET)-1 overexpression in the endothelium of adult mice caused sustained blood pressure (BP) elevation, vascular injury and early renal injury, which were reversed or reduced by a 2-week treatment with the ET<sub>A</sub> receptor antagonist atrasentan.

**2. What Is Relevant?**

- This novel model of inducible endothelial-restricted human endothelin-1 overexpression devoid of developmental confounding effects will facilitate understanding the role of endothelin-1 in the pathophysiology of hypertension.
- The study adds to a substantial body of evidence showing that ET<sub>A</sub> receptor antagonists could be beneficial in hypertension and other diseases associated with renal inflammation, particularly in patients with difficult to control or resistant hypertension.

**3. Summary**

Hypertension is the leading risk factor for global burden of disease. The ET system is activated in patients with moderate-to-severe hypertension and difficult to control or resistant hypertension. However, it has been difficult to demonstrate the pressor significance of ET-1 in hypertension. Here we show that when human ET-1 overexpression is induced for a long term in the endothelium of adult mice, it raises BP and caused vascular and renal injury via ET<sub>A</sub> receptors. These results should stimulate the development of novel ET<sub>A</sub> receptor blockers for the treatment of difficult to control or resistant hypertension, which has been delayed by adverse side effects of the antagonists developed in the past.

## Figures

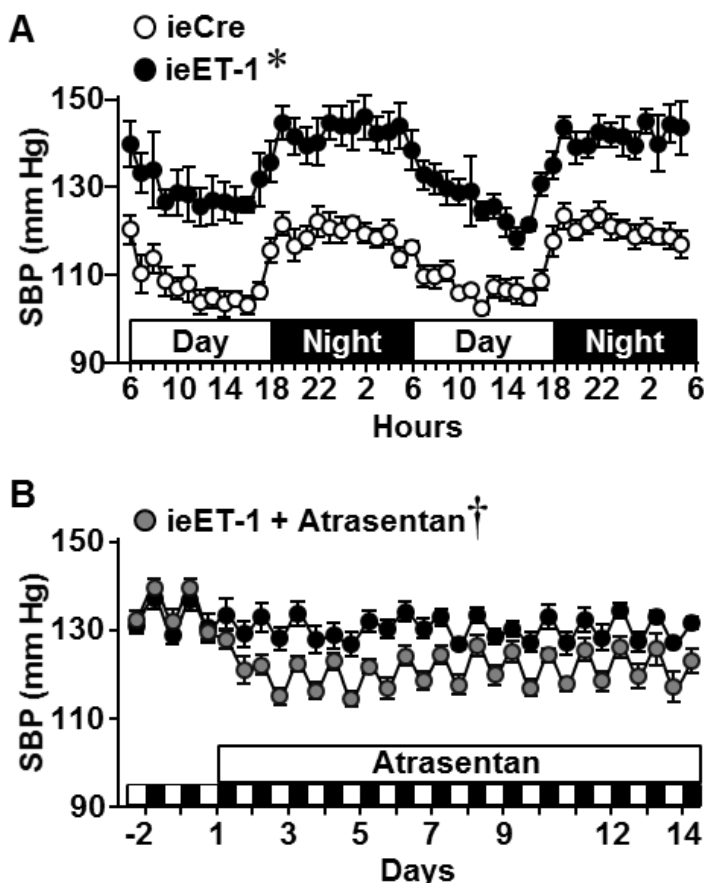


**Figure III-1. Long-term endothelial human endothelin-1 overexpression increased blood pressure in an ET type A receptor-dependent manner.**

**A.** Systolic blood pressure (SBP) was determined by telemetry in tamoxifen-treated inducible endothelium-restricted Cre recombinase (ieCre) and human endothelin-1 overexpressing (ieET-1) mice during the last two days of the third month after tamoxifen treatment. **B.** SBP was also measured in tamoxifen-treated ieET-1 mice two days before and during the last two weeks of the third month while they were treated or not with atrasentan. Data are presented as means  $\pm$  SEM,  $n = 5$  for ieCre and ieET-1 in **A** and 5 for ieET-1 and 6 for ieET-1 + Atrasentan in **B**. Days 2 to 14 were used to compare SBP in **B**. Data were analyzed using two-way ANOVA for repeated measures followed by a Student-Newman-Keuls *post hoc* test. \* $P < 0.001$  vs ieCre and † $P < 0.01$  vs ieET-1.

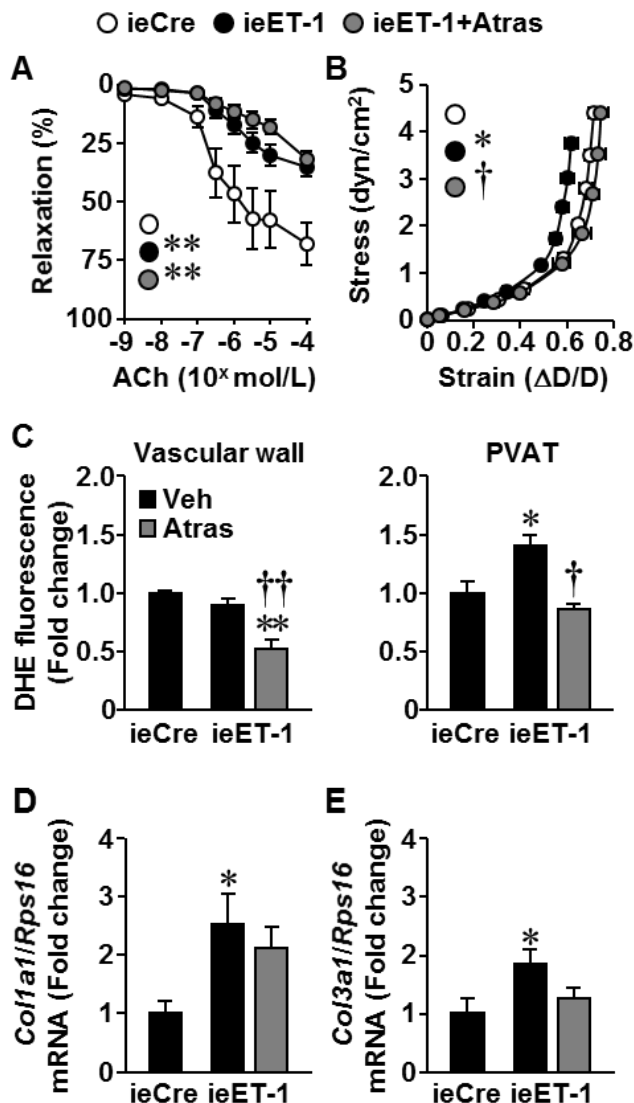


**Figure III-2. Long-term endothelial human endothelin-1 overexpression induced mesenteric artery endothelial dysfunction and vascular stiffening.**

Mesenteric artery (MA) relaxation responses to acetylcholine (A) and stress-strain relationships (B) by pressurized myography, reactive oxygen species (ROS) generation by dihydroethidium fluorescence in MA media and perivascular adipose tissue (PVAT) (C), and collagen type I alpha 1 (*Col1a1*, D) and III alpha 1 (*Col3a1*, E) expression in MA by reverse transcription/quantitative PCR were assessed in tamoxifen-treated inducible endothelium-restricted Cre recombinase (ieCre) and human endothelin-1 overexpressing (ieET-1) mice treated or not with atrasentan (Atras). Data are presented as means  $\pm$  SEM,  $n = 7$  for ieCre, 11 for ieET-1 and 9 for ieET-1 + Atras in A, 8 for

ieCre and 9 for ieET-1 and ieET-1 + Atras in **B**, 9 for ieCre + vehicle (Veh), 8 for ieET-1 + Veh and 6 for ieET-1 + Atras in **C** and 5 for ieCre + Veh, 8 for ieET-1 + Veh and 7 for ieET-1 + Atras in **D-E**. Data were analyzed using two-way ANOVA for repeated measures in **A** and one-way ANOVA in **B-E**, with all ANOVA followed by a Student-Newman-Keuls *post hoc* test. The displacement of the stress-strain curves was analyzed by comparing the strain at 140 mm Hg in **B**. \* $P < 0.05$  vs ieCre and † $P < 0.05$  vs ieET-1.

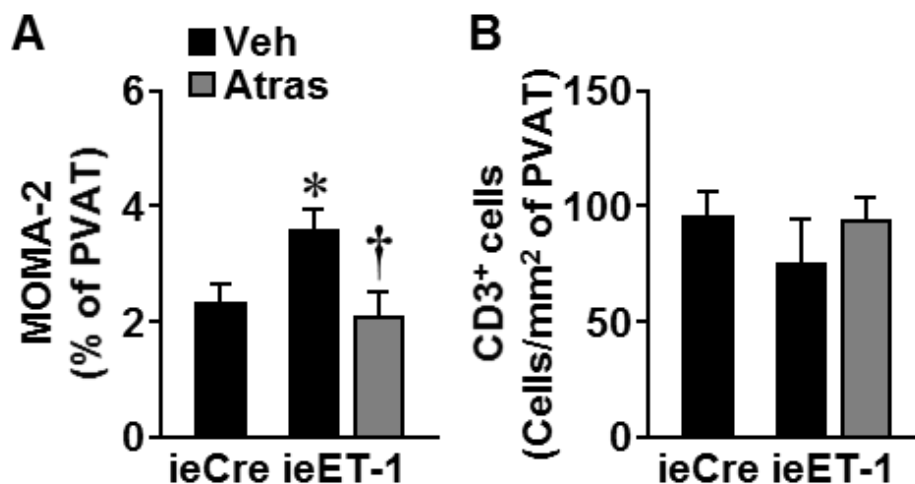


**Figure III-3. Long-term human endothelin-1 overexpression increased monocyte/macrophage infiltration in the perivascular adipose tissue of mesenteric arteries.**

Monocyte/macrophage infiltration using anti-MOMA-2 antibody (**A**) and T lymphocyte infiltration using anti-CD3 antibody (**B**) were determined by immunofluorescence in perivascular adipose tissue (PVAT) of tamoxifen-treated inducible endothelium-restricted Cre recombinase (ieCre) and human endothelin-1 overexpressing (ieET-1) mice treated or not with atrasentan (Atras). Data are presented as means  $\pm$  SEM,  $n = 7$  for ieCre and ieET-1 + vehicle (Veh) and 8 for ieET-1 + Atras in **A** and 7 for ieCre + Veh, 6 for ieET-1 + Veh and 7 for ieET-1 + Atras in **B**. Data were analyzed using one-way ANOVA followed by a Student-Newman-Keuls *post hoc* test. \* $P < 0.05$  and vs ieCre and † $P < 0.05$  vs ieET-1.

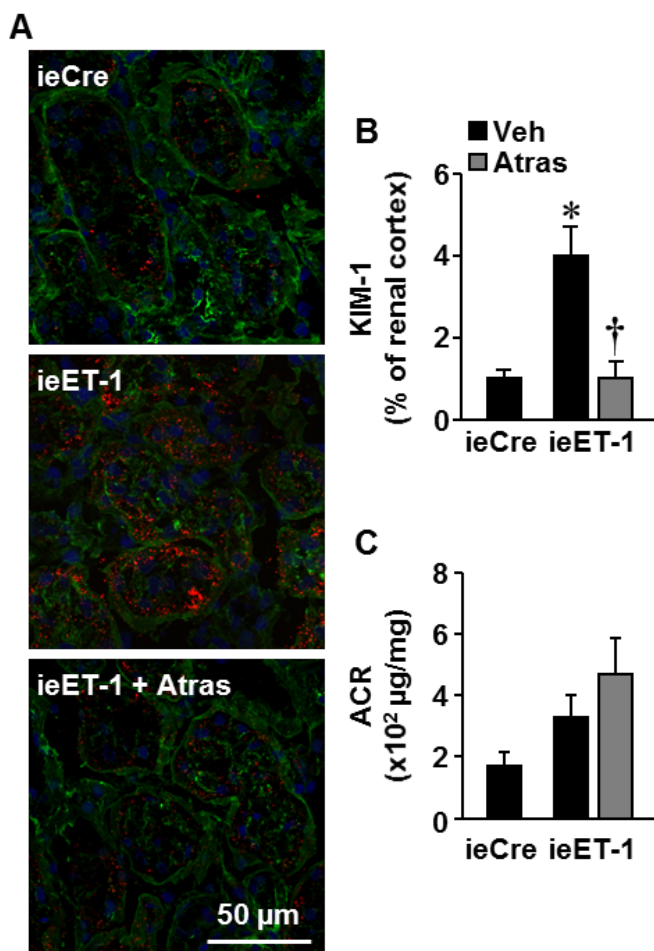


**Figure III-4. Long-term endothelial human ET-1 overexpression caused early renal damage.**

Kidney injury molecule-1 (KIM-1) expression by immunofluorescence in renal cortex (**A-B**) and albumin/creatinine ratio in 24-h urine (**C**) were determined in tamoxifen-treated inducible endothelium-restricted Cre recombinase (ieCre) and human endothelin-1 overexpressing (ieET-1) mice treated or not with atrasentan (Atras). Representative KIM-1 fluorescence images (red) in kidney sections are shown in **A**. Green and blue represent plasma membranes revealed with Alexa Fluor 647 wheat germ agglutinin, and 4',6-diamidino-2-phenylindole (DAPI) fluorescence, respectively. Data are presented as means  $\pm$  SEM,  $n = 11$  for ieCre and ieET-1 + vehicle (Veh) and 6 for ieET-1 + Atras in **A-B** and 6 for ieCre and ieET-1 + Veh and 7 for ieET-1 + Atras in **C**. Data were analyzed using one-way ANOVA followed by a Student-Newman-Keuls *post hoc* test. \* $P < 0.001$  vs ieCre and † $P < 0.01$  vs ieET-1.

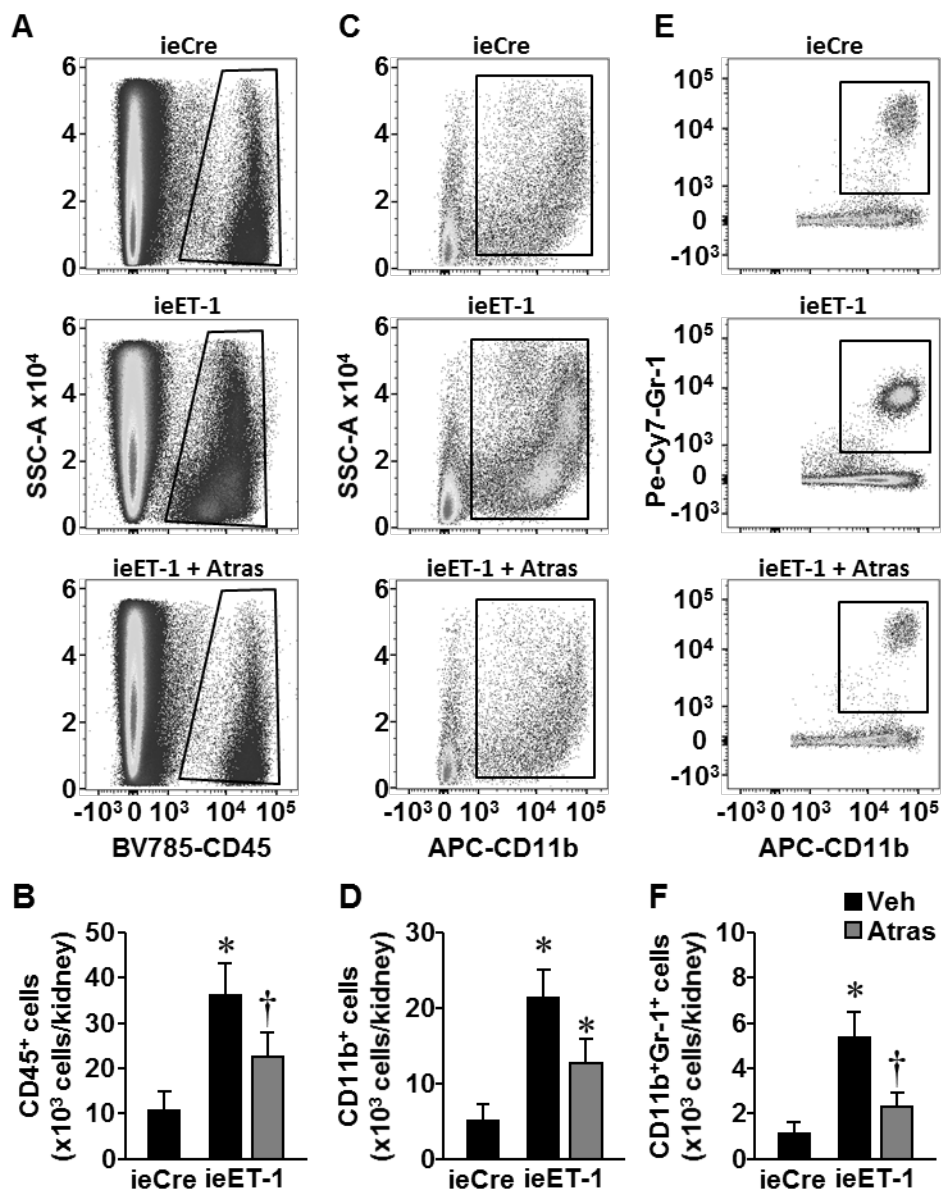


**Figure III-5. Long-term endothelial human endothelin-1 overexpression induced renal immune cell infiltration.**

The number of immune CD45<sup>+</sup> cells (**A-B**), myeloid cells (CD11b<sup>+</sup>, **C-D**) and myeloid-derived suppressor cells (MDSCs, CD11b<sup>+</sup>Gr-1<sup>+</sup>, **E-F**) was determined in the kidney by flow cytometry in tamoxifen-treated inducible endothelium-restricted Cre recombinase (ieCre) and human endothelin-1 overexpressing (ieET-1) mice treated or not with atrasentan (Atras). Representative gating of CD45<sup>+</sup> immune cells in the side scatter area (SSC-A)/Brilliant Violet 785-conjugated rat anti-mouse CD45 antibody (BV785-

CD45) grayscale plot (**A**), myeloid cells in the SSC-A/allophycocyanin-conjugated rat anti-mouse CD11b<sup>+</sup> antibody (APC-CD11b) grayscale plot (**C**) and MDSCs in the phycoerythrin-Cy7-conjugated rat anti-mouse Gr-1 antibody (PE-Cy7-Gr-1)/APC-CD11b+ grayscale plot (**E**) are shown. Data are presented as means  $\pm$  SEM, n = 6 for ieCre and ieET-1 + vehicle (Veh) and 5 for ieET-1 + Atras. Data were analyzed using one-way ANOVA followed by a Student-Newman-Keuls *post hoc* test. \* $P < 0.05$  vs ieCre and † $P < 0.05$  vs ieET-1.

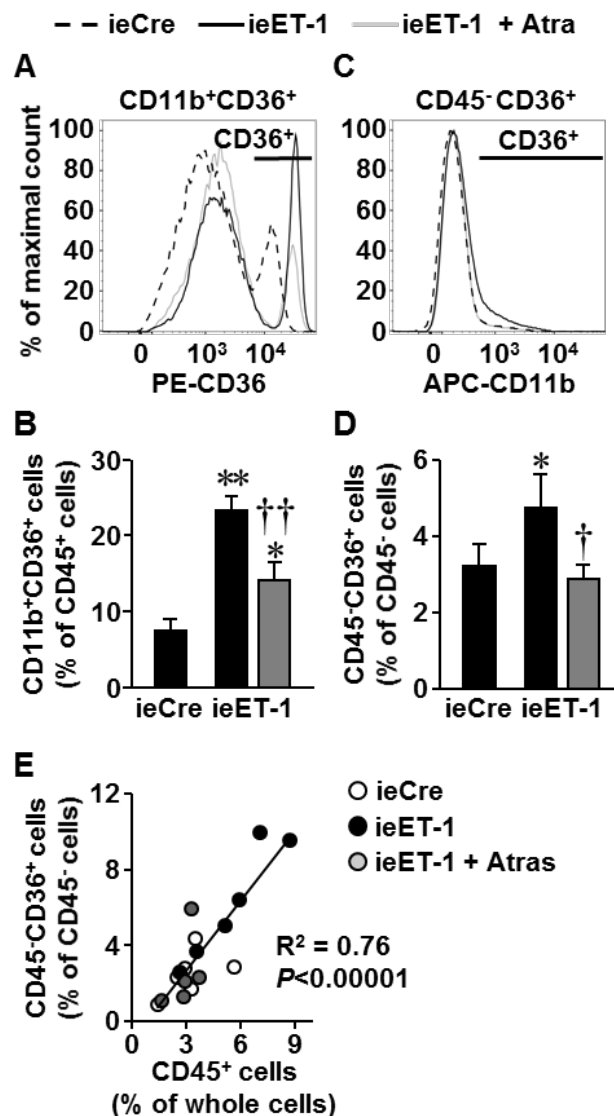


**Figure III-6.** After long-term endothelial human endothelin-1 overexpression, increased immune cell infiltration was associated with greater frequency of kidney and myeloid cells expressing the pattern-recognition receptor CD36.

The frequencies (%) of CD36-expressing myeloid cells (CD11b<sup>+</sup>CD36<sup>+</sup>, **A-B**) and kidney cells (CD45<sup>-</sup>CD36<sup>+</sup>, **C-D**) were determined in the kidney of tamoxifen-treated inducible endothelium-restricted Cre recombinase (ieCre) and human endothelin-1 overexpressing (ieET-1) mice treated or not with atrasentan (Atras). Representative histogram of CD11b<sup>+</sup>CD36<sup>+</sup> cells (**A**) and CD45<sup>-</sup>CD36<sup>+</sup> cells (**C**) are shown. The correlation between the frequencies (%) of CD45<sup>-</sup>CD36<sup>+</sup> and CD45<sup>+</sup> cells (**E**) was determined. Data are presented as means  $\pm$  SEM,  $n = 6$  for ieCre and ieET-1 + vehicle

(Veh) and 5 for ieET-1 + Atras. Data were analyzed using one-way ANOVA followed by a Student-Newman-Keuls *post hoc* test. \* $P < 0.05$  vs ieCre and † $P < 0.05$  vs ieET-1.

## Expanded materials and methods

### Experimental design

This study was approved by the Animal Care Committee of the Lady Davis Institute for Medical Research and McGill University, followed recommendations of the Canadian Council for Animal Care and was in agreement with the Guide for the Care and Use of Laboratory Animals published by the US National Institutes of Health. Control mice expressing a tamoxifen-inducible Cre recombinase (CreER<sup>T2</sup>)<sup>1</sup> under the control of the endothelium-specific *Tie2* promoter (named as ieCre) and tamoxifen-inducible endothelium-restricted human endothelin (ET)-1 overexpression (ieET-1) mice have been previously described<sup>2,3</sup> and were generated in our animal facility. The endothelial specificity of tamoxifen-induced Cre recombination was demonstrated previously<sup>3</sup> in mesenteric arteries, aorta, heart, liver and kidney using ieCre mice crossed with *ROSA26*<sup>mT-mG/+</sup> reporter mice, which expressed a loxP-flanked, membrane-targeted tandem dimer tomato (mT), before Cre mediated excision, and a membrane-targeted enhanced green fluorescent protein (mG) after excision, under the control of the CMV enhancer/chicken  $\beta$ -actin promoter (CAG) promoter driving the expression in all cell types. Nine-to-12 week-old male ieCre and ieET-1 mice were treated with tamoxifen (1 mg/day, S.C.) for 5 days and studied 3 months later. As previously described,<sup>3</sup> 24-hour urine was collected using metabolic cages to determine urinary albumin and creatinine in the week before or after the third month and renal artery flow was determined by ultrasound the following day.

In a subgroup of tamoxifen-treated ieCre and ieET-1 mice, blood pressure (BP) was determined by telemetry as described previously.<sup>4</sup> BP was assessed during the last 2 days of the third-month period and then mice were studied as above.

Another subset of tamoxifen-treated ieET-1 mice were treated with the ET type A receptor blocker, atrasentan (10 mg/kg/day PO), mixed with the food, during the last two weeks of the third month. BP was determined by telemetry two days before and during atrasentan treatment. Thereafter, mice were studied as above.

A separate group of ieCre and ieET-1 mice treated or not with atrasentan was used to examine the long-term effects of human ET-1 endothelial overexpression on the

expression of ET type A (*Ednra*) and B (*Ednrb*) receptors, collagen type 1A1 (*Col1A1*) and 3A1 (*Col3A1*) and renin (*Ren1*) in mesenteric artery (MA) or the kidney by reverse transcription/quantitative PCR (RT-qPCR).

### **Atrasentan treatment**

Mice were fed with soft food containing atrasentan (a generous gift from Abbott Laboratories, Abbott Park, IL). The soft food was prepared by combining 2 parts of 2918 Teklad global 18% protein diet powder (ENVIGO, Indianapolis, IN) with 1 part of tap water. Atrasentan was dissolved in the water used to prepare the food. Food daily consumption was determined during the 5 days before treatment initiation. This 5-day period was also used to acclimatize the mice to the new type of food. Initially, mice were provided 6.8 g of food dough in a metal cup. The amount of food dough was adjusted during the following days to daily food consumption. Thereafter, body weight was determined weekly, and food dough containing atrasentan was provided in slight excess of daily food consumption at 9 AM. The amount of food dough and atrasentan was adjusted weekly (or as needed) based on the amount of food remaining in the cup on the following morning and body weight change.

### **Metabolic cages**

Twenty-four-hour urine was collected as previously described.<sup>3</sup> In order to reduce stress, mice were first housed in metabolic cages (Tecniplast S.p.A., Buguggiate, VA, Italy) for two consecutive days, 3 days before the actual experiment to have them acclimatize to the environment and experimental procedure. Then, mice were housed in the metabolic cages for 2 days, and 24-hour urine collection was initiated early in the morning (between 8 and 9 AM). Urine was collected at the end of the first 24-hour period. Food powder and feces attached to the urine collector system were removed by rinsing extensively with water. The urine collector system was dried with paper towels and attached to the metabolic cage for the second 24-hour urine collection. At the end of the experiment, 24-hour urine was collected, cleared by centrifugation at 10,000 g for 10 min, and stored at -80°C until used. Albumin and creatinine were determined respectively in urine diluted 13 times using the Albuwell M direct competitive ELISA kit

and in urine diluted 4 times using the creatinine companion kit (Exocell, Philadelphia, PA).

### **Renal artery flow**

Right renal artery flow (RAF) was determined by ultrasound as previously described.<sup>3</sup> Mice were anesthetized with 3 % isoflurane and 2 L/min O<sub>2</sub>. Depth of anesthesia was confirmed by the rear foot squeezing. The mice were secured lightly on prone position on a warming pad adjusted to 38°C, and their posterior right back was shaved. Body temperature was measured using a rectal probe and maintained to 36-37°C by adjusting the intensity of an infrared lamp that is positioned over the mouse. The percentage of isoflurane was adjusted to maintain the heart rate (HR) at ~550 beats/min. Echography was performed using a Visual Sonic VEVO 770 ultrasound machine and a RMV™ 704 high frame rate scanhead with a center frequency of 40 MHz (VisualSonics Inc., Toronto, ON, Canada). A two-dimensional short axis view of the right kidney was obtained and a view of the renal artery emerging from the aorta was positioned at the focus level. The pulse wave (PW) Doppler sample volume was positioned into the renal artery in the focal zone, the scanhead was angled to achieve a beam/flow angle of less than 60 degrees, and the PW Doppler spectrum was recorded. The heart rate (HR) and renal artery velocity time integral (VTI) were determined from the PW Doppler waveform on five consecutive beats located between two respirations. The renal artery diameter measured from a two-dimensional guided M-mode image and HR were used to calculate the renal artery flow.

### **Blood pressure**

BP was determined by telemetry as previously described.<sup>4</sup> In brief, 10 days before the BP was to be measured, mice were anesthetized with 3% isoflurane mixed with O<sub>2</sub> at 1 L/min. The depth of anesthesia was confirmed by the rear foot squeezing. The non-steroidal anti-inflammatory drug carprofen (20 mg/kg) was administered subcutaneously to minimize post-operative pain. Mice were then surgically instrumented with PA-C10 telemetry transmitters as recommended by the manufacturer (Data Sciences International, St. Paul, MN). Carprofen was administered as above once daily for the

first 2 recovery days. Mice were allowed to recover for one additional day and BP determined every 5 min for 10 sec for the period indicated above.

### **Collection of tissues**

At the end of the protocol, mice were weighed and then anesthetized with isoflurane as indicated above. Blood was collected by cardiac puncture on EDTA for plasma ET-1 determination by ELISA. Blood samples were centrifuged at 1,000 x g for 15 min at 4°C to remove blood cells, followed by centrifugation at 10,000 x g for 10 min at 4°C to remove platelets. Plasma samples were stored at -80°C until tested. The MA vascular bed was harvested with the intestine in ice-cold Krebs solution (pH 7.4) containing (in mmol/L): 120 NaCl, 25 NaHCO<sub>3</sub>, 4.7 KCl, 1.18 KH<sub>2</sub>PO<sub>4</sub>, 1.18 MgSO<sub>4</sub>, 2.5 CaCl<sub>2</sub>, 0.026 EDTA and 5.5 glucose, that had been bubbled with 95% air and 5% CO<sub>2</sub>, and used for determination of endothelial function and vascular mechanics by pressurized myography. The heart, lung, kidneys and right tibia were harvested in ice-cold phosphate buffered saline (PBS). The renal capsule was removed. Tissues were weighed and tibia length determined. The right kidney was used for immune cell profiling by flow cytometry. Sections of MAs with perivascular adipose tissue (PVAT) and left kidney were embedded in VWR Clear Frozen Section Compound (VWR international, Edmonton, AB, Canada) for determination of reactive oxygen species (ROS) generation, fibronectin, and kidney injury molecule (KIM)-1 expression or monocyte/macrophage and T cell infiltration by immunofluorescence. Sections of MAs and left kidney were fixed with 4% paraformaldehyde in PBS for 48 h at 4°C, and embedded in paraffin for investigation of collagen content with Sirius red staining or kidney injury using Masson's trichrome and periodic acid Schiff (PAS) staining or immune cell infiltration using CD45 immunohistochemistry. The remaining tissues were frozen in liquid nitrogen and stored at -80°C until used.

In a separate set of mice, the total MA arcade was dissected from the attached intestine under RNase-free conditions, rinsed in ice-cold PBS and stored immediately in RNAlater (Life Technologies, Burlington, Ontario, Canada), and kidneys were collected in ice-cold PBS. The MAs were then dissected from surrounding tissues, perivascular fat and veins under the microscope, and stored in tubes containing RNAlater until RNA

extraction. The right kidney was meticulously dissected in ice-cold PBS under a dissecting microscope to separate the renal cortex and medulla. Tissues were frozen in liquid nitrogen and stored at  $-80^{\circ}\text{C}$  until use for RNA extraction.

### **Assessment of endothelial function and vessel mechanics**

Second-order MAs, of average lumen size  $\sim 220\ \mu\text{m}$ , were dissected from perivascular fat and vein, mounted on a pressurized myograph and endothelial function and vessel mechanics determined as previously described.<sup>5</sup>

### **Reactive oxygen species production**

Dihydroethidium (DHE) was used to evaluate the *in situ* production of reactive oxygen species (ROS) as previously described.<sup>5,6</sup> Five  $\mu\text{m}$  sections of MAs were thawed and incubated in DHE ( $2\ \mu\text{mol/l}$ ) in dark for 1 min at  $37^{\circ}\text{C}$  and then in cold PBS for 1 min. Fluorescence was visualized and captured with a fluorescence microscope with a CY3 filter as previously described.<sup>5</sup> DHE fluorescence intensity per total surface area in the media and PVAT was quantified separately using ImageJ software (<http://rsb.info.nih.gov/ij/>). The following steps were followed on each experimental day in order to ensure rigorous quantification of DHE fluorescence. One slide was handled at a time. The exposure time was determined with tissue sections expecting to have the greatest fluorescence to avoid signal saturation. DHE fluorescence was normalized to the control group acquired on the same day, to eliminate any variation due to changes in the oxidative environment on any given day.

### **Immunofluorescence**

Expression of MCP-1 and fibronectin in MAs, monocyte/macrophage (MOMA-2<sup>+</sup>) and CD3<sup>+</sup> T cell infiltration in MA PVAT and KIM-1 in renal cortex were determined by immunofluorescence microscopy on 5- $\mu\text{m}$  cryosections. Unless indicated, the following steps were made at room temperature. Tissue cryosections were air-dried for 30 min. Subsequently, sections were fixed in a staining dish with ice-cold acetone:methanol mixture (1:1) for 10 min (for MCP-1, fibronectin and MOMA-2) or with 4% paraformaldehyde solution for 20 min (for CD3 and KIM-1), and then washed with PBS

for 10 min in another staining dish. Thereafter, they were transferred to Shandon Sequenza™ Slide Racks (Thermo Fisher Scientific, Montreal, QC, Canada) for the remaining of the immunostaining procedure. PBS was added to each tissue section to keep them humidified. Paraformaldehyde-fixed sections were permeabilized with Tris buffered saline (TBS) containing 0.9% Triton X-100 for 5 min. Sections were blocked for 1 hour with TBS containing 0.1% Tween-20 (TBST) and 10% normal donkey serum (for MCP-1) or 10% normal goat serum (for fibronectin, MOMA-2, CD3 and KIM-1). Sections were incubated overnight at 4°C with goat anti-mouse MCP-1 antibodies (1:50, Santa Cruz Biotechnology, Santa Cruz, CA), rabbit anti-mouse fibronectin antibodies (1:100, EMD Millipore, Billerica, MA, USA), rat anti-mouse MOMA-2 antibodies (1:100, Abcam, Cambridge, MA), rat anti-mouse CD3 antibodies (1:200, eBiosciences - Thermo Fisher Scientific) or rabbit anti-mouse KIM-1 antibody (1:200, Abcam). The sections were then washed 3 times with 1 mL of TBST and blocked for 30 min with TBST containing 10% normal donkey serum (for MCP-1) or 10% normal goat serum (for fibronectin, MOMA-2, CD3 and KIM-1). Thereafter, sections were incubated for 1 hour with Alexa® Fluor 555 donkey anti-goat antibodies (1:150, Invitrogen - Thermo Fisher Scientific) for MCP-1, Alexa® Fluor 568 goat anti-rabbit antibodies (1:200) for fibronectin and KIM-1, Alexa® Fluor 568 goat anti-rat antibodies (1:200) for MOMA-2 and CD3. Sections were washed afterwards 3 times with 1 mL of TBST. Kidney sections were incubated with Alexa® Fluor 647 wheat germ agglutinin for KIM-1 (1:200, Molecular Probes - Thermo Fisher Scientific) for 30 min, washed afterwards with 1 mL of TBST and incubate 5 min. Subsequently, sections were stained with 4',6- diamidino-2-phenylindole (DAPI, 14.3 µmol/L, Life Technologies) for 5 min to label the nuclei, washed with 1 mL of TBST and then mounted with Fluoromount (Sigma-Aldrich Canada, Oakville, ON, Canada).

Fluorescence images were captured using a fluorescent microscope Leica DM2000 (Leica Microsystems, Richmond Hill, ON, Canada) for MCP-1, fibronectin, MOMA-2 and CD3 or with a Wave FX Spinning Disc Confocal Microscope (Quorum Technologies, ON, Canada) for KIM-1, and analyzed with ImageJ software. The expression of fibronectin and MCP-1 in MA wall were expressed as relative fluorescence units (RFU) per µm<sup>2</sup>. KIM-1 in renal cortex and monocyte/macrophage infiltration in MA adventitia and PVAT were determined by measuring the positive area

using color RGB thresholding, which was then expressed as % of studied area. CD3 infiltration was quantified in MA PVAT as the number of cells detected per  $\mu\text{m}^2$ .

### **Immunohistochemistry**

CD45<sup>+</sup> immune cell infiltration in the kidney was determined by immunofluorescence microscopy on 5  $\mu\text{m}$  sections of paraffin-embedded tissues as follows. Unless indicated, the following steps were made at room temperature. Paraffin sections were deparaffinized with two 10 min xylene baths, rehydrated in successive 5 min ethanol baths (100%, 100%, 95%, 95%, 70% and 50%), and followed by 5 min incubation in TBS. Tissue sections were left in TBS-triton X-100 0.1 % until the next step was ready. The antigens were unmasked by heat-induced epitope retrieval as follows. Tissue sections were incubated in 10 mM sodium citrate pH 6.0 in a Panasonic microwave model NN-H965WF (Panasonic Canada, Mississauga, ON, Canada) at medium power for 5 min to reach a temperature of 90-95°C at the end of the incubation. This step was repeated once more using a new slide container with fresh sodium citrate solution. Thereafter, slides were incubated for 5 min on the bench, next for 1 min in the microwave at medium power and then on the bench for 20 min. Slides were then dipped in 2 baths of distilled water to remove sodium citrate. To remove endogenous peroxidase, slides were incubated in 1% hydrogen peroxide for 5 min and dipped in distilled water and thereafter, slides were incubated in TBST for 5 min. Sections were transferred to Shandon Sequenza™ Slide Racks for the remaining of the immunostaining procedure. TBS was added to each tissue section to keep them humidified. Sections were incubated with TBST for 5 min, blocked for 1 hour with TBST containing 10% normal goat serum, 7% bovine serum albumin and 0.3 M glycine, and then incubated overnight at 4°C with rat anti-mouse CD45 antibodies (1/150, eBioscience) in the blocking solution. The sections were washed 3 times with 2 mL of TBST and blocked as above for 45 min. Thereafter, sections were incubated for 30 min with biotinylated goat anti-rat IgG antibodies (1/1000, Vector Laboratories, Burlingame, CA, USA) in the blocking solution. The sections were then washed 3 times with 2 mL of TBST, blocked as above for 1 hour. Next, sections were incubated for 30 min with horseradish peroxidase conjugated streptavidin (1:500, Perkin Elmer, Woodbridge, ON,

Canada) in the blocking solution, and then washed 3 times with 2 mL of TBST. The antigen-antibody complexes were revealed as follows in the dark. Sections were incubated 3 min in 3,3'-diaminobenzidine tetra-hydrochloride (DAB) solution and then washed with 3 successive 2 min baths of distilled water. DAB solution was made just before use and contained 0.05 % DAB (Sigma-Aldrich Canada), 0.009 % H<sub>2</sub>O<sub>2</sub> and 10 mmol/L imidazole dissolved in TBS. Subsequently, sections were counter stained with methyl green staining solution (1 % crystal violet free methyl green in 0.1 mol/L sodium acetate, pH 4) for 8 min. The sections were then washed twice by dipping the slides 5 times in a water bath, followed by 3 butanol baths, also dipping the slides 5 times in each of the first two baths followed by a 15 sec incubation in the last one. Slides were finally incubated twice in 2 min xylene baths and mounted in Eukitt Mounting Medium. Images were acquired by light microscopy using a Leica DM2000 microscope.

### **Collagen content**

Sections (5 µm) of paraffin-embedded tissues were stained with Sirius red to determine MA collagen type I and III content as previously described.<sup>7</sup> White and polarized light images were captured using an Olympus BX60F5 polarizing microscope (Olympus Canada, Richmond Hill, ON, Canada). Under polarized light collagen appears as green, red or yellow. However, it is not possible to distinguish the type of collagen using this technique as the absorbed amount of polarized light by the Sirius red dye is determined by the orientation of the collagen bundles.<sup>8</sup> Adventitia and MA wall collagen fraction was defined as the ratio of the adventitia and media stained area in polarized light to the media cross-sectional area in white light, and expressed as a percentage.

### **Histological assessment of kidney injury**

Kidney injury was assessed using Masson's trichrome and Periodic Acid-Schiff (PAS) staining as follows.

Five-µm sections of paraffin-embedded tissues were stained with Masson's trichrome stain to assess kidney injury as follows. Unless indicated, the following steps were made at room temperature. Paraffin sections were deparaffinized with two 3-min xylene baths, rehydrated in successive 5-min baths of ethanol (100% and 95%), and

followed by 5-min incubation in water. Tissue sections were then incubated in Bouin's solution for 1 hour at 56°C, and thereafter rinsed with running tap water set at ~20°C until the yellow color disappeared. Nuclear chromatin was stained with freshly made Weigert's iron-hematoxylin stain for 10 min. Excess stain was removed by dipping slides in water followed by soaking in another water bath for 5 min. Then, slides were transferred into a Biebrich scarlet-acid fuchsin solution for 2 min, dipped in water and soaked in another water bath for 30 sec. Thereafter, slides were placed in phosphomolybdic-phosphotungstic solution for 15 min, dipped in water and soaked in another water bath for 30 sec. Tissue sections were then stained for 5 min in Aniline Blue solution, and excess stain removed by dipping slides in water, followed by soaking in another water bath for 5 min. Slides were finally submerged in freshly made 1% acetic acid solution for 5 min and rinsed in water for 5 min. Tissue sections were then dehydrated in successive 5 min baths of ethanol (95%, 100%) and immersed in two baths of xylene for 3 min. Sections were then mounted using Eukitt Mounting Medium (Electron Microscopy Sciences, Hatfield, PA, USA). Images were acquired by light microscopy using a Leica DM2000 microscope. Masson's trichrome staining solutions are listed in Supplemental Table III-S3.

Five- $\mu$ m sections of paraffin-embedded tissues were stained with PAS stain as follows. Unless indicated, the following steps were made at room temperature. Where indicated solutions were preheated in a microwave. Paraffin sections were deparaffinized with two 5-min xylene baths, rehydrated in successive 2-min baths of ethanol (100%, 100%, 95%, 95%, 70% and 50%), and followed by 2-min incubation in water. For the negative control, the slides were incubated in diastase solution for 20 min and washed in running tap water set at ~20°C for 1 min. For the following step, the glassware was acid washed to prevent contamination. Tissue sections were incubated in periodic acid solution preheated at 60°C for 2 min, and rinsed with three 2-min distilled water bath. Tissue sections were then incubated in Schiff reagent preheated at 60°C for 2 min, and thereafter incubated with two 1-min 0.55% potassium metabisulfite baths to remove excess Schiff reagent. Following this they were rinsed with running tap water for 10 min to allow color to develop. Thereafter, slides were placed in acidified Harris hematoxylin solution for 30 sec, washed in running tap water to blue the

hematoxylin, dipped in 1% acid alcohol bath for 30 sec and then washed in running tap water for 5 min and successive 2 min baths of ethanol (70%, 95%, 95%, 100% and 100%). Slides were finally incubated for 2-min in 2 baths of xylene and mounted in Eukitt Mounting Medium. Images were acquired by light microscopy using a Leica DM2000 microscope. PAS staining solutions are listed in Supplemental Table III-S4.

### **Renal immune cell profiling**

The right kidney was transferred to a Petri dish containing ice-cold RPMI 1640 (Life Technologies, Burlington, ON, Canada) and crushed by forcing it through a 100  $\mu$ m nylon mesh cell strainer (BD Biosciences, Durham, NC, USA) pre-wetted with RPMI 1640 at 4°C, with the back of a 1 mL syringe plunger. The tissues were digested in a hybridization oven (VWR International, LLC Radnor, PA, USA) in 1 mL of enzyme digestion medium at 37°C for 1 h in a 1.5 mL conical tube with gentle agitation. The enzyme digestion medium was made of RPMI medium 1640 (Life Technologies, Burlington, Ontario, Canada) supplemented with 1 mg/ml of collagenase A (0.229 U/mg), 500 U/ml of collagenase type 2 (290 U/mg), 2 U/ml of elastase (4.41 U/mgP) and 250  $\mu$ g/ml of soybean trypsin inhibitor (1 mg SI inhibits 2 mg TRL) that was filtered with a 0.22  $\mu$ m Millex GP filter unit (EMD Millipore, Billerica, MA, USA). Collagenase A was obtained from Roche Diagnostics GmbH (Mannheim, Germany), and all other enzymes from Worthington Biochemical Corporation (Lakewood, NJ, USA). At the end of the digestion period, the cell suspension was passed through a 70- $\mu$ m BD Falcon nylon mesh cell strainer fitted on top of a 1.5 mL tube. The nylon mesh was washed with 0.5 mL of RPMI to collect any remaining cells. Cells were counted in 0.2% Trypan blue stain (Life Technologies) using a Neubauer cell counting hemacytometer (C.A. Hausser & son, Philadelphia, Pennsylvania, USA). One hundred fifty  $\mu$ L were transferred to a new tube that was used for control staining. Both tubes of cells were centrifuged at 410 g for 5 min at 4°C. The supernatant was removed and cells were suspended in 100  $\mu$ L of RPMI supplemented with 5% fetal bovine serum (FBS, qualified, Canadian origin, Life Technologies) containing specific antibodies or appropriate isotype control antibodies (Table III-S5), and incubated for 15 min at 4°C. They were then washed by adding 1.4 mL of PBS and centrifuged at 410 g for 5 min at

4°C. Cells were suspended in 200 µL of PBS and stored on ice until used for flow cytometry.

Flow cytometry was performed on the BD LSR Fortessa cell analyzer (BD Biosciences). Fluorescence minus one (FMO) was used to adjust the gates and isotype control antibodies to determine the fluorescence background. Data analysis was performed using FlowJo software (version 10.1, Tree Star Inc., Ashland, OR). Flow cytometry profiling gating strategy was performed as follows. Debris were excluded by gating cells using the side scatter-area (SSC-A)/forward scatter-area (FSC-A) plot. Singlet cells were gated using SSC-A over SSC-wide (SSC-W). CD45<sup>+</sup> and CD45<sup>-</sup> cells were gated in SSC-A/CD45 grayscale dot plot. CD11b<sup>+</sup> cells were gated in grayscale dot plot from the CD45<sup>+</sup> cell population, and CD11b<sup>+</sup>Gr-1<sup>+</sup> cells were then gated in grayscale dot plot from the CD11b<sup>+</sup> cell population. Thereafter, CD36<sup>+</sup> cells were gated in grayscale dot plot from the CD45<sup>-</sup> and CD11b<sup>+</sup> cell populations. Fluorophores were excited and analyzed with the appropriate laser and band pass filter (BP) (Brilliant Violet 785 (BV785): 405 nm with 780/60 BP, allophycocyanin (APC): 640 nm with 670/10 BP, phycoerythrin (PE): 561 nm with 582/15 BP, PE-cyanine 7 (Cy7): 561 nm with 780/60).

### **Quantification of mRNA expression**

The expression of *Ednra*, *Ednrb*, *Col1A1*, *Col3A1*, *Ren1* and ribosomal protein S16 (*Rps16*) was investigated in MAs or renal cortex and medulla by RT-qPCR. RNA was extracted from the kidney and MAs and processed as previously described.<sup>3</sup> RNA concentration was measured using a Nanodrop spectrophotometer ND-100 V3.1.2 (Thermo Fisher Scientific) and RNA quality was assessed by determining the rRNA and mRNA profiles by electrophoresis with a RNase free 1% agarose gel with 1X TAE electrophoresis buffer (2 M Tris-acetate and 50 mM EDTA) using 0.5 µg of RNA. Total RNA isolated from kidney (0.8 µg) and MAs (0.3 µg) was reverse-transcribed with the Quantitect RT kit (Qiagen, Foster City, CA, USA). QPCR was performed using the SsoFast EvaGreen Supermix (Bio-Rad Laboratories, Mississauga, ON, Canada) with the Mx3005P real-time PCR cycler (Agilent Technologies, Santa Clara, CA). qPCR oligonucleotides were designed to have a melting temperature (T<sub>m</sub>) of 60°C and a 3' GC clamp using Primer3<sup>9</sup> (Supplemental Table III-S6). Oligonucleotides were validated

to have a PCR efficiency between 95% and 105%, one amplicon with a  $T_m > 80^\circ\text{C}$  in the qPCR dissociation curve, and the right PCR product length using agarose gel electrophoresis. The qPCR conditions were 2 min at  $96^\circ\text{C}$ , followed by 40 cycles of 5 sec at  $96^\circ\text{C}$  and 30 sec at  $58^\circ\text{C}$ . Results were normalized with *Rps16* and expressed as fold change over control.

### **Plasma ET-1 and creatinine**

One hundred  $\mu\text{L}$  of plasma EDTA was used to assay the plasma concentration of ET-1 using a human ET-1 QuantiGlo ELISA Kit (R&D Systems Inc., Minneapolis, Minnesota, USA). Fifty  $\mu\text{L}$  of plasma EDTA was used to measure creatinine with a J&J Vitros 250 chemistry analyzer by Diagnostic Research Support Services at the Comparative Medicine and Animal Resource Centre of McGill University.

### **Data analysis**

Results are presented as means  $\pm$  SEM. Data were compared with two-way analysis of variance (ANOVA) for repeated measures or one-way ANOVA, with all ANOVA tests followed by a Student–Newman–Keuls *post-hoc* test, or with an unpaired *t*-test, as appropriate.  $P < 0.05$  was considered statistically significant.

## References

1. Indra AK, Warot X, Brocard J, Bornert JM, Xiao JH, Chambon P, Metzger D. Temporally-controlled site-specific mutagenesis in the basal layer of the epidermis: comparison of the recombinase activity of the tamoxifen-inducible Cre-ER(T) and Cre-ER(T2) recombinases. *Nucleic Acids Res.* 1999;27:4324-4327.
2. Korhonen H, Fisslthaler B, Moers A, Wirth A, Habermehl D, Wieland T, Schutz G, Wettschureck N, Fleming I, Offermanns S. Anaphylactic shock depends on endothelial Gq/G11. *J Exp Med.* 2009;206:411-420.
3. Rautureau Y, Coelho SC, Fraulob-Aquino JC, Huo KG, Rehman A, Offermanns S, Paradis P, Schiffrin EL. Inducible Human Endothelin-1 Overexpression in Endothelium Raises Blood Pressure via Endothelin Type A Receptors. *Hypertension.* 2015;66:347-355.
4. Barhoumi T, Kasal DA, Li MW, Shbat L, Laurant P, Neves MF, Paradis P, Schiffrin EL. T regulatory lymphocytes prevent angiotensin II-induced hypertension and vascular injury. *Hypertension.* 2011;57:469-476.
5. Leibovitz E, Ebrahimian T, Paradis P, Schiffrin EL. Aldosterone induces arterial stiffness in absence of oxidative stress and endothelial dysfunction. *J Hypertens.* 2009;27:2192-2200.
6. Rehman A, Leibowitz A, Yamamoto N, Rautureau Y, Paradis P, Schiffrin EL. Angiotensin type 2 receptor agonist compound 21 reduces vascular injury and myocardial fibrosis in stroke-prone spontaneously hypertensive rats. *Hypertension.* 2012;59:291-299.
7. Mian MO, Barhoumi T, Briet M, Paradis P, Schiffrin EL. Deficiency of T-regulatory cells exaggerates angiotensin II-induced microvascular injury by enhancing immune responses. *J Hypertens.* 2016;34:97-108.
8. Lattouf R, Younes R, Lutomski D, Naaman N, Godeau G, Senni K, Changotade S. Picrosirius red staining: a useful tool to appraise collagen networks in normal and pathological tissues. *J Histochem Cytochem.* 2014;62:751-758.

9. Rozen S, Skaletsky H. Primer3 on the WWW for general users and for biologist programmers. *Methods Mol Biol.* 2000;132:365-386.

## Supplemental figures and tables

**Table III-S1. Body and tissue weight**

Parameters	ieCre	ieET-1	ieET-1+Atras
n	7	9	6
BW (g)	29.1 ± 0.8	29.5 ± 0.5	32.0 ± 1.6
TL (mm)	19.3 ± 0.1	19.3 ± 0.1	19.1 ± 0.2
HW/TL (mg/mm)	7.6 ± 0.2	7.4 ± 0.2	7.2 ± 0.1
LuW/TL (mg/mm)	9.1 ± 0.7	11.3 ± 0.8	9.5 ± 0.9
KW/TL (mg/mm)	20.9 ± 0.7	20.9 ± 0.5	19.1 ± 0.2

Body weight (BW), tibia length (TL) and heart (HW), lung (LuW), and kidney (KW) weights were determined in tamoxifen-treated inducible endothelium-restricted Cre recombinase (ieCre) and human endothelin-1 overexpressing (ieET-1) mice, treated or not with atrasentan (Atras). n, number. Note Data are means ± SEM. Data were analyzed using one-way ANOVA followed by a Student-Newman-Keuls *post hoc* test.

**Table III-S2. Long-term human ET-1 overexpression in endothelium decreased renal artery flow**

Parameters	ieCre	ieET-1	ieET-1+Atras
n	10	13	9
RAF mL/min	3.01±0.26	1.74±0.20**	2.04±0.16*
RAD, mm	0.44±0.01	0.43±0.01	0.42±0.01
HR, bpm	563±4	548±6.0	547±7.0

Renal artery flow (RAF) and diameter (RAD), and heart rate (HR) were investigated in the right kidney renal artery using two-dimensional guided pulse wave (PW) Doppler in tamoxifen-treated inducible endothelium-restricted Cre recombinase (ieCre) and human endothelin-1 overexpressing (ieET-1) mice treated or not with atrasentan (Atras). n, number. Data are presented as means ± SEM. Data were analyzed using one-way ANOVA followed by a Student-Newman-Keuls *post hoc* test. \* $P < 0.01$  ieCre.

Table III-S3. Masson's trichrome staining solutions

Solutions and constituents	Company	Final concentration
<b>Bouin's solution</b>		
Picric acid, saturated aqueous solution	Sigma-Aldrich Canada	0.93%
Formaldehyde reagent (~37%)	Electron Microscopy Sciences	8.9%
Glacial acetic acid	Thermo Fisher Scientific	4.8%
<b>Weigert's iron hematoxylin solution</b>		
<b>Solution A:</b>		
Hematoxylin, certified biological stain	Thermo Fisher Scientific	1%
Ethanol, anhydrous	Commercial Alcohols	95%
<b>Solution B:</b>		
Iron (III) chloride, reagent grade	Sigma-Aldrich Canada	1.16%
Hydrochloric acid, certified ACS Plus	Thermo Fisher Scientific	1.2 N
<b>Working solution</b> is made just before use by mixing equal parts of solutions A and B.		
<b>Biebrich Scarlet-acid fuchsin solution</b>	Electron Microscopy Sciences	Ready to use
<b>Phosphomolybdic-phosphotungstic acid solution</b>		
Phosphotungstic acid	Electron Microscopy Sciences	2.5%
Phosphomolybdic acid	Electron Microscopy Sciences	2.5%
<b>Working solution</b> is made just before use.		
<b>Aniline Blue solution</b>		
Aniline Blue, certified dyes/stains	Electron Microscopy Sciences	2.5%
Glacial acetic acid	Thermo Fisher Scientific	2%

Table III-S4. Periodic Acid Schiff's staining solutions

Solutions and constituents	Company	Final concentration
<b>Phosphate citrate buffer, pH 5</b>		
Citric acid	Sigma	0.1 M
Dibasic sodium phosphate	Fisher	0.2 M
<b>Diastase solution</b>		
Diastase	Electron Microscopy Sciences	0.2%
Phosphate citrate buffer		
<i>Working solution was made just before use by dissolving the diastase in Phosphate citrate buffer.</i>		
<b>Periodic acid solution</b>		
Periodic acid	Acros Organics	0.5%
<i>Working solution was made just before by dissolving the Periodic acid in deionized water.</i>		
<b>Schiff's reagent</b>	Electron Microscopy Sciences	Ready to use
<b>Potassium metabisulfite</b>		
Potassium metabisulfite	Fisher scientific	0.55%
<i>Working solution was made just before by dissolving the Potassium metabisulfite acid in deionized water.</i>		
<b>Acidified Harris hematoxylin solution</b>	Polyscience Inc	Ready to use

**Table III-S5. Antibodies for flow cytometry profiling of T cells**

<b>Antibodies</b>	<b>Description</b>	<b>Clone, company</b>
CD45	BV785-conjugated rat IgG2b anti-mouse CD45 antibody	30F11, Biolegend
CD45 isotype	BV785-conjugated rat IgG2b $\kappa$ isotype control antibody	RTK4530, Biolegend
CD11b	APC-conjugated rat IgG2b $\kappa$ anti-mouse CD11b antibody	M1/70, eBioscience
CD11b isotype	APC-conjugated rat IgG2b $\kappa$ isotype control antibody	A95-1, eBioscience
Gr-1	PE-Cy7-conjugated rat IgG2b $\kappa$ anti-mouse Gr-1 antibody	RB6-8C5, eBioscience
Gr-1 isotype	PE-Cy7-conjugated rat IgG2b $\kappa$ isotype control antibody	A95-1, eBioscience
CD36	PE-conjugated rat IgG2a $\kappa$ anti-mouse CD36 antibody	72-1; eBioscience
CD36 isotype	PE-conjugated rat IgG2a $\kappa$ isotype control antibody	eBR2a, eBioscience
CD16/CD32	Rat IgG2b $\kappa$ anti-mouse CD16/CD32 Fc receptor block	2.4G2, BD pharmingen

APC, allophycocyanin, BV785, Brilliant Violet 785, Cy7, cyanine 7, PE, phycoerythrin.

**Table III-S6. Oligonucleotides used in quantitative PCR assays**

<b>mRNA</b>	<b>Forward</b>	<b>Reverse</b>
<i>Ednra</i>	5'-TGGCCCTTGGAGACCTTATC-3'	5'-GCTCGCCCTTGTATTCTGAAG-3'
<i>Ednrb</i>	5'-TGTTTCGTGCTAGGCATCATC-3'	5'-CTGCTGTCCATTTTGGAAACC-3'
<i>Ren1</i>	5'-ATCTTTGACACGGGTTTCAGC-3'	5'-AGAACACCGTCAAACCTTGGC-3'
<i>Col1A1</i>	5'-GGTGAGACTGGTCCTGCTG-3'	5'-GACCGTTGAGTCCGTCTTTG-3'
<i>Col3A1</i>	5'-ATAAGCCCTGATGGTTCTCG-3'	5'-AGCTGCACATCAACGACATC-3'
<i>Col12A1</i>	5'-CTGGAAAAGATGGTGCAATG-3'	5'-GGCTGGTTTTCGACTTGAGTG-3'
<i>Rps16</i>	5'-ATCTCAAAGGCCCTGGTAGC-3'	5'-ACAAAGGTAAACCCCGATCC-3'

*Ednra* and *Ednrb*, endothelin type A and B receptors, *Ren1*, renin, *Col1A1* and *Col3A1* collagen type I alpha 1 and III alpha 1. Ribosomal protein 16 (*Rps16*) gene was chosen as a reference gene for relative quantification.

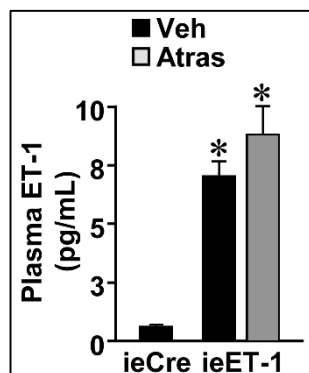


**Figure III-S1. Long-term endothelial human ET-1 overexpression enhanced plasma ET-1 levels.**

Plasma ET-1 levels were measured at the end of the study by ELISA in tamoxifen-treated inducible endothelium-restricted Cre recombinase (ieCre) and human endothelin-1 overexpressing (ieET-1) mice treated or not with atrasentan (Atras). Data are presented as mean  $\pm$  SEM,  $n = 9$  for ieCre + vehicle (Veh), 7 for ieET-1 + Veh and 5 for ieET-1 + Atras. Data were analyzed using one-way ANOVA followed by a Student-Newman-Keuls *post hoc* test. \* $P < 0.001$  vs ieCre.

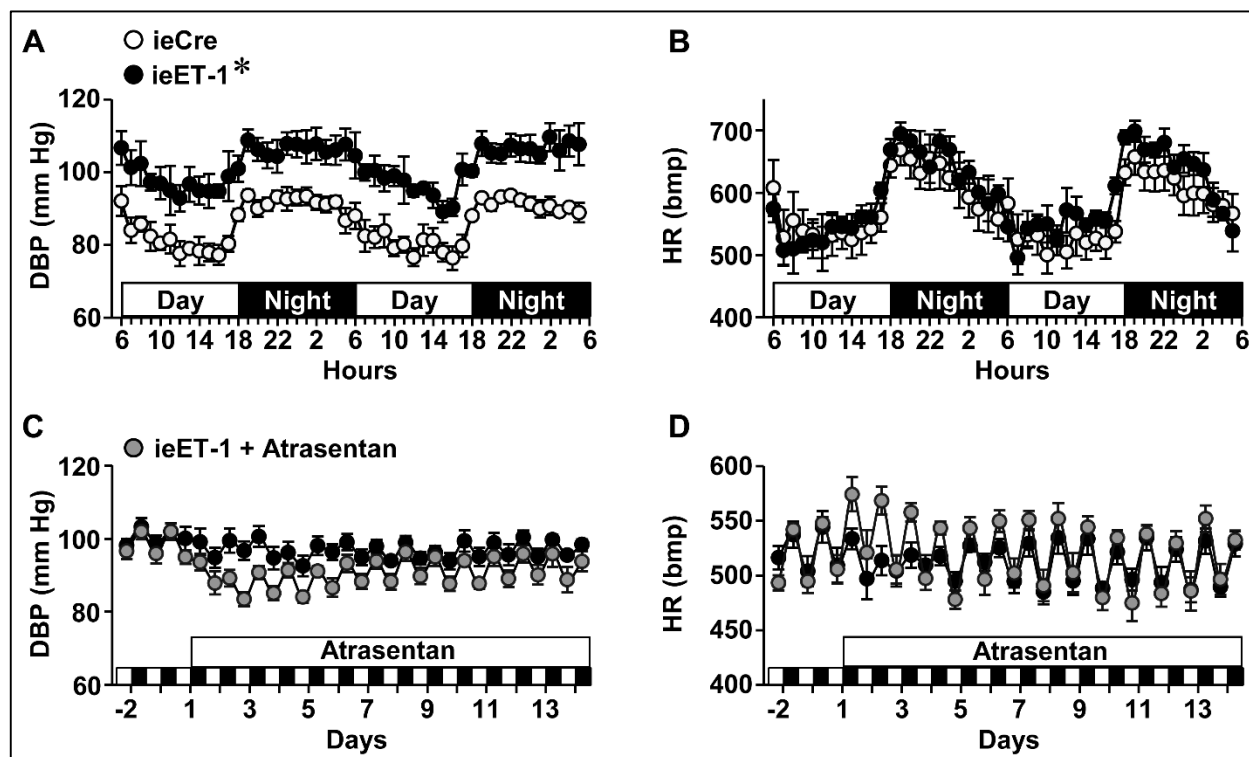


**Figure III-S2. Long-term endothelial human endothelin-1 overexpression increased blood pressure in an ET type A receptor-dependent manner.**

**A.** Diastolic blood pressure (DBP) and heart rate (HR) were determined by telemetry in tamoxifen-treated inducible endothelium-restricted Cre recombinase (ieCre) and human endothelin-1 overexpressing (ieET-1) mice during the last two days of the third month after tamoxifen treatment. **B.** DBP and HR were also measured in tamoxifen-treated ieET-1 mice two days before and during the last two weeks of the third month while they were treated or not with atrasentan. Data are presented as means  $\pm$  SEM,  $n=5$  for ieCre and ieET-1 in **A** and **B** and 5 for ieET-1 and 6 for ieET-1 + Atrasentan in **C** and **D**. Days 2 to 14 were used to compare DBP in **B**. Data were analyzed using two-way ANOVA for repeated measures followed by a Student-Newman-Keuls *post hoc* test. \* $P<0.01$  vs ieCre.

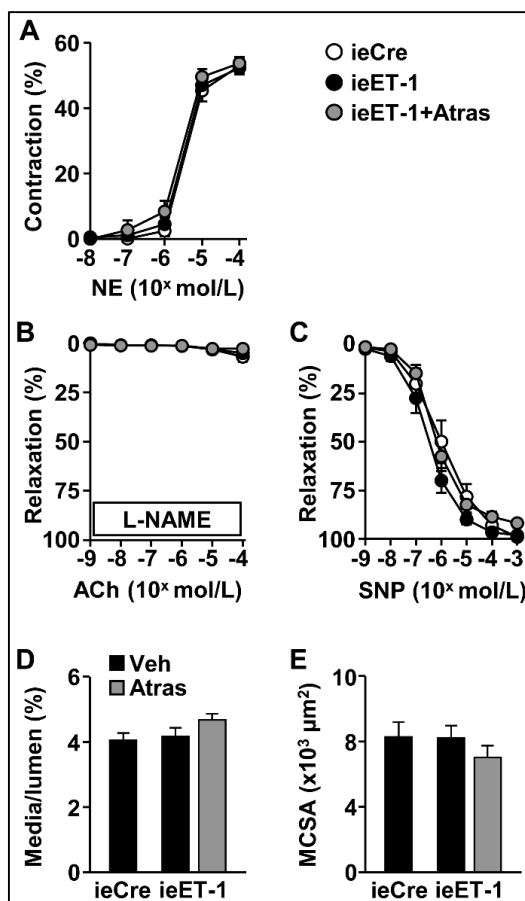


**Figure III-S3. Long-term endothelial human endothelin-1 overexpression did not affect mesenteric artery contractile responses to norepinephrine (NE), relaxation responses to acetylcholine (ACh) after inhibition of nitric oxide synthase (NOS) and to sodium nitroprusside (SNP), and caused vascular remodeling.**

Contractile responses to NE (**A**), relaxation responses to ACh in presence of the NOS inhibitor N<sup>ω</sup>-nitro-L-arginine methyl ester (L-NAME, **B**) and to SNP (**C**), media/lumen (**D**) and media cross-sectional area (MCSA, **E**) were assessed at the end of the study using pressurized myography in mesenteric arteries from tamoxifen-treated inducible endothelium-restricted Cre recombinase (ieCre) and human endothelin-1 overexpressing (ieET-1) mice treated or not with atrasentan (Atras). Data are presented as mean ± SEM, n = 7 for ieCre, 11 for ieET-1 and 9 for ieET-1+Atras in **A-C** and 8 for ieCre + vehicle (Veh), and 9 for ieET-1 + Veh and ieET-1 + Atras in **D-E**. Data were analyzed using two-way ANOVA for repeated measures in **A-C** and one-way ANOVA in **D-E**, with all ANOVA followed by a Student-Newman-Keuls *post hoc* test.

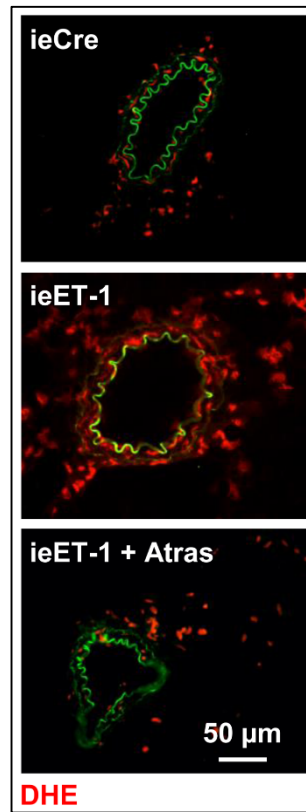


**Figure III-S4. Long-term endothelial human endothelin-1 overexpression increased oxidative stress in mesenteric artery perivascular adipose tissue.**

Representative images of reactive oxygen species (ROS) generation by dihydroethidium fluorescence (red) in mesenteric artery media and perivascular adipose tissue from tamoxifen-treated inducible endothelium-restricted Cre recombinase (ieCre) and human endothelin-1 overexpressing (ieET-1) mice treated or not with atrasentan (Atras) are shown. Green fluorescence represents elastin autofluorescence. n = 9 for ieCre, 8 for ieET-1 and 6 for ieET-1 + Atras.

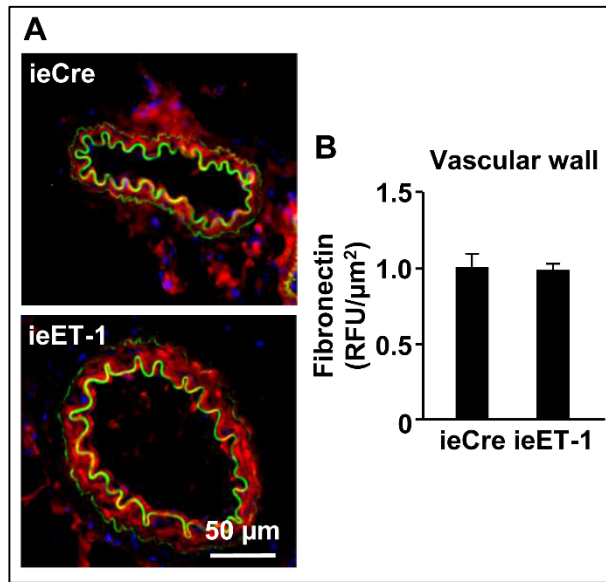


**Figure III-S5. Long-term endothelial human endothelin-1 overexpression did not modify mesenteric artery fibronectin expression.**

Fibronectin expression was determined by immunofluorescence in mesenteric arteries of tamoxifen-treated inducible endothelium-restricted Cre recombinase (ieCre) and human endothelin-1 overexpressing (ieET-1) mice (**A-B**). Representative fibronectin fluorescence images (red) are shown in **A**. Green and blue represent elastin autofluorescence and 4',6- diamidino-2-phenylindole (DAPI) fluorescence, respectively. RFU, relative light unit. Data are presented as means  $\pm$  SEM,  $n = 6$  for ieCre and ieET-1. Data were analyzed with an unpaired  $t$ -test.

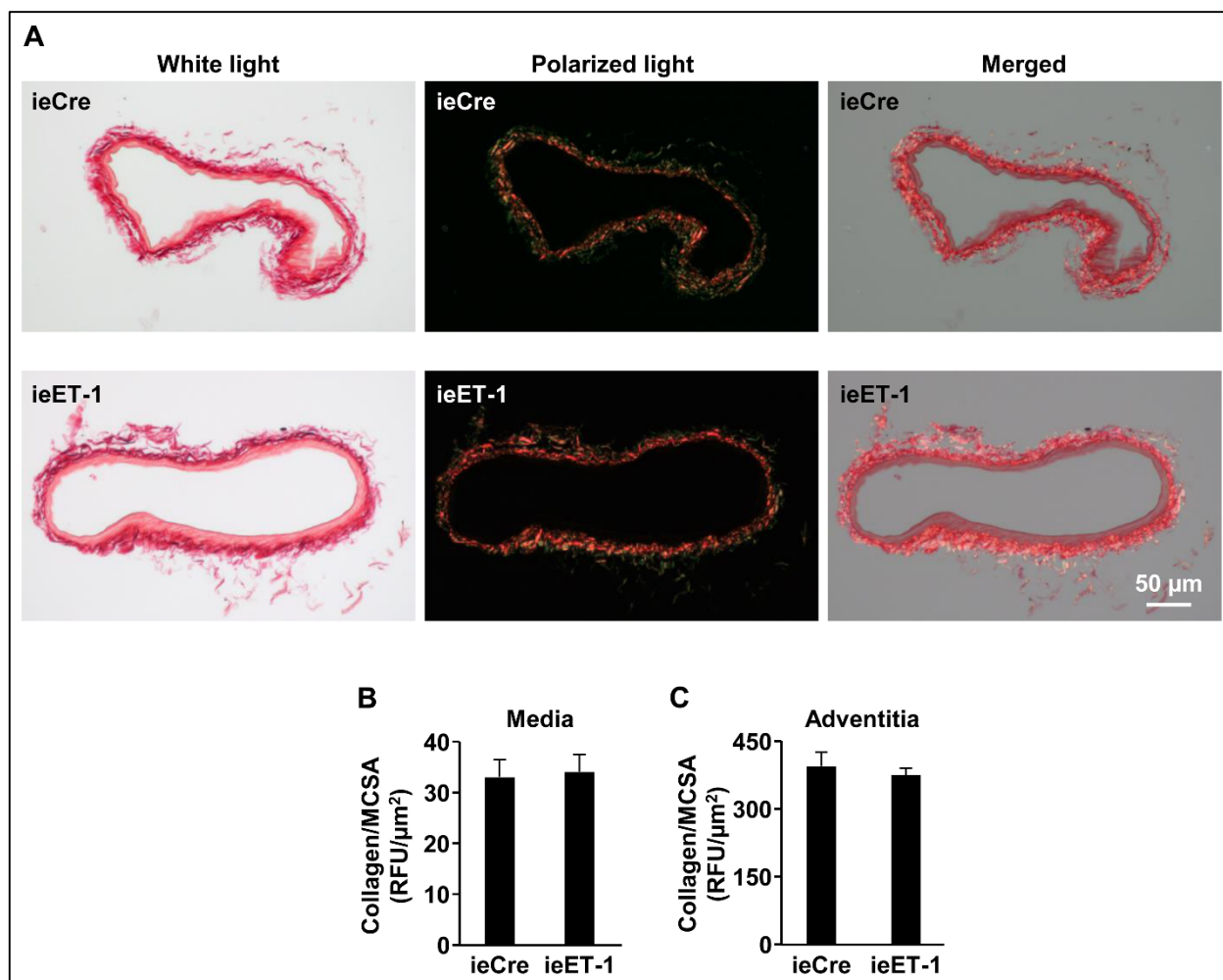


**Figure III-S6. Long-term endothelial human endothelin-1 overexpression did not affect mesenteric artery collagen content.**

Collagen content was assessed in adventitia (**A** and **B**) and media (**A** and **C**) of mesenteric arteries by Sirius red staining in tamoxifen-treated inducible endothelium-restricted Cre recombinase (ieCre) and human endothelin-1 overexpressing (ieET-1) mice (**A-C**). Representative white light, polarized light and merged images of Sirius red-stained mesenteric arteries are shown in **A**. MCSA, media cross-sectional area, RFU, relative light unit. Data are presented as means  $\pm$  SEM,  $n = 6$  for ieCre and 5 for ieET-1. Data were analyzed with an unpaired *t*-test.

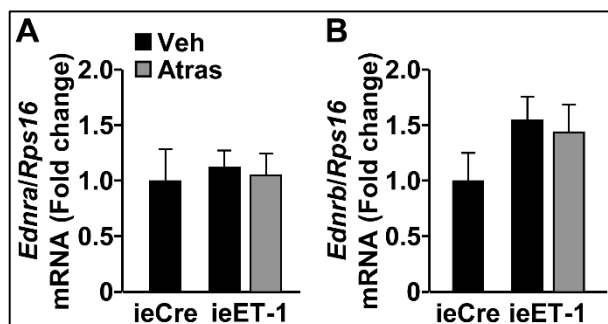


**Figure III-S7. Long-term endothelial human endothelin-1 overexpression did not alter the mRNA expression of ET<sub>A</sub> or ET<sub>B</sub> receptors in the mesenteric arteries.**

The mRNA expression of ET<sub>A</sub> (*Ednra*, **A**) and ET<sub>B</sub> (*Ednrb*, **B**) receptors, and ribosomal protein S16 (*Rps16*, reference gene for relative quantification) were determined by reverse transcription/quantitative PCR in mesenteric arteries of tamoxifen-treated inducible endothelium-restricted Cre recombinase (ieCre) and human endothelin-1 overexpressing (ieET-1) mice treated or not with atrasentan (Atras). Data are presented as means  $\pm$  SEM,  $n = 6$  for ieCre + and ieET-1 vehicle (Veh) and 7 for ieET-1 + Atras. Data were analyzed using one-way ANOVA followed by a Student-Newman-Keuls *post hoc* test.

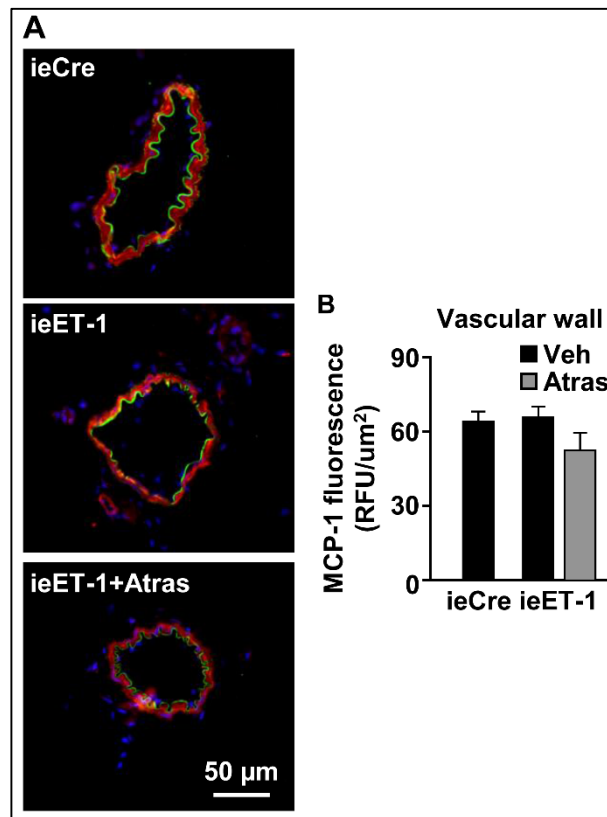


**Figure III-S8 Long-term endothelial human endothelin-1 overexpression did not alter the expression of monocyte chemoattractant protein (MCP)-1 in mesenteric arteries.**

MCP-1 expression was determined by immunofluorescence in mesenteric arteries (MA) of tamoxifen-treated inducible endothelium-restricted Cre recombinase (ieCre) and human endothelin-1 overexpressing (ieET-1) mice treated or not with atrasentan (Atras). Representative fluorescence images of MCP-1 (red) are shown in **A**. Green and blue represent elastin autofluorescence and 4',6- diamidino-2-phenylindole (DAPI) fluorescence, respectively. Data are presented as means  $\pm$  SEM,  $n = 7$  for ieCre + vehicle (Veh) and 6 for the two other groups. Data were analyzed using one-way ANOVA followed by a Student-Newman-Keuls *post hoc* test.

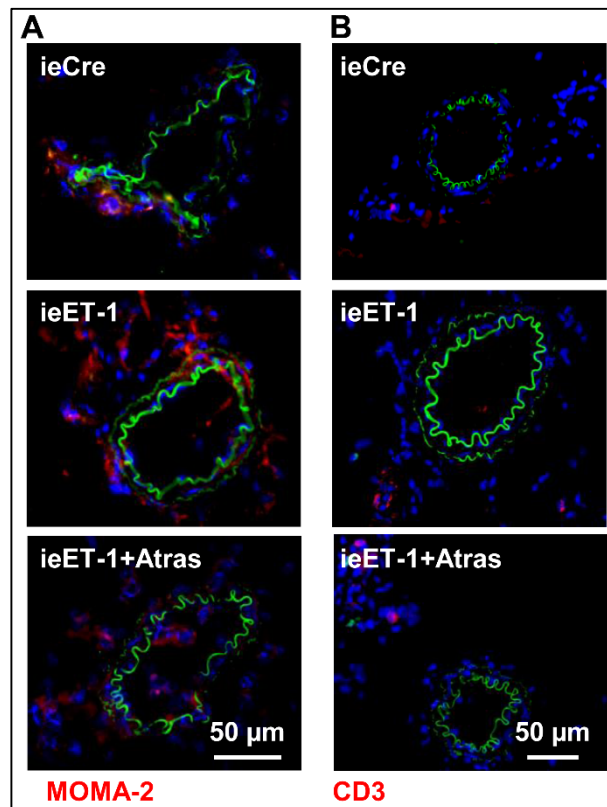


**Figure III-S9. Long-term endothelial human endothelin-1 overexpression increased monocyte/macrophage infiltration in the perivascular adipose tissue of mesenteric arteries.**

Monocyte/macrophage infiltration using anti-MOMA-2 antibody (**A**) and T lymphocyte infiltration using anti-CD3 antibody (**B**) were determined by immunofluorescence in perivascular adipose tissue (PVAT) of tamoxifen-treated inducible endothelium-restricted Cre recombinase (ieCre) and human endothelin-1 overexpressing (ieET-1) mice treated or not with atrasentan (Atras). Representative fluorescence images of MOMA-2 (red, **A**) and CD3 (red, **B**) are shown. Green and blue represent elastin autofluorescence and 4',6- diamidino-2-phenylindole (DAPI) fluorescence, respectively. n = 7 for ieCre and ieET-1 and 8 for ieET-1 + Atras in **A** and 7 for ieCre, 6 for ieET-1 and 7 for ieET-1 + Atras in **B**.

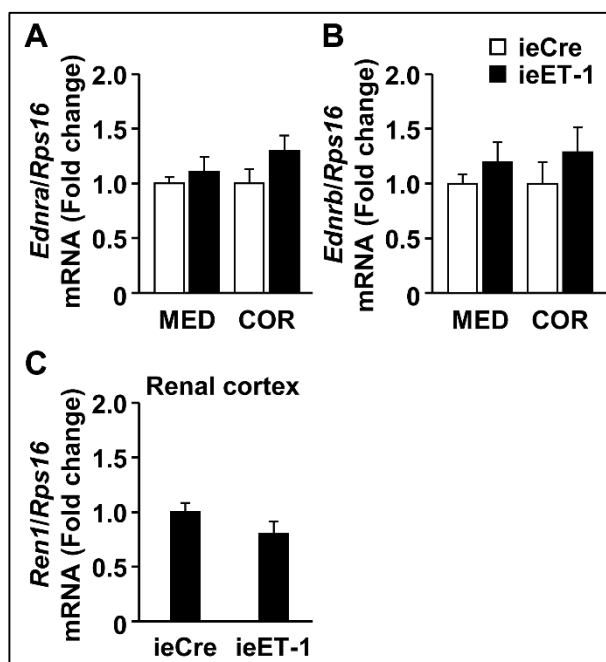


**Figure III-S10. Long-term endothelial human endothelin-1 overexpression did not alter the mRNA expression of renal ET<sub>A</sub>, ET<sub>B</sub> receptors or renal cortex renin.**

The mRNA expression of ET<sub>A</sub> (*Ednra*, **A**) and ET<sub>B</sub> (*Ednrb*, **B**) receptors, renin (*Ren1*, **C**) and ribosomal protein S16 (*Rps16*, reference gene for relative quantification) were determined by reverse transcription/quantitative PCR in renal cortex (COR) or renal medulla (MED) of tamoxifen-treated inducible endothelium-restricted Cre recombinase (ieCre) and human endothelin-1 overexpressing (ieET-1). Data are presented as means  $\pm$  SEM,  $n = 7$  for all the groups in **A-B** and 7 for ieCre and 6 for ieET-1 in **C**. Data were analyzed using an unpaired *t*-test.

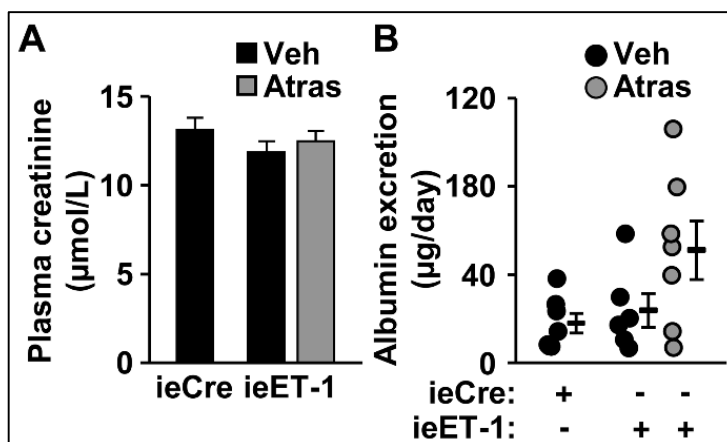


**Figure III-S11. Long-term endothelial human endothelin-1 overexpression did not alter plasma creatinine or urinary albumin excretion rate.**

Plasma Creatinine (**A**) and albumin excretion (**B**) were determined in tamoxifen-treated inducible endothelium-restricted Cre recombinase (ieCre) and human endothelin-1 overexpressing (ieET-1) mice treated or not with atrasentan (Atras). Data are presented as means  $\pm$  SEM,  $n = 7$  for all the groups in **A** and 6 for ieET-1 + vehicle (Veh) and 7 for the other groups in **B**. Data were analyzed using one-way ANOVA followed by a Student-Newman-Keuls post hoc test.

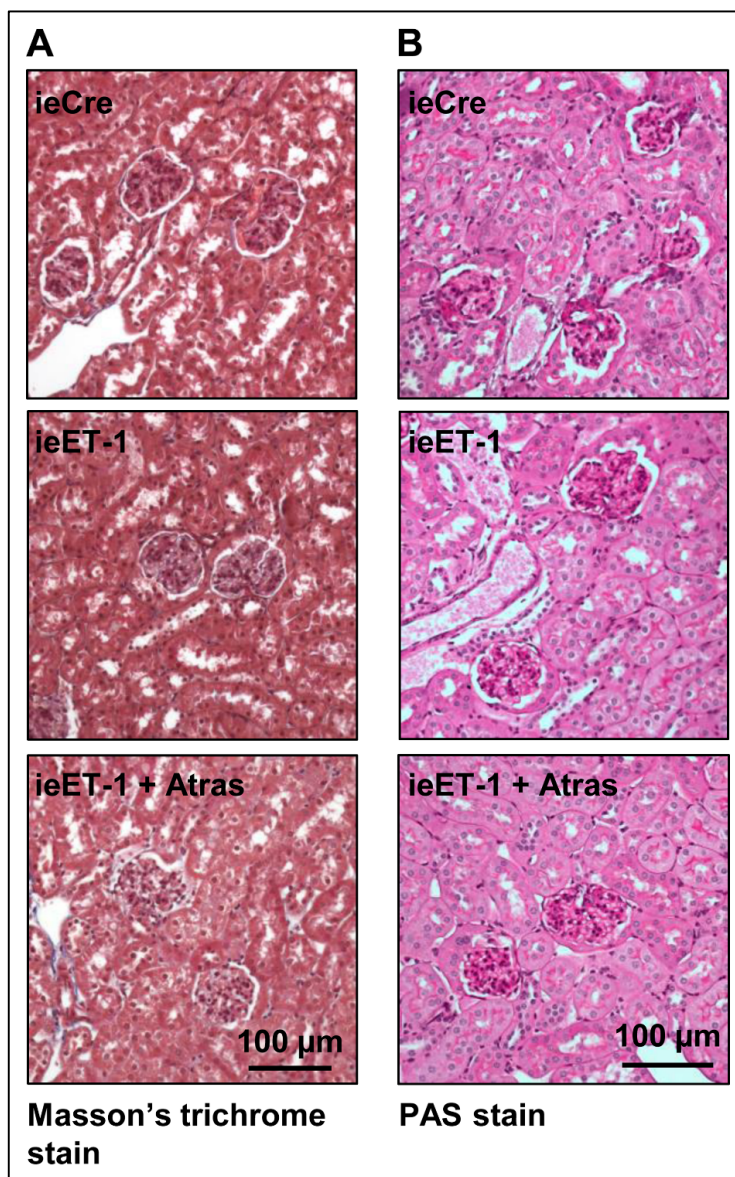


**Figure III-S12. Long-term endothelial human endothelin-1 overexpression did not cause evident kidney injury.**

Kidney injury was assessed using Masson's trichrome (**A**) and Periodic Acid Schiff (PAS)-stained kidney sections (**B**) of tamoxifen-treated inducible endothelium-restricted Cre recombinase (ieCre) and human endothelin-1 overexpressing (ieET-1) mice treated or not with atrasentan (Atras). Representative images of Masson's trichrome (**A**) and PAS (**B**) stained kidney sections are shown.  $n = 7$  for ieCre, 5 for ieET-1 and 8 for ieET-1 + Atras in **A** and 7 for all the groups in **B**.

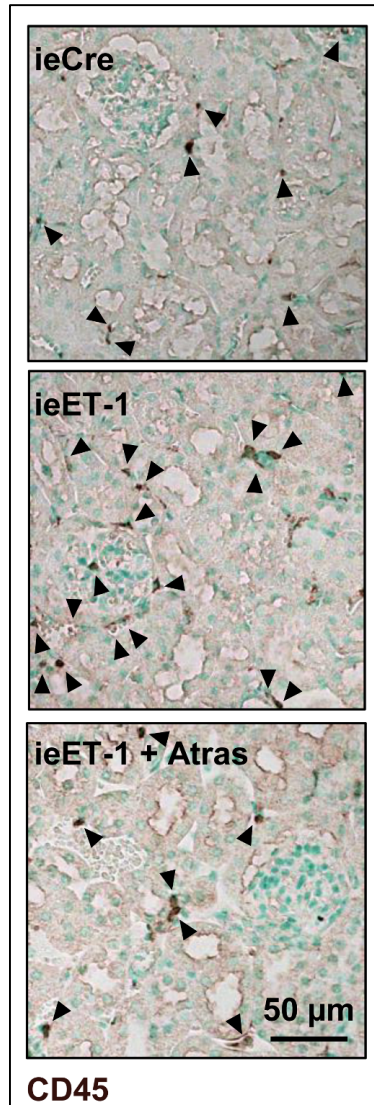


**Figure III-S13. Long-term endothelial human endothelin-1 overexpression increased immune cell infiltration in the kidney.**

Immune cell infiltration using anti-CD45 antibody was examined by immunohistochemistry in kidneys of tamoxifen-treated inducible endothelium-restricted Cre recombinase (ieCre) and human endothelin-1 overexpressing (ieET-1) mice treated or not with atrasentan (Atras). Representative immunohistochemistry images of CD45 (brown) are shown. Black arrow heads pointed toward CD45<sup>+</sup> cells. n = 7 for all the groups.

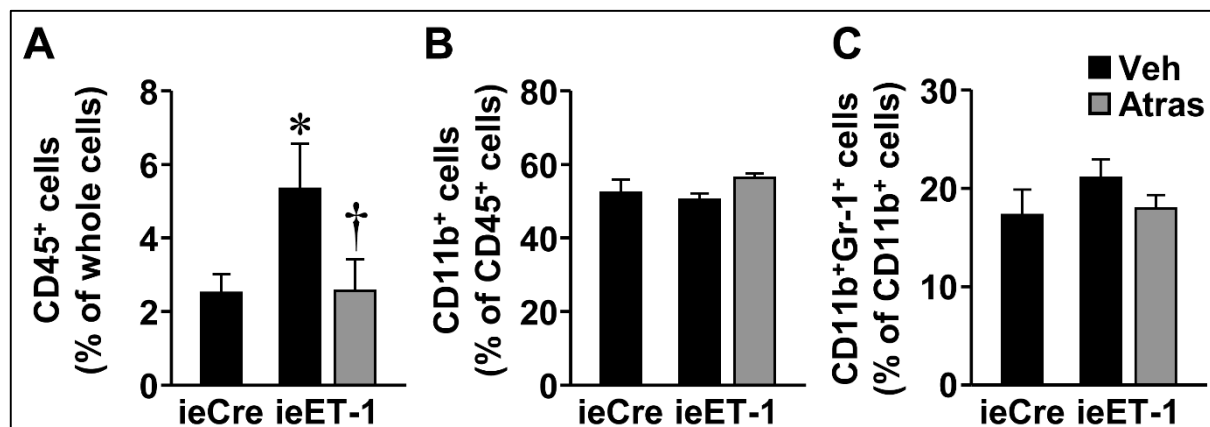


**Figure III-S14. Long-term endothelial human endothelin-1 overexpression increased the frequency of renal immune cell infiltration.**

The frequency of immune CD45<sup>+</sup> cells (**A**), myeloid cells (CD11b<sup>+</sup>, **B**) and of myeloid-derived suppressor cells (MDSCs, CD11b<sup>+</sup>Gr-1<sup>+</sup>, **C**) was determined in the kidney by flow cytometry in tamoxifen-treated inducible endothelium-restricted Cre recombinase (ieCre) and human endothelin-1 overexpressing (ieET-1) mice treated or not with atrasentan. Data are presented as means  $\pm$  SEM, n = 6 for ieCre and ieET-1 + vehicle (Veh) and 5 for ieET-1 + Atras. Data were analyzed using one-way ANOVA followed by a Student-Newman-Keuls *post hoc* test. \* $P$ <0.05 vs ieCre and † $P$ <0.05 vs ieET-1.

**CHAPTER IV: Discussion and conclusion**

## 7. Discussion

The studies described in this thesis aimed to explore the pathophysiological contribution of ET-1 in HTN using a new mouse model with inducible EC-restricted *EDN1* overexpression. The first study demonstrated that in the short-term (3 weeks), *EDN1* overexpression induced ET<sub>A</sub>R-dependent BP elevation without vascular dysfunction or changes in vascular properties in small arteries. Renal function was normal and no apparent renal injury was observed. Extending these findings, the second study showed that longer term effects (3 months) of *EDN1* overexpression resulted in sustained ET<sub>A</sub>R-dependent BP elevation and small artery endothelial dysfunction and stiffening, which was associated with enhanced PVAT-derived oxidative stress and monocyte/macrophage infiltration. In addition, initiation of renal damage and immune cells infiltration were observed. Atrasentan, an ET<sub>A</sub>R antagonist, reversed all the long-term ET-1-induced effects with the exception of endothelial dysfunction. Taken together, these results indicate that ET-1 plays an important role in the development and maintenance of hypertension, and in the initiation of vascular and renal injury and inflammation.

### 7.1. Role of ET-1 in development and maintenance of hypertension

A large body of evidence has demonstrated that high levels of plasma ET-1 or greater mRNA expression of ET-1 in several tissues are associated with an increase in BP in different animal models of HTN.<sup>121, 124, 289</sup> ET<sub>A</sub>R<sup>122, 125, 290</sup> or non-selective ETR antagonists<sup>129</sup> reverse the elevated BP in these hypertensive models. Likewise, EC-restricted ET-1 knockout mice<sup>291</sup> and smooth muscle-restricted ET<sub>A</sub>R knockout mice<sup>292</sup> presented low BP. Interestingly, constitutive eET-1 overexpression did not induce a significant increase in BP, although systolic BP tracked 10mm Hg above that of wild type mice.<sup>127</sup> Perhaps a developmental adaptation altered the phenotype of these animals as the *Tie2* promoter is expressed in vessels at early embryonic stages to induce vasculogenesis and angiogenesis.<sup>132</sup> In addition, an adaptation to life-long exposure to high concentrations of ET-1 in plasma or in tissue could explain the absence of significant blood pressure elevation. Ontogenic adaptation has been

proposed in other animal models, as heterozygous ET-1 knockout mice were reported to show an increase in BP,<sup>108</sup> whereas heterozygous ET<sub>A</sub>R knockout mice do not show a significant change in BP.<sup>293</sup> It is important to note that our inducible mouse model is devoid of adverse side-effects that may be caused by developmental or life-long exposure to ET-1. As shown in the first study (chapter II) of this thesis, ieET-1 mice in which ET-1 overexpression has not yet been induced present low levels of plasma ET-1. Thus, this model allows the assessment of ET-1-mediated effects without other confounding factors. In contrast to BP levels in eET-1 mice, short-term ET-1 overexpression progressively increased BP which persisted over a longer time. This BP elevation was associated with high levels of plasma ET-1. A causal relationship between elevated plasma ET-1 and BP could be established since atrasentan treatment reversed BP elevation. Our finding confirms previous observations that show the participation of ET-1 in the BP regulation in various animal models of HTN<sup>122, 125, 128, 290-292, 294-297</sup> and hypertensive patients.<sup>115, 118, 264, 298, 299</sup> Most importantly, our studies indicate for the first time that ET-1 can play an important role in the development and maintenance of HTN in an ET<sub>A</sub>-dependent manner.

## **7.2. Role of ET-1 in the vascular function and mechanical properties**

Our laboratory has demonstrated that ET-1 is involved in pathological changes of vascular structure, function and mechanical properties. We have shown that ET-1 exacerbated vascular hypertrophy in DOCA and salt-treated SHR,<sup>123</sup> in DOCA-salt hypertensive rats,<sup>129</sup> and in unilaterally nephrectomized DOCA-salt-treated rats.<sup>300</sup> Constitutive ET-1 overexpression induced endothelial dysfunction, vascular hypertrophic, remodeling and oxidative stress in small resistance vessels of eET-1 mice,<sup>127</sup> of eET-1 loaded with a high salt-diet,<sup>133</sup> and exacerbated diabetes-induced endothelial dysfunction in eET-1 mice.<sup>134</sup> ET-1 action was associated with endothelial dysfunction and hypertrophic remodeling of resistance arteries as well in Dahl salt-sensitive rats.<sup>125, 290</sup> Although ET-1 induces profound vasoconstriction, pro-inflammatory actions, mitogenic and proliferative effects, ROS formation and platelet activation,<sup>16, 301</sup> induction of ET-1 overexpression for 21 days did not cause vascular dysfunction, remodeling, or stiffening even though BP was already elevated at this time point. A

conceivable reason is that 3 weeks of ET-1 overexpression are not sufficient to induce vascular changes. Only long exposure to ET-1 in cultured murine aortic rings impaired acetylcholine-induced relaxation.<sup>302</sup> In addition, ET-1-induced vascular changes observed from eET-1 mice were a result of long exposure to ET-1 overexpression,<sup>127</sup> time that differed from our short-term study. Overexpression of ET-1 for a short period of time may have only initiated vascular effects, as indicated by a decrease in mRNA expression levels of ETRs. Vascular effects could become pronounced with a combination of different factors, such as Ang II, inflammation and ROS formation over time. HTN is a multifactorial disease, and a result of dysregulation of hormones, pro-inflammatory process, presence of cardiovascular disease and aging.<sup>87, 104, 303, 304</sup> Thus, an additional insult such as salt, Ang II or aldosterone excess, and reduced kidney function can exacerbate short-term ET-1 effects on the vasculature as observed in another animals models of HTN.<sup>123, 289, 300</sup>

In the second study (chapter III) of this thesis, we have shown that longer exposure to ET-1 overexpression maintained BP elevation at the level that was observed in the short-term experiments, and induced small artery endothelial dysfunction, and stiffening but no remodeling. Our results are in agreement with Amiri *et al.*, who showed that ET-1 overexpression induced vascular changes in eET-1 mice<sup>127</sup> as well as other studies.<sup>122, 134, 283</sup>

There is considerable debate whether endothelial dysfunction precedes or is a consequence of HTN.<sup>305</sup> A study conducted by Rossi *et. al* supported the hypothesis that endothelial dysfunction can occur at early stage of HTN, which contributes to further BP augmentation.<sup>306</sup> Another study, however, provided longitudinal evidence supporting the idea that endothelial dysfunction is a consequence of HTN,<sup>307</sup> contributing to further increase in peripheral vascular resistance and risk of adverse cardiovascular events. Considering both studies of this thesis, endothelial dysfunction only appears over longer exposure to ET-1 and sustained BP elevation. This indicates that endothelial dysfunction could be the consequence of ET-1-induced HTN in this model.

In the second study (chapter III), endothelial dysfunction could be explained by an increase in ROS generation in the PVAT area. Reduction of NO bioavailability due to

an increase in ROS generation<sup>308</sup> is one of the major causes of endothelial dysfunction in HTN.<sup>309</sup> In addition, previous studies have shown that ET-1 participates in the generation of vascular ROS formation via the ET<sub>A</sub>R-NAD(P)H oxidase pathway.<sup>127, 140</sup> Differently from our current findings, the cellular localization of ET-1-induced ROS formation was also observed in VSMCs.<sup>138</sup>

The PVAT and its participation in the modulation of vascular function have been recently receiving considerable attention. PVAT adipocytes and immune cells are a rich source of adipokines, cytokines, and ROS.<sup>99</sup> These PVAT mediators can in turn act in a paracrine fashion to stimulate or inhibit the underlying VSMCs and ECs. PVAT has important vascular anticontractile effects that can be mediated by two distinct mechanisms: a transferable PVAT-derived relaxing factor that induces endothelium-dependent relaxation through the production of NO,<sup>310</sup> and PVAT-derived H<sub>2</sub>O<sub>2</sub> production that stimulates endothelium-independent relaxation through activation of soluble GC in the underlying VSMCs.<sup>100</sup> PVAT-mediated anticontractile effects have been described to be attenuated in pathological conditions such as HTN.<sup>311, 312</sup> Inflammation and oxidative stress within the PVAT have been shown to contribute to vascular dysfunction in a mouse model of the metabolic syndrome.<sup>101</sup> Abnormalities in adiponectin-mediated anticontractile properties of PVAT were also described in subcutaneous adipose tissue of obese subjects with metabolic syndrome.<sup>102</sup> Thus, we initially speculated that ET-1-induced ROS formation in the PVAT could be a mechanism leading to the vascular dysfunction observed in our long-term study, due a decrease in PVAT anti-contractile effects. However, although atrasentan treatment normalized BP and abolished ROS formation detected in the PVAT, it did not improve endothelial function. Perhaps, the duration of atrasentan treatment was not enough to revert a 3-month period of ET-1-induced endothelial dysfunction or long-term ET-1 overexpression may have irreversibly altered the mechanisms responsible for setting baseline vascular tone to a more contractile state. Previous studies have reported an increase in the vasoconstrictor response of coronary arteries to ET-1 with age.<sup>313, 314</sup> Increasing the treatment time with atrasentan could potentially have reverted endothelial dysfunction, since it has been shown that ETR antagonists reduce BP elevation and improve endothelial dysfunction.<sup>133, 290</sup>

Long-term induction of ET-1 overexpression caused vascular stiffening that was associated with an increase in *Col1a1* and *Col3a1* mRNA expression. Vascular stiffness is dependent on the balance between biosynthesis of collagen and degradation of elastin. These proteins provide structural integrity and elasticity to vessels and are regulated by MMPs, which in turn are inhibited by TIMPs.<sup>315</sup> Decrease in MMP activity contributes to enhanced collagen deposition that participates in vascular stiffening and remodeling in CVD.<sup>152</sup> Hemodynamic forces and hormonal factors regulate the dynamic mechanism leading to vascular stiffening. ET-1 is one of these factors that mediates early vascular changes by activating MMP-2 and MMP-9 expression and activity via ET<sub>A</sub>R activation, independently of changes in BP.<sup>157</sup> Moreover, ROS and proinflammatory cells can modulate MMP activity and TIMP expression.<sup>316, 317</sup> As observed in the second study of this thesis (chapter III), long-term ET-1 overexpression, increased ROS formation and proinflammatory cells might have modulated the expression and/or activity of MMPs and TIMPs, thus, altering the expression of collagen, and resulting in stiffening of the small vessels of ieET-1 mice.

Vascular remodeling in small resistance arteries was not observed in our inducible mouse model. ET-1 has been shown to have growth factor activity on VSMCs<sup>188</sup> due to its potent mitogenic action<sup>189</sup> and capability to stimulate DNA synthesis<sup>318</sup> in VSMCs. These effects may contribute to vascular hypertrophy and remodeling. Indeed, there is strong evidence showing a direct effect of ET-1 in vascular remodeling in DOCA-salt SHR, DOCA-salt hypertensive rats, Dahl sat rats and stroke-prone SHR.<sup>122, 123, 125, 129</sup> Thus, the absence of vascular remodeling in our inducible model is unexpected. A possible explanation for the absence of remodeling of small vessels in our inducible mouse model compared with other animal models of HTN,<sup>170</sup> is that ET-1 alone cannot induce vascular remodeling even in the presence of persistent BP elevation. It is worth noting that animal models of HTN used in other studies are genetically prone to develop HTN<sup>122, 125</sup> and/or are salt-loaded.<sup>129, 297</sup> Another conceivable reason is that the level of BP observed in our model is not high enough to induce changes in the interaction between ECM components of resistance vessels, to trigger vascular fibrosis and cell growth.<sup>162</sup> The observed BP elevation is considerably

greater (e.g.  $\geq 200$  mm Hg) in other animal models of HTN that exhibit vascular changes compared with what was observed in our model.

In a previous study from our laboratory, vascular changes were observed independently of changes on BP, as constitutive eET-1 mice exhibited vascular remodeling in the absence of BP elevation.<sup>127</sup> It is worth mentioning that the constitutive ET-1 overexpressing mouse model was exposed to high levels of plasma ET-1 since the developmental stage, which may have altered the final phenotype. Perhaps ET-1 overexpression in utero primes VSMC such that they become sensitized to proliferate, thereby leading to vascular remodeling in the adult even in absence of elevated BP. ET-1 is physiologically distributed throughout the vascular endothelium of the human placenta and in cultured umbilical vein ECs.<sup>319</sup> As observed in women with preeclampsia, higher immunoreactive ET-1 concentrations<sup>320</sup> may lead to cardiovascular changes.<sup>321</sup> Our inducible mouse model, however, is devoid of confounding developmental effects that are present in eET-1 mice. Thus, further studies investigating the differences of VSMC response to ET-1 exposure during development and adulthood could shed light on this matter.

### **7.3. ET-1 and the immune system in HTN**

Innate and adaptive immunity contribute to hypertension and vascular injury.<sup>207, 322</sup> Constitutive ET-1 overexpression induced vascular inflammation as demonstrated by an increase in monocyte/macrophage infiltration, associated with an upregulation of endothelial adhesion molecules and chemoattractant factors.<sup>283</sup> Furthermore, suppression of monocyte/macrophage-dependent inflammation in eET-1 mice prevented ET-1-induced endothelial dysfunction, oxidative stress and vascular remodeling.<sup>203</sup> There are few data showing the participation of the adaptive immune response in vascular inflammation in ET-1-induced HTN. However, studies using animal models of HTN in which ET-1 plays a role strongly suggest that ET-1 signaling participates in enhancing vascular inflammation and the immune response. Depletion of B and T cells by an immunosuppressant decreased BP elevation in DOCA-salt rats.<sup>323</sup> In a model of high fat diet-induced atherosclerosis, our laboratory has previously shown that constitutive eET-1 overexpression exacerbates CD4<sup>+</sup> T cell infiltration in aortic

PVAT<sup>144</sup> Expression levels of ET-1 are higher in the placenta of normal pregnant rats that received adoptive transfer from placental ischemia-stimulated CD4<sup>+</sup> T cells.<sup>210</sup> This observation was followed by an increase in BP, which was reduced by an ET<sub>A</sub>R antagonist. In addition, adoptive transfer of placental ischemia-stimulated CD4<sup>+</sup> T cells also increased circulating pro-inflammatory cytokines such as TNF- $\alpha$ , IL-1 and IL-17 in recipient pregnant rats.<sup>211</sup> These results suggest that ET-1 and innate and adaptive immunity can interact. The second study in this thesis (chapter III) has shown that long-term induction of ET-1 overexpression may have initiated innate immune activation as indicated by an increase in monocyte/macrophage infiltration in MA PVAT, which was blunted by atrasentan treatment. Increased monocyte/macrophage infiltration in MA PVAT was not likely mediated by MCP-1, as its expression in small arteries was unaltered. Our results corroborate previous findings that demonstrate the role of innate immunity in ET-1-induced vascular inflammation.<sup>203, 283</sup> Moreover, long-term treatment with ETR antagonists exerted anti-inflammatory effects that were associated with clinical and hemodynamic improvement in patients with PAH.<sup>324</sup>

Decreased concentrations of NO, increased concentrations of ET-1, and monocyte/macrophage infiltration in PVAT and vascular dysfunction have been observed in the carotid artery of rabbits fed a high fat diet.<sup>325</sup> C-reactive protein treatment further exacerbated the imbalance between NO and ET-1 concentrations, increased macrophage infiltration in PVAT and aggravated endothelial dysfunction in arteries with PVAT. Likewise, endothelial dysfunction was associated with a proinflammatory PVAT phenotype in obese mice.<sup>326</sup> Thus, along with ROS, monocyte/macrophage infiltration in PVAT could have contributed to vascular dysfunction in our inducible mouse model. As atrasentan treatment reversed monocyte/macrophage infiltration in PVAT, ROS formation and BP elevation but did not reduce endothelial dysfunction, other ET-1-independent mechanisms might be at play.

In contrast, ET-1 overexpression seems not to trigger local adaptive immune responses, as PVAT CD3<sup>+</sup> T cell infiltration was not enhanced. However, this does not rule out ET-1-mediated systemic activation of adaptive immunity,<sup>327</sup> which was not examined in our studies. Low-grade inflammation in PVAT of resistance arteries and absence of adaptive immune participation might explain the absence of vascular

remodeling and the mild BP elevation in ieET-1 mice. Exposure to an inflammatory insult can possibly contribute to the triggering of vascular remodeling and exacerbate vascular dysfunction and stiffening. Patients with PAH and systemic sclerosis, a disease with an autoimmune component, have an increase in the interaction between T cells and ECs to promote cell infiltration and fibroblast activation inducing ECM deposition in the skin and organs.<sup>328</sup> Bosentan treatment decreased this detrimental interaction as shown by a reduction of peripheral blood T cells expressing leukocyte function-associated antigen-1, which is a protein involved in the immune cell infiltration process and a counter-receptor of ICAM-1.

#### **7.4. ET-1 and renal damage during HTN**

The ET-1 system modulates the ability of the kidneys to regulate BP by altering renal hemodynamics, controlling renin secretion and sodium and water excretion through activation of its receptors.<sup>55</sup> Indeed, vasoconstriction of afferent renal arteries reduces glomerular filtration rate and stimulates the release of renin. These effects result in activation of RAAS and induction of sodium and water retention, which consequently cause BP elevation.<sup>227</sup> Although short-term ET-1 overexpression induced BP elevation, it did not cause changes in kidney perfusion or function. Likewise, long-term ET-1 overexpression did not alter renal function; however, it decreased RAF, which was not corrected by atrasentan treatment. The fact that atrasentan treatment decreased BP without restoring RAF suggests that renal hemodynamics do not play a critical role in ET-1-induced BP elevation in our model. Perhaps, at this time point, alterations in vascular function and mechanical properties along with vascular inflammation<sup>329</sup> are the major factors determining the development and maintenance of HTN.

Renin mRNA expression in the renal cortex was unaltered in both short-term and long-term studies. It is unclear why renin mRNA expression level is not altered at least after a longer exposure to ET-1 when RAF is reduced. Although there is no difference in renin mRNA expression level, this does not rule out the possibility that there are changes at the protein activity or changes in other components of the RAS throughout the nephron. Indeed, plasma aldosterone levels are increased in both studies (Unpublished data). Aldosterone is known to participate in the development of

hypertension by increasing blood volume through enhanced renal sodium and water reabsorption,<sup>330</sup> and inducing vascular fibrosis and stiffening.<sup>331</sup> ET-1 directly regulates aldosterone secretion<sup>332</sup> by adrenal zona glomerulosa cells.<sup>333</sup> Aldosterone induces transepithelial sodium transport via ENaC in the distal nephron and collecting duct, as well as in the medullary collecting duct. In the absence of aldosterone, inhibitory components such as Nedd4-2 and Raf-1 are physically bound to ENaC, limiting its activity. In the presence of aldosterone, stimulatory signaling proteins such as SGK1 and GILZ1 are activated and recruited into the ENaC-regulatory complex, thereby interfering with Nedd4-2 and Raf-1 inhibitory activity.<sup>334</sup> Aldosterone upregulates mRNA expression levels of ENaC, SGK1 and GILZ1 in the rat kidney.<sup>335</sup> However, in both studies of this thesis, short and long-term ET-1 overexpression associated with elevated circulating aldosterone was not accompanied by changes in the transcriptional levels of ENaC and its regulators in the renal cortex or medulla (Unpublished data). Although the system is overloaded with ET-1 and aldosterone, the lack of changes in mRNA expression of ENaC and its regulators is in agreement with the absence of changes in sodium excretion after 3 months. There could be a counterbalancing effect between the ET-1-mediated natriuretic effect and sodium retention induced by aldosterone.<sup>336</sup>

ETRs are differentially distributed and widely expressed in different cell types of the kidney.<sup>233-235</sup> Short-term ET-1 overexpression increased mRNA expression levels of ET<sub>A</sub>Rs in the renal cortex and ET<sub>B</sub>Rs in the renal cortex and medulla. Long-term ET-1 overexpression did not modify renal ETR expression, at least at the level of mRNA. Acute changes in ETR mRNA expression levels suggest some renal functional adaptation to short-term ET-1 overexpression or BP elevation. Renal ET-1 is mainly produced by collecting duct epithelial cells,<sup>245, 246</sup> and ET<sub>B</sub>Rs are predominantly expressed in the outer and inner medullary collecting duct epithelial cells, whereas ET<sub>A</sub>R expression is detectable in the cortical collecting duct.<sup>233, 235</sup> Thus, a renal functional adaptation could be expected to occur at the tubular level, which could affect the ET-1-dependent natriuretic and diuretic effects.<sup>254, 255</sup> However, sodium and water excretion are not altered, which further supports the hypothesis that ET-1-mediated natriuretic and diuretic effects might have been counterbalanced by a sodium-retaining hormone such as aldosterone.<sup>336</sup> Renal functional adaptation is no longer present when

ieET-1 mice were exposed to long-term ET-1 overexpression with sustained BP elevation. The lack of changes in renal ETR expression levels suggests renal adaptation to longer exposure to ET-1 overexpression. The consequences of this effect are unclear. Changes in ETR expression could have altered ET-1-mediated natriuretic and diuretic effects, or BP elevation.<sup>337</sup>

The participation of ET-1 in the development of renal injury and progression of CKD has been documented.<sup>338</sup> Transgenic mice overexpressing human ET-1 in different cells of the kidney present glomerular and interstitial injury.<sup>339</sup> Suppression of ET-1 attenuates renal ischemia/reperfusion-induced tubular injury, oxidative stress and inflammation.<sup>340</sup> In the first study (chapter II), short-term exposure to ET-1 overexpression did not cause renal injury. Although urinary albumin excretion and detectable histologic lesions were absent, long-term exposure to endothelial ET-1 increased the expression level of KIM-1, an early marker of kidney injury, which suggests presence of an initial renal damage. Mild BP elevation goes along with a minimal renal damage, as the progression of ET-1-induced BP elevation is associated with the level of kidney injury.<sup>341</sup> Such subtle renal damage is unlikely to occur in other animal models with moderate HTN,<sup>342</sup> obesity<sup>343</sup> and CKD.<sup>344</sup>

Initial renal damage was associated with an increase in infiltration of myeloid cells and a myeloid-derived suppressor cell (MDSCs) subpopulation. It has been shown that MDSCs are increased in experimental models of HTN.<sup>345, 346</sup> These cells have anti-inflammatory properties as these cells have diminished inflammation, BP elevation and renal injury. The increase in renal MDSC infiltration may have counteracted ET-1-induced renal damage in our model, explaining the absence of established renal damage. Myeloid cells and kidney non-immune cells expressed the pro-inflammatory B scavenger/pattern recognition receptor CD36, which could contribute to the development of kidney injury. Indeed, it has been shown that *Cd36* knockout prevents renal inflammation, oxidative stress and injury in *ApoE*<sup>-/-</sup> mice exposed to a high fat diet.<sup>347</sup> In our mouse model, initial renal damage and increases in immune and non-immune cell infiltration were reduced by atrasentan treatment. Taken together, these results indicate that endothelial ET-1 plays an important role in the development of kidney injury. ET-1 blockade attenuated BP elevation, as well as vascular and renal

damage and inflammation. Further experiments reducing BP with a non-ET-related antihypertensive agent such as hydralazine will clarify whether the vascular and renal effects of ET-1 are BP-dependent or not.

## 8. Conclusion

Several studies have shown the participation of ET-1 in different animal models of HTN. These models, differently from ours, presented genetic gain-or-loss of function or were treated with DOCA-salt or a high fat diet. Since hypertension is a complex disease, the addition of different factors such as developmental/genomic effects, different diets or treatments could alter the final observed outcome. Thus, the first study demonstrates the successful generation of an inducible EC-restricted *EDN1* overexpression mouse model. This inducible mouse model has the advantage of allowing the study of the role of ET-1 on BP regulation in the absence of any confounding factors. Short-term ET-1 overexpression caused ET-1-dependent BP elevation mediated by ET<sub>A</sub>R, unaccompanied by vascular injury or evident alteration of kidney function or kidney injury. The second study demonstrated that longer exposure to ET-1 overexpression caused sustained BP elevation, small artery endothelial dysfunction and stiffening, and vascular inflammation. Furthermore, ET-1 overexpression impaired renal hemodynamics and caused initial renal damage associated with activation of innate immunity. The studies of this thesis indicate that ET-1 plays an important role in the development and maintenance of HTN in an ET<sub>A</sub> receptor-dependent manner. ET-1-induced sustained BP elevation and vascular and renal inflammation, which might be important contributors to further induce vascular and renal injury.

## 9. Limitations

Sex differences have been reported for the ET-1 system.<sup>348</sup> In this study, the effects of ET-1 overexpression were determined only in male mice. Different results might be observed in female mice, as plasma ET-1 levels are lower under physiological and pathological conditions. This difference needs to be addressed in further studies. The

results obtained in male mice can be translated to HTN in men and postmenopausal women.

## 10. Perspectives

HTN is a major risk factor for CVD, yet the prevalence of uncontrolled HTN has increased worldwide despite the availability of various classes of anti-hypertensive drugs. The pathophysiology of HTN is complex and not completely understood. ET-1, a powerful vasoconstrictor, is known to be involved in the pathophysiology of HTN. Although, ETR antagonists have been approved to treat PAH, they have a high incidence of side effects such as liver toxicity, headache and peripheral edema. This novel mouse model of inducible EC-restricted *EDN1* overexpression devoid of developmental confounding effects will help to understand the role of ET-1 in the pathophysiology of HTN. Moreover, it should stimulate development of novel ET-1 antagonists with fewer side effects, ameliorating the success rate to treat HTN, especially in resistant HTN.

### References:

1. Ho KK, Pinsky JL, Kannel WB, Levy D. The epidemiology of heart failure: The framingham study. *Journal of the American College of Cardiology*. 1993;22:6A-13A
2. Tozawa M, Iseki K, Iseki C, Kinjo K, Ikemiya Y, Takishita S. Blood pressure predicts risk of developing end-stage renal disease in men and women. *Hypertension*. 2003;41:1341-1345
3. MacMahon S, Peto R, Cutler J, Collins R, Sorlie P, Neaton J, Abbott R, Godwin J, Dyer A, Stamler J. Blood pressure, stroke, and coronary heart disease. Part 1, prolonged differences in blood pressure: Prospective observational studies corrected for the regression dilution bias. *Lancet*. 1990;335:765-774
4. Carretero OA, Oparil S. Essential hypertension. Part i: Definition and etiology. *Circulation*. 2000;101:329-335
5. Hall GYHLaJE. *Comprehensive hypertension*. Mosby Elsevier; 2007.
6. Myat A, Redwood SR, Qureshi AC, Spertus JA, Williams B. Resistant hypertension. *Bmj*. 2012;345:e7473
7. Pimenta E, Calhoun DA. Resistant hypertension: Incidence, prevalence, and prognosis. *Circulation*. 2012;125:1594-1596
8. Bromfield S, Muntner P. High blood pressure: The leading global burden of disease risk factor and the need for worldwide prevention programs. *Current hypertension reports*. 2013;15:134-136
9. Danaei G, Finucane MM, Lin JK, Singh GM, Paciorek CJ, Cowan MJ, Farzadfar F, Stevens GA, Lim SS, Riley LM, Ezzati M, Global Burden of Metabolic Risk Factors of Chronic Diseases Collaborating G. National, regional, and global trends in systolic blood pressure since 1980: Systematic analysis of health examination surveys and epidemiological studies with 786 country-years and 5.4 million participants. *Lancet*. 2011;377:568-577
10. Kearney PM, Whelton M, Reynolds K, Muntner P, Whelton PK, He J. Global burden of hypertension: Analysis of worldwide data. *Lancet*. 2005;365:217-223

11. Hickey KA, Rubanyi G, Paul RJ, Highsmith RF. Characterization of a coronary vasoconstrictor produced by cultured endothelial cells. *The American journal of physiology*. 1985;248:C550-556
12. Yanagisawa M, Kurihara H, Kimura S, Tomobe Y, Kobayashi M, Mitsui Y, Yazaki Y, Goto K, Masaki T. A novel potent vasoconstrictor peptide produced by vascular endothelial cells. *Nature*. 1988;332:411-415
13. Kloog Y, Ambar I, Sokolovsky M, Kochva E, Wollberg Z, Bdolah A. Sarafotoxin, a novel vasoconstrictor peptide: Phosphoinositide hydrolysis in rat heart and brain. *Science*. 1988;242:268-270
14. Inoue A, Yanagisawa M, Kimura S, Kasuya Y, Miyauchi T, Goto K, Masaki T. The human endothelin family: Three structurally and pharmacologically distinct isopeptides predicted by three separate genes. *Proceedings of the National Academy of Sciences of the United States of America*. 1989;86:2863-2867
15. Saida K, Mitsui Y, Ishida N. A novel peptide, vasoactive intestinal contractor, of a new (endothelin) peptide family. Molecular cloning, expression, and biological activity. *J Biol Chem*. 1989;264:14613-14616
16. Davenport AP, Hyndman KA, Dhaun N, Southan C, Kohan DE, Pollock JS, Pollock DM, Webb DJ, Maguire JJ. Endothelin. *Pharmacological reviews*. 2016;68:357-418
17. Barton M, Yanagisawa M. Endothelin: 20 years from discovery to therapy. *Canadian journal of physiology and pharmacology*. 2008;86:485-498
18. Rodriguez-Pascual F, Redondo-Horcajo M, Lamas S. Functional cooperation between smad proteins and activator protein-1 regulates transforming growth factor-beta-mediated induction of endothelin-1 expression. *Circulation research*. 2003;92:1288-1295
19. Dorfman DM, Wilson DB, Bruns GA, Orkin SH. Human transcription factor gata-2. Evidence for regulation of preproendothelin-1 gene expression in endothelial cells. *J Biol Chem*. 1992;267:1279-1285
20. Matsuura A, Yamochi W, Hirata K, Kawashima S, Yokoyama M. Stimulatory interaction between vascular endothelial growth factor and endothelin-1 on each gene expression. *Hypertension*. 1998;32:89-95

21. Marsen TA, Simonson MS, Dunn MJ. Thrombin induces the preproendothelin-1 gene in endothelial cells by a protein tyrosine kinase-linked mechanism. *Circulation research*. 1995;76:987-995
22. Woods M, Bishop-Bailey D, Pepper JR, Evans TW, Mitchell JA, Warner TD. Cytokine and lipopolysaccharide stimulation of endothelin-1 release from human internal mammary artery and saphenous vein smooth-muscle cells. *Journal of cardiovascular pharmacology*. 1998;31 Suppl 1:S348-350
23. Stow LR, Jacobs ME, Wingo CS, Cain BD. Endothelin-1 gene regulation. *FASEB J*. 2011;25:16-28
24. Malek AM, Greene AL, Izumo S. Regulation of endothelin 1 gene by fluid shear stress is transcriptionally mediated and independent of protein kinase c and camp. *Proceedings of the National Academy of Sciences of the United States of America*. 1993;90:5999-6003
25. Spinella F, Caprara V, Cianfrocca R, Rosano L, Di Castro V, Garrafa E, Natali PG, Bagnato A. The interplay between hypoxia, endothelial and melanoma cells regulates vascularization and cell motility through endothelin-1 and vascular endothelial growth factor. *Carcinogenesis*. 2014;35:840-848
26. Itoh Y, Yanagisawa M, Ohkubo S, Kimura C, Kosaka T, Inoue A, Ishida N, Mitsui Y, Onda H, Fujino M, et al. Cloning and sequence analysis of cDNA encoding the precursor of a human endothelium-derived vasoconstrictor peptide, endothelin: Identity of human and porcine endothelin. *FEBS Lett*. 1988;231:440-444
27. Fabbrini MS, Valsasina B, Nitti G, Benatti L, Vitale A. The signal peptide of human preproendothelin-1. *FEBS Lett*. 1991;286:91-94
28. Blais V, Fugere M, Denault JB, Klarskov K, Day R, Leduc R. Processing of proendothelin-1 by members of the subtilisin-like pro-protein convertase family. *FEBS Lett*. 2002;524:43-48
29. Pernow J, Kaijser L, Lundberg JM, Ahlborg G. Comparable potent coronary constrictor effects of endothelin-1 and big endothelin-1 in humans. *Circulation*. 1996;94:2077-2082
30. Kishi F, Minami K, Okishima N, Murakami M, Mori S, Yano M, Niwa Y, Nakaya Y, Kido H. Novel 31-amino-acid-length endothelins cause constriction of vascular

- smooth muscle. *Biochemical and biophysical research communications*. 1998;248:387-390
31. Hoffman A, Abassi ZA, Brodsky S, Ramadan R, Winaver J. Mechanisms of big endothelin-1-induced diuresis and natriuresis : Role of et(b) receptors. *Hypertension*. 2000;35:732-739
  32. Hunter RW, Moorhouse R, Farrah TE, MacIntyre IM, Asai T, Gallacher PJ, Kerr D, Melville V, Czopek A, Morrison EE, Ivy JR, Dear JW, Bailey MA, Goddard J, Webb DJ, Dhaun N. First-in-man demonstration of direct endothelin-mediated natriuresis and diuresis. *Hypertension*. 2017;70:192-200
  33. Russell FD, Davenport AP. Secretory pathways in endothelin synthesis. *British journal of pharmacology*. 1999;126:391-398
  34. Huskisson APDEKPWMJBS. Endothelin-converting enzyme in human tissues. *Histochemical Journal*. 1998;30:359-374
  35. Xu D, Emoto N, Giaid A, Slaughter C, Kaw S, deWit D, Yanagisawa M. Ece-1: A membrane-bound metalloprotease that catalyzes the proteolytic activation of big endothelin-1. *Cell*. 1994;78:473-485
  36. Emoto N, Yanagisawa M. Endothelin-converting enzyme-2 is a membrane-bound, phosphoramidon-sensitive metalloprotease with acidic ph optimum. *J Biol Chem*. 1995;270:15262-15268
  37. Schweizer A, Valdenaire O, Nelbock P, Deuschle U, Dumas Milne Edwards JB, Stumpf JG, Loffler BM. Human endothelin-converting enzyme (ece-1): Three isoforms with distinct subcellular localizations. *Biochem J*. 1997;328 ( Pt 3):871-877
  38. Valdenaire O, Lepailleur-Enouf D, Egidy G, Thouard A, Barret A, Vranckx R, Tougard C, Michel JB. A fourth isoform of endothelin-converting enzyme (ece-1) is generated from an additional promoter molecular cloning and characterization. *Eur J Biochem*. 1999;264:341-349
  39. Nakano A, Kishi F, Minami K, Wakabayashi H, Nakaya Y, Kido H. Selective conversion of big endothelins to tracheal smooth muscle-constricting 31-amino acid-length endothelins by chymase from human mast cells. *J Immunol*. 1997;159:1987-1992

40. Maguire JJ, Kuc RE, Davenport AP. Vasoconstrictor activity of novel endothelin peptide, et-1(1 - 31), in human mammary and coronary arteries in vitro. *British journal of pharmacology*. 2001;134:1360-1366
41. Watts SW, Thakali K, Smark C, Rondelli C, Fink GD. Big et-1 processing into vasoactive peptides in arteries and veins. *Vascular pharmacology*. 2007;47:302-312
42. Fecteau MH, Honore JC, Plante M, Labonte J, Rae GA, D'Orleans-Juste P. Endothelin-1 (1-31) is an intermediate in the production of endothelin-1 after big endothelin-1 administration in vivo. *Hypertension*. 2005;46:87-92
43. Nagata N, Niwa Y, Nakaya Y. A novel 31-amino-acid-length endothelin, et-1(1-31), can act as a biologically active peptide for vascular smooth muscle cells. *Biochemical and biophysical research communications*. 2000;275:595-600
44. Cui P, Tani K, Kitamura H, Okumura Y, Yano M, Inui D, Tamaki T, Sone S, Kido H. A novel bioactive 31-amino acid endothelin-1 is a potent chemotactic peptide for human neutrophils and monocytes. *J Leukoc Biol*. 2001;70:306-312
45. Fernandez-Patron C, Radomski MW, Davidge ST. Vascular matrix metalloproteinase-2 cleaves big endothelin-1 yielding a novel vasoconstrictor. *Circulation research*. 1999;85:906-911
46. Lowenstein CJ, Morrell CN, Yamakuchi M. Regulation of weibel-palade body exocytosis. *Trends Cardiovasc Med*. 2005;15:302-308
47. Harrison VJ, Barnes K, Turner AJ, Wood E, Corder R, Vane JR. Identification of endothelin 1 and big endothelin 1 in secretory vesicles isolated from bovine aortic endothelial cells. *Proceedings of the National Academy of Sciences of the United States of America*. 1995;92:6344-6348
48. Barnes K, Brown C, Turner AJ. Endothelin-converting enzyme: Ultrastructural localization and its recycling from the cell surface. *Hypertension*. 1998;31:3-9
49. Russell FD, Skepper JN, Davenport AP. Evidence using immunoelectron microscopy for regulated and constitutive pathways in the transport and release of endothelin. *Journal of cardiovascular pharmacology*. 1998;31:424-430

50. Doi Y, Kudo H, Nishino T, Yamamoto O, Nagata T, Nara S, Morita M, Fujimoto S. Enhanced expression of endothelin-1 and endothelin-converting enzyme-1 in acute hypoxic rat aorta. *Histol Histopathol*. 2002;17:97-105
51. Russell FD, Skepper JN, Davenport AP. Human endothelial cell storage granules: A novel intracellular site for isoforms of the endothelin-converting enzyme. *Circulation research*. 1998;83:314-321
52. Davenport AP. International union of pharmacology. Xxix. Update on endothelin receptor nomenclature. *Pharmacological reviews*. 2002;54:219-226
53. Arai H, Hori S, Aramori I, Ohkubo H, Nakanishi S. Cloning and expression of a cDNA encoding an endothelin receptor. *Nature*. 1990;348:730-732
54. Sakurai T, Yanagisawa M, Takawa Y, Miyazaki H, Kimura S, Goto K, Masaki T. Cloning of a cDNA encoding a non-isopeptide-selective subtype of the endothelin receptor. *Nature*. 1990;348:732-735
55. Kohan DE, Rossi NF, Inscho EW, Pollock DM. Regulation of blood pressure and salt homeostasis by endothelin. *Physiol Rev*. 2011;91:1-77
56. Luscher TF, Barton M. Endothelins and endothelin receptor antagonists: Therapeutic considerations for a novel class of cardiovascular drugs. *Circulation*. 2000;102:2434-2440
57. Khimji AK, Rokey DC. Endothelin--biology and disease. *Cell Signal*. 2010;22:1615-1625
58. Simonson MS, Dunn MJ. Cellular signaling by peptides of the endothelin gene family. *FASEB J*. 1990;4:2989-3000
59. Mazzuca MQ, Khalil RA. Vascular endothelin receptor type b: Structure, function and dysregulation in vascular disease. *Biochem Pharmacol*. 2012;84:147-162
60. Schiffrin EL, Touyz RM. Vascular biology of endothelin. *Journal of cardiovascular pharmacology*. 1998;32 Suppl 3:S2-13
61. Liu S, Premont RT, Kontos CD, Huang J, Rokey DC. Endothelin-1 activates endothelial cell nitric-oxide synthase via heterotrimeric g-protein betagamma subunit signaling to protein kinase B/Akt. *J Biol Chem*. 2003;278:49929-49935
62. Sandoo A, van Zanten JJ, Metsios GS, Carroll D, Kitas GD. The endothelium and its role in regulating vascular tone. *Open Cardiovasc Med J*. 2010;4:302-312

63. Palmer RM, Ashton DS, Moncada S. Vascular endothelial cells synthesize nitric oxide from L-arginine. *Nature*. 1988;333:664-666
64. de Nucci G, Thomas R, D'Orleans-Juste P, Antunes E, Walder C, Warner TD, Vane JR. Pressor effects of circulating endothelin are limited by its removal in the pulmonary circulation and by the release of prostacyclin and endothelium-derived relaxing factor. *Proceedings of the National Academy of Sciences of the United States of America*. 1988;85:9797-9800
65. Tirapelli CR, Casolari DA, Yogi A, Montezano AC, Tostes RC, Legros E, D'Orleans-Juste P, de Oliveira AM. Functional characterization and expression of endothelin receptors in rat carotid artery: Involvement of nitric oxide, a vasodilator prostanoid and the opening of k<sup>+</sup> channels in etb-induced relaxation. *British journal of pharmacology*. 2005;146:903-912
66. Wright HM, Malik KU. Prostacyclin formation elicited by endothelin-1 in rat aorta is mediated via phospholipase d activation and not phospholipase c or a2. *Circulation research*. 1996;79:271-276
67. Chang J, Musser JH, McGregor H. Phospholipase a2: Function and pharmacological regulation. *Biochem Pharmacol*. 1987;36:2429-2436
68. Kang KT. Endothelium-derived relaxing factors of small resistance arteries in hypertension. *Toxicol Res*. 2014;30:141-148
69. Busse R, Edwards G, Feletou M, Fleming I, Vanhoutte PM, Weston AH. Edhf: Bringing the concepts together. *Trends Pharmacol Sci*. 2002;23:374-380
70. Nakashima M, Vanhoutte PM. Endothelin-1 and -3 cause endothelium-dependent hyperpolarization in the rat mesenteric artery. *The American journal of physiology*. 1993;265:H2137-2141
71. Bremnes T, Paasche JD, Mehllum A, Sandberg C, Bremnes B, Attramadal H. Regulation and intracellular trafficking pathways of the endothelin receptors. *J Biol Chem*. 2000;275:17596-17604
72. Maguire JJ, Davenport AP. Endothelin receptors and their antagonists. *Semin Nephrol*. 2015;35:125-136

73. Vizza CD, Fedele F, Pezzuto B, Rubin LJ. Safety and efficacy evaluation of ambrisentan in pulmonary hypertension. *Expert Opin Drug Saf.* 2012;11:1003-1011
74. de Zeeuw D, Coll B, Andress D, Brennan JJ, Tang H, Houser M, Correa-Rotter R, Kohan D, Lambers Heerspink HJ, Makino H, Perkovic V, Pritchett Y, Remuzzi G, Tobe SW, Toto R, Viberti G, Parving HH. The endothelin antagonist atrasentan lowers residual albuminuria in patients with type 2 diabetic nephropathy. *Journal of the American Society of Nephrology : JASN.* 2014;25:1083-1093
75. Nelson JB, Fizazi K, Miller K, Higano C, Moul JW, Akaza H, Morris T, McIntosh S, Pemberton K, Gleave M. Phase 3, randomized, placebo-controlled study of zibotentan (zd4054) in patients with castration-resistant prostate cancer metastatic to bone. *Cancer.* 2012;118:5709-5718
76. Don GW, Joseph F, Celermajer DS, Corte TJ. Ironic case of hepatic dysfunction following the global withdrawal of sitaxentan. *Intern Med J.* 2012;42:1351-1354
77. Maguire JJ, Davenport AP. Endothelin@25 - new agonists, antagonists, inhibitors and emerging research frontiers: luphar review 12. *British journal of pharmacology.* 2014;171:5555-5572
78. Vijayaraghavan J, Scicli AG, Carretero OA, Slaughter C, Moomaw C, Hersh LB. The hydrolysis of endothelins by neutral endopeptidase 24.11 (enkephalinase). *J Biol Chem.* 1990;265:14150-14155
79. Yamaguchi T, Kohrogi H, Kawano O, Ando M, Araki S. Neutral endopeptidase inhibitor potentiates endothelin-1-induced airway smooth muscle contraction. *Journal of applied physiology.* 1992;73:1108-1113
80. Yamaguchi T, Fukase M, Arao M, Sugimoto T, Chihara K. Endothelin 1 hydrolysis by rat kidney membranes. *FEBS Lett.* 1992;309:303-306
81. Wang TL, Chang H. Intravenous morphine reduces plasma endothelin 1 concentration through activation of neutral endopeptidase 24.11 in patients with myocardial infarction. *Ann Emerg Med.* 2001;37:445-449
82. Metsarinne KP, Vehmaan-Kreula P, Kovanen PT, Saijonmaa O, Baumann M, Wang Y, Nyman T, Fyhrquist FY, Eklund KK. Activated mast cells increase the

- level of endothelin-1 mRNA in cocultured endothelial cells and degrade the secreted peptide. *Arteriosclerosis, thrombosis, and vascular biology*. 2002;22:268-273
83. Fukuroda T, Fujikawa T, Ozaki S, Ishikawa K, Yano M, Nishikibe M. Clearance of circulating endothelin-1 by etb receptors in rats. *Biochemical and biophysical research communications*. 1994;199:1461-1465
  84. Johnstrom P, Fryer TD, Richards HK, Harris NG, Barret O, Clark JC, Pickard JD, Davenport AP. Positron emission tomography using 18f-labelled endothelin-1 reveals prevention of binding to cardiac receptors owing to tissue-specific clearance by et b receptors in vivo. *British journal of pharmacology*. 2005;144:115-122
  85. Gasic S, Wagner OF, Vierhapper H, Nowotny P, Waldhausl W. Regional hemodynamic effects and clearance of endothelin-1 in humans: Renal and peripheral tissues may contribute to the overall disposal of the peptide. *Journal of cardiovascular pharmacology*. 1992;19:176-180
  86. Kelland NF, Kuc RE, McLean DL, Azfer A, Bagnall AJ, Gray GA, Gulliver-Sloan FH, Maguire JJ, Davenport AP, Kotelevtsev YV, Webb DJ. Endothelial cell-specific etb receptor knockout: Autoradiographic and histological characterisation and crucial role in the clearance of endothelin-1. *Canadian journal of physiology and pharmacology*. 2010;88:644-651
  87. Schiffrin EL. Vascular endothelin in hypertension. *Vascular pharmacology*. 2005;43:19-29
  88. Rodriguez-Pascual F, Busnadiego O, Lagares D, Lamas S. Role of endothelin in the cardiovascular system. *Pharmacol Res*. 2011;63:463-472
  89. Tedgu BILaA. Morphologic aspects of the large artery vascular wall In: Bernard I, Levy AT, ed. *Biology of the arterial wall*. Kluwer Academic Publishers; 1999:284.
  90. Schiffrin EL. The endothelium and control of blood vessel function in health and disease. *Clin Invest Med*. 1994;17:602-620
  91. Aird WC. Phenotypic heterogeneity of the endothelium: I. Structure, function, and mechanisms. *Circulation research*. 2007;100:158-173

92. Wagenseil JE, Mecham RP. Vascular extracellular matrix and arterial mechanics. *Physiol Rev.* 2009;89:957-989
93. Burton AC. Relation of structure to function of the tissues of the wall of blood vessels. *Physiol Rev.* 1954;34:619-642
94. Di Wang H, Ratsep MT, Chapman A, Boyd R. Adventitial fibroblasts in vascular structure and function: The role of oxidative stress and beyond. *Canadian journal of physiology and pharmacology.* 2010;88:177-186
95. Haurani MJ, Pagano PJ. Adventitial fibroblast reactive oxygen species as autocrine and paracrine mediators of remodeling: Bellwether for vascular disease? *Cardiovascular research.* 2007;75:679-689
96. Shekhonin BV, Domogatsky SP, Muzykantov VR, Idelson GL, Rukosuev VS. Distribution of type i, iii, iv and v collagen in normal and atherosclerotic human arterial wall: Immunomorphological characteristics. *Coll Relat Res.* 1985;5:355-368
97. Brown NK, Zhou Z, Zhang J, Zeng R, Wu J, Eitzman DT, Chen YE, Chang L. Perivascular adipose tissue in vascular function and disease: A review of current research and animal models. *Arteriosclerosis, thrombosis, and vascular biology.* 2014;34:1621-1630
98. Szasz T, Webb RC. Perivascular adipose tissue: More than just structural support. *Clinical science.* 2012;122:1-12
99. Szasz T, Bomfim GF, Webb RC. The influence of perivascular adipose tissue on vascular homeostasis. *Vasc Health Risk Manag.* 2013;9:105-116
100. Gao YJ, Lu C, Su LY, Sharma AM, Lee RM. Modulation of vascular function by perivascular adipose tissue: The role of endothelium and hydrogen peroxide. *British journal of pharmacology.* 2007;151:323-331
101. Marchesi C, Ebrahimian T, Angulo O, Paradis P, Schiffrin EL. Endothelial nitric oxide synthase uncoupling and perivascular adipose oxidative stress and inflammation contribute to vascular dysfunction in a rodent model of metabolic syndrome. *Hypertension.* 2009;54:1384-1392
102. Greenstein AS, Khavandi K, Withers SB, Sonoyama K, Clancy O, Jeziorska M, Laing I, Yates AP, Pemberton PW, Malik RA, Heagerty AM. Local inflammation

- and hypoxia abolish the protective anticontractile properties of perivascular fat in obese patients. *Circulation*. 2009;119:1661-1670
103. Wagner OF, Christ G, Wojta J, Vierhapper H, Parzer S, Nowotny PJ, Schneider B, Waldhausl W, Binder BR. Polar secretion of endothelin-1 by cultured endothelial cells. *J Biol Chem*. 1992;267:16066-16068
  104. Schiffrin EL. Role of endothelin-1 in hypertension and vascular disease. *American journal of hypertension*. 2001;14:83S-89S
  105. Taddei S, Virdis A, Ghiadoni L, Sudano I, Magagna A, Salvetti A. Role of endothelin in the control of peripheral vascular tone in human hypertension. *Heart failure reviews*. 2001;6:277-285
  106. Haynes WG, Webb DJ. Contribution of endogenous generation of endothelin-1 to basal vascular tone. *Lancet*. 1994;344:852-854
  107. Haynes WG, Ferro CJ, O'Kane KP, Somerville D, Lomax CC, Webb DJ. Systemic endothelin receptor blockade decreases peripheral vascular resistance and blood pressure in humans. *Circulation*. 1996;93:1860-1870
  108. Kurihara Y, Kurihara H, Suzuki H, Kodama T, Maemura K, Nagai R, Oda H, Kuwaki T, Cao WH, Kamada N, et al. Elevated blood pressure and craniofacial abnormalities in mice deficient in endothelin-1. *Nature*. 1994;368:703-710
  109. Verhaar MC, Strachan FE, Newby DE, Cruden NL, Koomans HA, Rabelink TJ, Webb DJ. Endothelin-a receptor antagonist-mediated vasodilatation is attenuated by inhibition of nitric oxide synthesis and by endothelin-b receptor blockade. *Circulation*. 1998;97:752-756
  110. Goligorsky MS, Tsukahara H, Magazine H, Andersen TT, Malik AB, Bahou WF. Termination of endothelin signaling: Role of nitric oxide. *J Cell Physiol*. 1994;158:485-494
  111. Boulanger C, Luscher TF. Release of endothelin from the porcine aorta. Inhibition by endothelium-derived nitric oxide. *The Journal of clinical investigation*. 1990;85:587-590
  112. Luscher TF, Yang Z, Tschudi M, von Segesser L, Stulz P, Boulanger C, Siebenmann R, Turina M, Buhler FR. Interaction between endothelin-1 and

- endothelium-derived relaxing factor in human arteries and veins. *Circulation research*. 1990;66:1088-1094
113. Radomski MW, Palmer RM, Moncada S. The role of nitric oxide and cgmp in platelet adhesion to vascular endothelium. *Biochemical and biophysical research communications*. 1987;148:1482-1489
114. Garg UC, Hassid A. Nitric oxide-generating vasodilators and 8-bromo-cyclic guanosine monophosphate inhibit mitogenesis and proliferation of cultured rat vascular smooth muscle cells. *The Journal of clinical investigation*. 1989;83:1774-1777
115. Schiffrin EL, Deng LY, Sventek P, Day R. Enhanced expression of endothelin-1 gene in resistance arteries in severe human essential hypertension. *Journal of hypertension*. 1997;15:57-63
116. Ergul S, Parish DC, Puett D, Ergul A. Racial differences in plasma endothelin-1 concentrations in individuals with essential hypertension. *Hypertension*. 1996;28:652-655
117. Saito Y, Nakao K, Mukoyama M, Imura H. Increased plasma endothelin level in patients with essential hypertension. *The New England journal of medicine*. 1990;322:205
118. Shichiri M, Hirata Y, Ando K, Emori T, Ohta K, Kimoto S, Ogura M, Inoue A, Marumo F. Plasma endothelin levels in hypertension and chronic renal failure. *Hypertension*. 1990;15:493-496
119. Cernacek P, Stewart DJ. Immunoreactive endothelin in human plasma: Marked elevations in patients in cardiogenic shock. *Biochemical and biophysical research communications*. 1989;161:562-567
120. Tomoda H. Plasma endothelin-1 in acute myocardial infarction with heart failure. *Am Heart J*. 1993;125:667-672
121. Lariviere R, Thibault G, Schiffrin EL. Increased endothelin-1 content in blood vessels of deoxycorticosterone acetate-salt hypertensive but not in spontaneously hypertensive rats. *Hypertension*. 1993;21:294-300
122. Sharifi AM, He G, Touyz RM, Schiffrin EL. Vascular endothelin-1 expression and effect of an endothelin eta antagonist on structure and function of small arteries

- from stroke-prone spontaneously hypertensive rats. *Journal of cardiovascular pharmacology*. 1998;31 Suppl 1:S309-312
123. Schiffrin EL, Lariviere R, Li JS, Sventek P, Touyz RM. Deoxycorticosterone acetate plus salt induces overexpression of vascular endothelin-1 and severe vascular hypertrophy in spontaneously hypertensive rats. *Hypertension*. 1995;25:769-773
  124. Ikeda T, Ohta H, Okada M, Kawai N, Nakao R, Siegl PK, Kobayashi T, Maeda S, Miyauchi T, Nishikibe M. Pathophysiological roles of endothelin-1 in dahl salt-sensitive hypertension. *Hypertension*. 1999;34:514-519
  125. d'Uscio LV, Barton M, Shaw S, Moreau P, Luscher TF. Structure and function of small arteries in salt-induced hypertension: Effects of chronic endothelin-subtype-a-receptor blockade. *Hypertension*. 1997;30:905-911
  126. Sventek P, Turgeon A, Garcia R, Schiffrin EL. Vascular and cardiac overexpression of endothelin-1 gene in one-kidney, one clip goldblatt hypertensive rats but only in the late phase of two-kidney one clip goldblatt hypertension. *Journal of hypertension*. 1996;14:57-64
  127. Amiri F, Viridis A, Neves MF, Iglarz M, Seidah NG, Touyz RM, Reudelhuber TL, Schiffrin EL. Endothelium-restricted overexpression of human endothelin-1 causes vascular remodeling and endothelial dysfunction. *Circulation*. 2004;110:2233-2240
  128. Leung JW, Wong WT, Koon HW, Mo FM, Tam S, Huang Y, Vanhoutte PM, Chung SS, Chung SK. Transgenic mice over-expressing et-1 in the endothelial cells develop systemic hypertension with altered vascular reactivity. *PloS one*. 2011;6:e26994
  129. Li JS, Lariviere R, Schiffrin EL. Effect of a nonselective endothelin antagonist on vascular remodeling in deoxycorticosterone acetate-salt hypertensive rats. Evidence for a role of endothelin in vascular hypertrophy. *Hypertension*. 1994;24:183-188
  130. Endemann DH, Schiffrin EL. Endothelial dysfunction. *Journal of the American Society of Nephrology : JASN*. 2004;15:1983-1992

131. Korhonen J, Lahtinen I, Halmekyto M, Alhonen L, Janne J, Dumont D, Alitalo K. Endothelial-specific gene expression directed by the tie gene promoter in vivo. *Blood*. 1995;86:1828-1835
132. Schlaeger TM, Bartunkova S, Lawitts JA, Teichmann G, Risau W, Deutsch U, Sato TN. Uniform vascular-endothelial-cell-specific gene expression in both embryonic and adult transgenic mice. *Proceedings of the National Academy of Sciences of the United States of America*. 1997;94:3058-3063
133. Amiri F, Ko EA, Javeshghani D, Reudelhuber TL, Schiffrin EL. Deleterious combined effects of salt-loading and endothelial cell restricted endothelin-1 overexpression on blood pressure and vascular function in mice. *Journal of hypertension*. 2010;28:1243-1251
134. Idris-Khodja N, Ouerd S, Mian MO, Gornitsky J, Barhoumi T, Paradis P, Schiffrin EL. Endothelin-1 overexpression exaggerates diabetes-induced endothelial dysfunction by altering oxidative stress. *American journal of hypertension*. 2016
135. Wedgwood S, McMullan DM, Bekker JM, Fineman JR, Black SM. Role for endothelin-1-induced superoxide and peroxynitrite production in rebound pulmonary hypertension associated with inhaled nitric oxide therapy. *Circulation research*. 2001;89:357-364
136. Bedard K, Krause KH. The nox family of ros-generating nadph oxidases: Physiology and pathophysiology. *Physiol Rev*. 2007;87:245-313
137. Touyz RM, Yao G, Viel E, Amiri F, Schiffrin EL. Angiotensin ii and endothelin-1 regulate map kinases through different redox-dependent mechanisms in human vascular smooth muscle cells. *Journal of hypertension*. 2004;22:1141-1149
138. Sedeek MH, Llinas MT, Drummond H, Fortepiani L, Abram SR, Alexander BT, Reckelhoff JF, Granger JP. Role of reactive oxygen species in endothelin-induced hypertension. *Hypertension*. 2003;42:806-810
139. Elmarakby AA, Loomis ED, Pollock JS, Pollock DM. Nadph oxidase inhibition attenuates oxidative stress but not hypertension produced by chronic et-1. *Hypertension*. 2005;45:283-287

140. Li L, Fink GD, Watts SW, Northcott CA, Galligan JJ, Pagano PJ, Chen AF. Endothelin-1 increases vascular superoxide via endothelin(a)-nadph oxidase pathway in low-renin hypertension. *Circulation*. 2003;107:1053-1058
141. Duerrschmidt N, Wippich N, Goettsch W, Broemme HJ, Morawietz H. Endothelin-1 induces nad(p)h oxidase in human endothelial cells. *Biochemical and biophysical research communications*. 2000;269:713-717
142. Ketonen J, Shi J, Martonen E, Mervaala E. Periadventitial adipose tissue promotes endothelial dysfunction via oxidative stress in diet-induced obese c57bl/6 mice. *Circ J*. 2010;74:1479-1487
143. Viridis A, Duranti E, Rossi C, Dell'Agnello U, Santini E, Anselmino M, Chiarugi M, Taddei S, Solini A. Tumour necrosis factor-alpha participates on the endothelin-1/nitric oxide imbalance in small arteries from obese patients: Role of perivascular adipose tissue. *Eur Heart J*. 2015;36:784-794
144. Li MW, Mian MO, Barhoumi T, Rehman A, Mann K, Paradis P, Schiffrin EL. Endothelin-1 overexpression exacerbates atherosclerosis and induces aortic aneurysms in apolipoprotein e knockout mice. *Arteriosclerosis, thrombosis, and vascular biology*. 2013;33:2306-2315
145. Schiffrin EL. Remodeling of resistance arteries in essential hypertension and effects of antihypertensive treatment. *American journal of hypertension*. 2004;17:1192-1200
146. Lee RM, Dickhout JG, Sandow SL. Vascular structural and functional changes: Their association with causality in hypertension: Models, remodeling and relevance. *Hypertens Res*. 2017;40:311-323
147. Rizzoni D, Porteri E, Boari GE, De Ciuceis C, Sleiman I, Muiesan ML, Castellano M, Miclini M, Agabiti-Rosei E. Prognostic significance of small-artery structure in hypertension. *Circulation*. 2003;108:2230-2235
148. Chistiakov DA, Sobenin IA, Orekhov AN. Vascular extracellular matrix in atherosclerosis. *Cardiol Rev*. 2013;21:270-288
149. Ooshima A, Fuller GC, Cardinale GJ, Spector S, Udenfriend S. Increased collagen synthesis in blood vessels of hypertensive rats and its reversal by

- antihypertensive agents. *Proceedings of the National Academy of Sciences of the United States of America*. 1974;71:3019-3023
150. Kim S, Ohta K, Hamaguchi A, Omura T, Yukimura T, Miura K, Inada Y, Ishimura Y, Chatani F, Iwao H. Angiotensin ii type i receptor antagonist inhibits the gene expression of transforming growth factor-beta 1 and extracellular matrix in cardiac and vascular tissues of hypertensive rats. *J Pharmacol Exp Ther*. 1995;273:509-515
  151. Intengan HD, Deng LY, Li JS, Schiffrin EL. Mechanics and composition of human subcutaneous resistance arteries in essential hypertension. *Hypertension*. 1999;33:569-574
  152. Wang M, Kim SH, Monticone RE, Lakatta EG. Matrix metalloproteinases promote arterial remodeling in aging, hypertension, and atherosclerosis. *Hypertension*. 2015;65:698-703
  153. Laviades C, Varo N, Fernandez J, Mayor G, Gil MJ, Monreal I, Diez J. Abnormalities of the extracellular degradation of collagen type i in essential hypertension. *Circulation*. 1998;98:535-540
  154. Ergul A, Portik-Dobos V, Hutchinson J, Franco J, Anstadt MP. Downregulation of vascular matrix metalloproteinase inducer and activator proteins in hypertensive patients. *American journal of hypertension*. 2004;17:775-782
  155. Wang M, Zhang J, Telljohann R, Jiang L, Wu J, Monticone RE, Kapoor K, Talan M, Lakatta EG. Chronic matrix metalloproteinase inhibition retards age-associated arterial proinflammation and increase in blood pressure. *Hypertension*. 2012;60:459-466
  156. Wang M, Jiang L, Monticone RE, Lakatta EG. Proinflammation: The key to arterial aging. *Trends Endocrinol Metab*. 2014;25:72-79
  157. Ergul A, Portik-Dobos V, Giulumian AD, Molero MM, Fuchs LC. Stress upregulates arterial matrix metalloproteinase expression and activity via endothelin a receptor activation. *American journal of physiology. Heart and circulatory physiology*. 2003;285:H2225-2232

158. Pu Q, Neves MF, Virdis A, Touyz RM, Schiffrin EL. Endothelin antagonism on aldosterone-induced oxidative stress and vascular remodeling. *Hypertension*. 2003;42:49-55
159. Park JB, Schiffrin EL. Et(a) receptor antagonist prevents blood pressure elevation and vascular remodeling in aldosterone-infused rats. *Hypertension*. 2001;37:1444-1449
160. Sachidanandam K, Portik-Dobos V, Kelly-Cobbs AI, Ergul A. Dual endothelin receptor antagonism prevents remodeling of resistance arteries in diabetes. *Canadian journal of physiology and pharmacology*. 2010;88:616-621
161. Gras E, Belaidi E, Briancon-Marjollet A, Pepin JL, Arnaud C, Godin-Ribuot D. Endothelin-1 mediates intermittent hypoxia-induced inflammatory vascular remodeling through hif-1 activation. *Journal of applied physiology*. 2016;120:437-443
162. Intengan HD, Schiffrin EL. Structure and mechanical properties of resistance arteries in hypertension: Role of adhesion molecules and extracellular matrix determinants. *Hypertension*. 2000;36:312-318
163. Mitchell GF. Effects of central arterial aging on the structure and function of the peripheral vasculature: Implications for end-organ damage. *Journal of applied physiology*. 2008;105:1652-1660
164. Mitchell GF, Parise H, Benjamin EJ, Larson MG, Keyes MJ, Vita JA, Vasan RS, Levy D. Changes in arterial stiffness and wave reflection with advancing age in healthy men and women: The framingham heart study. *Hypertension*. 2004;43:1239-1245
165. O'Rourke MF, Nichols WW. Aortic diameter, aortic stiffness, and wave reflection increase with age and isolated systolic hypertension. *Hypertension*. 2005;45:652-658
166. Olivetti G, Melissari M, Marchetti G, Anversa P. Quantitative structural changes of the rat thoracic aorta in early spontaneous hypertension. Tissue composition, and hypertrophy and hyperplasia of smooth muscle cells. *Circulation research*. 1982;51:19-26

167. Owens GK, Schwartz SM. Vascular smooth muscle cell hypertrophy and hyperploidy in the goldblatt hypertensive rat. *Circulation research*. 1983;53:491-501
168. Diep QN, Li JS, Schiffrin EL. In vivo study of at(1) and at(2) angiotensin receptors in apoptosis in rat blood vessels. *Hypertension*. 1999;34:617-624
169. Sharifi AM, Schiffrin EL. Apoptosis in vasculature of spontaneously hypertensive rats: Effect of an angiotensin converting enzyme inhibitor and a calcium channel antagonist. *American journal of hypertension*. 1998;11:1108-1116
170. Schiffrin EL. Vascular remodeling in hypertension: Mechanisms and treatment. *Hypertension*. 2012;59:367-374
171. Pauletto P, Chiavegato A, Giuriato L, Scatena M, Faggin E, Grisenti A, Sarzani R, Paci MV, Fulgeri PD, Rappelli A, et al. Hyperplastic growth of aortic smooth muscle cells in renovascular hypertensive rabbits is characterized by the expansion of an immature cell phenotype. *Circulation research*. 1994;74:774-788
172. Park JB, Schiffrin EL. Small artery remodeling is the most prevalent (earliest?) form of target organ damage in mild essential hypertension. *Journal of hypertension*. 2001;19:921-930
173. Intengan HD, Schiffrin EL. Vascular remodeling in hypertension: Roles of apoptosis, inflammation, and fibrosis. *Hypertension*. 2001;38:581-587
174. Intengan HD, Thibault G, Li JS, Schiffrin EL. Resistance artery mechanics, structure, and extracellular components in spontaneously hypertensive rats : Effects of angiotensin receptor antagonism and converting enzyme inhibition. *Circulation*. 1999;100:2267-2275
175. Endemann D, Touyz RM, Li JS, Deng LY, Schiffrin EL. Altered angiotensin ii-induced small artery contraction during the development of hypertension in spontaneously hypertensive rats. *American journal of hypertension*. 1999;12:716-723
176. Diep QN, El Mabrouk M, Cohn JS, Endemann D, Amiri F, Viridis A, Neves MF, Schiffrin EL. Structure, endothelial function, cell growth, and inflammation in blood vessels of angiotensin ii-infused rats: Role of peroxisome proliferator-activated receptor-gamma. *Circulation*. 2002;105:2296-2302

177. Rosei EA, Rizzoni D, Castellano M, Porteri E, Zulli R, Muiesan ML, Bettoni G, Salvetti M, Muiesan P, Giulini SM. Media: Lumen ratio in human small resistance arteries is related to forearm minimal vascular resistance. *Journal of hypertension*. 1995;13:341-347
178. Korsgaard N, Aalkjaer C, Heagerty AM, Izzard AS, Mulvany MJ. Histology of subcutaneous small arteries from patients with essential hypertension. *Hypertension*. 1993;22:523-526
179. Schiffrin EL, Park JB, Intengan HD, Touyz RM. Correction of arterial structure and endothelial dysfunction in human essential hypertension by the angiotensin receptor antagonist losartan. *Circulation*. 2000;101:1653-1659
180. Lee RM, Richardson M, McKenzie R. Vascular changes associated with deoxycorticosterone-nacl-induced hypertension. *Blood Vessels*. 1989;26:137-156
181. Lee RM, Triggle CR. Morphometric study of mesenteric arteries from genetically hypertensive dahl strain rats. *Blood Vessels*. 1986;23:199-224
182. Mulvany MJ, Baandrup U, Gundersen HJ. Evidence for hyperplasia in mesenteric resistance vessels of spontaneously hypertensive rats using a three-dimensional disector. *Circulation research*. 1985;57:794-800
183. Deng LY, Schiffrin EL. Effects of endothelin on resistance arteries of doca-salt hypertensive rats. *The American journal of physiology*. 1992;262:H1782-1787
184. Korsgaard N, Mulvany MJ. Cellular hypertrophy in mesenteric resistance vessels from renal hypertensive rats. *Hypertension*. 1988;12:162-167
185. Rizzoni D, Porteri E, Castellano M, Bettoni G, Muiesan ML, Muiesan P, Giulini SM, Agabiti-Rosei E. Vascular hypertrophy and remodeling in secondary hypertension. *Hypertension*. 1996;28:785-790
186. Li JS, Knafo L, Turgeon A, Garcia R, Schiffrin EL. Effect of endothelin antagonism on blood pressure and vascular structure in renovascular hypertensive rats. *The American journal of physiology*. 1996;271:H88-93
187. Schiffrin EL. Endothelin: Potential role in hypertension and vascular hypertrophy. *Hypertension*. 1995;25:1135-1143

188. Bobik A, Grooms A, Millar JA, Mitchell A, Grinpukel S. Growth factor activity of endothelin on vascular smooth muscle. *The American journal of physiology*. 1990;258:C408-415
189. Hirata Y, Takagi Y, Fukuda Y, Marumo F. Endothelin is a potent mitogen for rat vascular smooth muscle cells. *Atherosclerosis*. 1989;78:225-228
190. Chua BH, Krebs CJ, Chua CC, Diglio CA. Endothelin stimulates protein synthesis in smooth muscle cells. *The American journal of physiology*. 1992;262:E412-416
191. Thomas KA. Vascular endothelial growth factor, a potent and selective angiogenic agent. *J Biol Chem*. 1996;271:603-606
192. Caillon A, Schiffrin EL. Role of inflammation and immunity in hypertension: Recent epidemiological, laboratory, and clinical evidence. *Current hypertension reports*. 2016;18:21
193. Harrison DG, Guzik TJ, Lob HE, Madhur MS, Marvar PJ, Thabet SR, Vinh A, Weyand CM. Inflammation, immunity, and hypertension. *Hypertension*. 2011;57:132-140
194. Olsen F. Transfer of arterial hypertension by splenic cells from doca-salt hypertensive and renal hypertensive rats to normotensive recipients. *Acta Pathol Microbiol Scand C*. 1980;88:1-5
195. Svendsen UG. The role of thymus for the development and prognosis of hypertension and hypertensive vascular disease in mice following renal infarction. *Acta Pathol Microbiol Scand A*. 1976;84:235-243
196. Schiffrin EL. Inflammation, immunity and development of essential hypertension. *Journal of hypertension*. 2014;32:228-229
197. Janeway CA Jr TP, Walport M, et al. Principles of innate and adaptive immunity. *Immunobiology: The Immune System in Health and Disease*. 2001
198. Alberts B JA, Lewis J, et al. Innate immunity. *Molecular Biology of the Cell*. 2002
199. Yoshida H, Hayashi S, Kunisada T, Ogawa M, Nishikawa S, Okamura H, Sudo T, Shultz LD, Nishikawa S. The murine mutation osteopetrosis is in the coding region of the macrophage colony stimulating factor gene. *Nature*. 1990;345:442-444

200. Wiktor-Jedrzejczak W, Bartocci A, Ferrante AW, Jr., Ahmed-Ansari A, Sell KW, Pollard JW, Stanley ER. Total absence of colony-stimulating factor 1 in the macrophage-deficient osteopetrotic (op/op) mouse. *Proceedings of the National Academy of Sciences of the United States of America*. 1990;87:4828-4832
201. De Ciuceis C, Amiri F, Brassard P, Endemann DH, Touyz RM, Schiffrin EL. Reduced vascular remodeling, endothelial dysfunction, and oxidative stress in resistance arteries of angiotensin ii-infused macrophage colony-stimulating factor-deficient mice: Evidence for a role in inflammation in angiotensin-induced vascular injury. *Arteriosclerosis, thrombosis, and vascular biology*. 2005;25:2106-2113
202. Ko EA, Amiri F, Pandey NR, Javeshghani D, Leibovitz E, Touyz RM, Schiffrin EL. Resistance artery remodeling in deoxycorticosterone acetate-salt hypertension is dependent on vascular inflammation: Evidence from m-csf-deficient mice. *American journal of physiology. Heart and circulatory physiology*. 2007;292:H1789-1795
203. Javeshghani D, Barhoumi T, Idris-Khodja N, Paradis P, Schiffrin EL. Reduced macrophage-dependent inflammation improves endothelin-1-induced vascular injury. *Hypertension*. 2013;62:112-117
204. Wenzel P, Knorr M, Kossmann S, Stratmann J, Hausding M, Schuhmacher S, Karbach SH, Schwenk M, Yogev N, Schulz E, Oelze M, Grabbe S, Jonuleit H, Becker C, Daiber A, Waisman A, Munzel T. Lysozyme m-positive monocytes mediate angiotensin ii-induced arterial hypertension and vascular dysfunction. *Circulation*. 2011;124:1370-1381
205. Jakubzick CV, Randolph GJ, Henson PM. Monocyte differentiation and antigen-presenting functions. *Nat Rev Immunol*. 2017
206. O'Shea JJ, Paul WE. Mechanisms underlying lineage commitment and plasticity of helper cd4+ t cells. *Science*. 2010;327:1098-1102
207. Idris-Khodja N, Mian MO, Paradis P, Schiffrin EL. Dual opposing roles of adaptive immunity in hypertension. *Eur Heart J*. 2014;35:1238-1244
208. Guzik TJ, Hoch NE, Brown KA, McCann LA, Rahman A, Dikalov S, Goronzy J, Weyand C, Harrison DG. Role of the t cell in the genesis of angiotensin ii induced

- hypertension and vascular dysfunction. *The Journal of experimental medicine*. 2007;204:2449-2460
209. Wu J, Thabet SR, Kirabo A, Trott DW, Saleh MA, Xiao L, Madhur MS, Chen W, Harrison DG. Inflammation and mechanical stretch promote aortic stiffening in hypertension through activation of p38 mitogen-activated protein kinase. *Circulation research*. 2014;114:616-625
210. Wallace K, Novotny S, Heath J, Moseley J, Martin JN, Jr., Owens MY, LaMarca B. Hypertension in response to cd4(+) t cells from reduced uterine perfusion pregnant rats is associated with activation of the endothelin-1 system. *Am J Physiol Regul Integr Comp Physiol*. 2012;303:R144-149
211. Wallace K, Richards S, Dhillon P, Weimer A, Edholm ES, Bengten E, Wilson M, Martin JN, Jr., LaMarca B. Cd4+ t-helper cells stimulated in response to placental ischemia mediate hypertension during pregnancy. *Hypertension*. 2011;57:949-955
212. Madhur MS, Lob HE, McCann LA, Iwakura Y, Blinder Y, Guzik TJ, Harrison DG. Interleukin 17 promotes angiotensin ii-induced hypertension and vascular dysfunction. *Hypertension*. 2010;55:500-507
213. Tanaka K, Yoshioka K, Tatsumi K, Kimura S, Kasuya Y. Endothelin regulates function of il-17-producing t cell subset. *Life sciences*. 2014;118:244-247
214. Barhoumi T, Kasal DA, Li MW, Shbat L, Laurant P, Neves MF, Paradis P, Schiffrin EL. T regulatory lymphocytes prevent angiotensin ii-induced hypertension and vascular injury. *Hypertension*. 2011;57:469-476
215. Kasal DA, Barhoumi T, Li MW, Yamamoto N, Zdanovich E, Rehman A, Neves MF, Laurant P, Paradis P, Schiffrin EL. T regulatory lymphocytes prevent aldosterone-induced vascular injury. *Hypertension*. 2012;59:324-330
216. Mian MO, Barhoumi T, Briet M, Paradis P, Schiffrin EL. Deficiency of t-regulatory cells exaggerates angiotensin ii-induced microvascular injury by enhancing immune responses. *Journal of hypertension*. 2016;34:97-108
217. Kassin M, Galan M, Partyka M, Trebak M, Matrougui K. Interleukin-10 released by cd4(+)/cd25(+) natural regulatory t cells improves microvascular endothelial

- function through inhibition of nadph oxidase activity in hypertensive mice. *Arteriosclerosis, thrombosis, and vascular biology*. 2011;31:2534-2542
218. Barhoumi T, Briet M, Kasal DA, Fraulob-Aquino JC, Idris-Khodja N, Laurant P, Paradis P, Schiffrin EL. Erythropoietin-induced hypertension and vascular injury in mice overexpressing human endothelin-1: Exercise attenuated hypertension, oxidative stress, inflammation and immune response. *Journal of hypertension*. 2014;32:784-794
219. Miner JH. The glomerular basement membrane. *Exp Cell Res*. 2012;318:973-978
220. Kawachi H, Miyauchi N, Suzuki K, Han GD, Orikasa M, Shimizu F. Role of podocyte slit diaphragm as a filtration barrier. *Nephrology (Carlton)*. 2006;11:274-281
221. Greger R. Physiology of renal sodium transport. *Am J Med Sci*. 2000;319:51-62
222. Mullins LJ, Bailey MA, Mullins JJ. Hypertension, kidney, and transgenics: A fresh perspective. *Physiol Rev*. 2006;86:709-746
223. Atlas SA. The renin-angiotensin aldosterone system: Pathophysiological role and pharmacologic inhibition. *J Manag Care Pharm*. 2007;13:9-20
224. Santos RA. Angiotensin-(1-7). *Hypertension*. 2014;63:1138-1147
225. Lavoie JL, Sigmund CD. Minireview: Overview of the renin-angiotensin system--an endocrine and paracrine system. *Endocrinology*. 2003;144:2179-2183
226. Stockand JD, Sansom SC. Regulation of filtration rate by glomerular mesangial cells in health and diabetic renal disease. *American journal of kidney diseases : the official journal of the National Kidney Foundation*. 1997;29:971-981
227. Navar LG. Intrarenal renin-angiotensin system in regulation of glomerular function. *Current opinion in nephrology and hypertension*. 2014;23:38-45
228. Navar LG, Mitchell KD, Harrison-Bernard LM, Kobori H, Nishiyama A. Review: Intrarenal angiotensin ii levels in normal and hypertensive states. *J Renin Angiotensin Aldosterone Syst*. 2001;2:S176-S184
229. Kobori H, Nangaku M, Navar LG, Nishiyama A. The intrarenal renin-angiotensin system: From physiology to the pathobiology of hypertension and kidney disease. *Pharmacological reviews*. 2007;59:251-287

230. Vignon-Zellweger N, Heiden S, Miyauchi T, Emoto N. Endothelin and endothelin receptors in the renal and cardiovascular systems. *Life sciences*. 2012;91:490-500
231. Pupilli C, Brunori M, Misciglia N, Selli C, Ianni L, Yanagisawa M, Mannelli M, Serio M. Presence and distribution of endothelin-1 gene expression in human kidney. *The American journal of physiology*. 1994;267:F679-687
232. Kohan DE, Inscho EW, Wesson D, Pollock DM. Physiology of endothelin and the kidney. *Comprehensive Physiology*. 2011;1:883-919
233. Terada Y, Tomita K, Nonoguchi H, Marumo F. Different localization of two types of endothelin receptor mRNA in microdissected rat nephron segments using reverse transcription and polymerase chain reaction assay. *The Journal of clinical investigation*. 1992;90:107-112
234. Wendel M, Knels L, Kummer W, Koch T. Distribution of endothelin receptor subtypes eta and etb in the rat kidney. *J Histochem Cytochem*. 2006;54:1193-1203
235. Chow LH, Subramanian S, Nuovo GJ, Miller F, Nord EP. Endothelin receptor mRNA expression in renal medulla identified by in situ rt-pcr. *The American journal of physiology*. 1995;269:F449-457
236. Qiu C, Samsell L, Baylis C. Actions of endogenous endothelin on glomerular hemodynamics in the rat. *The American journal of physiology*. 1995;269:R469-473
237. Loutzenhiser R, Epstein M, Hayashi K, Horton C. Direct visualization of effects of endothelin on the renal microvasculature. *The American journal of physiology*. 1990;258:F61-68
238. Endlich K, Hoffend J, Steinhausen M. Localization of endothelin eta and etb receptor-mediated constriction in the renal microcirculation of rats. *J Physiol*. 1996;497 ( Pt 1):211-218
239. Inscho EW, Imig JD, Cook AK, Pollock DM. Eta and etb receptors differentially modulate afferent and efferent arteriolar responses to endothelin. *British journal of pharmacology*. 2005;146:1019-1026

240. Lanese DM, Yuan BH, McMurtry IF, Conger JD. Comparative sensitivities of isolated rat renal arterioles to endothelin. *The American journal of physiology*. 1992;263:F894-899
241. Gurbanov K, Rubinstein I, Hoffman A, Abassi Z, Better OS, Winaver J. Differential regulation of renal regional blood flow by endothelin-1. *The American journal of physiology*. 1996;271:F1166-1172
242. Rubinstein I, Gurbanov K, Hoffman A, Better OS, Winaver J. Differential effect of endothelin-1 on renal regional blood flow: Role of nitric oxide. *Journal of cardiovascular pharmacology*. 1995;26 Suppl 3:S208-210
243. Evans RG, Madden AC, Oliver JJ, Lewis TV. Effects of et(a) - and et(b)-receptor antagonists on regional kidney blood flow, and responses to intravenous endothelin-1, in anaesthetized rabbits. *Journal of hypertension*. 2001;19:1789-1799
244. Just A, Olson AJ, Arendshorst WJ. Dual constrictor and dilator actions of et(b) receptors in the rat renal microcirculation: Interactions with et(a) receptors. *American journal of physiology. Renal physiology*. 2004;286:F660-668
245. Kohan DE. Endothelin synthesis by rabbit renal tubule cells. *The American journal of physiology*. 1991;261:F221-226
246. Ujiie K, Terada Y, Nonoguchi H, Shinohara M, Tomita K, Marumo F. Messenger rna expression and synthesis of endothelin-1 along rat nephron segments. *The Journal of clinical investigation*. 1992;90:1043-1048
247. Claria J, Jimenez W, La Villa G, Asbert M, Castro A, Llibre JL, Arroyo V, Rivera F. Effects of endothelin on renal haemodynamics and segmental sodium handling in conscious rats. *Acta Physiol Scand*. 1991;141:305-308
248. Harris PJ, Zhuo J, Mendelsohn FA, Skinner SL. Haemodynamic and renal tubular effects of low doses of endothelin in anaesthetized rats. *J Physiol*. 1991;433:25-39
249. Schnermann J, Lorenz JN, Briggs JP, Keiser JA. Induction of water diuresis by endothelin in rats. *The American journal of physiology*. 1992;263:F516-526
250. Denton KM, Anderson WP. Vascular actions of endothelin in the rabbit kidney. *Clinical and experimental pharmacology & physiology*. 1990;17:861-872

251. Ahn D, Ge Y, Stricklett PK, Gill P, Taylor D, Hughes AK, Yanagisawa M, Miller L, Nelson RD, Kohan DE. Collecting duct-specific knockout of endothelin-1 causes hypertension and sodium retention. *The Journal of clinical investigation*. 2004;114:504-511
252. Ge Y, Ahn D, Stricklett PK, Hughes AK, Yanagisawa M, Verbalis JG, Kohan DE. Collecting duct-specific knockout of endothelin-1 alters vasopressin regulation of urine osmolality. *American journal of physiology. Renal physiology*. 2005;288:F912-920
253. Ge Y, Stricklett PK, Hughes AK, Yanagisawa M, Kohan DE. Collecting duct-specific knockout of the endothelin a receptor alters renal vasopressin responsiveness, but not sodium excretion or blood pressure. *American journal of physiology. Renal physiology*. 2005;289:F692-698
254. Ge Y, Bagnall A, Stricklett PK, Strait K, Webb DJ, Kotelevtsev Y, Kohan DE. Collecting duct-specific knockout of the endothelin b receptor causes hypertension and sodium retention. *American journal of physiology. Renal physiology*. 2006;291:F1274-1280
255. Ge Y, Bagnall A, Stricklett PK, Webb D, Kotelevtsev Y, Kohan DE. Combined knockout of collecting duct endothelin a and b receptors causes hypertension and sodium retention. *American journal of physiology. Renal physiology*. 2008;295:F1635-1640
256. Lynch IJ, Welch AK, Kohan DE, Cain BD, Wingo CS. Endothelin-1 inhibits sodium reabsorption by et(a) and et(b) receptors in the mouse cortical collecting duct. *American journal of physiology. Renal physiology*. 2013;305:F568-573
257. Bugaj V, Mironova E, Kohan DE, Stockand JD. Collecting duct-specific endothelin b receptor knockout increases enac activity. *Am J Physiol Cell Physiol*. 2012;302:C188-194
258. Bugaj V, Pochynyuk O, Mironova E, Vandewalle A, Medina JL, Stockand JD. Regulation of the epithelial na<sup>+</sup> channel by endothelin-1 in rat collecting duct. *American journal of physiology. Renal physiology*. 2008;295:F1063-1070

259. Schneider MP, Ge Y, Pollock DM, Pollock JS, Kohan DE. Collecting duct-derived endothelin regulates arterial pressure and na excretion via nitric oxide. *Hypertension*. 2008;51:1605-1610
260. Eiam-Ong S, Hilden SA, King AJ, Johns CA, Madias NE. Endothelin-1 stimulates the na<sup>+</sup>/h<sup>+</sup> and na<sup>+</sup>/hco<sub>3</sub><sup>-</sup> transporters in rabbit renal cortex. *Kidney international*. 1992;42:18-24
261. Gallego MS, Ling BN. Regulation of amiloride-sensitive na<sup>+</sup> channels by endothelin-1 in distal nephron cells. *The American journal of physiology*. 1996;271:F451-460
262. Firth JD, Ratcliffe PJ, Raine AE, Ledingham JG. Endothelin: An important factor in acute renal failure? *Lancet*. 1988;2:1179-1182
263. Vuurmans JL, Boer P, Koomans HA. Effects of endothelin-1 and endothelin-1-receptor blockade on renal function in humans. *Nephrology, dialysis, transplantation : official publication of the European Dialysis and Transplant Association - European Renal Association*. 2004;19:2742-2746
264. Goddard J, Johnston NR, Hand MF, Cumming AD, Rabelink TJ, Rankin AJ, Webb DJ. Endothelin-a receptor antagonism reduces blood pressure and increases renal blood flow in hypertensive patients with chronic renal failure: A comparison of selective and combined endothelin receptor blockade. *Circulation*. 2004;109:1186-1193
265. Shindo T, Kurihara H, Maemura K, Kurihara Y, Ueda O, Suzuki H, Kuwaki T, Ju KH, Wang Y, Ebihara A, Nishimatsu H, Moriyama N, Fukuda M, Akimoto Y, Hirano H, Morita H, Kumada M, Yazaki Y, Nagai R, Kimura K. Renal damage and salt-dependent hypertension in aged transgenic mice overexpressing endothelin-1. *Journal of molecular medicine*. 2002;80:105-116
266. Kassab S, Miller MT, Novak J, Reckelhoff J, Clower B, Granger JP. Endothelin-a receptor antagonism attenuates the hypertension and renal injury in dahl salt-sensitive rats. *Hypertension*. 1998;31:397-402
267. Okada M, Kobayashi M, Maruyama H, Takahashi R, Ikemoto F, Yano M, Nishikibe M. Effects of a selective endothelin a-receptor antagonist, bq-123, in

- salt-loaded stroke-prone spontaneously hypertensive rats. *Clinical and experimental pharmacology & physiology*. 1995;22:763-768
268. Li JS, Schiffrin EL. Effect of chronic treatment of adult spontaneously hypertensive rats with an endothelin receptor antagonist. *Hypertension*. 1995;25:495-500
269. Ohno A, Naruse M, Kato S, Hosaka M, Naruse K, Demura H, Sugino N. Endothelin-specific antibodies decrease blood pressure and increase glomerular filtration rate and renal plasma flow in spontaneously hypertensive rats. *Journal of hypertension*. 1992;10:781-785
270. Neuhofer W, Pittrow D. Role of endothelin and endothelin receptor antagonists in renal disease. *Eur J Clin Invest*. 2006;36 Suppl 3:78-88
271. Sasser JM, Pollock JS, Pollock DM. Renal endothelin in chronic angiotensin ii hypertension. *Am J Physiol Regul Integr Comp Physiol*. 2002;283:R243-248
272. Vogel V, Backer A, Heller J, Kramer HJ. The renal endothelin system in the prague hypertensive rat, a new model of spontaneous hypertension. *Clinical science*. 1999;97:91-98
273. Hughes AK, Cline RC, Kohan DE. Alterations in renal endothelin-1 production in the spontaneously hypertensive rat. *Hypertension*. 1992;20:666-673
274. Hoffman A, Grossman E, Goldstein DS, Gill JR, Jr., Keiser HR. Urinary excretion rate of endothelin-1 in patients with essential hypertension and salt sensitivity. *Kidney international*. 1994;45:556-560
275. Zoccali C, Leonardis D, Parlongo S, Mallamaci F, Postorino M. Urinary and plasma endothelin 1 in essential hypertension and in hypertension secondary to renoparenchymal disease. *Nephrology, dialysis, transplantation : official publication of the European Dialysis and Transplant Association - European Renal Association*. 1995;10:1320-1323
276. Kohan DE. Endothelins in the normal and diseased kidney. *American journal of kidney diseases : the official journal of the National Kidney Foundation*. 1997;29:2-26

277. Forbes JM, Jandeleit-Dahm K, Allen TJ, Hewitson TD, Becker GJ, Jones CL. Endothelin and endothelin a/b receptors are increased after ischaemic acute renal failure. *Exp Nephrol.* 2001;9:309-316
278. Bruzzi I, Corna D, Zoja C, Orisio S, Schiffrin EL, Cavallotti D, Remuzzi G, Benigni A. Time course and localization of endothelin-1 gene expression in a model of renal disease progression. *Am J Pathol.* 1997;151:1241-1247
279. Gellai M, DeWolf R, Pullen M, Nambi P. Distribution and functional role of renal et receptor subtypes in normotensive and hypertensive rats. *Kidney international.* 1994;46:1287-1294
280. Boesen EI, Krishnan KR, Pollock JS, Pollock DM. Eta activation mediates angiotensin ii-induced infiltration of renal cortical t cells. *Journal of the American Society of Nephrology : JASN.* 2011;22:2187-2192
281. Tostes RC, Touyz RM, He G, Chen X, Schiffrin EL. Contribution of endothelin-1 to renal activator protein-1 activation and macrophage infiltration in aldosterone-induced hypertension. *Clinical science.* 2002;103 Suppl 48:25S-30S
282. Saleh MA, Boesen EI, Pollock JS, Savin VJ, Pollock DM. Endothelin-1 increases glomerular permeability and inflammation independent of blood pressure in the rat. *Hypertension.* 2010;56:942-949
283. Amiri F, Paradis P, Reudelhuber TL, Schiffrin EL. Vascular inflammation in absence of blood pressure elevation in transgenic murine model overexpressing endothelin-1 in endothelial cells. *Journal of hypertension.* 2008;26:1102-1109
284. Dhaun N, Goddard J, Kohan DE, Pollock DM, Schiffrin EL, Webb DJ. Role of endothelin-1 in clinical hypertension: 20 years on. *Hypertension.* 2008;52:452-459
285. Indra AK, Warot X, Brocard J, Bornert JM, Xiao JH, Chambon P, Metzger D. Temporally-controlled site-specific mutagenesis in the basal layer of the epidermis: Comparison of the recombinase activity of the tamoxifen-inducible cre-er(t) and cre-er(t2) recombinases. *Nucleic acids research.* 1999;27:4324-4327
286. Rautureau Y, Coelho SC, Fraulob-Aquino JC, Huo KG, Rehman A, Offermanns S, Paradis P, Schiffrin EL. Inducible human endothelin-1 overexpression in

- endothelium raises blood pressure via endothelin type a receptors. *Hypertension*. 2015;66:347-355
287. Leibovitz E, Ebrahimian T, Paradis P, Schiffrin EL. Aldosterone induces arterial stiffness in absence of oxidative stress and endothelial dysfunction. *Journal of hypertension*. 2009;27:2192-2200
288. Rozen S, Skaletsky H. Primer3 on the www for general users and for biologist programmers. *Methods in molecular biology*. 2000;132:365-386
289. Lariviere R, Day R, Schiffrin EL. Increased expression of endothelin-1 gene in blood vessels of deoxycorticosterone acetate-salt hypertensive rats. *Hypertension*. 1993;21:916-920
290. Barton M, d'Uscio LV, Shaw S, Meyer P, Moreau P, Luscher TF. Et(a) receptor blockade prevents increased tissue endothelin-1, vascular hypertrophy, and endothelial dysfunction in salt-sensitive hypertension. *Hypertension*. 1998;31:499-504
291. Kisanuki YY, Emoto N, Ohuchi T, Widyantoro B, Yagi K, Nakayama K, Kedzierski RM, Hammer RE, Yanagisawa H, Williams SC, Richardson JA, Suzuki T, Yanagisawa M. Low blood pressure in endothelial cell-specific endothelin 1 knockout mice. *Hypertension*. 2010;56:121-128
292. Donato AJ, Lesniewski LA, Stuart D, Walker AE, Henson G, Sorensen L, Li D, Kohan DE. Smooth muscle specific disruption of the endothelin-a receptor in mice reduces arterial pressure, and vascular reactivity and affects vascular development. *Life sciences*. 2014;118:238-243
293. Clouthier DE, Hosoda K, Richardson JA, Williams SC, Yanagisawa H, Kuwaki T, Kumada M, Hammer RE, Yanagisawa M. Cranial and cardiac neural crest defects in endothelin-a receptor-deficient mice. *Development*. 1998;125:813-824
294. Bazil MK, Lappe RW, Webb RL. Pharmacologic characterization of an endothelina (eta) receptor antagonist in conscious rats. *Journal of cardiovascular pharmacology*. 1992;20:940-948
295. Nishikibe M, Tsuchida S, Okada M, Fukuroda T, Shimamoto K, Yano M, Ishikawa K, Ikemoto F. Antihypertensive effect of a newly synthesized endothelin

- antagonist, bq-123, in a genetic hypertensive model. *Life sciences*. 1993;52:717-724
296. Okada M, Fukuroda T, Shimamoto K, Takahashi R, Ikemoto F, Yano M, Nishikibe M. Antihypertensive effects of bq-123, a selective endothelin eta receptor antagonist, in spontaneously hypertensive rats treated with doca-salt. *European journal of pharmacology*. 1994;259:339-342
297. Schiffrin EL, Sventek P, Li JS, Turgeon A, Reudelhuber T. Antihypertensive effect of an endothelin receptor antagonist in doca-salt spontaneously hypertensive rats. *British journal of pharmacology*. 1995;115:1377-1381
298. Petramala L, Olmati F, Mancone M, Concistre A, Galassi M, Marinelli C, Tonnarini G, Lucia P, Costi U, Iannucci G, Sardella G, Letizia C. Plasma endothelin-1 levels in patients with resistant hypertension: Effects of renal sympathetic denervation. *Ann Med*. 2017;49:396-403
299. Krum H, Viskoper RJ, Lacourciere Y, Budde M, Charlon V. The effect of an endothelin-receptor antagonist, bosentan, on blood pressure in patients with essential hypertension. Bosentan hypertension investigators. *The New England journal of medicine*. 1998;338:784-790
300. Schiffrin EL, Lariviere R, Li JS, Sventek P. Enhanced expression of the endothelin-1 gene in blood vessels of doca-salt hypertensive rats: Correlation with vascular structure. *J Vasc Res*. 1996;33:235-248
301. Bohm F, Pernow J. The importance of endothelin-1 for vascular dysfunction in cardiovascular disease. *Cardiovascular research*. 2007;76:8-18
302. Zemse SM, Hilgers RH, Simkins GB, Rudic RD, Webb RC. Restoration of endothelin-1-induced impairment in endothelium-dependent relaxation by interleukin-10 in murine aortic rings. *Canadian journal of physiology and pharmacology*. 2008;86:557-565
303. Thijssen DH, Hopman MT, Levine BD. Endothelin and aged blood vessels: One more reason to get off the couch? *Hypertension*. 2007;50:292-293
304. Pernow J, Shemyakin A, Bohm F. New perspectives on endothelin-1 in atherosclerosis and diabetes mellitus. *Life sciences*. 2012;91:507-516

305. Quyyumi AA, Patel RS. Endothelial dysfunction and hypertension: Cause or effect? *Hypertension*. 2010;55:1092-1094
306. Rossi R, Chiurlia E, Nuzzo A, Cioni E, Origliani G, Modena MG. Flow-mediated vasodilation and the risk of developing hypertension in healthy postmenopausal women. *Journal of the American College of Cardiology*. 2004;44:1636-1640
307. Shimbo D, Muntner P, Mann D, Viera AJ, Homma S, Polak JF, Barr RG, Herrington D, Shea S. Endothelial dysfunction and the risk of hypertension: The multi-ethnic study of atherosclerosis. *Hypertension*. 2010;55:1210-1216
308. Diederich D, Skopec J, Diederich A, Dai FX. Cyclosporine produces endothelial dysfunction by increased production of superoxide. *Hypertension*. 1994;23:957-961
309. McIntyre M, Bohr DF, Dominiczak AF. Endothelial function in hypertension: The role of superoxide anion. *Hypertension*. 1999;34:539-545
310. Kimura K, Tsuda K, Baba A, Kawabe T, Boh-oka S, Ibata M, Moriwaki C, Hano T, Nishio I. Involvement of nitric oxide in endothelium-dependent arterial relaxation by leptin. *Biochemical and biophysical research communications*. 2000;273:745-749
311. Li R, Andersen I, Aleke J, Golubinskaya V, Gustafsson H, Nilsson H. Reduced anti-contractile effect of perivascular adipose tissue on mesenteric small arteries from spontaneously hypertensive rats: Role of kv7 channels. *European journal of pharmacology*. 2013;698:310-315
312. Galvez-Prieto B, Somoza B, Gil-Ortega M, Garcia-Prieto CF, de Las Heras AI, Gonzalez MC, Arribas S, Aranguez I, Bolbrinker J, Kreutz R, Ruiz-Gayo M, Fernandez-Alfonso MS. Anticontractile effect of perivascular adipose tissue and leptin are reduced in hypertension. *Front Pharmacol*. 2012;3:103
313. Korzick DH, Muller-Delp JM, Dougherty P, Heaps CL, Bowles DK, Krick KK. Exaggerated coronary vasoreactivity to endothelin-1 in aged rats: Role of protein kinase c. *Cardiovascular research*. 2005;66:384-392
314. Goodwin AT, Amrani M, Marchbank AJ, Gray CC, Jayakumar J, Yacoub MH. Coronary vasoconstriction to endothelin-1 increases with age before and after ischaemia and reperfusion. *Cardiovascular research*. 1999;41:554-562

315. Ziemann SJ, Melenovsky V, Kass DA. Mechanisms, pathophysiology, and therapy of arterial stiffness. *Arteriosclerosis, thrombosis, and vascular biology*. 2005;25:932-943
316. Rajagopalan S, Meng XP, Ramasamy S, Harrison DG, Galis ZS. Reactive oxygen species produced by macrophage-derived foam cells regulate the activity of vascular matrix metalloproteinases in vitro. Implications for atherosclerotic plaque stability. *The Journal of clinical investigation*. 1996;98:2572-2579
317. Gonzalez W, Fontaine V, Pueyo ME, Laquay N, Messika-Zeitoun D, Philippe M, Arnal JF, Jacob MP, Michel JB. Molecular plasticity of vascular wall during n(g)-nitro-l-arginine methyl ester-induced hypertension: Modulation of proinflammatory signals. *Hypertension*. 2000;36:103-109
318. Nakaki T, Nakayama M, Yamamoto S, Kato R. Endothelin-mediated stimulation of DNA synthesis in vascular smooth muscle cells. *Biochemical and biophysical research communications*. 1989;158:880-883
319. Wilkes BM, Susin M, Mento PF. Localization of endothelin-1-like immunoreactivity in human placenta. *J Histochem Cytochem*. 1993;41:535-541
320. Taylor RN, Varma M, Teng NN, Roberts JM. Women with preeclampsia have higher plasma endothelin levels than women with normal pregnancies. *J Clin Endocrinol Metab*. 1990;71:1675-1677
321. Gilbert JS, Ryan MJ, LaMarca BB, Sedeek M, Murphy SR, Granger JP. Pathophysiology of hypertension during preeclampsia: Linking placental ischemia with endothelial dysfunction. *American journal of physiology. Heart and circulatory physiology*. 2008;294:H541-550
322. Mian MO, Paradis P, Schiffrin EL. Innate immunity in hypertension. *Current hypertension reports*. 2014;16:413
323. Boesen EI, Williams DL, Pollock JS, Pollock DM. Immunosuppression with mycophenolate mofetil attenuates the development of hypertension and albuminuria in deoxycorticosterone acetate-salt hypertensive rats. *Clinical and experimental pharmacology & physiology*. 2010;37:1016-1022
324. Karavolias GK, Georgiadou P, Gkouziouta A, Kariofillis P, Karabela G, Tsiapras D, Sbarouni E, Chaidaroglou A, Degiannis D, Adamopoulos S, Voudris V. Short

- and long term anti-inflammatory effects of bosentan therapy in patients with pulmonary arterial hypertension: Relation to clinical and hemodynamic responses. *Expert Opin Ther Targets*. 2010;14:1283-1289
325. Chen Y, Wang X, Mai J, Zhao X, Liang Y, Gu M, Chen Z, Nie R, Wang J. C-reactive protein promotes vascular endothelial dysfunction partly via activating adipose tissue inflammation in hyperlipidemic rabbits. *Int J Cardiol*. 2013;168:2397-2403
326. Huang Cao ZF, Stoffel E, Cohen P. Role of perivascular adipose tissue in vascular physiology and pathology. *Hypertension*. 2017;69:770-777
327. Elisa T, Antonio P, Giuseppe P, Alessandro B, Giuseppe A, Federico C, Marzia D, Ruggero B, Giacomo M, Andrea O, Daniela R, Mariaelisa R, Claudio L. Endothelin receptors expressed by immune cells are involved in modulation of inflammation and in fibrosis: Relevance to the pathogenesis of systemic sclerosis. *J Immunol Res*. 2015;2015:147616
328. Iannone F, Riccardi MT, Guiducci S, Bizzoca R, Cinelli M, Matucci-Cerinic M, Lapadula G. Bosentan regulates the expression of adhesion molecules on circulating t cells and serum soluble adhesion molecules in systemic sclerosis-associated pulmonary arterial hypertension. *Ann Rheum Dis*. 2008;67:1121-1126
329. Schiffrin EL. Immune mechanisms in hypertension and vascular injury. *Clinical science*. 2014;126:267-274
330. Briet M, Schiffrin EL. Aldosterone: Effects on the kidney and cardiovascular system. *Nat Rev Nephrol*. 2010;6:261-273
331. Savoia C, Touyz RM, Amiri F, Schiffrin EL. Selective mineralocorticoid receptor blocker eplerenone reduces resistance artery stiffness in hypertensive patients. *Hypertension*. 2008;51:432-439
332. Zeng ZP, Naruse M, Guan BJ, Naruse K, Sun ML, Zang MF, Demura H, Shi YF. Endothelin stimulates aldosterone secretion in vitro from normal adrenocortical tissue, but not adenoma tissue, in primary aldosteronism. *J Clin Endocrinol Metab*. 1992;74:874-878

333. Cozza EN, Gomez-Sanchez CE, Foecking MF, Chiou S. Endothelin binding to cultured calf adrenal zona glomerulosa cells and stimulation of aldosterone secretion. *The Journal of clinical investigation*. 1989;84:1032-1035
334. Soundararajan R, Pearce D, Ziera T. The role of the enac-regulatory complex in aldosterone-mediated sodium transport. *Mol Cell Endocrinol*. 2012;350:242-247
335. Muller OG, Parnova RG, Centeno G, Rossier BC, Firsov D, Horisberger JD. Mineralocorticoid effects in the kidney: Correlation between alphaenac, gilz, and sgk-1 mrna expression and urinary excretion of na<sup>+</sup> and k<sup>+</sup>. *Journal of the American Society of Nephrology : JASN*. 2003;14:1107-1115
336. Lynch IJ, Welch AK, Gumz ML, Kohan DE, Cain BD, Wingo CS. Effect of mineralocorticoid treatment in mice with collecting duct-specific knockout of endothelin-1. *American journal of physiology. Renal physiology*. 2015;309:F1026-1034
337. Rothermund L, Luckert S, Kossmehl P, Paul M, Kreutz R. Renal endothelin et(a)/et(b) receptor imbalance differentiates salt-sensitive from salt-resistant spontaneous hypertension. *Hypertension*. 2001;37:275-280
338. De Miguel C, Speed JS, Kasztan M, Gohar EY, Pollock DM. Endothelin-1 and the kidney: New perspectives and recent findings. *Current opinion in nephrology and hypertension*. 2016;25:35-41
339. Hocher B, Thone-Reineke C, Rohmeiss P, Schmager F, Slowinski T, Burst V, Siegmund F, Quertermous T, Bauer C, Neumayer HH, Schleuning WD, Theuring F. Endothelin-1 transgenic mice develop glomerulosclerosis, interstitial fibrosis, and renal cysts but not hypertension. *The Journal of clinical investigation*. 1997;99:1380-1389
340. Arfian N, Emoto N, Vignon-Zellweger N, Nakayama K, Yagi K, Hirata K. Et-1 deletion from endothelial cells protects the kidney during the extension phase of ischemia/reperfusion injury. *Biochemical and biophysical research communications*. 2012;425:443-449
341. Benigni A, Zoja C, Corna D, Orisio S, Longaretti L, Bertani T, Remuzzi G. A specific endothelin subtype a receptor antagonist protects against injury in renal disease progression. *Kidney international*. 1993;44:440-444

342. Johnson RJ, Alpers CE, Yoshimura A, Lombardi D, Pritzl P, Floege J, Schwartz SM. Renal injury from angiotensin ii-mediated hypertension. *Hypertension*. 1992;19:464-474
343. Hall JE. The kidney, hypertension, and obesity. *Hypertension*. 2003;41:625-633
344. Picken M, Long J, Williamson GA, Polichnowski AJ. Progression of chronic kidney disease after acute kidney injury: Role of self-perpetuating versus hemodynamic-induced fibrosis. *Hypertension*. 2016;68:921-928
345. Shah KH, Shi P, Giani JF, Janjulia T, Bernstein EA, Li Y, Zhao T, Harrison DG, Bernstein KE, Shen XZ. Myeloid suppressor cells accumulate and regulate blood pressure in hypertension. *Circulation research*. 2015;117:858-869
346. Zhang C, Wang S, Li J, Zhang W, Zheng L, Yang C, Zhu T, Rong R. The mtor signal regulates myeloid-derived suppressor cells differentiation and immunosuppressive function in acute kidney injury. *Cell Death Dis*. 2017;8:e2695
347. Kennedy DJ, Chen Y, Huang W, Viterna J, Liu J, Westfall K, Tian J, Bartlett DJ, Tang WH, Xie Z, Shapiro JI, Silverstein RL. Cd36 and na/k-atpase-alpha1 form a proinflammatory signaling loop in kidney. *Hypertension*. 2013;61:216-224
348. Tostes RC, Fortes ZB, Callera GE, Montezano AC, Touyz RM, Webb RC, Carvalho MH. Endothelin, sex and hypertension. *Clinical science*. 2008;114:85-97